2023-08

Interactions of neurofibrosis and oligodendrogenesis following demyelination: Modulation by aging and exercise

Lozinski, Brian Mark

UNIVERSITY OF CALGARY

Interactions of neurofibrosis and oligodendrogenesis following demyelination: Modulation by aging and exercise

by

Brian Mark Lozinski

A THESIS

SUBMITTED TO THE FACULTY OF GRADUATE STUDIES

IN PARTIAL FULFILMENT OF THE REQUIREMENTS FOR THE

DEGREE OF DOCTOR OF PHILOSOPHY

GRADUATE PROGRAM IN NEUROSCIENCE

CALGARY, ALBERTA

AUGUST, 2023

Abstract

The central nervous system does not undergo significant amounts of regeneration following injury. Despite this, cellular repair processes occur that help to limit the spread of injuries, maintain tissue integrity, and in some cases regenerate lost cells. Here I introduce central nervous system fibroblasts as regulators of regenerative processes in the central nervous system, and present aging and exercise as factors regulating fibroblasts and the lesioned environment. Fibroblasts are connective tissue cells that are found throughout the body. Under pathological conditions they contribute to tissue scarification by secreting excessive amounts of extracellular matrix that impairs regeneration. Fibroblasts in the central nervous system are normally found at the border regions in the meninges, perivascular space, and choroid plexus. In the injured central nervous system fibroblasts are elevated in the parenchyma and impair regenerative processes like axon regeneration. In this thesis I characterized the elevation of fibroblasts in the toxin induced lysolecithin model of central nervous system injury. One primary observation was the association of fibroblasts with microglia/macrophage responses, as well as the ability of macrophages to promote fibroblast migration in vitro. Central nervous system fibroblasts spatially obscured newly myelinating oligodendrocytes in lysolecithin lesions and inhibited the differentiation of oligodendrocyte progenitor cells in vitro. I explored the impact of age on the fibroblast response to lysolecithin injury. I found that age affected the proportion of the lysolecithin lesion occupied by fibroblasts, attenuated the immune response, and ablated the chemoattractant capacity of macrophages in vitro. Lastly, I described the changes that occur in the proteome of naïve and lysolecithin lesioned spinal cords and serum from exercising and sedentary mice. I also examined the effects of exercise on the young and middle-aged fibroblast response. I found that acute voluntary access to a running wheel resulted in significant protein changes related to metabolism, oxidative stress, and synaptic transmission. However, voluntary wheel running did not result in any changes to the fibroblast response in lysolecithin lesions in young and middle-aged mice. This thesis highlights the role of fibroblasts in central nervous system injuries, details the potential causes and outcomes of their elevation in the parenchyma, and also highlights the implications of aging and exercise for the fibroblast response and broader lysolecithin lesion environment.

Preface

This thesis is the original work of the author, Brian M. Lozinski, prepared in manuscript style format. Figures appear in the text in the sections in which they are mentioned.

Chapter 1 of this thesis is an expanded version of published and unpublished reviews. Portions of the introductory text are used with permission from SAGE publishing and Lozinski and Yong (2020) of which I am an author. Figure 1.5 is from figure 1 in Lozinski and Yong (2020).

Lozinski BM, Yong VW. Exercise and the brain in multiple sclerosis. Multiple Sclerosis Journal. 2020;28(8):1167-1172. Published October 2020. doi:10.1177/1352458520969099

Lozinski BM, Ghorbani S, Yong VW. Unnamed fibrosis review. In preparation for submission.

Chapter 2 is a portion of a manuscript in preparation for submission.

Chapter 3 is a portion of a manuscript in preparation for submission.

Chapter 4 of this thesis has been published as Lozinski et al, “Exercise rapidly alters proteomes in mice following spinal cord demyelination”. Multiple sclerosis journal, Vol 11, Issue 1. The full citation can be found below.

Lozinski, B. M., de Almeida, L. G. N., Silva, C., Dong, Y., Brown, D., Chopra, S., Yong, V. W., & Dufour, A. (2021). Exercise rapidly alters proteomes in mice following spinal cord demyelination. Scientific reports, 11(1), 7239. https://doi.org/10.1038/s41598-021-86593-5

Acknowledgements

Firstly, I want to earnestly thank and acknowledge my supervisor, Dr. Wee Yong, for giving me the opportunity to pursue research as a Master's student 5 years ago despite my lack of experience. I appreciate the consistent guidance and support he has provided me, as well as, his ability to bring extraordinary individuals together and maintain an environment of comradery and scientific interest has made the duration of my graduate program a joy.

Thank you to my committee members: Dr. Keith Sharkey and Dr. Hedwich Kuipers, who made my committee meetings so engaging and enjoyable. I also want to extend a special thank you to Dr. Sharkey for his guidance in pursuing graduate school. When I came to you as an undergraduate student you saw my potential and motivated me to improve and apply myself to my studies and research.

I also want to acknowledge my undergraduate professors, Dr's. Benediktsson, Bird, and Chik without whom I never would have discovered my appreciation for research.

Additionally, I want to acknowledge the post-doctoral fellows, Dr's. Jeff Dong, Samira Ghorbani, and Rajiv Jain, as well as everyone else in the Yong lab who were always around for engaging discussion, guidance, collaboration, and generally made every day in the lab enjoyable.

I want to acknowledge the animal technicians and veterinarians for caring for our animals, and to the HBI AMP facility for maintaining the equipment I relied on. I also want to extend my gratitude to Vincent Ebacher, Kelvin Poon, and David Elliot for their consistent technical assistance.

I am so grateful to my parents, Larry and Diane Lozinski, without whom I would not have the privilege of pursuing this doctorate, as well as for their constant support and interest in my work. I want to thank my brother for his support and interest in my work, and for being the standard that I aspire to emulate. I also want to thank my in-laws, John and Sue Choi, and my

brother-in-law, Caden Choi, for their encouragement over the last 5 years. Particularly Sue for her food.

Lastly, I want to thank my wife, Emily Choi-Lozinski, for always supporting me, putting up with the often irregular work hours, and for providing me with the inspiration, motivation, and love that I needed.

Dedication

This is dedicated to my family

c'est dédié à ma famille

це присвячено моїй родині

내 가족에게 바칩니다

Welcome to the family Emelia Lozinski

Table of Contents

List of Figures

List of Symbols, Abbreviations, and Nomenclature

4-HNE: 4-hydroxynonenal (4-HNE).

8-OhDG: 8-Oxo-2′-deoxyguanosine

AAV: Adeno-associated virus

ACN: Acetonitrile

Acsl1: long chain fatty acid CoA ligase 1

ACVR: activin A receptor

ADAM10: a disintegrin and metalloprotease 10

AKT: Protein kinase B

Aldh1A2: Aldehyde Dehydrogenase 1 Family Member A2

Aldh3a2: (aldehyde dehydrogenase

AMPK: AMP activated protein kinase

Ank2: Ankyrin 2

AP-1: Activator protein 1

ApoA4: Apolipoprotein A-4

ApoB: Apolipoprotein B-100

ApoE: Apolipoprotein E

Areg: Amphiregulin

Arg1: Arginase 1

ATP: Adenosine triphosphate

BBB: Blood-brain barrier

BCA: Bicinchoninic acid assay

BDNF: Brain derived neurotrophic factor

Bgn: Biglycan

BMDM: Bone marrow derived macrophage

BMP: Bone morphogenetic proteins

Brk1: BRICK1 Subunit Of SCAR/WAVE Actin Nucleating Complex

BSA: Bovine serum albumin

CC1: Antibody clone against adenomatous polyposis coli (APC)

CCL: (C-C) Motif chemokine Ligand

CCL2: (C-C) Motif chemokine Ligand 2

CCL3/MIP1a: (C-C) Motif chemokine Ligand 3/ Macrophage inflammatory protein-1 alpha

CCL4/MIP1b: (C-C) Motif chemokine Ligand 4/ Macrophage inflammatory protein-1 beta

CCL5/RANTES: (C-C) Motif chemokine Ligand 5/ Regulated upon Activation, Normal T Cell Expressed and Presumably Secreted

CCR: (C-C) Motif chemokine receptor

CCR2: (C-C) Motif chemokine receptor 2

CD4: T-Cell Surface Glycoprotein CD4

CD8: T-Cell Surface Glycoprotein CD8

CD31: Platelet endothelial cell adhesion molecule (PECAM-1)

CD44: CD44 antigen

CD45: lymphocyte common antigen

Cdk17/18: Cyclin dependent kinase 17 or 18

Chmp5: Charged Multivesicular Body Protein 5

CIS: Clinically isolated syndrome

Clic1: Chloride intracellular channel 1

CM: Conditioned medium

CNPase: 2′,3′-Cyclic-nucleotide 3'-phosphodiesterase

CNS: Central nervous system

Col15a1: Collagen Type XV Alpha 1 Chain

Col1a1: Collagen Type I Alpha 1 Chain

Col24a1: Collagen Type XXIV Alpha 1 Chain

Copa: Coatomer submit alpha

CRABP2: Cellular Retinoic Acid Binding Protein 2

CSF: Cerebral spinal fluid

CSPG: Chondroitin sulfate proteoglycan

CSPG4: chondroitin sulfate proteoglycan 4/ Neuron-glial antigen 2 (NG2)

Cst3: Cystatin C

CX3CR1: (C-X3-C) Motif chemokine receptor 1/fractalkine receptor

CXCL1/KC: (C-X-C) Motif chemokine ligand 1/ keratinocytes-derived chemokine

CXCL9: (C-X-C) Motif chemokine ligand 9

CXCL10: (C-X-C) Motif chemokine ligand 10

CXCL12: (C-X-C) Motif chemokine ligand 12

CXCL13: (C-X-C) Motif chemokine ligand 13

DAMP: Damage associated molecular pattern

DAPI: 4′,6-diamidino-2-phenylindole

Dctn4: dynactin subunit 4

DMEM: Dulbecco's modified eagle medium

DMSO: Dimethyl sulfoxide

DNA: Deoxyribonucleic acid

DNase: Deoxyribonuclease

Dnm1: Dynamin 1

dpi: Days post injury/injection

dpl: Days post lesion

Dpt: Dermatopontin

DT: Diphtheria toxin

DTR: Diphtheria toxin receptor

E: embryonic day

EAE: Experimental autoimmune encephalomyelitis

EBV: Epstein-Barr Virus

EC: Eriochrome cyanine

ECM: Extracellular matrix

Ecm1: extracellular matrix protein 1

EDTA: ethylenediaminetetraacetic acid buffer

Ehd1: EH domain- containing protein 1

Eif3b: Eukaryotic Translation Initiation Factor 3 Subunit B

Eif4g1/2: eukaryotic translation initiation factor 4 gamma 1 or 3

Epn1: Epsin-1

Exog: Exo/endonuclease G

FACS: fluorescence-activated cell sorting

FDR: False discovery rate

Fgb: fibrinogen beta chain

FGF: Fibroblast growth factor

FN1: Fibronectin

Fnta: protein farnesyltransferase

FoxO3: Forkhead box O3

FoxP1: Forkhead box protein P1

FXYD5: FXYD Domain Containing Ion Transport Regulator 5

GAG: glycosaminoglycan

Gaparapl2: gamma-aminobutyric acid receptor-associated protein-like 2

Gart: Trifunctional purine biosynthetic protein adenosine-3

G-CSF: Granulocyte colony stimulating factor

GCV: Ganciclovir

GFAP: Glial fibrillary acid protein

GFP: Green fluorescent protein

Ggt7: Gamma-Glutamyltransferase7

Git1: ARF GTPase-activating protein GIT1

GJB1: connexin 32

GlialCAM: Glial cell adhesion molecule

GM: Gray matter

GM-CSF: Granulocyte-macrophage colony-stimulating factor

Gmpda1/2: glucosamine-6-phosphate isomerase 1 or 2

Gnpda1: Glucosamine-6-phosphate isomerase 1

Gpx3: Glutathione peroxidase 3

Gstk1: glutathione S-transferase kappa 1

GWAS: Genome wide association study

H&E: Hematoxylin & Eosin

HBSS: Hanks buffered salt solution

HCAR: Hydrocarboxylic acid receptor

Hccs: cytochrome c-type heme lyase

HCl: Hydrochloric acid

HDAC: Histone deacetylase

HEPES: N-2-hydroxyethylpiperazine-N-2-ethane sulfonic acid

HPLC: High performance liquid chromatography

HSPG: Heparin sulfate proteoglycan

HSV: Herpes simplex virus

IBA1: Ionized calcium binding adaptor molecule 1

IFN: Interferon

IFN-γ: Interferon-gamma/ type II interferon

IGF: Insulin-like growth factor

IGF1: Insulin-like growth factor 1

IL: Interleukin

IL-1α: Interleukin 1 alpha/ hematopoietin 1

IL-1β: Interleukin 1 beta

IL-4: Interleukin 4

IL-5: Interleukin 5

IL-6: Interleukin 6

IL-13: Interleukin 13

IL-17: Interleukin 17

IL-25: Interleukin 25/IL-17E

IL-33: Interleukin 33

iNOS: Inducible nitric oxide synthase

IRF: Interferon regulatory factors

LAR: Leukocyte common antigen-related

LFB: Luxol fast blue

Lgals3: Galectin-3

LINGO1: Leucine rich repeat and Immunoglobin-like domain-containing protein 1

LPC: Lysophosphatidylcholine/

LPS: Lipopolysaccharides

Ly6A: lymphocyte antigen 6 family member A

lysolecithin

m/z: mass-to-charge ratio

M-CSF: Macrophage colony stimulating factor

mAChR: Muscarinic acetylcholine receptor

Mapt: Microtubule associated protein tau

MBP: Myelin basic protein

MDA: Malondialdehyde

MEM: Minimum essential medium

Mgll: monoglyceride lipase

Mgst1: microsomal glutathione S-transferase 1

MHCII: Major Histocompatibility Complex class 2

MOG: Myelin oligodendrocyte glycoprotein

MPO: Myeloperoxidase

MRC1/CD206: Macrophage mannose receptor

MRI: Magnetic resonance imaging

MS: Multiple sclerosis

MS2: fragment ions

MSFC: multiple sclerosis functional composite

mt-Nd3: Mitochondrially Encoded NADH:Ubiquinone Oxidoreductase Core Subunit 3

MyD88: Myeloid differentiation primary response 88

MYRF: Myelin regulatory factor

NAGM: Normal appearing gray matter

NAWM: Normal appearing white matter

Ncald: neurocalcin delta

Ndufb9: NADH dehydrogenase [ubiquinone] 1 beta subcomplex subunit 9

Ndufv3: NADH:Ubiquinone Oxidoreductase Subunit V3

NEAA: Non-essential amino acids

NFH: Neurofilament heavy chain

NFkB: Nuclear factor kappa B

NGFR: Nerve Growth Factor Receptor

NgR: Nogo Receptor

NMDAR: N-methyl-D-aspartate receptor

NRF2: Nuclear factor erythroid 2-related factor 2

O4: Antibody against sulfatide, seminolipid, and cholesterol

OLIG2: Oligodendrocyte transcription factor 2

OPC: Oligodendrocyte progenitor cell

Orm1: Alpha-1-acid glycoprotein-1

Orm2: Alpha-1-acid glycoprotein-2

P: postnatal day

Pacs2: phosphofurin acidic cluster sorting protein 2

PAMP: pathogen associated molecular pattern

PBS: Phosphate buffered saline

PDGF: Platelet derived growth factor

PDGFRα: Platelet derived growth factor receptor α

PDGFRβ: Platelet derived growth factor receptor β

PFA: Paraformaldehyde

Pgam2: phosphoglycerate mutase 2

PGC1a: PPAR gamma coactivator

PGE2: Prostaglandin E2

Pi16: Peptidase inhibitor 16

PKD2: Polycystin 2

PLP: Proteolipid protein

Plxnb3: Plexin B3

pMn: Motor neural progenitor domain

POSTN: Periostin

PPAR: Peroxisome proliferator-activated receptors

PPMS: Primary progressive MS

Prdx2: Peroxiredoxin-1

Prph: peripherin/vimentin

PTPσ: Receptor-type tyrosine-protein phosphatase S

PwMS: People with MS

Rap1gap: Rap1 GTPase-activating protein 1

Rbp1: Retinol Binding Protein 1

ROI: Region of interest

ROS: Reactive oxygen species

Rpm: Revolutions per minute

RPMI: Roswell Park Memorial Institute

RRMS: Relapsing remitting MS

RT: Room temperature

RXR: Retinoid X receptor

S100A6: S100 calcium-binding protein A6

SAMS: Southern Alberta Mass Spectrometry

SCWM: Spinal cord white matter

Serpin1b: leukocyte elastase inhibitor B

Slc25a1: mitochondrial phosphate carrier protein

SNP: Single nucleotide polymorphism

Snx2: sorting nexin-2

Sod1: Superoxide dismutase type 1

SOX: SRY-Box Transcription Factor

SPMS: Secondary progressive MS

Spp1: Osteopontin

Stam: Signal transducing adapter molecule 1

Tbx18: T -box transcription factor 18

TdTom: TdTomato

TFA: trifluoroacetic acid

TGF-β: Transforming growth factor-beta

Th: T helper

TK: Thymidine kinase

TLR: Toll-like receptor

TMEM119: Transmembrane protein 119

TMT: Tandem mass tags

TNF: Tumor necrosis factor

Tsp1: Thrombospondin 1

Vim: Vimentin

WM: White matter

Chapter 1: Introduction

Chapter 1 was written by combining materials from published and unpublished materials and was a joint effort of Brian M. Lozinski, and Dr. Wee Yong. The published work in this chapter is listed below:

Lozinski, B. M., & Yong, V. W. (2022). Exercise and the brain in multiple sclerosis. Multiple sclerosis (Houndmills, Basingstoke, England), 28(8), 1167–1172. This is a pre-copyedited author-produced version of an article published in Multiple Sclerosis Journal. The version of record is available online at https://journals.sagepub.com/doi/10.1177/1352458520969099 and https://doi.org/10.1177/1352458520969099

1.1) Multiple sclerosis (MS)

1.1.1) Overview

Multiple sclerosis (MS) is a neuroinflammatory disease characterized by chronic inflammation and demyelination of the central nervous system (CNS). MS is the most prevalent neurological disabling disease affecting 1 in 400 people or 93,500 Canadians(Reich et al., 2018). Symptoms of MS are sensory, motor, or cognitive in nature and include vision loss, gait imbalance, and impaired processing speeds(Filippi et al., 2018). The criteria to diagnose MS requires evidence of damage disseminated in space and time(Thompson et al., 2018). Dissemination in space can be done through identification of injury in more than one region and dissemination in time by the identification of lesions in two separate regions(Brownlee et al., 2017). These criteria rely on magnetic resonance imaging (MRI), recognition of oligoclonal bands in the cerebrospinal fluid (CSF), or further relapses(Brändle et al., 2016). The first clinical presentation of a disease with characteristics of inflammatory demyelination that has not met these criteria is referred to as clinically isolated syndrome (CIS)(D'Alessandro et al., 2013). When a diagnosis is made, roughly 85% of people with MS (PwMS) are diagnosed with relapsing

remitting MS (RRMS)(Reich et al., 2018). RRMS is characterized by irregular periods of neurological deficits and complete or partial recovery(Filippi et al., 2018). Symptom presentation occurs in conjunction with the region that lesions occur(Filippi et al., 2018). The majority of PwMS with RRMS will transition to a secondary progressive MS (SPMS) stage of disease(Klineova & Lublin, 2018). Conversion to SPMS is associated with continuous and irreversible neurological decline unrelated to relapses(Thompson et al., 2018). Approximately 15% of PwMS are diagnosed from the beginning with primary progressive MS (PPMS)(Filippi et al., 2018). This presentation is similar to SPMS with nearly non-existent relapses and progressive cognitive decline(Kantarci et al., 2016). Diagnosis of MS occurs primarily between 20-35 years of age for RRMS and approximately 40 years of age for PPMS(Thompson et al., 2018). MS prevalence is highest in North America and Europe in northern latitudes, and there is lower risk of MS in Africans, Asians and North American Indigenous peoples(Olsson et al., 2016). Sex is also likely involved in the risk of MS as it is twice as prevalent in females than males though males have a greater association with progression(Filippi et al., 2018; Olsson et al., 2016). Other lifestyle factors contribute to both susceptibility and severity of MS including smoking, vitamin D deficiency, childhood obesity, and adolescent exposure to Epstein-Barr virus (EBV)(Bjornevik et al., 2022; Jagannath et al., 2018; Wesnes et al., 2017). Genetic heritability of MS is roughly 13.5% based on data from monozygotic and dizygotic twin studies(Baranzini et al., 2010; Beecham et al., 2013). Genome wide association studies (GWAS) have identified more than 200 MS associated single nucleotide polymorphisms (SNPs) for risk of developing MS(Baranzini & Oksenberg, 2017; International Multiple Sclerosis Genetics Consortium et al., 2023). Many of these SNPs are found in immune response associated genes such as HLA-DRB1*1501(Baranzini & Oksenberg, 2017). More recently, a gene variant has also been identified for progression of disability in MS(International Multiple Sclerosis Genetics Consortium et al., 2023). The specific cause of MS is not known though interactions between lifestyle, environment, and genetics are likely critical for the conditions required for MS.

1.1.2) Pathology of MS

The pathological hallmark of MS are confluent demyelinating lesions in the CNS gray matter (GM) and white matter (WM)(Lassmann, 2018). Regions that lesions can occur are heterogeneous and will vary from one person to the next, but common sites include the optic nerve, cerebellum, brain stem, spinal cord, deep GM, along the ventricles, and subcortically(Dendrou et al., 2015) (Fig 1.1a). Development of MS is associated with the presence of infiltrating immune cells in the border regions of the meninges, choroid plexus, and perivascular space of postcapillary venules, as well as in the tissue parenchyma(Böttcher et al., 2020; Machado-Santos et al., 2018; Magliozzi et al., 2010). Demyelinating lesions are divided into active, inactive, and remyelinating lesions although chronically active slowly expanding lesions have also been described (Fig 1.1b)(Absinta et al., 2021; Kuhlmann et al., 2017). There can be a significant amount of heterogeneity in the immunopathological appearance of lesions. Active lesions are hypercellular with accumulation of CD8+ T cells and to a lesser extent CD4+ T cells, phagocytes such as monocyte derived macrophages and CNS resident microglia, and B cells(Kutzelnigg & Lassmann, 2014; Popescu et al., 2013). Inactive lesions are characterized by a lack of inflammation, the presence of reactive astrocytes, significant and ongoing axonal loss, few oligodendrocyte progenitor cells (OPCs), and variable amounts of remyelination(Kuhlmann et al., 2017). Remyelinating lesions are highly variable within a lesion, between lesions, and between PwMS(Strijbis et al., 2017). Due to a thinner layer of myelin around remyelinated axons remyelinated lesions are identified by fainter appearance of common histological myelin stains and are referred to as shadow plaques(Prineas & Connell, 1979; Strijbis et al., 2017). Some PwMS undergo significant remyelination, as much as 60%, while others show little evidence of repair(Albert et al., 2007; Patani et al., 2007; Patrikios et al., 2006). Remyelination is associated with higher axonal densities and lower levels of amyloid precursor protein positive damaged axons(Bodini et al., 2016; I. D. Duncan et al., 2009; Mei et al., 2016; Schultz et al., 2017). However, due to the post-mortem nature of the analysis it is unclear if surviving axons are remyelinated or if remyelination protected these axons.

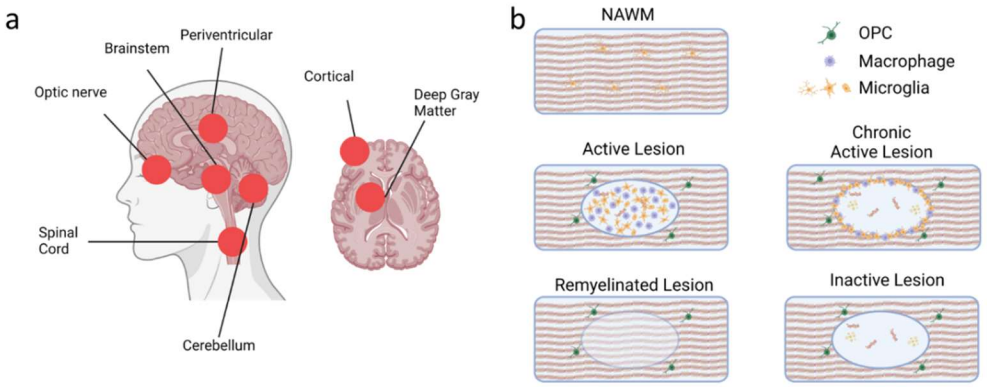

Figure 1.1) Common locations of lesions and types of lesions. a) Demyelination of the optic nerve is associated with visual impairment while cerebellar demyelination is associated with motor deficits(Filippi et al., 2018). Other areas where demyelinating lesions frequently form include the deep gray matter, subcortically, along the ventricles, in the brainstem, and the spinal cord. b) MS lesions are divided into active hypercellular lesions, chronic active lesions with a rim of activity, inactive lesions that are hypocellular, and remyelinated lesions that have thin myelin internodes. Created in BioRender.

The development of lesions can be tracked using the content of microglia/macrophages laden with lipid rich myelin debris and myelin associated proteins(Marschallinger et al., 2020). Early active lesions are identifiable based on microglia/macrophages positive for minor myelin proteins myelin oligodendrocyte glycoprotein (MOG) and 2',3'-Cyclic-nucleotide 3'-phosphodiesterase (CNPase)(Kuhlmann et al., 2017). Conversely, microglia/macrophages in late active lesions are positive only for major myelin proteins myelin basic protein (MBP) and proteolipid protein (PLP)(Kuhlmann et al., 2017). Besides inflammation, active lesions show signs of oligodendrocyte loss, variable OPC recruitment, axonal swelling and transections, and astrocyte reactivity(Ferguson et al., 1997; Masuda et al., 2019; Trapp et al., 1998; Wheeler et al., 2020).

There is also pathology in the normal appearing white matter (NAWM) and gray matter (NAGM)(Allen et al., 2001; Howell et al., 2015; Zrzavy et al., 2017). In the NAWM microglia become activated and cluster in nodules, axons show signs of Wallerian degeneration, and vasculature show signs of blood-brain barrier (BBB) disruption(Allen et al., 2001; Gay & Esiri, 1991; Kermode et al., 1990; Lassmann, 2018; Zrzavy et al., 2017). Unlike immune accumulation in demyelinating lesions microglia nodules do not localize around injured blood vessels or microvasculature(J. van Horssen et al., 2012). There is a greater extent of NAWM pathology in progressive MS indicative of diffuse white matter injury during progressive MS(Kutzelnigg et al., 2005).

1.1.3) Immune abnormalities in MS

The impact of the immune system on MS pathology has been shown through pre-clinical, post-mortem, biomarker, and imaging studies(Absinta et al., 2021; Ghorbani et al., 2022; Howell et al., 2015; Thouvenot et al., 2019). Auto-reactive lymphocytes escape immune tolerance in the periphery and traffic to the CNS(Dong & Yong, 2019). It is unclear what causes this escape from tolerance but lymphocytes recognizing self-antigens including MOG, MBP, PLP, and glial cell adhesion molecule (GlialCAM) have been identified(Brändle et al., 2016; Goverman, 2011; Krogsgaard et al., 2000; Lanz et al., 2022). Infiltration of the CNS by peripheral immune cells

occurs at three major border regions: the blood-meningeal barrier in the leptomeninges, the blood-CSF barrier in the choroid plexus, and the BBB at the cerebral vasculature(Engelhardt et al., 2017). Entrance into the CNS by clonally expanded activated lymphocytes requires recognition of surface ligands by homing receptors such as integrin α4β1/very late antigen-4 and intercellular adhesion molecule-1 (Bö et al., 1996; Dong & Yong, 2019; Kivisäkk et al., 2003; Scalabrini et al., 2005; Steffen et al., 1996). Immune cell infiltration of the CNS first requires them to enter across the endothelial barrier into the perivascular space which becomes swollen with immune cells forming a perivascular cuff(Stephenson et al., 2018). Crossing from here into the tissue parenchyma requires further degeneration of the glial limitans through protease secretion(Agrawal et al., 2006).

1.1.4) Models of MS

Since MS is a disease specific to humans and does not occur naturally in animals there are no direct models available. Therefore, several models have been developed to imitate specific aspects of MS pathology. Animal models achieve demyelination similar to that seen in MS by autoimmune inflammation, viral infection, and toxin-based models(Ghorbani et al., 2022; Lozinski et al., 2021; Murray et al., 2001). Experimental autoimmune encephalomyelitis (EAE) is the most common model used and produces demyelination through inoculation of animals with a CNS specific peptide such as myelin oligodendrocyte glycoprotein peptides 35-to-55 (MOG_{35-55}) or proteolipid protein peptides 139-to-151 ($PLP_{139-151}$) to generate chronic or relapsing remitting disease course, respectively(Ghorbani et al., 2022; Krasemann et al., 2017). Characterized by ascending paralysis, EAE is a beneficial model for studying the inflammatory aspects of MS and has contributed to our understanding of autoimmunity, neuroinflammation, cytokine biology and immunogenetics(Ajami et al., 2011; Christy et al., 2013; Ghorbani et al., 2022; Giles et al., 2018; Haimon et al., 2022; Mundt et al., 2019; Ransohoff, 2012; Sun et al., 2022). The major limitations of EAE are that it does not model progression, it is a poor model to study remyelination, it primarily affects the spinal cord, and it does not adequately model the CD8+ cell and B cell

contributions to MS(R. W. Jain & Yong, 2021; Magliozzi et al., 2010; Ransohoff, 2012; Rojas et al., 2019).

Viral induced demyelination occurs following the resolution of encephalitis caused by Theiler's murine encephalomyelitis virus and mouse hepatitis virus(Murray et al., 2001; Ransohoff, 2012). Though these models have been beneficial in understanding the clearance of viruses from the CNS they are less commonly used as they do not model the persistent viral infection seen in MS(Lassmann & Bradl, 2017).

Toxin induced demyelination is achieved through oral administration of the copper chelator cuprizone and stereotaxic injection of lysophosphatidylcholine (LPC), oxidized phosphatidylcholine(Dong et al., 2021) or ethidium bromide(Blakemore et al., 1977; Keough et al., 2015; Triarhou & Herndon, 1986). Oral administration of cuprizone for several weeks causes demyelination primarily of the corpus callosum and hippocampus although demyelination also occurs in the cortex and deep gray matter(Zirngibl et al., 2022). Withdrawal of cuprizone from the chow results in extensive and rapid remyelination of the corpus callosum(Zirngibl et al., 2022). Cuprizone is a useful model for the study of remyelination and mimics the GM and WM pathologies seen in MS. However, opposite to what is seen in MS, WM tracts in cuprizone remyelinate more efficiently than GM(Ransohoff, 2012). Furthermore, while MS lesions seen in progressive MS and cuprizone lesions both are sparsely populated with T cells the former do not contain complement while cuprizone lesions do. Despite these shortcomings cuprizone provides a good model of the processes of de- and remyelination.

Finally, injection of LPC, and formerly ethidium bromide, into the CNS white matter provides the ability to study de- and remyelination by induction of focal demyelinated lesions(Keough et al., 2015). The LPC model has allowed for the study of de- and remyelination with spatiotemporal predictability(Keough et al., 2015; Ransohoff, 2012). Immediately after LPC there is the accumulation of myelin debris, axonal swelling and injury, cell death, and the formation of an astroglial scar that persists throughout the course of injury(Plemel, Michaels, et al., 2017). Soon after, microglia and then monocyte derived macrophages enter the lesion after

which microglia become the predominant myeloid population(Plemel et al., 2020). Phagocytes such as microglia/macrophages are critical to the removal of myelin and cellular debris from the lesion(Rawji et al., 2020). There has been some indication of lymphocytes such as T cells in LPC lesions during the immediate days following injury though they are transient and not believed to play a significant part in the pathology(Ousman & David, 2000). However, most studies do not follow the lesion to chronic stages and so may miss later contribution of T cells. After 3 days there is accumulation of OPCs at the rim of the LPC lesion which enter the lesion around 7 days and mature into myelinating oligodendrocytes from 14 to 21 days post induction(Keough et al., 2015; Ruckh et al., 2012). As many as 30% of axons are lost within the LPC lesion and the remaining axons are fully remyelinated within 28 days(Ruckh et al., 2012). While LPC is a useful model it lacks the ongoing immune activity present in MS, and due to a lack of specificity for oligodendrocytes and myelin causes non-specific cell death(Plemel, Michaels, et al., 2017).

1.2) Oligodendrocytes and remyelination

1.2.1) Developmental myelinogenesis

The myelination of the CNS occurs in several stages: proliferation and migration of OPCs, recognition of axons, differentiation into oligodendrocytes, wrapping of the axon, and compaction of the myelin sheath(Charles et al., 2000; Emery et al., 2009; Herbert et al., 2017; Nawaz et al., 2015; Snaidero et al., 2014, 2017; Windrem et al., 2004; Zuchero et al., 2015). Oligodendrocytes are derived from three waves of OPC development(J. Cai et al., 2005; Orentas et al., 1999; Vallstedt et al., 2005). The first arise from the ventral ventricular zone of the forebrain and the motor neural progenitor (pMN) domain in the spinal cord during development around embryonic day 12.5 (E12.5) in mice, or roughly gestational week 6.5 in humans(Bergles & Richardson, 2016). The second wave of development comes from radial glial cells in the dorsal spinal cord and the ventricular zone in the forebrain at around E15.5(Goldman & Kuypers, 2015). The third wave of OPC development consists of local proliferation in the developing cortex and spinal cord at postnatal day 0 (P0)(Goldman & Kuypers, 2015). Migrating throughout the CNS, OPCs tile the parenchyma by migrating along the developing vasculature, responding to

guidance cues including semaphorins and netrin, and through contact inhibition with other OPCs(Hughes et al., 2013; Tsai et al., 2016).

Maturation of OPCs into myelinating oligodendrocytes begins before birth and continues for several decades in humans(Yeung et al., 2014). OPCs first become pre-myelinating oligodendrocytes, extending processes out that contact axons(Fancy et al., 2009; Stadelmann et al., 2019). OPCs choose which axons to myelinate based on several factors including axon diameter, cell surface proteins that positively regulate myelination such as N-cadherin and neuregulin I/III, and negative regulators like LINGO-1 and PSA-NCAM(Almeida, 2018; Charles et al., 2000; Demerens et al., 1996; Gibson et al., 2014; Mi et al., 2005). Maturation of OPCs through the pre-myelinating stage to myelinating oligodendrocytes is regulated by the transcription factor myelin regulatory factor (MYRF) which is maintained by transcription factors Olig2 and Sox10(Emery et al., 2009). Downstream genes of MYRF including PLP and MBP are required for proper myelin formation and compaction(Emery et al., 2009). The process of wrapping the axon in concentric sheets of lipid membrane is driven by actin polymerization at the leading edge and occurs like a croissant expanding out from the centre(Nawaz et al., 2015). Finally, compaction of the myelin sheath occurs once the membrane components such as CNPase, MBP, and contactin-associated protein (CASPr) needed for adequate function are trafficked to the appropriate positions(G. J. Duncan et al., 2021). The compaction of the myelin into tight layers is driven by the formation of a polymeric network of MBP that pushes the cytoplasm from the myelin sheath into the edges of the sheath and forming the major dense and interperiod lines(Snaidero et al., 2017). The length of myelin that covers the axon is divided into sections: starting adjacent to the node of Ranvier is the paranode, followed by the juxtaparanode, and finally the internode(Stadelmann et al., 2019). At the paranode, myelin tethers to the axon by an adhesion complex of contactin, CASPr, and neurofascin(Stadelmann et al., 2019). Further anchoring is found in the juxtaparanode between complexes of contactin and CASPr, and in the internode between myelin adjacent protein and gangliosides(Stadelmann et al., 2019). These divisions are important to maintaining saltatory conduction of the axon by separating voltage gated sodium and potassium channels in the node of Ranvier and paranode

respectively(Freeman et al., 2015; Kaplan et al., 1997, 2001; Susuki et al., 2013). Each layer of myelin is connected via gap-junctional proteins and cytosolic channels maintained by CNPase(Lappe-Siefke et al., 2003; Snaidero et al., 2017). Importantly, covering of the axon by myelin isolates the axon from nutrients found in the extracellular environment(Micu et al., 2017). Therefore, the oligodendrocyte must provide metabolic trophic support to the axon. The cytoplasmic channels and gap junctions linking myelin layers are critical for transmission of trophic factors to the inner membrane of the myelin sheath for export into the periaxonal space(Snaidero et al., 2017).

Myelination is influenced by other CNS resident cells such as astrocytes and microglia. Oligodendrocytes are connected to astrocytes through gap-junctions allowing them to meet the metabolic demands of myelinating up to 50 separate axons(Chong et al., 2012; Kettenmann & Ranson, 1988; Philippot et al., 2021; Waxman et al., 1990). Astrocytes are in turn connected to the vasculature by their endfeet providing nutrients to the oligodendrocytes through this pan glial syncytium(Díaz-Castro et al., 2023; G. R. J. Gordon et al., 2008). Myelin does not remain static throughout life but dynamically changes its length, extending and retracting in response to neuronal activity such as occurs when learning new skills(Gibson et al., 2014; Hughes et al., 2018; Jensen & Yong, 2016). Microglia are critical to the maintenance and plasticity of myelin sheaths in adult mice indicated by hypermyelination occurring in microglia deficient mice that precedes the loss of myelin integrity and demyelination (McNamara et al 2023). Oligodendrocyte stability varies between white matter tracts of mice from 90% survival over 2 years in the corpus callosum to 60% in the spinal cord(R. B. Tripathi et al., 2017). Surprisingly, oligodendrocytes are believed to be more stable in humans with a turnover rate of just 0.32% per year(Yeung et al., 2014). The process of myelination continues in humans into our thirties after which white matter volumes begin to decline(Bethlehem et al., 2022).

1.2.2) Remyelination

Remyelination occurs spontaneously following demyelination of the brain and spinal cord(Franklin & Simons, 2022). Like developmental myelination, remyelination is the result of

OPC migration, proliferation, and differentiation (Fig 1.2a)(Boyd et al., 2013; Fancy et al., 2009; Levine & Reynolds, 1999). Remyelination in both humans and mice is associated with greater neuroprotection and axonal survival(Kornek et al., 2000; Mei et al., 2016; Schultz et al., 2017). Re-establishment of the myelin sheath restores saltatory conduction, metabolic support, and provides mechanical protection from injury (Fig 1.2b)(Coman et al., 2006; Irvine & Blakemore, 2008; Jeffery & Blakemore, 1997; Lappe-Siefke et al., 2003; Micu et al., 2017; K. J. Smith et al., 1979, 1981). Ultrastructurally, remyelinated myelin consists of a paranode, juxtaparanode, and internode as well as major dense and interperiod lines consistent with compact myelin(Coman et al., 2006; Sasaki et al., 2006). The major difference between developmental and remyelinated myelin is a thinner myelin sheath following remyelination(I. D. Duncan et al., 2017).

Remyelination has been described extensively in experimental models though it is less well characterized in humans. Post-mortem studies of MS samples suggest that remyelination occurs to varying degrees between both lesions and individuals(Patani et al., 2007; Patrikios et al., 2006; Strijbis et al., 2017). Remyelination is more commonly seen in perivascular, deep white matter, and cortical lesions and is more extensive in the gray matter than the white matter suggesting a role of anatomical location in remyelination efficiency(Albert et al., 2007; Goldschmidt et al., 2009; Merkler et al., 2005). In vivo imaging studies using positron emission tomography and myelin specific probes indicate an inverse correlation of remyelination with clinical disability(Bodini et al., 2016). However, it is unclear if this is due to a protective effect of remyelination or a lack of activity allowing remyelination to occur. Indeed, remyelination negatively correlates with disease activity(Bramow et al., 2010; Patrikios et al., 2006). Unfortunately, remyelination often fails to occur sufficiently for functional benefits(Boyd et al., 2013).

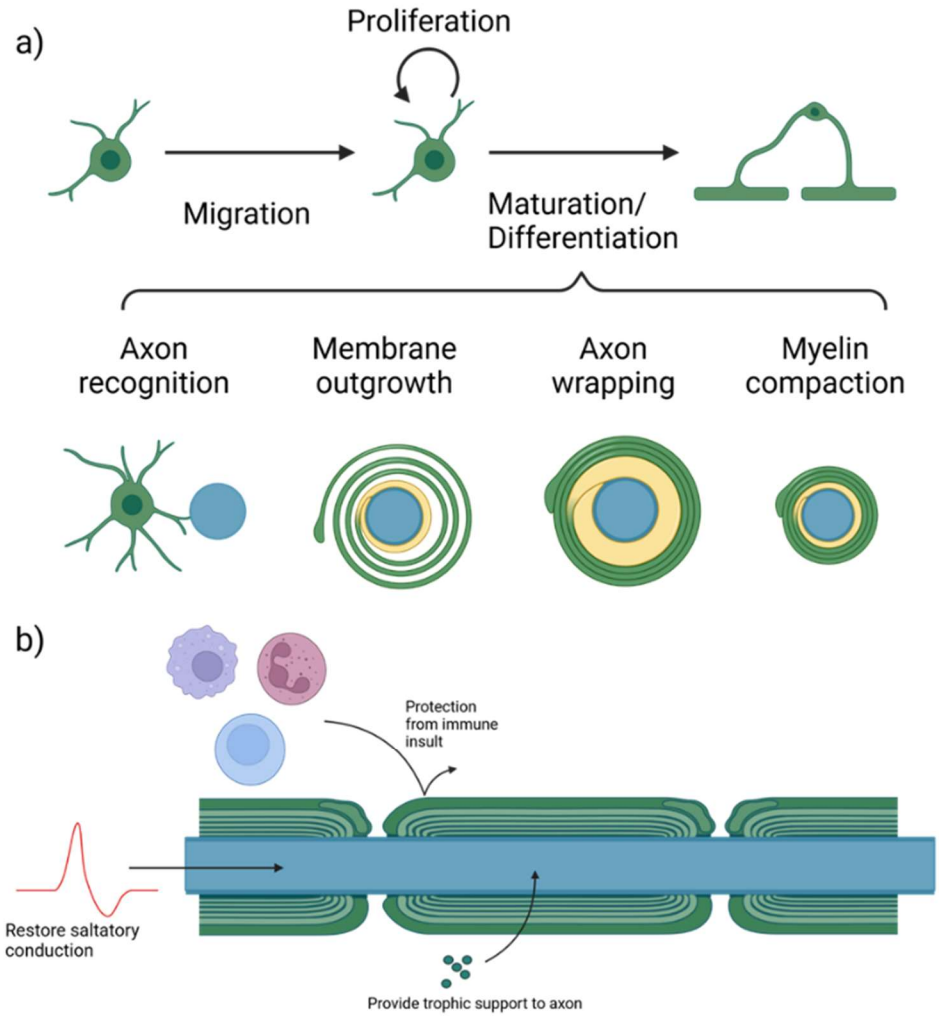

Figure 1.2) Process and benefits of remyelination. a) Developmental myelination and remyelination result from the migration, proliferation, and differentiation of oligodendrocyte progenitor cells (OPCs). Differentiation of OPCs into myelinating oligodendrocytes occurs over several stages: OPCs target and contact an axon, membrane trafficking outgrowth, lateral and radially wrapping of the axon, and finally compaction of the myelin sheath. b) myelination and remyelination provide benefits for the underlying axons that include maintenance of saltatory conduction by clustering of voltage gated channels around the nodes of Ranvier, providing trophic support including lactate to the otherwise isolated axon, and providing physical protection from immune mediated injury. Made in BioRender.

1.2.3) Remyelination failure

Remyelination fails due to an imbalance in permissive and inhibitory signals together with the ability of OPCs to respond to them (Fig 1.3). These signals affect OPC proliferation, migration, and differentiation. One hypothesis asserts that a bottleneck during OPC differentiation is the primary cause of remyelination failure. Histological analyses of MS lesions indicates that they possess OPCs in comparable numbers across lesion types and pre-myelinating oligodendrocytes that lack compact myelin(Chang et al., 2000, 2002; Kuhlmann et al., 2008; Lucchinetti et al., 1999; Maeda et al., 2001; Scolding et al., 1998; Wolswijk, 1998; Yeung et al., 2019). It can be inferred from these studies that OPCs are able to enter lesions but fail to mature into myelinating oligodendrocytes. This hypothesis was tested in a model of experimental demyelination in which the OPC proliferative signal platelet derived growth factor (PDGF)-AA was over expressed leading to increased OPC numbers but not remyelination(Woodruff et al., 2004). Critically, PDGFAA promotes OPC proliferation but also impairs differentiation and could explain the lack of observed remyelination(Frost et al., 2003; Wolswijk & Noble, 1992). As well, post-mortem studies represent snapshots in time and do not contain the resolution to represent all possible context within lesions. An alternative possibility is that OPCs are present in insufficient numbers for extensive remyelination. Other studies have indicated that there are reduced OPC numbers in MS lesions and significant accumulation of macromolecules that impede OPC migration(Boyd et al., 2013; D. M. Chari et al., 2003). It is likely that deregulation affects many aspects of the OPC response including intrinsic and extrinsic factors (Fig 1.3). As such, there is evidence that suggests that impaired remyelination may depend on the stage of lesion formation (Hess et al 2020). Hess et al identified a subset of active lesions that lacked myelin sheaths despite mature oligodendrocytes being present, and significant loss of oligodendrocytes in mixed/inactive lesions due to the hostile environment within these lesions. Two important regulators of remyelination efficiency are age-related attenuation and the accumulation of extracellular matrix (ECM) molecules(Ghorbani et al., 2022; Neumann et al., 2019; S. Shen et al., 2008; Stephenson et al., 2018).

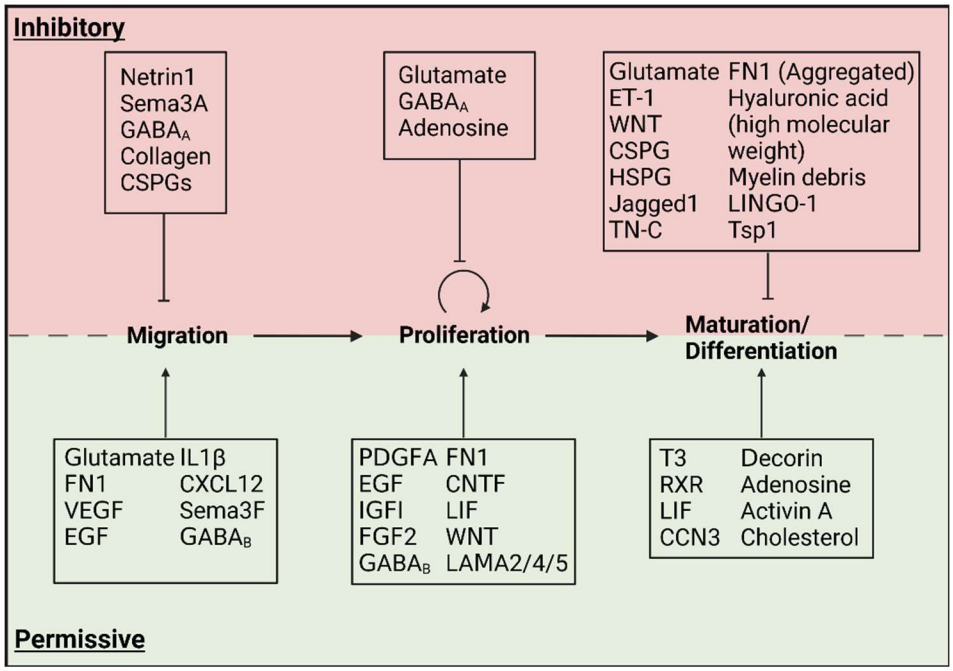

Figure 1.3) Permissive and inhibitory regulators of OPC function. OPC development and remyelination are regulated by many positive and negative factors. Regulators can be divided into membrane bound proteins (e.g. LINGO1), intracellular proteins (e.g. RXR), extracellular proteins (e.g. Wnt), Semaophorins (e.g. Sema3A), growth factors (e.g. PDGFA), cytokines (e.g. IL1β), chemokines (e.g. CXCL12), and ECM components (e.g. CSPGs). Many factors promote one stage of response while inhibiting another. For example, PDGFA inhibits OPC differentiation by promoting proliferation. Other factors can be permissive or inhibitory depending on the receptors they act on. For instance, γ-aminobutyric acid (GABA) signaling through $GABA_A$ receptors inhibits OPC migration and proliferation while GABA signaling through $GABA_B$ receptors promotes OPC migration and proliferation. Made in BioRender

1.2.4) Aging

Aging is the accumulation of cellular dysfunctions that lead to decline in physical and cognitive functions(López-Otín et al., 2023). Though aging is not associated with an elevated incidence of MS it has been linked to progression(Koch et al., 2007). Importantly, many PwMS live long lives and age-related changes at the cellular and organ level are important considerations for pathology and treatment(McGinley et al., 2021). Age-related cellular dysfunction includes certain hallmarks such as chronic inflammation, stem cell exhaustion, and a decline in tissue regeneration(Eming et al., 2014; López-Otín et al., 2023). While there have been studies of an age-related effect on remyelination in human samples, much of our understanding of age and remyelination comes from animal models(Goldschmidt et al., 2009; Patani et al., 2007; Patrikios et al., 2006). From these studies the accumulation of cellular dysfunction with age clearly delays the remyelination process(Shields et al., 1999). Delaying OPC response can result in them missing the defined window in which they can extend processes to enwrap axons(Czopka et al., 2013). This loss of myelin sheath results in axon pathology that has been described in MS lesions such as retraction bulbs and swellings and contributes to disability(Gritsch et al., 2014; Locatelli et al., 2012; Oluich et al., 2012; Pohl et al., 2011; Trapp et al., 1998).

Age-related remyelination impairment is multifactorial and affects intrinsic and extrinsic factors. Accumulation of intrinsic factors in OPCs reduces their ability to respond to chemical and mechanical environmental signals (Fig 1.4). In OPCs histone deacetylases (HDACs) are important to promote the expression of pro-differentiation transcription factors through the inhibition of differentiation inhibitors Hes5 and Id2(S. Shen et al., 2008). In aged OPCs HDAC recruitment to the promoters of these inhibitors are impaired leading to elevated levels of the differentiation inhibitors. As well, due to accumulation of DNA damage and reduced mitochondrial function aged OPCs have impaired capacity to respond to soluble signals in the environment including growth signals that promote differentiation(Neumann et al., 2019). Additional deficits in aged OPCs include a reduced ability to respond to neuronal activity that results from reduced levels of N-methyl-D-aspartate receptors (NMDAR)(S. O. Spitzer et al., 2019). Interestingly,

OPCs are also affected with age by mechanical signals from the environment. The aged CNS becomes increasingly rigid due to the accumulation of ECM and impairs OPC proliferation and differentiation due to the mechanosensitive ion channel Piezo1 expressed on OPCs(Segel et al., 2019). The ECM that accumulates in the aged CNS includes inhibitory ECM such as chondroitin sulfate proteoglycans (CSPGs), hyaluronan, collagen, and fibronectin(Ghorbani et al., 2022; Jong et al., 2019; Mohan et al., 2010; Sobel, 2001; Sobel & Mitchell, 1989; J. van Horssen et al., 2006). Aside from inhibitory ECM, MS lesions accumulate other macromolecules such as oxidized lipids and myelin debris remnants(Dong et al., 2021; Kuhlmann et al., 2017). Myelin debris remnants that accumulate in MS lesions impair OPC differentiation(Plemel et al., 2013). Under normal conditions phagocytes like microglia and macrophages remove and process myelin and cellular debris(D. Chari et al., 2006; Dong et al., 2021; Kotter et al., 2005). With age, the phagocytic and processing capacity of these immune cells is impaired leading to formation of cholesterol crystals within cells and accumulation of inflammatory foamy macrophages(Bosch-Queralt et al., 2018; Rawji et al., 2020). Though ECM is known to be inhibitory to OPC function there is little known about how it is affected by age.

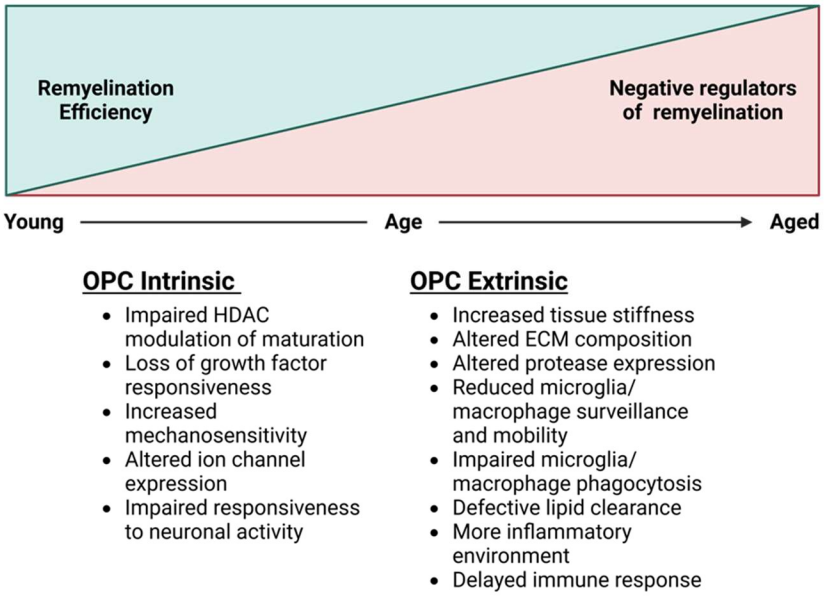

Figure 1.4) Intrinsic and extrinsic age-associated dysfunctions regulating OPC function. Age impacts OPC responses intrinsically by reduced epigenetic regulation, growth factor sensitivity, neuronal response, and increased sensitivity to environmental stiffness. These contribute to impairing OPC migration, proliferation, and differentiation. Extracellular factors also contribute to age associated OPC impairment. Increasing tissue stiffness, altered extracellular matrix (ECM) composition, accumulation of debris, and a more inflammatory environment all contribute to impair OPC responses. Made in BioRender

1.2.5) Extracellular Matrix (ECM)

The ECM is an organized macromolecular substrate that provides physical support for tissue integrity and maintenance of tissue homeostasis(Bonnans et al., 2014). It acts as a ligand for cell surface receptors to regulate cellular functions including proliferation, migration, and differentiation(Bonnans et al., 2014; Petersen et al., 2017; Sellers et al., 2009; Stoffels et al., 2014). In the healthy CNS the ECM in the parenchyma consists primarily of hyaluronan, tenascins, and CSPGs(Ghorbani & Yong, 2021; Sorokin, 2010). The basement membrane of the vasculature is composed of a cross-linked network of collagen VII, collagen IV, and laminins(Ghorbani & Yong, 2021; J. V. Horssen et al., 2005; S. Wang et al., 2006). The functional role of the ECM is to provide structural support for cells, transmit information mechanically, bind and sequester growth factors, and regulate inflammation(Massagué, 2012; Sorokin, 2010). These functions are contextual and can be altered if proteolytically cleaved or damaged following injury. Following tissue damage ECM is deposited as a part of the ongoing tissue remodeling to restore the tissue to a similar state as prior to the injury(Eming et al., 2014; Ito et al., 2007; Lorenz et al., 1993; Talbott et al., 2022). In this scenario the ECM in the parenchyma may vary from de novo ECM in content or abundance. MS lesions contain greater amounts of ECM compared to uninjured or NAWM(Mohan et al., 2010; Sobel, 2001; J. van Horssen et al., 2006). As well, ECM is found in greater amounts in inactive lesions compared to active suggesting ongoing tissue remodeling and wound healing(Mohan et al., 2010). In MS lesions the ECM also has spatial variability with CSPGs and hyaluronan aggregated at the lesion edge while heparin sulfate proteoglycans (HSPGs), biglycan, decorin, fibronectin, collagens, laminins, and thrombospondin are distributed throughout the lesion centre(Ghorbani & Yong, 2021; Van Horssen et al., 2007).

OPC responses are regulated by ECM interactions both directly through receptor binding and indirectly through modulation of immune and other CNS cells(Andreuzzi et al., 2022; Ghorbani et al., 2022; Stoffels et al., 2014; Suzuki et al., 2019; R. B. Tripathi et al., 2017). Direct interactions of ECM with OPCs occurs through ECM ligands binding to cell surface receptors on OPCs(Ghorbani & Yong, 2021; Pu et al., 2018). OPCs express several ECM receptors including

integrin-αvβ1, integrin-α6β1, integrin-αvβ3, CD44, toll like receptor 2 (TLR2), TLR4, activin A receptor 1 (ACVR1), leukocyte common antigen (LAR), protein tyrosine phosphatase (PTPσ), and Nogo receptor (NgR)(Ghorbani & Yong, 2021; Harlow et al., 2015; J.-Y. Huang et al., 2012; Miron et al., 2013; Srivastava et al., n.d.). By expressing a wide array of receptors OPCs recognize many ECM components and respond to environmental changes and injury. The effect of OPC-ECM interactions is dependent on the structural and biochemical properties of the ECM components, some of which will be discussed below.

Fibronectin is a glycoprotein that forms dimers and acts as a scaffold for cell adhesion and migration(Pu et al., 2018; Sobel & Mitchell, 1989) (Pu 2018). The aggregated and fibrillar forms of fibronectin lead it to have inhibitory and permissive effects on OPC responses(Buttery, 1999; Milner et al., 1996; Qin et al., 2017; Stoffels et al., 2014; A. Tripathi et al., 2017; Werkman et al., 2020). Unaggregated fibrillar fibronectin binds to OPC αvβ3 and αvβ6 integrins promoting their migration and proliferation(Milner et al., 1996). Conversely, aggregated fibronectin, which accumulates in MS lesions, impairs OPC differentiation and acts as a scaffold for other inhibitory ECM such as thrombospondin 1 (Tsp1)(Ghorbani & Yong, 2021; Sikkema et al., 2018).

Hyaluronan is the most abundant ECM component in the healthy CNS and is found as a high molecular weight polymer in MS lesions(Back et al., 2005). Structurally, hyaluronan is composed of unsulfated polymers of glycosaminoglycan (GAG) chains(Pu et al., 2018). High molecular weight hyaluronan is produced during inflammation by astrocytes and interacts with other ECM such as the CSPG versican forming a scaffold for cell adhesion(Seyfried et al., 2005). OPCs binding of high molecular weight hyaluronan polymers through TLR4 inhibits expression of pro-differentiation genes by inactivating protein kinase B (AKT)/forkhead box O3 (FoxO3) signaling(Srivastava et al., n.d., 2020). During injury hyaluronan is cleaved into fragments that bind TLR2 on OPCs and signal through myeloid differentiation primary response 88 (MyD88) impairing their differentiation and remyelination(Sloane et al., 2010).

CSPGs are sulfated proteoglycans covalently linked to one or more sulfated GAG chains(Stephenson et al., 2018). The family of CSPGs is composed of aggrecan, versican,

brevican, neurocan, phosphacan, and neuron-glial antigen 2(Pu et al., 2018). In the healthy CNS they contribute to the tissue substrate by forming aggregates with tenascins and hyaluronan(Pu et al., 2018; Sorokin, 2010; Wu et al., 2005). The function of CSPGs will vary based on differences in the core protein and GAG side chains(Pu et al., 2018). They have been implicated as inhibitors of CNS regeneration due to their abundance in spinal cord injuries and repulsive effects on axon regrowth(Sofroniew, 2018). OPCs interact with CSPGs through LAR, PTPσ, and NgR1/3(Dickendesher et al., 2012; Fisher et al., 2011; Y. Shen et al., 2009). As such, CSPGs impair OPC differentiation and process outgrowth contributing to remyelination failure(Lau et al., 2012; Pendleton et al., 2013). Indirectly, versican and aggrecan can bind to microglia/macrophage TLR2/6 causing MyD88/Nuclear factor kappa B (NFkB) signaling and expression of inflammatory mediators like tumor necrosis factor (TNF)-α, interleukin (IL)-6, and reactive oxygen species(Kang et al., 2017; S. Kim et al., 2009; Stephenson et al., 2018). As well, versican promotes polarization of T cells to cytotoxic T helper (Th)1 and Th17 phenotypes(Ghorbani et al., 2022). Interferon (IFN)-γ and IL-17 produced by Th1 and Th17 cells impair OPC differentiation and cause apoptosis(Ghorbani et al., 2022; Moore et al., 2015; Psenicka et al., 2021).

Collagen is a triple helix of three polypeptide α-chains of varying lengths that form homo and hetero trimers(Shoulders & Raines, 2009). There are 28 identified collagens with several collagens found in the glial limitans and basement membrane(Sorokin, 2010). As essential structural components of the basement membrane collagen VII, collagen IV and laminins form cross-linked structures that provide tensile strength to the tissue and support for cellular anchoring(Mouw et al., 2014). Not normally present in the CNS parenchyma, collagen is found to be elevated in demyelinating MS lesions(Mohan et al., 2010; J. van Horssen et al., 2006). The role of collagen in MS lesions is not well defined. However, OPCs growth on collagen substrates have impaired differentiation(Soderblom et al., 2013). As well collagen impairs the expression of CCL2 by microglia/macrophages important for further immune recruitment(Kotter et al., 2005; Mohan et al., 2010).

HSPGs are structurally similar to CSPGs differing in the polysaccharides that make up their GAG side chains(Kjellén & Lindahl, 1991, 2018). Members of the HSPG family include glypican, syndecan, perlecan, agrin, collagen XVIII, CD44, neuropilin-1, betaglycan, and serglycin(Pu et al., 2018). HSPGs bind growth factors including fibroblast growth factor-2 (FGF2) and PDGF(Bonnans et al., 2014; Kjellén & Lindahl, 1991). Both FGF2 and PDGF promote OPC migration, and proliferation while impairing their differentiation(Armstrong et al., 2002; Bansal et al., 2003; McKinnon et al., 1990, 1993; Winkler et al., 2002).

Laminins are fibrous glycoproteins that bind to many ECM including collagen IV, HSPGs, nidogen, and dystroglycan(Leiton et al., 2015). As with most ECM, laminins are important for structural support. As well, laminin α2 promotes OPC survival and differentiation while laminin α4 and α5 bind to α6β1-integrin and positively regulate OPC migration and survival(De La Fuente et al., 2017; Relucio et al., 2012).

1.2.6 Promoting Remyelination

Seeking to improve remyelination efficiency is a growing area of interest. Remyelination has many benefits for PwMS and is the most extensive form of regeneration in the CNS(Franklin & Simons, 2022). Strategies to promote remyelination seek to improve OPC function and/or overcome inhibitors in the lesion environment(Plemel, Liu, et al., 2017). OPC function can be improved both pharmacologically and holistically. Targeting inhibitors of remyelination such as leucine rich repeat and immunoglobin-like domain-containing protein 1 (LINGO1) have also shown promising results to promote remyelination(Jepson et al., 2012). Genetic deletion and monoclonal antibodies targeting LINGO1 resulted in reduced EAE scores, increased remyelination, and axon survival(Mi et al., 2005). Clinical trials of anti-LINGO1 monoclonal antibodies marketed under the name Opicinumab have indicated it is well tolerated and moderately improved conduction latency of visually evoked potential(Tran et al., 2014).

Therapeutically improving cellular functions targeting intrinsic dysfunction has also been done. Pharmacological antagonism of the muscarinic acetylcholine receptors (mAChR) on OPCs

with Benzatropine, Quetiapine, or Clemastine was shown to improve OPC differentiation in vitro and in vivo, promote remyelination, and increase axon density(Green et al., 2017; Mei et al., 2014, 2016). Additionally, retinoid x receptor (RXR) γ and α were implicated in defective OPC and microglia/macrophage functions respectively(J. K. Huang et al., 2011; Natrajan et al., 2015). In separate studies, treatment with 9-cis retinoic acid reversed age-associated declines in OPC differentiation and myelination, and microglia/macrophage phagocytosis. However, in a phase 2a trial an RXR agonist, bexarotene, was not well tolerated and its use was recommended against(Brown et al., 2021). This highlighted the need for well tolerated therapeutics. One such candidate was Vitamin B3, also known as niacin, which had been shown to improve remyelination outcomes in experimental demyelination(Rawji et al., 2020). Niacin binds hydroxycaroboxylic acid receptor 2 on microglia/macrophages reversing the effects of age and increasing phagocytosis leading to greater amounts of remyelination(Rawji et al., 2020). Niacin is also converted into nicotinamide adenine dinucleotide (NAD), a critical coenzyme for redox reactions involved in metabolism as well as a cofactor in non-redox NAD-dependent enzyme functions(Covarrubias et al., 2021). By being converted to NAD+ niacin can affect many aspects of age such as cell senescence, DNA repair, and immune aging(Covarrubias et al., 2021). Indeed, microglia are interesting candidates to target for the promotion of remyelination as they can produce permissive factors such as IGF1 and play an important role in maintaining myelin health (McNamara et al 2023, Bellver-Landete et al 2019). The antidiabetic drug metformin has also shown positive results in restoring age related OPC dysfunction and increasing remyelination(Neumann et al., 2019). Metformin restores OPC function in an AMP dependent kinase (AMPK) dependent manner. AMPK has been shown to also be modulated by calorie restriction and exercise. The benefits of exercise for remyelination and PwMS generally will now be discussed.

1.2.7) Exercise

Exercise was previously thought to be harmful to PwMS due to overheating and the potential to exacerbate symptoms(van Praag, 2009). Exercise has now been shown to confer a range of benefits for PwMS including improvements to fatigue, quality of life, cognition, and

depression, as well as mobility and balance (Fig 1.5)(Motl et al., 2017). However, there are many challenges for PwMS when engaging in regular exercise including heat insensitivity, fatigue, and decreased mobility leading to PwMS exercising less than the average population(Klaren et al., 2013). Recently, opinions have shifted to the point that exercise is proposed to treat symptoms and even prevent or delay MS in those at risk(Dalgas et al., 2019). This shift is due to a growing body of literature showing exercise to be both safe and beneficial to PwMS(Learmonth et al., 2021).

Analysis of the EnvIMS database of 1904 cases and 3694 controls in three European countries found that self-reported vigorous (increased respiratory rate and perspiring) but not light (no increase in respiratory rate or perspiration) exercise was inversely associated with the risk of developing MS(Wesnes et al., 2017). Recent clinical trials also found exercise to improve cognition and mobility and noted that those with poor fitness level at baseline may benefit more(Sandroff et al., 2019). Also, a 6-month randomized controlled trial of internet delivered behavioral modification successfully increased physical activity in PwMS, and improved fatigue and mental health (depression and anxiety)(Pilutti et al., 2014). In a longitudinal study of youth with pediatric-onset MS, those with higher levels of moderate-to-vigorous physical activity were associated with lower depression and fatigue(Stephens et al., 2019).

This has led to the development of recommended guidelines for clinicians to promote activity in PwMS based on differing levels of disability(Kalb et al., 2020). It was recommended that ≥150 minutes per week of moderate-to-vigorous exercise or lifestyle activity should be the target for most people with considerations for increasing disability and other challenges(Kalb et al., 2020). One survey of PwMS found that 62% of respondents were interested in receiving exercise programs and 69% were interested in information regarding exercise and physical activity(Flachenecker et al., 2020; Kalron et al., 2021). The interest in exercise and information related to it suggests that recommended levels of exercise are more likely to be adopted when key findings of the benefits of exercise for the CNS beyond fatigue, cognition, and mental health are highlighted. The terms “exercise” and “physical activity” are used interchangeably though

physical activity involves movement while exercise is physical activity performed in a regimented fashion with the purpose of improving physical fitness(Motl et al., 2017).

Most of our understanding of the benefits of exercise and physical activity come from animal models. Understanding how exercise affects disease can be informed by how pathology changes when exercise is initiated at different stages of disease. Prophylactic initiation of exercise close or prior to immunization has shown broad benefits. Rats that began running 1 day post-immunization had resultant delayed onset of clinical signs and lower duration of the first relapse(Le Page et al., 1994). Similarly, both forced swimming and voluntary running paradigms begun prior to immunization reduced the amount of demyelination and preserved dendritic spines and axonal loss(Rossi et al., 2009; Shahidi et al., 2020). Functionally, exercise prevented EAE associated memory decline by increasing hippocampal neurogenesis when initiated prior to and during EAE(T. W. Kim & Sung, 2017). Interestingly, male mice were more responsive to reduction of EAE severity than female mice in a voluntary wheel running paradigm suggesting sex-specific effects(Mifflin et al., 2017). It should be noted that employing an exercise paradigm initiated before clinical signs of EAE are apparent could prevent immune abnormalities that give rise to disease. However, it is challenging to initiate exercise in mice that are severely afflicted with the paralysis characteristic of EAE, so most studies do not address whether exercise directly improves CNS functions after EAE pathology has been established.

Following cuprizone induced demyelination, mice allowed voluntary access to a running wheel had attenuated axonal injury, reduced decline in levels of myelin proteins, and diminished microglia activation(Mandolesi et al., 2019). Similarly, exercise after lysolecithin demyelination has shown that exercise impinges on cells of the oligodendrocyte lineage. Specifically, running wheel activity activated PGC1α ((peroxisome proliferator-activated receptor (PPAR) gamma co-activator-1α) within OPCs and increased the number of remyelinated axons, along with thicker myelin sheaths, compared to sedentary controls(Jensen et al., 2018). Other indirect effects of exercise may also influence remyelination such as increased axonal activity promoting OPC recruitment or decreasing oxidative stress leading to neuron survival(Barres & Raff, 1993; Souza

et al., 2016). Interestingly, remyelination by exercise was bolstered when combined with clemastine. Indeed, the combination of medication and exercise in mice led to more surviving axons after lysolecithin demyelination compared to exercise or clemastine alone groups, and ~98% of axons were remyelinated(Jensen et al., 2018). Whether this is due to exercise creating a more tractable environment for remyelination, altering the immune landscape, or supporting axon survival is not clear.

There are several mechanisms by which exercise improves CNS function. Exercise elevates levels of important neurotrophic factors such as brain-derived neurotrophic factor (BDNF)(Marlatt et al., 2012), growth hormones, neurotransmission(Jensen et al., 2018), and multiple signaling pathways in brain cells(Di Liegro et al., 2019). As well, exercise lowers levels of transcripts of genes related to the Nogo inhibitory pathway for CNS regeneration(Shahidi et al., 2020). Endurance (treadmill running) but not strength (climbing) training decreased oxidative stress in the spinal cord, while increasing levels of the nuclear factor erythroid 2–related factor 2 (Nrf2) transcription factor and downstream anti-oxidant glutathione peroxidase and glutathione levels(Souza et al., 2016).

Exercise also has important effects on the immune system. In EAE, exercise modulates both the innate and adaptive immune responses in peripheral blood as well as in the brain(Gentile et al., 2019). Running wheel activity decreased the proliferation of microglia and increased their expression of insulin-like growth factor-1 (IGF-1)(Kohman et al., 2012). EAE severity was attenuated in naïve mice following adoptive transfer of lymph node cells from treadmill exercising compared with sedentary mice; cells from higher intensity running were less pro-inflammatory than those from lower intensity running(Fainstein et al., 2019).

Maintaining the integrity of the BBB is important in MS as increased permeability is associated with leukocyte extravasation into the parenchyma and formation of demyelinating lesions. In aging mice and in EAE, exercise reduced BBB dysfunction through the upregulation of gap junction proteins(Souza et al., 2016). In aging mice, this was found to be associated with increased numbers of pericytes in blood vessels(Soto et al., 2015). Pericytes can increase the

proliferation and differentiation of OPCs within a demyelinated lesion through the secretion of laminin α2(De La Fuente et al., 2017). As well, in the hippocampus of exercising mice, improved neurogenesis was associated with increased angiogenesis(Baek, 2016). Exercise is known to increase cerebral angiogenesis through interaction of lactate with its receptor hydroxycarboxylic acid receptor 1 on pericytes(Morland et al., 2017). This presents a potential therapeutic avenue by which exercise, through expanding pericyte numbers and their coverage of blood vessels, can decrease BBB dysfunction, increase angiogenesis, and promote the OPC regenerative response for remyelination.

Neuronal activity influences OPCs to remyelinate denuded axons(Barres & Raff, 1993; Guo et al., 2019). Recent studies found that motor learning immediately after cuprizone induced demyelination, when neurons were hyperexcitable, did not have the same benefit of increased oligodendrogenesis and myelin sheath plasticity as delaying the learning task by several days, when partial remyelination has restored neuronal function(Bacmeister et al., 2020). There may be a period following specific injuries in which the CNS is particularly amenable to repair by physical activity, and this remains to be investigated in future studies.

In summary, exercise in models of MS shapes the immune response to reduce its pro-inflammatory potential, and it also acts directly on oligodendrocyte lineage cells to reduce myelin loss or to promote their regeneration(Guo et al., 2019). Exercise also has the effect of improving the lesion microenvironment to make it more conducive for regenerative processes.

It has long been recognized that activity dependent tasks such as piano playing, juggling, and general cognitive training increase the organization and integrity of brain white matter(Bengtsson et al., 2005). Functional MRI studies in PwMS have shown that exercise improves connectivity among different brain regions(Akbar et al., 2020). In addition, 8 weeks of voluntary upper limb task–oriented movement restored normal brain activity in PwMS with mild upper limb sensorimotor deficits as shown by functional MRI; this restoration coincided with reduced compensatory activity from other brain areas decreasing the overall brain burden(Bonzano et al., 2019). Transcranial magnetic stimulation (TMS) has also supported the

contention that exercise induces connectivity. PwMS with poor fitness have a longer corticospinal silent period measured by TMS; encouragingly, a single 40-minute bout of harness-supported treadmill walking in highly disabled PwMS reversed the TMS deficit and increased cortical excitability(Chaves et al., 2020).

MRI studies document that exercise reduces the loss of brain volume in PwMS in several areas including the cortex and deep gray matter(Feys et al., 2017; Kjolhede et al., 2018; Motl & Sandroff, 2015). In pediatric-onset PwMS, those with a high level of physical activity have lower MRI brain lesion burden and greater dentate gyrus volume than those with low activity(Longoni et al., 2018). Several methods of physiotherapy have been studied for how they may impact white matter in PwMS. In one study, the use of facilitation physiotherapy in which PwMS were given sensorimotor stimuli and stretching was shown to increase fractional anisotropy and decrease mean diffusivity and axial diffusivity in diffusion tensor imaging of the corpus callosum(Ibrahim et al., 2011). Another study using video game balance board training showed increased fractional anisotropy and radial diffusivity in the superior cerebellar peduncle, which the authors suggested to be due to enhanced remyelination; however, the imaging changes did not persist following the 12-week training period(Prosperini et al., 2014). In support of exercise-induced repair as occurs in animal models, resistance training over 24 weeks in PwMS improved multiple sclerosis functional composite (MSFC) scores and brain cortical thickness on MRI, which the authors suggested to be a possible indication of neuroprotection or even repair(Kjolhede et al., 2018).

A substantial literature in preclinical models, and sparse but emerging data in clinical studies, support the contention that exercise promotes well-being of the CNS with regard to neurogenesis and oligodendrogenesis, neuroprotection, connectomics, and remyelination. More data are required to link exercise and brain functions and repair. Moreover, several unknowns are evident, including whether exercise will have broad benefits for the CNS in the majority of PwMS, or whether this is influenced by age and the stage of disability in PwMS. For the likely responders, it remains unclear whether the intensity and type of exercise regimen, or the period of time after a relapse, affects brain function. As well, as seen in the balance board study, the

benefits of exercise may be transient if the program is not maintained(Prosperini et al., 2014). There is evidence to support exercise promoting oligodendrocyte, pericyte, and immune changes. If progressive forms of MS have less adaptive versus innate immune responses compared to relapsing-remitting MS, does this affect the outcome of exercise on the brain? Moreover, how does one maximize benefits of exercise without exacerbating other issues such as heat sensitivity or pain? These are all issues to be addressed in future studies. Finally, at least in animals with lysolecithin demyelination, exercise alters many signaling cascades, indices of neurotransmission, and phagocytic functions within lesions(Jensen et al., 2018) which may allow the microenvironment of a lesion to be particularly conducive for a pro-remyelinating medication to act upon. In this regard, the result aforementioned that the addition of clemastine to exercise after lysolecithin demyelination resulted in more surviving axons and near complete remyelination compared to either intervention alone invites the hypothesis that other pro-remyelinating medications with direct effects on OPCs or oligodendrocytes may also benefit from the more conducive lesion microenvironment, and regulatory/anti-inflammatory immune changes, that an exercise regimen confers(Jensen et al., 2018).

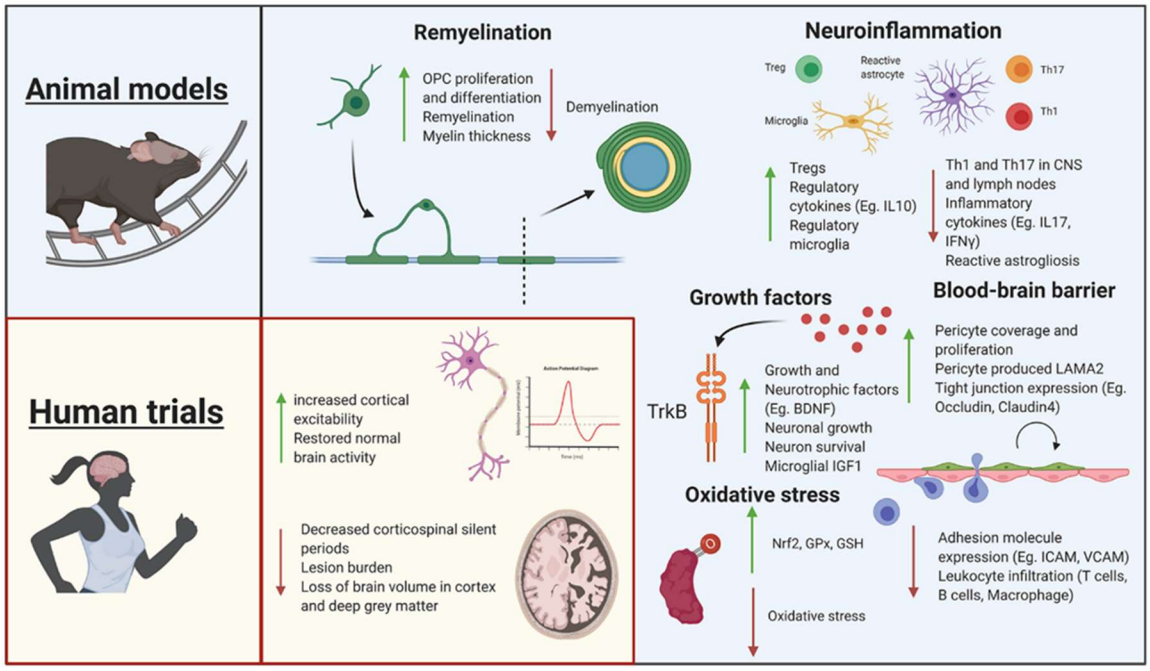

Figure 1.5) Postulated mechanisms of action of exercise in the CNS. Exercise exerts effects in both the peripheral circulation as well as the CNS. Within the CNS findings from animal models indicate exercise influences remyelination, neuroinflammation, growth factor levels, and blood–brain barrier integrity. This leads to reduced demyelination, adhesion molecules and leukocyte trafficking into the CNS parenchyma, inflammatory cytokine levels, and reactive astrogliosis; in addition, exercise is documented to increase remyelination including myelin thickness, BDNF and NGF levels, microglial IGF1, pathways that detoxify oxidative stress, tight junction proteins, and pericyte coverage of the vasculature. These results from animal models appear to translate to PwMS, as human trials show exercise to restore brain activity and to reduce lesion burden and loss of brain volume. Images were created with BioRender software(Lozinski & Yong, 2020).

1.3) Wound healing and CNS fibrosis

1.3.1) Stages of wound healing and fibrosis

A proper wound healing response is vital for tissue regeneration and involves discrete stages of inflammation, tissue remodeling, and their resolution(Talbott et al., 2022). The inflammatory response is critical for the removal of pathogens and debris from the injury site. It also recruits and activates tissue specific effector cells. Immune and effector cells then deposit a variety of ECM molecules to reconstitute matrix lost to injury(Talbott et al., 2022). Successful wound healing recapitulates the tissue environment and restores function(Rodrigues et al., 2019). Deregulation of wound healing following repeated, chronic, or pronounced injury leads to fibrotic scarring due to excessive build-up of cells and ECM(Soliman et al., 2021; Talbott et al., 2022).

Fibrosis is characterized by increased tissue stiffness and disrupted tissue architecture (Figure 1.6)(Distler et al., 2019). It is identified by markers of accumulation of ECM components, altered protease expression, increased levels of pro-fibrotic signaling molecules, and the presence of pro-fibrotic cells such as fibroblasts and myofibroblasts(Talbott et al., 2022). Even in conditions not classically associated with fibrosis, disease outcomes such as hypoxia and epigenetic reprogramming of cells are described with fibrosis-linked responses such as progressive scarification and exacerbated tissue injury(Distler et al., 2019; Henderson et al., 2020).

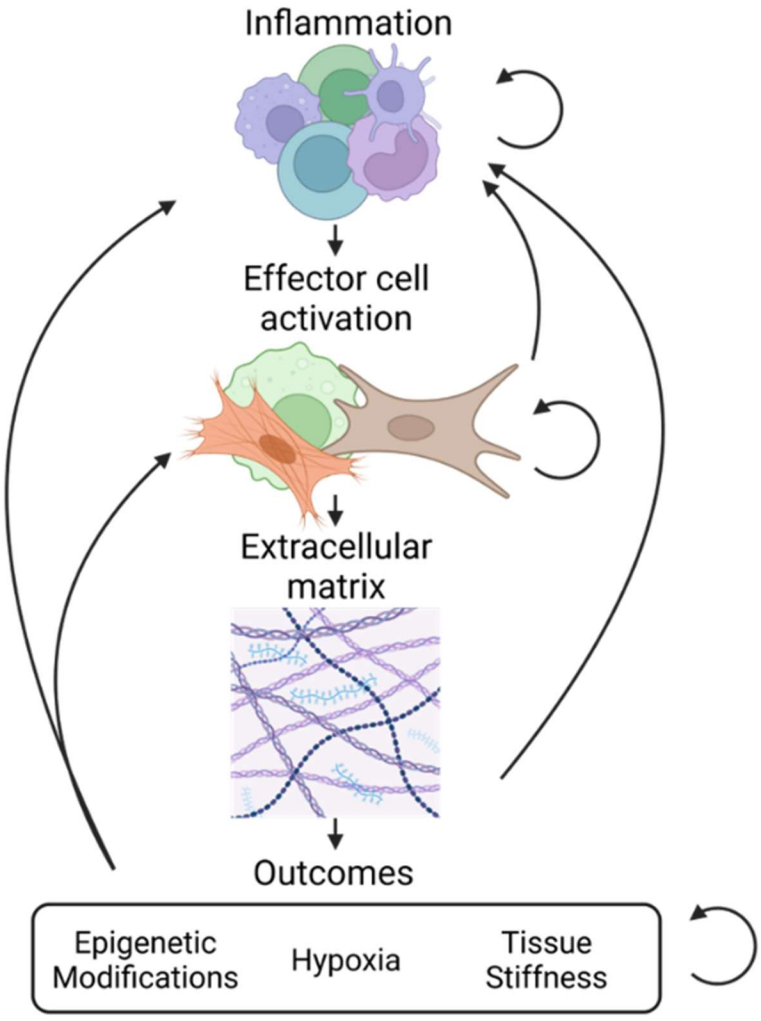

Figure 1.6) Overview of fibrosis and interconnectivity of stages. Fibrosis progresses through several stages. The first stage of inflammation involves accumulation of a heterogeneous population of cells such as macrophages, dendritic cells, and lymphocytes (top). This is followed by the activation of effector cells such as fibroblasts, myofibroblasts, and fibrocytes, that drive the process of tissue remodeling (middle). The result of effector cell activation is the production and deposition of extracellular matrix components including collagen, fibronectin, laminins, and proteoglycans (bottom). As a result of fibrosis there can be secondary injury that results from epigenetic modification of cells, tissue hypoxia, and increased tissue stiffness. Made in BioRender

Fibrosis occurring in many organs has shared and unique tissue specific characteristics(Distler et al., 2019). The primary injury varies based on anatomical location and trigger(Henderson et al., 2020). For instance, liver and kidney fibrosis can occur due to viral hepatitis and diabetes, respectively. Resident and infiltrating immune cells contribute to fibrosis during initial innate and later adaptive responses(Soliman et al., 2021) (Figure 2). Two primary signaling axes, IL-4/IL-13 and IL-1/IL-17A/transforming growth factor-β (TGFβ), are core pro-fibrosis pathways (Fig 1.7)(Wilson et al., 2010). Macrophages, the most abundant immune cell type in fibrosis, are recruited by damage associated molecular patterns (DAMPs), pathogen associated molecular patterns (PAMPs), and chemokines(Wynn & Vannella, 2016). Early arriving macrophages possess an inflammatory phenotype and secrete pro-inflammatory TNF-α, IL-1β and IFN-γ which fuel inflammation(Wynn & Vannella, 2016). Later stage macrophages assume a tissue remodeling regulatory phenotype characterized by the expression of TGF-β, IL-10, and mannose receptor 1(MRC1/CD206) (Wynn & Vannella, 2016). Inflammatory macrophages contribute to fibrosis by exacerbating the injury, while regulatory macrophages stimulate effector cells to deposit ECM and express other tissue remodeling genes(Henderson et al., 2020).

Effector cells responsible for tissue remodeling originate from resident and/or recruited fibroblasts, epithelial cells, endothelial cells, and other tissue resident cells and immune cells(Distler et al., 2019). Effector cells are recruited by chemokines and growth factors elaborated at sites of injury where they then proliferate and upregulate ECM, proteases, and growth factors(Pakshir et al., 2019). Often, positive feedback loops between effector and immune cells and the fibrotic environment promote further fibrosis by upregulation of pro-fibrotic genes(Henderson et al., 2013; Parker et al., 2014; Xia et al., 2008).

Organ failure and increased morbidity are outcomes of fibrosis-related disorders such as cardiac fibrosis following myocardial infarction(Bitterman & Henke, 1991). Prominently, fibrosis-related disorders are responsible for 45% of fatalities in the United States of America(Bitterman & Henke, 1991). This highlights the severity of fibrosis for tissue function and recovery which is made more significant in a tissue environment that is not prone to regeneration, such as the CNS.

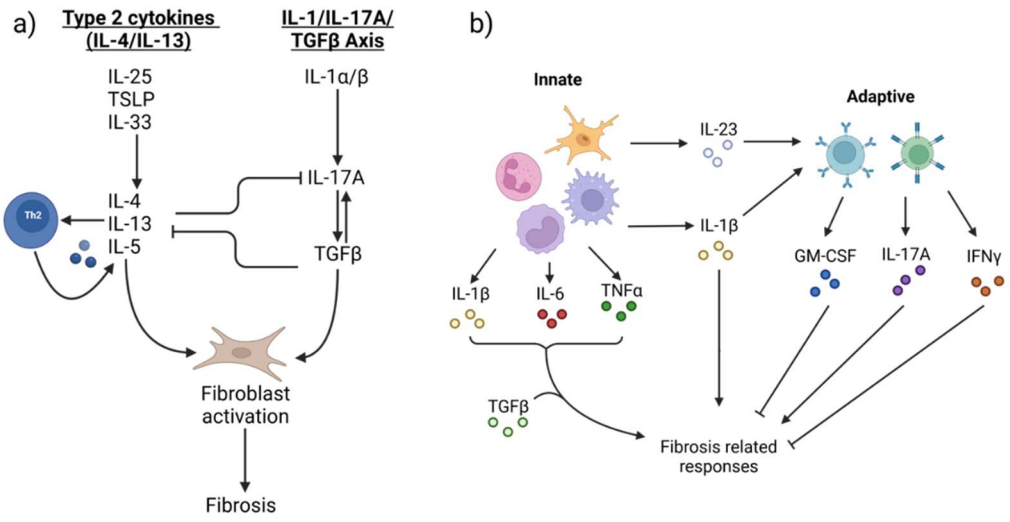

Figure 1.7) Fibrosis-related signaling pathways. a) Fibrosis canonically occurs through type 2 cytokines including IL-4 and IL-13 and the IL-1/IL-17/TGF-β signaling axis. Type 2 cytokines promote fibrosis in TGF-β dependent or independent ways. DAMPs including TSLP, IL-33, and IL-25 stimulate the production of IL-4, IL-13, and IL-5. These cytokines cause Th2 cells to produce more type 2 cytokines, macrophages to produce TGF-β, and stromal cells, including fibroblasts, to produce ECM components. The second pathway stimulating fibrosis is the IL-1/IL-17/TGF-β axis. IL-1, along with other inflammatory cytokines like IL-6 and TNF-α, stimulates IL-17A expression in neutrophils and T cells. IL-17A increases expression of TGF-β and fibroblast expression of TGFβRIII leading to greater fibrosis. b) Fibrosis is regulated by innate and adaptive immunity. Early phases of fibrosis are influenced more by innate immune cells including macrophages, neutrophils, monocytes, and microglia (in the CNS). Cytokines such as IL-1β, IL-6, and IL-23 affect both fibrosis and immune responses. During later stages of fibrosis lymphocyte derived IL-17A, IFN-γ, and granulocyte-macrophage colony stimulating factor (GM-CSF) promote and impede fibrosis-related responses. IFN-γ may impede fibrosis by limiting Th2 differentiation and type 2 cytokine signaling but can contribute to fibrosis by stimulating immune infiltration leading to greater tissue injury. GM-CSF is anti-fibrotic and dampens pro-fibrotic cytokine production and alternatively activated macrophage polarization. Made in BioRender

1.3.2) CNS Fibrosis

Functional regeneration of the CNS does not occur in adult humans(Rentsch & Rust, 2022) due to factors including age-related changes in neural cells and the tissue environment, and the formation of inhibitory scar tissue after injury(Franklin & Simons, 2022; Sofroniew, 2020). Scarring of the CNS comes in two forms: fibroblast-based scarring and astrocyte-based gliosis; even though interactions between many cell types occur similarly. In spinal cord injury, fibroblasts occupy the centre of the lesion while reactive scar forming astrocytes either surround the lesion or retain their original locations; in MS lesions, these cells are more intermingled(Anderson et al., 2018; D. Dias, 2020). The fibroblast scar is composed of meningeal and perivascular fibroblasts, and perhaps pericytes, that become elevated in the parenchyma following injury(D. O. Dias et al., 2021; Dorrier, Aran, et al., 2021; Goritz et al., 2011; Yahn et al., 2020). This contributes to impairment of axonal regrowth due to elevated deposition of collagens and CSPGs into the lesion(Shearer et al., 2003). However, there are complexities as complete depletion of CNS associated fibroblasts results in the loss of tissue integrity and an open tissue defect(Goritz et al., 2011) while partial depletion maintains tissue integrity and promotes increased axon regrowth(D. O. Dias et al., 2018). Part of the complexity may arise from the common use of platelet derived growth factor receptor-β (PDGFRβ)-driven Cre-recombinase based transgenic mouse lines to identify mural cells including pericytes and smooth muscle cells(Henderson et al., 2020), but PDGFRβ is highly expressed in fibroblasts(Vanlandewijck et al., 2018).

The molecular impediments to CNS regeneration within fibrotic lesions include inhibitory molecules, reduced levels of growth signals, and products of particular inflammatory cells(Dorrier, Jones, et al., 2021; Sofroniew, 2020). In neonatal mice infiltration by peripheral macrophages is resolved rapidly compared to adult mice, implying that it is microglia that act to promote axonal regeneration following crush injury(Y. Li et al., 2020). Additionally, there is a clear interconnectedness of the cells within CNS lesions as highlighted by altered levels of astrocytes, macrophages, and fibroblasts following depletion of each individually(D. O. Dias et al., 2018; Wanner et al., 2013; Zhu et al., 2015). Indeed, both astrocytes and fibroblasts interact reciprocally

with immune cells informing each cell's phenotype (Fig 1.8)(Dorrier, Aran, et al., 2021; Rawji et al., 2020). This emphasizes the importance of the cellular components of CNS injury to the success of regeneration.

While tissue stiffness generally increases in fibrosis-related non-CNS disorders, many forms of CNS injury are reported to result in reduced stiffness(Wuerfel et al., 2010). This may be due to the acute period of CNS injury in which measurement is taken as chronicity of the insult does associate with increasing stiffness(Cooper et al., 2020). Thus, neurofibrosis can be considered a form of fibrosis and presents further questions about the role of fibrosis-related responses in CNS pathologies including MS.

1.3.3) Fibroblasts

Fibroblasts occupy all organs, including the CNS, and are responsible for the secretion and maintenance of connective tissues (Fig 1.9)(Buechler, Fu, et al., 2021; Plikus et al., 2021). As well, fibroblasts play important roles in wound healing, tissue repair, immune regulation, mechanotransduction, metabolism, and progenitor renewal(Abbasi et al., 2020; Buechler, Fu, et al., 2021; Lappano et al., 2020; Mascharak et al., 2021). Most fibroblasts originate from paraxial and lateral plate mesoderm precursors and neural crest mesenchyme(Herriges & Morrisey, 2014; Soriano, 1997). Fibroblasts can also arise from epithelial and endothelial-to-mesenchymal transition driven by TGF-β, PDGF, Wnt, and other signals within the organs they occupy(Plikus et al., 2021). Several markers are thought to be universal identifiers of fibroblasts such as platelet derived growth factor-α (PDGFRα), Thy1, dermatopontin (Dpt), peptidase inhibitor (Pi16), and collagen 15a1(Buechler, Pradhan, et al., 2021). Other common markers used to identify fibroblasts include collagen 1a1, PDGFRβ, and vimentin (Vim)(Mascharak et al., 2021; Plikus et al., 2021).

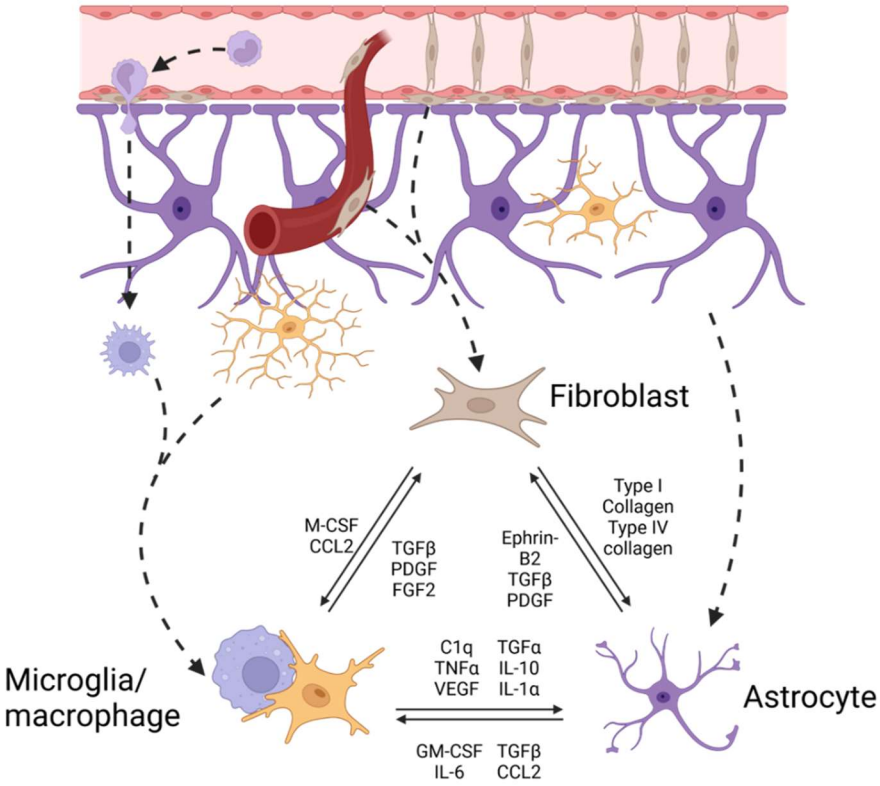

Figure 1.8) Fibroblast interactions with resident CNS cells. There is significant interconnectedness between cell types. Cell-cell, cell-ECM-cell, and soluble factors signal between effector cells leading to reduced or greater stimulation of fibrosis-related pathways such as TGF-β signaling in fibroblasts or collagen-1 activation of astrocytes. Made in BioRender

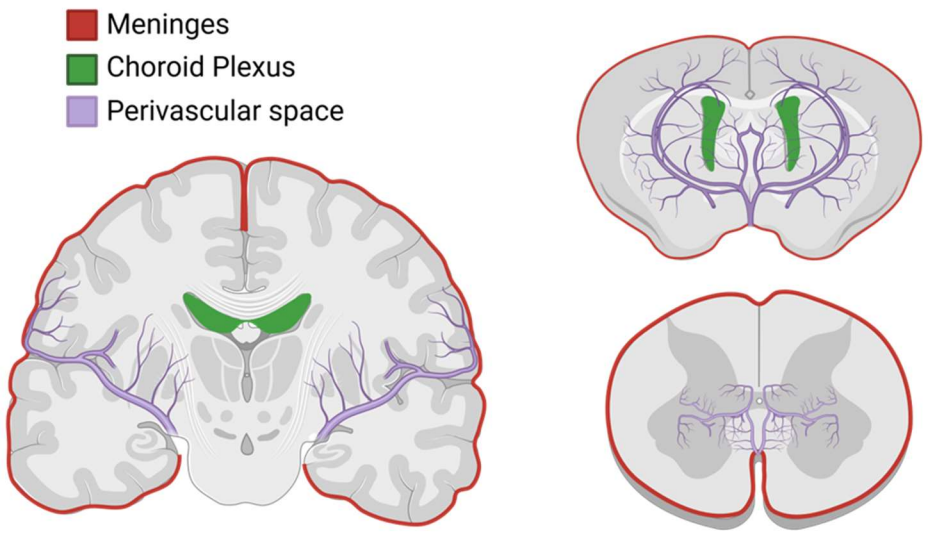

Figure 1.9) Regions of the CNS occupied by fibroblasts. Fibroblasts occupy border regions of the CNS including the meninges, chordoid plexus, and perivascular spaces. Meningeal fibroblasts in the spinal cord, midbrain, and hindbrain arise from the somatic and cephalic mesoderm and forebrain fibroblasts arise from neural crest cells. Perivascular fibroblasts originate from meningeal fibroblasts postnatally. Choroid plexus fibroblasts are thought to come from stromal fibroblasts and head mesenchyme. Made in BioRender

Following injury, fibroblasts become activated and transition into a myofibroblast that contributes to tissue regeneration as an effector cell. In the process of becoming activated, fibroblasts upregulate contractile and ECM related genes(Bageghni et al., 2019; Boothby et al., 2021; Jones et al., 2009; Nouchi et al., 1991). Fibroblast activation is prominently controlled by TGF-β mediated expression of α-smooth muscle actin (αSMA) and ECM related genes through SMAD2/3 signaling(Kuppe et al., 2021; Nouchi et al., 1991; Peng et al., 2022; Verrecchia et al., 2001). As well, migration of fibroblasts to the injury and their proliferation are driven by PDGFRα/β signaling. After fibroblasts have secreted large amounts of ECM into the injury, they promote collagen stabilization through synergizing of PDGF and TGF-β signaling(Walker et al., 2019; X. Zhou et al., 2018). PDGF isoforms PDGF-AA, PDGF-AB, and PDGF-BB bind to PDGFRα/β and activate several signaling cascades including MAPK and PI3K important for fibroblast self-renewal, proliferation, and migration(Donovan et al., 2013). The regenerative capacity of fibroblasts appears to be an autonomous characteristic that is retained even after transplantation into new tissue niches(Sinha et al., 2022). However, to some degree fibroblasts are informed by the environment they occupy as shown in vitro by the upregulation of ECM genes in fibroblasts cultured on pulmonary fibrosis related ECM(Parker et al., 2014). Similarly, in vivo comparisons of fibroblast populations in rheumatoid and osteoarthritic synovium describe differing expansion of lining and sublining fibroblasts based on NOTCH3 expression and proximity to endothelial cells(M. H. Smith et al., 2023; K. Wei et al., 2020). Cancer associated fibroblasts have also been shown to rely on stiffer matrix to maintain their phenotype(Calvo et al., 2013; M. H. Smith et al., 2023; Zhang et al., 2016).

Within the injury, activated fibroblasts/myofibroblasts secrete a plethora of ECM including fibronectin, collagen, laminin, proteoglycans, elastin, and other microfibrillar proteins(Plikus et al., 2021). As well, cell contraction polarizes the ECM matrix and transmits mechanical signals to other cells (Fig 1.10)(D. Cai et al., 2014; McWhorter et al., 2013; Tse et al., 2011). This allows fibroblasts to transmit positional cues, generate regional niches, and regulate immune recruitment and activation(Brügger & Basler, 2023; Buechler, Pradhan, et al., 2021; Ceccato et al., 2020; McGee et al., 2013). Macrophages and other immune cells are densely packed into sites of tissue

damage and closely associate with fibroblasts(Buechler, Fu, et al., 2021). Fibroblast-macrophage interactions have been described as a biological circuit that maintains their numbers through paracrine and autocrine signaling(X. Zhou et al., 2018). Fibroblasts secrete a variety of cytokines, chemokines, and growth factors including those critical for macrophage homeostasis(X. Zhou et al., 2022). Fibroblast derived macrophage colony stimulating factor (M-CSF) and macrophage derived PDGF act in paracrine and autocrine manners to maintain fibroblast and macrophage numbers within a stable range(X. Zhou et al., 2022).

Much of our understanding of age-related cellular decline originates from in vitro study of fibroblasts. This includes the description of replicative senescence and Hayflick numbers resulting from repeated passage of fibroblasts in culture(Hayflick, 1965). More recently, studies have shown aged fibroblasts to be more activated and express inflammatory cytokines like TNF-α and IL-1β, and chemokines such as CCL2 and CXCL11(Mahmoudi et al., 2019; Tinaburri et al., 2021; Vidal et al., n.d.). As well, aged fibroblasts have a reduced wound healing capacity, increasing expression of cytoskeletal proteins and becoming increasingly stiff(Schulze et al., 2010). Interestingly, aged dermal fibroblasts lose their cellular identity becoming ill-defined and gaining adipogenic and inflammatory traits(Salzer et al., 2018). These changes contribute to an overall reduction in regenerative capacity with age.

In the CNS fibroblasts are much less abundant than the heart, skin, or lung. The parenchyma of the CNS is devoid of fibroblasts, and they instead occupy the meninges, perivascular space, and choroid plexus borders of the CNS(Dorrier, Jones, et al., 2021). Meningeal fibroblasts in the midbrain, hindbrain, and spinal cord arise from mesoderm progenitors while forebrain meningeal fibroblasts are derived from neural crest cells(Couly et al., 1992; Couly & Douarin, 1987; Jiang et al., 2002). Conversely, perivascular fibroblasts develop postnatally possibly from meningeal fibroblasts in the pia(Dorrier, Jones, et al., 2021). Little is known about choroid plexus fibroblast development although ultrastructural studies suggest they may be derived from head mesenchyme(Wilting & Christ, 1989).

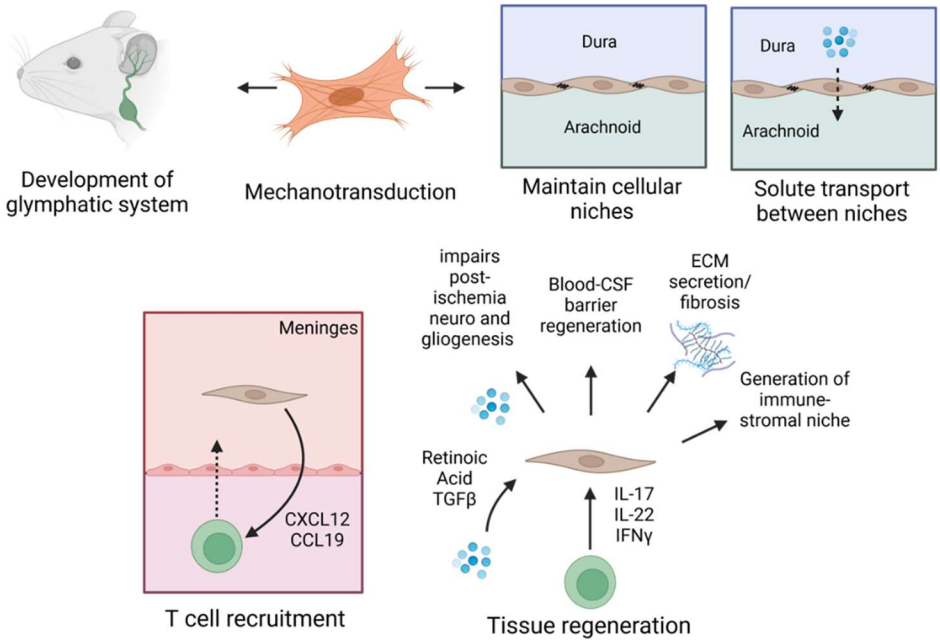

Figure 1.10) Functions of CNS fibroblasts. CNS fibroblasts have a number of critical functions in healthy and inflammatory states. Developmentally they are thought to contribute to the development of the CNS glymphatic system. As well, fibroblasts maintain tissue niche such as the dura and arachnoid in the meninges. In their position maintaining these niches, fibroblasts contract to transmit mechanical signals and polarize the surrounding tissue. They also aid in solute transport across tissue boundaries. During inflammation fibroblasts contribute to immune regulation by promoting T cell recruitment and maintaining immune-stromal niche in the meninges. Furthermore, they are involved in aiding and impairing regeneration in response to inflammatory signals including TGF-β and IFN-γ. Made in BioRender

Different populations of CNS fibroblasts can be identified by specific lineage markers. Fibroblasts that occupy the different layers of the meninges can be identified by certain markers; pial fibroblasts express S100 Calcium Binding Protein A6 (S100A6) and nerve growth factor receptor (NGFR), arachnoid fibroblasts express Cellular retinoic acid-binding protein 2 (CRABP2) and Aldehyde Dehydrogenase 1 Family Member A2 (ALDH1A2), and dural fibroblasts express Forkhead box protein P1 (FOXP1) and XYD Domain Containing Ion Transport Regulator 5 (FXYD5)(DeSisto et al., 2020). The function of the different populations of CNS fibroblasts are not well understood. However, like fibroblasts in all organs, CNS fibroblasts provide structural support within and between their occupied niches(DeSisto et al., 2020; Pikor et al., 2015). Choroid plexus fibroblasts express nestin suggesting that they may function as a progenitor cell pool although it is unclear for what cells(Dani et al., 2021). Some studies have suggested that perivascular fibroblasts are involved in fluid transfer of CSF transfer though it is not certain(Lam et al., 2017; Rasmussen et al., 2022).

Despite their well-defined involvement in wound healing and tissue regeneration there is little known about the involvement of fibroblasts in CNS injury and disease. Fibroblasts are known to become elevated in the parenchyma after acute injury such as in spinal cord injury or stroke(D. Dias, 2020; D. O. Dias et al., 2021; Goritz et al., 2011; Shibahara, Ago, Nakamura, et al., 2020). They have also been described in EAE and implicated in maintaining an immunogenic niche in the meninges(Dorrier, Aran, et al., 2021; Pikor et al., 2015; Yahn et al., 2020). Despite this, fibroblasts have not been directly described in MS. Some descriptions of their existence suggest that they remain in the border areas(Iacobaeus et al., 2017). However, given their position at the site of injury onset, their expression of ECM, and their ability to inform immune responses makes them worthy or additional study. As well, it is unclear what effect fibroblast derived tissue fibrosis that follows acute CNS injury has on remyelination, or whether it is altered during aging.

1.4) Concluding remarks

Remyelination is the most abundant form of regeneration that occurs in the CNS and contributes to functional recovery(Franklin & Simons, 2022). The failure of remyelination to occur sufficiently for functional benefits is mediated in part by age and accumulation of inhibitory ECM. In this chapter, we have highlighted the process and benefits of remyelination as well as inhibitors and promoters of it. As well, I have described the central role of fibroblasts in wound healing and fibrosis, and the minimal literature of their involvement in CNS pathology.

CNS fibroblasts express substantial amounts of ECM important for structural support, but which is inhibitory for regeneration. As well, fibroblasts are found in close proximity to microglia/macrophages and astrocytes and have the capacity to inform their functions(Anderson et al., 2016; Dorrier, Aran, et al., 2021; Wanner et al., 2013). In peripheral injury fibroblasts are known to secrete cytokines, chemokines, and growth factors that polarize immune phenotypes. With age, fibroblasts lose their regenerative capacity and express more inflammatory mediators. It has recently been shown that fibroblasts become elevated in EAE lesions in response to lymphocyte derived IFN-γ and may influence oligodendrocyte responses(Dorrier, Aran, et al., 2021).

Many outstanding questions remain including whether age affects accumulation of CNS fibroblasts in lesions. As well, fibroblasts are known to associate with microglia/macrophage in CNS injuries though it is not clear what role these myeloid cells have in the fibroblast response. Fibroblasts produce many of the ECM inhibitory to OPC responses, but it is not known whether their elevation within CNS lesions contributes to impaired remyelination. Finally, physical activity has been shown to promote remyelination(Jensen et al., 2018), contribute to the regenerative capacity of muscle fibroblast populations(Saito et al., 2020), and influence the niches that fibroblasts occupy in the CNS(He et al., 2017). It is of interest to study whether physical activity may contribute to CNS regeneration by affecting fibroblast responses to injury.

1.5) Hypothesis and Aims

In this proposal I will test the hypothesis that CNS fibroblasts became elevated within CNS lesions, negatively influence OPC responses, and are impacted by age. I will also test the hypothesis that voluntary running wheel exercise alters the LPC lesion environment and fibroblast response. My thesis has three aims:

1. Characterize the fibroblast response in LPC lesions and determine the causes and outcomes of this response.
2. Examine the effect of aging on the LPC fibroblast response and determine mechanisms contributing to these changes.
3. Investigate the effect of voluntary physical activity on CNS injuries, including the fibroblast response to LPC injury.

Overall, my thesis seeks to provide clarity and greater understanding of how central nervous system fibroblasts contribute to CNS regeneration and factors that influence it. There is currently little to no data on how age affects CNS fibroblast responses to injury or how physical activity influences CNS lesions including fibroblast accumulation. My work provides insights into the regulation of CNS regeneration by CNS fibroblasts, including how this is affected by age and physical activity.

Chapter 2: Response of fibroblasts to CNS injury

2.1) Abstract

The purpose of this chapter was to characterize the response of fibroblasts to lysolecithin (LPC) induced CNS injury and investigate the causes and outcomes of this response. The main findings of this chapter include the observation that fibroblasts are elevated in LPC lesions, and express markers of activation. This response corresponded with the onset of inflammation in LPC lesions, and macrophages were able to stimulate fibroblast migration in vitro. Regions of the LPC lesion occupied by fibroblasts were devoid of oligodendrocytes and newly myelinating oligodendrocytes. This was seen in vitro as fibroblasts impaired oligodendrocyte progenitor cell (OPC) differentiation in co-cultures. We attempted several methods of perturbing the system using transgenic mice that unfortunately were unsuccessful. Thus, fibroblasts are elevated in LPC lesions, their migration is stimulated by macrophages, and they inhibit OPC differentiation.

The findings presented in this chapter are in preparation for publication.

Author contributions to this chapter include S. Ghorbani for tamoxifen treatment of mice used in figures 2.12 and AAV injections in figure 2.11, C. Li and D. Moezzi helped harvesting meningeal tissue used to generate fibroblast cultures used in figures 2.9 and 2.10, M. MØrch for tamoxifen treatments in figure 2.4 and BMDMs used in figure 2.3. F. Visser provided AAV for figure 2.11. Lab of G. Gordon provided PDGFRβ-Cre mice used in figure 2.11. All other experiments, and the writing of this chapter, were completed by B.M. Lozinski. V.W. Yong supervised B.M. Lozinski, M. MØrch, C. Li, D. Moezzi, and S. Ghorbani, and contributed input.

2.2) Introduction

Multiple sclerosis (MS) is a neuroinflammatory disease of the central nervous system (CNS) characterized by demyelination, axon loss, and lifelong disability(Lassmann, 2018). Remyelination is the endogenous regenerative response to demyelination and restores myelin sheaths and function of denuded axons(Franklin & Simons, 2022). During remyelination oligodendrocyte progenitor cells (OPCs) migrate, proliferate, and mature into myelinating oligodendrocytes(Emery, 2010). Outcomes of remyelination are heterogeneous and it often fails(Rawji et al., 2020). The CNS does not normally undergo significant amounts of regeneration due to scarring those forms and impedes regenerative processes(Y. Li et al., 2020; Sofroniew, 2018, p. 201). Fibrosis is the scarification of tissue that results from accumulation of cells and inhibitory extracellular matrix (ECM)(Henderson et al., 2020). Accumulation of inhibitory ECM contributes to remyelination failure by impeding OPC migration, proliferation, and differentiation(Lassmann, 2018). For example, hyaluronan binds toll-like receptor (TLR)4 on OPCs impairing their differentiation by inhibiting AMP-activated protein kinase (AMPK) signaling(Srivastava et al., n.d., 2020). Hyaluronan and other ECM including chondroitin sulfate proteoglycan (CSPGs), collagens, and laminins are elevated in MS lesions(Back et al., 2005; Ghorbani et al., 2022; Mohan et al., 2010; J. van Horssen et al., 2006).

In non-CNS tissue, fibroblasts are the primary cells involved in fibrosis and fibrosis-related disorders like pulmonary fibrosis(Wynn & Vannella, 2016). By producing significant amounts of many types of ECM fibroblasts normally contribute to the structural support needed in connective tissues(Plikus et al., 2021). Under pathological conditions fibroblasts are activated and upregulate contractile and ECM genes transitioning to a myofibroblast phenotype(Plikus et al., 2021; Shook et al., 2018). As well, they contribute to inflammation by polarizing immune responses through secreting cytokines and chemokines including macrophage-colony stimulating factor (M-CSF), C-X-C motif chemokine 12 (CXCL12), and transforming growth factor (TGF)-β(Buechler, Pradhan, et al., 2021). Innate immunity is critical for tissue remodeling but can contribute to fibrotic scarring in severe or chronic inflammation(Wynn & Vannella, 2016).

In the CNS fibroblasts are restricted to the meninges, perivascular space, and choroid plexus(Dorrier, Jones, et al., 2021). Upon injury to the brain or spinal cord, fibroblasts become elevated in the parenchyma(D. O. Dias et al., 2021). These cells are necessary for maintaining tissue integrity but contribute to impeding axon regrowth(Anderson et al., 2018; D. O. Dias et al., 2018; Goritz et al., 2011). In the experimental autoimmune encephalomyelitis (EAE) model of MS CNS fibroblasts are elevated by interferon (IFN)-γ signaling(Dorrier, Aran, et al., 2021). However, little else is known about the mechanisms regulating fibroblast elevation in the parenchyma following injury or the outcomes of it.

In this chapter we sought to characterize the fibroblast response to toxin induced focal demyelination focusing on their role in impairing remyelination and the mechanisms regulating their elevation. We examined the time-course of the fibroblast response including how it compared to the microglia/macrophage response. The outcome of these experiments contributes to our understanding of fibroblast responses to CNS injury and the implications of this for CNS regeneration.

2.3) Materials and Methods

2.3.1) MS Specimens

Postmortem frozen brain tissues from people with MS brain tissue were obtained from The Multiple Sclerosis and Parkinson's Tissue Bank situated at Imperial College, London (https://www.imperial.ac.uk/ medicine/multiple-sclerosis-and-parkinsons-tissue-bank). All samples at their local sites were collected with full informed consent for autopsy, and their use for research has been approved by local institutional ethics committee. The use of these human tissues in Calgary for research was approved by the Conjoint Health Research Ethics Board at the University of Calgary (Ethics ID REB15-0444). MS sections were characterized using Luxol fast blue (LFB) and Hematoxylin & Eosin (H&E) to identify lesions. Autopsy samples were preserved, and lesions were classified using Luxol fast blue and H&E staining as previously described (Dong 2021).

2.3.2) Mice

All experiments were conducted with ethics approval from the Animal Care Committee at the University of Calgary under regulations of the Canadian Council of Animal Care. Female C57BL/6J mice were acquired from Jackson laboratories. CX3CR1^{CreER} (JAX 021160), iDTR [Rosa26^{iDTR} (JAX 007900)], PDGFRβ-P2A-CreER^{T2} (JAX 030201), Ai9 [Rosa26^{TdTomato} (JAX 007905)], NG2^{CreER} (JAX 008538), and Tau^{mGFP} (JAX 021162) mice were acquired from The Jackson Laboratory. CX3CR1^{CreER} and Rosa26^{iDTR} were bred in the single barrier mouse unit at the University of Calgary to produce female CX3CR1-iDTR mice, which were used for microglia/macrophage depletion experiments. PDGFRβ-P2A-CreER^{T2}, Rosa26^{TdTomato}, and Rosa26^{iDTR} mice were bred in the single barrier mouse unit at the University of Calgary to produce female PDGFRβ-Ai9 and PDGFRβ-iDTR mice, which were used in fate mapping and depletion experiments, respectively. NG2^{CreER} and Tau^{mGFP} mice were bred in the single barrier mouse unit at the University of Calgary to produce female NG2-Mapt^{eGFP} mice, which were used in myelin genesis experiments. All young female mice were 6-10 weeks of age, and all middle-aged female mice were 48-52 weeks of age. Pdgfrb-Cre (Jax #008046) mice were used for AAV experiments (gift from Dr. Grant Gordon). Male and female CD1 pups P0-2 were used for OPC and meningeal fibroblast cultures. C57BL6 female mice 6-10 weeks of age were used for BMDM cultures. All mice were maintained on a 12-h light/dark cycle with food (Pico-Vac Mouse Diet 20) and water given ad libitum.

2.3.3) Microglia/Macrophage Depletion

CX3CR1-iDTR mice were intraperitoneally injected with 2mg tamoxifen (20mgml^{-1}; T5648, Sigma) dissolved in corn oil (C8267) once a day for 3 consecutive days to induce diphtheria toxin receptor (DTR) expression on microglia/macrophages. Tamoxifen treated C-X3-C Motif Chemokine Receptor 1 (CX3CR1)-iDTR mice were intraperitoneally injected with phosphate buffered saline (PBS) or 1µg of diphtheria toxin (DT) on D0, D1, D3, and D5 or D5, D7, D9, and D10 after surgery. Wildtype C57BL6 mice were treated I.P. with C-C chemokine receptor type 2 (CCR2)-antagonist

(RS504393; Tocris Cat # 2517) for 7 days prior to surgery and 7 days following. RS503492 was dissolved in 10% Dimethyl sulfoxide (DMSO) in PBS.

2.3.4) Spinal Cord Surgery

Lysolecithin/lysophosphatidylcholine (LPC) demyelination was accomplished as previously described(Keough et al., 2015). Mice were anaesthetized with intraperitoneal injections of ketamine (100 $mgkg^{-1}$) and xylazine (10 $mgkg^{-1}$). Buprenorphine (0.05 $mgkg^{-1}$) was injected subcutaneously immediately prior to surgery and 12 h post-surgery as an analgesic. The surgery site was shaved and disinfected with 70% ethanol and betadine. Ophthalmic gel was applied to both eyes to prevent drying throughout the surgery and recovery period. Animals were positioned on a stereotaxic frame and a midline incision 2-3 cm long was made between the shoulder blades using a #11 scalpel blade. The T2 vertebra was exposed by separating the muscle and adipose tissue with a retractor. The intervertebral space between T3 and T4 was identified using T2 as a landmark. The T3-T4 tissue was blunt dissected apart and the dura was removed using a 30-gauge metal needle. Using a 32-gauge needle attached to a 10 µL Hamilton syringe, 0.5 µL of 1% w/v LPC (Sigma-Aldrich, L1381) was injected into the ventral column of the spinal cord at a rate of 0.25 $\mu Lmin^{-1}$ for 2 min. The needle was left in place for 2 min following the injection to avoid back flow. The muscle and skin were then sutured, and mice were placed in a thermally controlled environment for recovery.

2.3.5) Spinal Cord Tissue Isolation

LPC mice were anaesthetized with intraperitoneal injections of ketamine (100 $mgkg^{-1}$) and xylazine (10 $mgkg^{-1}$). LPC spinal cords were collected at 3-, 7-, 14-, or 21-days post-surgery. Mice were then transcardially perfused with a total of 15mL of PBS. Spinal cords were dissected from the back of the mouse, and the tissue between the lower cervical and lower thoracic regions was collected into 4% paraformaldehyde (PFA) in PBS for 24-hour fixation. Spinal cords were then transferred to 30% w/v sucrose solution for cyroprotection for at least 72-hours. Spinal cords were then frozen in FSC 22 frozen section media (Leica). Using a cryostat (ThermoFisher Scientific),

spinal cord tissue was coronally cut in 20μm sections onto Superfrost Plus microscope slides (VWR) and stored at -20^{o}C until analysis.

2.3.6) Immunofluorescence staining

Slides were thawed at room temperature then rehydrated with PBS for 10 minutes and permeabilized with 0.2% TritonX-100 in PBS for 10 minutes. Tissue was blocked by adding horse serum blocking solution (0.01 M PBS, 10% horse serum, 1% bovine serum albumin (BSA), 0.1% cold fish skin gelatin, 0.1% Triton-X100, and 0.05% Tween-20) for 1 hour at room temperature. Primary antibodies were resuspended in antibody dilution buffer (PBS, 1% BSA, 0.1% cold fish stain gelation, 0.1% Triton X-100) and added to tissue overnight at RT. Slides were then washed three times, 5 minutes each, using PBS, and stained with TrueBlack Lipofuscin Autofluorescence Quencher according to the manufacturer's instructions (Biotium) for 2 min at room temperature. Tissues were washed three more times, 5 minutes each, then incubated with secondary antibodies and 1 μgmL^{-1} of DAPI resuspended in antibody dilution buffer for 1 hour at RT. Slides were then washed three more times, 5 minutes each, and coverslips were mounted onto slides using Fluoromount-G solution (SouthernBiotech). EAE slides were thawed at RT, fixed with 4% PFA for 10 minutes, washed twice with PBS. All remaining steps were the same as above. Antibodies used for immunofluorescence identification of specific targets: anti-mouse myelin basic protein (MBP, BioLegend, PA1-10008), anti-mouse Periostin (POSTN, R&D Systems, AF2955), anti-mouse α-smooth muscle actin-Cy3 (αSMA, Millipore, C6198), anti-mouse Fibronectin (FN1, Millipore, AB2033), anti-human leukocyte common antigen (CD45, Thermofisher, MA5-17687), anti-mouse/human platelet derived growth factor receptor β (PDGFRβ, R&D Systems, AF1042), anti-mouse ionized calcium-binding adaptor molecule1 (Iba1, Wako, 019-19741), anti-mouse CD45-AF488 (Biolegend, 103122), Collagen Type I Alpha 1 Chain (Col1a1, Invitrogen, PA1-26204), anti-mouse glial fibrillary acidic protein (GFAP, Biolegend, PCK-591P), anti-mouse neurofilament-heavy chain (NFH, RPCA-NF-H), anti-mouse platelet derived growth factor receptor α (PDGFRα, R&D Systems, AF1062), anti-mouse Olig2 (Millipore, ab9610), GFP (Aveslab, GFP-1020), anti-mouse sulfatide O4 (R&D Systems, MAB1326). The following secondary antibodies from Jackson

ImmunoResearch were used at 1:400 dilution: Alexa Fluor 488 donkey anti-mouse IgM, Alexa Fluor 488 donkey anti-rabbit IgG, Alexa Fluor 488 donkey anti-rat IgG, Alexa Fluor 488 donkey anti-goat IgG, cyanine Cy3 donkey anti-goat IgG, cyanine Cy3 donkey anti-chicken IgY, Alexa Fluor 647 donkey anti-rat IgG, Alexa Fluor 647 donkey anti-rabbit IgG.

2.3.7) Confocal Immunofluorescence Microscopy

Laser confocal immunofluorescence images were acquired at RT using the Leica TCS Sp8 laser confocal microscope or Leica Sp8 Falcon. Images acquired on the Leica TCS were done using a ×25/0.5 NA water objective. The 405-nm, 488-nm, 552-nm and 640-nm lasers were used to excite the fluorophores from antibodies bound to samples and detected by two low-dark-current Hamamatsu PMT detectors and two high-sensitivity hybrid detectors on the Sp8. Images acquired on the Leica SP8 Falcon were done using a x20/0.8 NA air objective with 405nm and white light laser (470-670nm) used to excite the fluorophores from antibodies bound to samples. Fluorescence was detected by one low-dark-current Hamamatsu PMT detector, one cooled high sensitivity, single molecule detection hybrid detector, and two high sensitivity hybrid detectors. All images were acquired using the following parameters: in 8 bits, in a z-stack using unidirectional scanning, 1 times frame averaging, 1 airy unit pinhole, ×1 zoom, 0.57 µm or 1 µm per optical section, and 2,048 x 2,048 or 1024 x 1024 pixels x–y resolution. Equal laser, gain and offset settings to maximize contrast and minimize saturation were consistently used for all samples within each set of experiments. For volume measurements every section with a lesion was imaged. For all other analysis, lesion epicentres were acquired.

2.3.8) Cell Culture

2.3.8.1) Mouse meningeal fibroblasts

Brains from postnatal day P0-2 CD1 mouse pups were isolated, the meninges were removed using a dissection microscope and transferred to serum free RPMI buffer (Sigma) on ice until all meninges were collected. Meninges were then digested for 18 minutes at 37^{o}C in 1 µgmL^{-}

[1] DNase I (Sigma) and 3.7 μgmL^{-1} collagenase D (Sigma) triturating every 6 minutes. Meninges were centrifuged at 300xg for 3 minutes and supernatant was discarded. Cells were resuspended in growth medium (DMEM (Gibco) supplemented with 10% FBS, 1% non-essential amino-acids (NEAA), 1% GlutaMAX, 1% sodium pyruvate, and 1% Penicillin- Streptomycin (all from Gibco)). Cells were then transferred to T-75 flasks and incubated at 37^{o}C with 5% CO_2. Medium was changed every 3 days and cells were passaged when 90% confluent. Cells were passaged by adding 2.5% trypsin for 5 minutes at 37^{o}C. Trypsin was inactivated by adding growth medium, then cells were centrifuged at 300xg for 10 minutes. Cells were resuspended in 10mL of growth medium and run through 100 μm filter. Filtered cells were transferred to either T-75 flasks, or 96-well plates. Cells were used after at least one passage.

2.3.8.2) Mouse oligodendrocyte progenitor cells (OPCs)

Mouse OPCs were cultured as previously described(Ghorbani et al., 2022). Briefly, cortices from P0 CD1 pups were removed and dissociated with a digestion cocktail containing papain (1.54 mg/ml, Worthington), DNase (60 μg/ml, Sigma), and L-cysteine (360 μg/ml, Sigma) for 30 minutes at 37 °C. Cells were cultured in mixed glial culture growth medium (DMEM (Gibco) supplemented with 10% FBS, 1% GlutaMAX, 1% sodium pyruvate, and 1% Penicillin- Streptomycin (all from Gibco)) in T-75 culture flasks pre-coated with poly-L-lysine (100 μg/ mL, Sigma). Medium changes were performed after 3–4 h, on day 3 and 6. Medium was supplemented with 5 μg/ml insulin (Sigma) from day 6. On day 9, flasks were shaken for 45 minutes on an orbital shaker at 50 rpm and then medium was replaced with 10-12mL of fresh mixed glial culture medium supplemented with 5ug/mL insulin. Flasks were then shaken at 220 rpm overnight at 37 °C, 5% CO_2. The supernatant containing OPCs and microglia were transferred to a 100 mm tissue culture dish and incubated at 37 °C and 5% CO_2 for 30 min with gentle swirling by hand after 15 minutes. Medium enriched with unadhered OPCs were harvested and centrifuged at 300xg for 10 min. Cells were seeded at a density of 3,200 cells/cm^2 in 100 μL of oligodendrocyte differentiating medium (DMEM containing 2% (v/v) B27 supplement (Gibco), 1% (v/v) oligodendrocyte supplement cocktail (see below), 1% (v/v) GlutaMAX™ (Gibco), 100 μM sodium pyruvate (Gibco), 1% (v/ v) Penicillin-Streptomycin

(Gibco), 50 µg/mL holo-transferrin (Sigma), 5 µg/mL N-acetyl-L-cysteine (Sigma), 50 ng/mL ciliary neurotrophic factor (PeProTech), 10 µg/ml Biotin (Sigma) and 0.01% (v/v) Trace Elements B (Fisher Scientific)) and grown at 37 °C and 8.5% CO_2 for 24–72 h. 96-well flat bottom black/clear plates pre-coated with poly-L-lysine was used.

2.3.8.3) Mouse bone marrow-derived macrophages (BMDMs)

Mice were sterilized and hair and skin cleared from the lower half of the mouse to expose the lower limbs. Femurs from C57BL6 mice <6 months old were collected in calcium and magnesium free Hank's buffered salt solution (HBSS), and then cells from bone marrow were collected by flushing with DMEM supplemented with 10% FBS, 1% Penicillin- Streptomycin and 1% Glutamax (all Gibco) using a 12mL syringe and 25g needle. Samples were then centrifuged at 300xg for 10 minutes, supernatant was discarded, and cells were then resuspended in BMDM culture medium (10% supernatant from L929 cell line enriched in macrophage-colony stimulating factor], 10% FBS, 1% penicillin-streptomycin, 2% minimum essential medium (MEM) nonessential amino acid solution (all except L929 from Gibco). Cells were cultured in 100 mm culture plates at 37^{o}C with 8.5% CO_2 for 9 days with half-medium change at day 5 and full change at day 7. At day 9 BMDMs were collected by adding 3mL of cold PBS and scraping cells off of the plates. Cell suspensions were collected into 50mL tubes and centrifuged at 300xg for 10 minutes, then supernatant was discarded, and cells were resuspended in 1mL of BMDM culture medium for counting.

2.3.8.4) Cocultures

OPCs and meningeal fibroblasts were added to poly-L-lysine coated 96-well plates at the same time in 100 µL of OPC differentiating medium. Cocultures were incubated at 37^{o}C with 8.5% CO_2 for 72 hours. Cells were fixed by adding 33 µL of 16% PFA for 10 minutes and stored in 100 µL of PBS until staining. Cells were blocked with 50 µL of Licor Blocking Buffer at RT for 1 hour on an orbital shaker. Licor blocking buffer were aspirated and mouse anti-O4 primary antibody was added in Licor antibody dilution buffer at 1:250 dilution overnight at 4^{o}C. Cells were washed 3 times

for 5 minutes each in PBS and incubated with donkey anti-mouse IgM AF488 secondary antibodies at 1:200 dilution for 1 hour at RT covered in tinfoil on an orbital shaker. Cells were washed 3 times for 5 minutes each in PBS and permeabilized for 5 minutes with 0.02% Triton-X100 in PBS. Permeabilizing solution was removed and cells were washed once with Licor blocking buffer, then incubated overnight at 4^{o}C with anti-PDGFRβ (1:50; R&D systems;AF1042) and anti-MBP (1:100; Abcam; ab7349). Cells were then washed in PBS-Tween 0.1% and stained with secondary antibodies 1:200 in Licor blocking buffer for 1 hour at RT on an orbital shaker. Cells were washed 3 more times for 5 minutes each and suspended in 100uL of PBS with 1ug/mL DAPI. Plates were kept at 4^{o}C in tinfoil until ready to image.

2.3.9) Transwell migration assay

BMDMs were plated in 24 well plates at a density of 260,000 cells/cm^2 overnight at 37^{o}C with 8.5% CO_2. Cells were serum starved in BMDM culture medium with 1% FBS for 24 hours prior to experiments. Meningeal fibroblasts were added to transwell inserts (Corning, 29442-120) at a density of 150,000 cells/cm^2. Fibroblasts were allowed to migrate for 16-18 hours after which they were fixed and stained. Cells remaining in the upper chamber were removed using a cotton swab after which inserts were fixed with acid alcohol (1% HCl in 95% ethanol) for 15 minutes, washed in PBS for 5 minutes, transferred to hematoxylin for 15 minutes, and washed in PBS again for 1 minutes. Inserts were cut out using a #11 scalpel and mounted on Superfrost Plus microscope slides (VWR) using a small amount of water to adhere and Fluoromount-G solution (SouthernBiotech) to apply coverslips. Mounted transwell inserts were imaged on an Olympus VS110 slide scanner on a 10x/0.4 NA objective and VS-ASW-S5 (V2.9) with Batch Converter software.

2.3.10) Fluorescent image analysis

Leica Application Suite X was used for image acquisition, ImageJ was used for image threshold and particle analysis, and QuPath 0.3.1 was used for transwell and slide scanner image analysis. The z-stacks of confocal images were analyzed using ImageJ. For each image z-stack,

maximum-intensity projections were created for each channel/marker. All images were blinded prior to analysis. ROI for lesions were drawn using DAPI or MBP for LPC lesions. Fibroblast occupied regions were defined using PDGFRβ. Threshold intensity was determined using at least 3 images. The Analyze Particles function was then used to create a mask and to quantify the positive signals in each ROI using size exclusion of 2-infinity. Threshold intensity, size exclusion, and circularity settings for particle analysis were kept constant across all samples for each experimental set. For the representative images shown, the maximum-intensity projection of each channel/marker in a z-stack was merged and displayed using pseudocolors in ImageJ. Only the brightness and contrast settings were adjusted, and consistently between samples, to better display the images. Oligodendrocytes were counted manually using Olig2 and DAPI as a guide.

2.3.11) Quantitative fluorescence microscopy analysis

Labeled cells in 96-well flat-bottom black/clear plates were imaged using a ×10/0.5 NA air objective on an ImageXpress Micro XLS High-Content Analysis system (Molecular Devices). The following filters were used for detection: DAPI, excitation of 387/11 and emission of 447/60; FITC, excitation of 482/35 and emission of 536/40; Cy3, excitation of 531/40 and emission of 593/40; and Cy5, excitation of 628/40 and emission of 692/40. For each well of cells, 9–12 FOVs were imaged for quantitative analysis. Multiwavelength cell scoring analysis in the MetaXpress High-Content Image Acquisition and Analysis software (Molecular Devices) was used to quantify cell survival from the fluorescence microscopy images gathered. For fold change values, all numbers were divided by the mean of the control samples. The fold-change values from all samples and experiments were then plotted for statistical analysis. For the representative images shown, each channel/marker for the sample was merged and displayed using pseudocolors. Only the brightness and contrast settings were adjusted, and consistently between samples, to better display the images.

2.3.12) Fibroblast depletion experiments

Pdgfrb-Cre (Jax #008046) mice were retro-orbitally injected with 3x10^11gV/mouse of PHP.eB adeno associated-virus (AAV) loaded with a CAG-DIO-TK-T2A-eGFP construct 14 days prior to LPC surgery. HSV-TK plasmid was obtained from addgene (Addgene plasmid # 22053). Following LPC surgery mice were treated twice daily with GCV or saline for 14 days. Tissue was collected as previously described.

2.3.13) Statistical analysis

Data were collated using Microsoft Excel. Graphs were generated using GraphPad Prism 8. Data shown are the individual data points, whereby each point on a bar graph represents a biological replicate (for in vivo experiments) or replicate (for in vitro experiments), and the mean ± s.d. No statistical methods were used to predetermine sample sizes, but our sample sizes were similar to those reported in previous publications(Dong et al., 2021; Plemel et al., 2020; Rawji et al., 2020). No inclusion or exclusion criteria were used unless otherwise stated. Animals and tissue culture samples were randomized when assigned to various experimental groups and conditions. Data collection and analysis were not performed blind to the conditions of the experiment (unless otherwise stated), as all image and data analysis were completed with the same acquisition conditions and analysis thresholds. Statistical tests are as listed in figure legends. Asterisks indicate significance where *P < 0.05, **P < 0.01, ***P < 0.001.

2.4) Results

2.4.1) Fibroblasts are elevated in LPC lesions

We began with characterization of LPC lesions at timepoints that correspond with the beginning of the OPC response (7 day post-injury, dpi) and when remyelination is robust (21 dpi)(Keough et al., 2015). To confirm the presence of fibroblasts in the CNS parenchyma following toxin induced demyelination, lysophosphatidylcholine (LPC) was injected into the ventral spinal cord white matter (SCWM) of PDGFRβ-Ai9 mice (Fig 2.1a.) (Keough et al., 2015). Though PDGFRβ is expressed by fibroblasts, pericytes, and smooth muscle cells it was recently shown that pericytes and smooth muscle cells do not contribute to fibrotic scarring in the spinal cord(Dorrier, Aran, et al., 2021). Lesions were identified by immunofluorescence staining for nuclei accumulation (DAPI) and myelin basic protein (MBP) disruption (Figure 2.1e). Fibroblasts were present within LPC lesions 7- and 21 dpi (Fig 2.1b-e). Total lesion volume was reduced at 21 dpi compared to 7 dpi (Fig 2.1b, f,i). The total TdTom+ volume remained unchanged (Fig 2.1c,d) and the proportion of lesion volume occupied by fibroblasts was greater twenty-one dpi compared with seven dpi (Fig 2.1g,h). As well, the area of the lesion epicenters decreased over time (Figure 1b), and the proportion of the lesion epicenter occupied by fibroblasts increased over time (Fig 2.1d,k).

Since activated fibroblasts are associated with greater ECM and tissue fibrosis, we next characterized fibroblast activation within LPC lesions. Sections were stained for markers of activation including the contractile protein smooth muscle actin (SMA), and ECM molecules periostin (POSTN) and fibronectin (FN1) (Fig 2.1j). There was significant overlap of TdTom with all activation markers (Fig 2.1l-n). POSTN+TdTom+ and SMA+TdTom+ levels increased from 7-to-21-dpi while FN1+TdTom+ levels decreased over that period (Fig 2.1l, m, n). SMA expression was present throughout the lesion and FN1 and POSTN were primarily located in close proximity to TdTom+ fibroblasts. Overall, these results show that activated fibroblasts are elevated in LPC lesions throughout the course of injury.

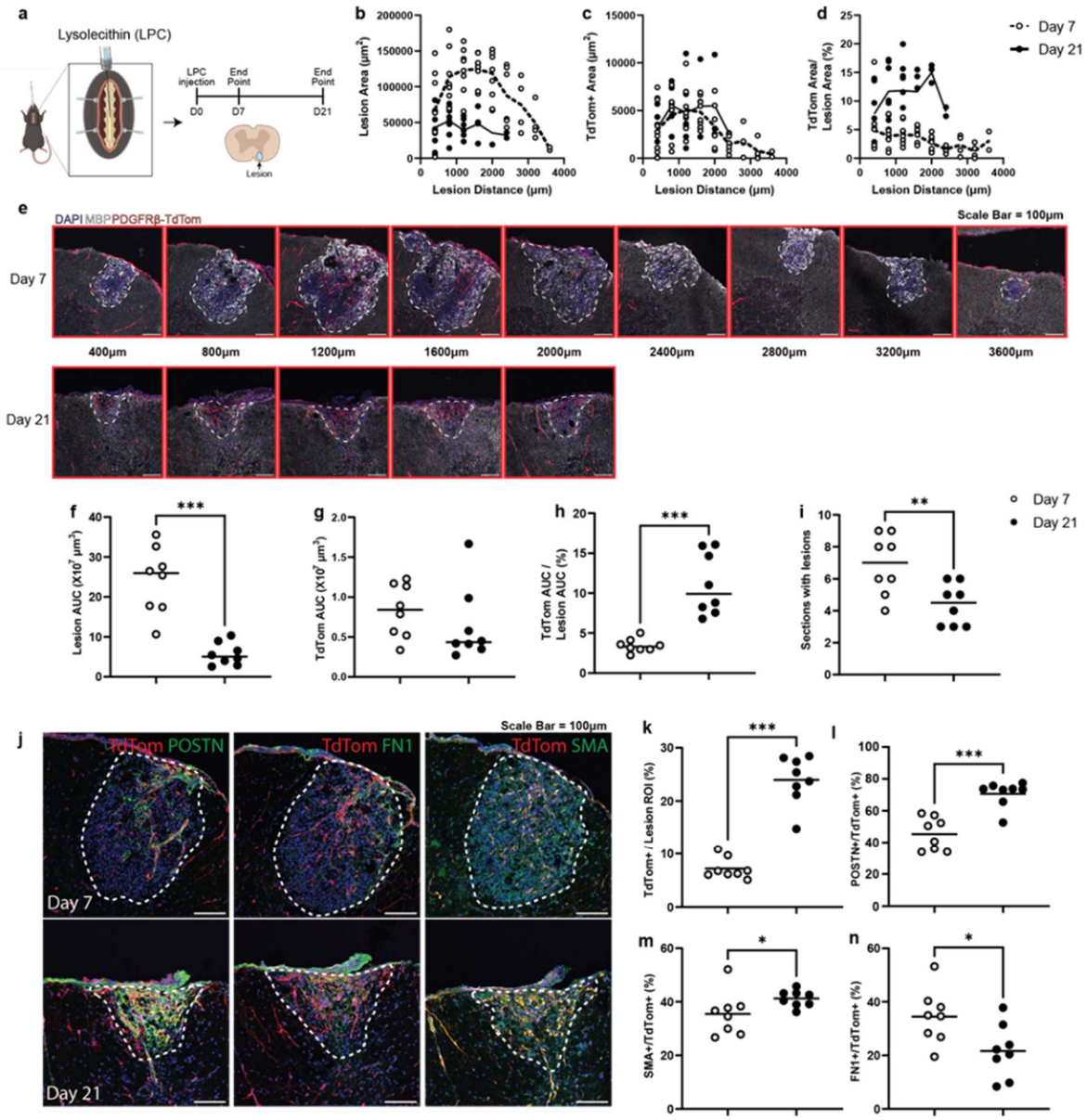

Figure 2.1) Characterization of PDGFRβ+ fibroblasts in LPC lesion. a) Schematic of experimental procedure and time course. b-d) Histograms comparing spinal cord lesion and TdTomato spread b) total lesion volume based on intense MBP disruption, c) total TdTom volume, d) TdTom-positive proportion of spinal cord lesion. e) Representative serial images of immunofluorescent labeling of day 7 and day 21 after LPC injection. f-i) Graphs quantifying histograms in b-d comparing day 7 and day 21 after LPC injection. f) Total lesion volume area under the curve, g) total TdTom volume area under the curve, h) TdTom-positive proportion of lesion volume, i) number of tissue sections with lesions. j) Representative confocal images of TdTom (Red) with periostin (POSTN), fibronectin

(FN1), and smooth muscle actin (SMA) (green; left to right). k) percentage of the lesion region of interest (ROI) occupied by TdTom. l-n) percentage of TdTom positive for l) POSTN, m) SMA, n) FN1. Data were collected from two experiments. Sample size n = as shown number of mice from two experiments. Significance is indicated as *P < 0.05, **P < 0.01, ***P < 0.001. Two-tailed, unpaired *t*-test comparing 7- and 21-days post injection. Mean shown as horizontal lines.

2.4.2) Fibroblasts are present in MS lesions

Having shown that fibroblasts are elevated in toxin induced demyelinating lesions we asked whether fibroblasts could be detected in MS lesions. To determine the presence of fibroblasts in MS, three frozen MS sections from different donors were stained for PDGFRβ and CD45 for immune cells. PDGFRβ+ cells were visible in all three sections (Fig 2.2a). Anatomically, PDGFRβ+ cells appeared located in close proximity to blood vessels (Fig 2.2a, b). Immunoreactivity was prominent in close proximity to CD45+ leukocytes (Fig 2.2b). PDGFRβ+ cells were identifiable both in lesions, and at the lesion boundary and NAWM.

2.4.3) Macrophages promote meningeal fibroblast migration in vitro

Macrophages are critical regulators of fibrosis(Duffield, Forbes, et al., 2005; Duffield, Tipping, et al., 2005) and together with microglia are the primary immune cells in LPC(Ousman & David, 2000; Plemel et al., 2020). We asked whether macrophages were involved in the fibroblast response. We looked first at 3, 7, 14, and 21 dpi for markers of microglia/macrophage (Iba1) and fibroblasts (PDGFRβ) (Figure 2.3a). The area of the lesions did not significantly change at 3, 7, and 14 dpi though day 21 was reduced (Figure 2.3b). The microglia/macrophage response increased significantly from occupying approximately 10% of the lesion at 3 dpi to >40% at 7dpi (Fig 2.3a, c). The fibroblast response followed a similar course increasing from 3 to 7dpi though there was no detectable immunoreactivity at 3dpi (Fig 2.3a, d). While the microglia/macrophage response peaked at 7 dpi the fibroblast appeared to plateau at 7 – 21 dpi (Fig 2.3c, d). The data at 3 dpi indicate that the immune response begins prior to the elevation of fibroblasts in the lesion.

Next, to answer whether macrophages could stimulate fibroblast migration we utilized a transwell migration assay. Meningeal fibroblasts were added to transwell inserts in the presence of bone marrow derived macrophages (BMDMs) or medium alone for 24 hours after which they were fixed and stained with hematoxylin (Figure 2.3e). After 24 hours fibroblasts on the underside of the insert had an elongated morphology and the hematoxylin-positive % area of the insert was greater in the BMDM+ wells. (Fig 2.3f,g).

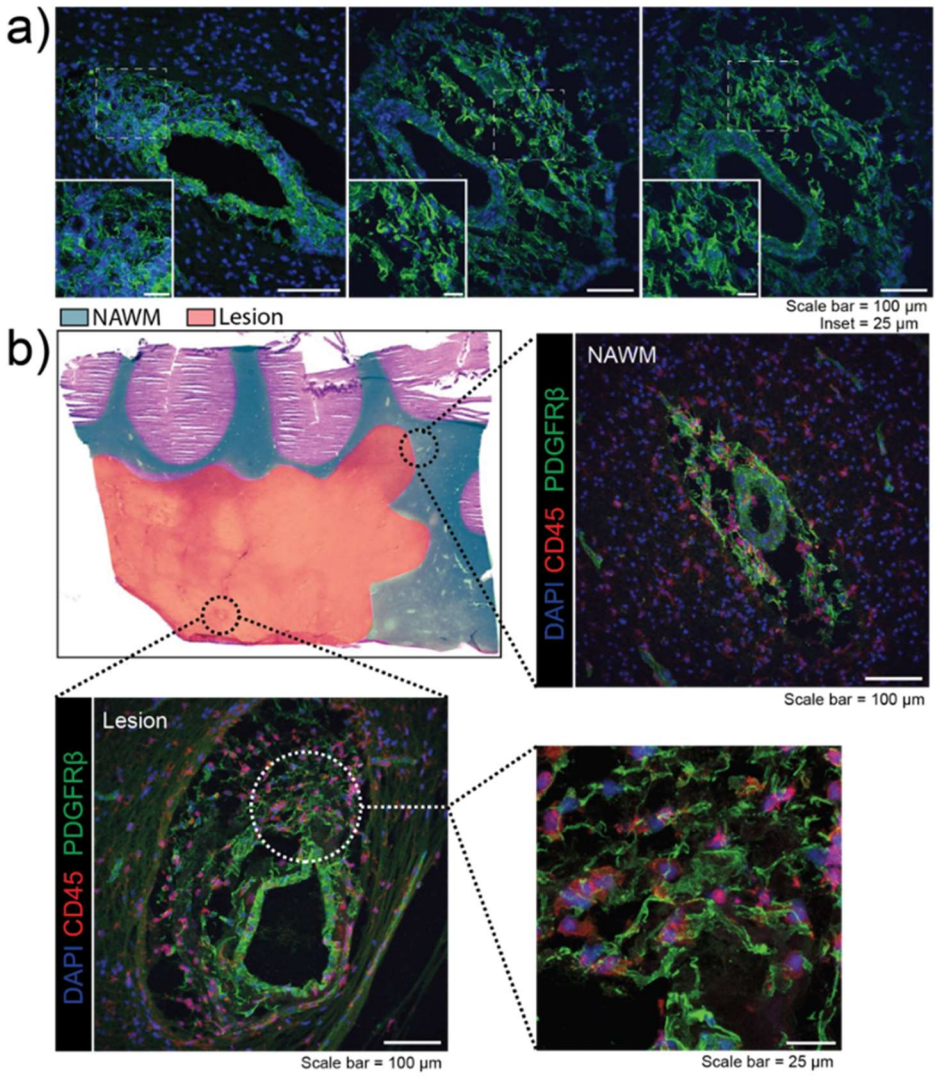

Figure 2.2) PDGFRβ-positive fibroblasts are present in MS tissues. a) Representative confocal images of PDGFRβ (green) and DAPI (blue) in MS tissue sections from three separate donors. b) Representative images from AB172 PD1-B2, top left) hematoxylin and eosin stain labeled with lesion and normal appearing white matter (NAWM) boundary, top right) confocal image of PDGFRβ (green) DAPI (blue) and CD45 (red) at the lesion border/NAWM, bottom left) confocal image of PDGFRβ (green) DAPI (blue) and CD45 (red) within the lesion, bottom right) high magnification inset identifying PDGFRβ-positive fibroblasts and CD45-positive leukocytes.

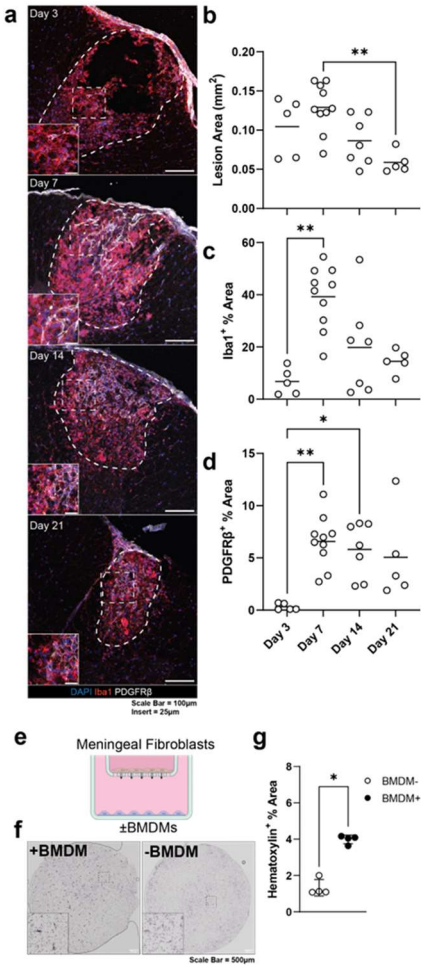

Figure 2.3) Microglia/macrophage precedes fibroblast response and promote fibroblast migration. a) Representative confocal images of PDGFRβ and Iba1 immunoreactivity 3-, 7-, 14-, and 21- days post LPC injection. b-d) Graphs comparing b) lesion ROI, c) Iba1-positive proportion of lesion ROI, d) PDGFRβ-positive proportion of lesion ROI. e) Schematic of Boyden chamber-transwell migration assay. Meningeal macrophages are added to the upper chamber with or without bone marrow derived macrophages (BMDMs) added to the bottom chamber. f) Representative brightfield images of hematoxylin stained transwell inserts after 16-18 hours with or without BMDMs added. g) Graph of percentage of the insert positive for hematoxylin comparing BMDM and no BMDM groups. Significance is indicated as *P < 0.05, **P < 0.01, ***P < 0.001, ****P < 0.0001. Sample sizes n = as shown, a) number of mice across at least two experiments, b) number of technical replicates. b-d) Kruskal-Wallis followed by a Dunn's multiple comparisons; g) Two-tailed, unpaired t-test comparing groups. Mean shown as horizontal line.

2.4.4) Elevation of fibroblasts in LPC lesions occurs independent of microglia/macrophage response

We hypothesized that macrophages contributed to the elevation of fibroblasts seen in LPC lesions by promoting their migration. To test this hypothesis in vivo we utilized the CX3CR1-iDTR model to deplete microglia/macrophages. Mice were treated for 3 days with tamoxifen after which LPC was induced within 2 weeks to avoid hematopoietic cell turnover. Mice were then treated with diphtheria toxin (DT) or saline on days 0, 1,3, 5, or 5, 6, 8, 10. Tissues were collected at 10 dpi, 6 hours after the final injection. The tissue was then stained for CD45 to label all leukocytes and Iba1 to label microglia/macrophages. There were no observable changes in lesion area, nor the proportion of the lesion positive for CD45, Iba1, PDGFRβ, and Col1a1 (Fig 2.4a-e). The similar density of Iba1+ or CD45+ cells between the DT or PBS groups would suggest that the DT did not adequately ablate the targeted microglia.

We also tried another method of limiting macrophage involvement in LPC lesions in which mice were treated with a CCR2 antagonist RS504393 for one week prior to LPC then daily for one week at which point tissue was collected. Treatment with the CCR2-antagonist resulted in greater lesion area though it did not affect the proportion positive for Iba1, PDGFRβ, or Col1a1 (Fig 2.5). At this point the in vivo role of microglia/macrophages on the fibroblast response is inconclusive though there is evidence to suggest reciprocal interactions between fibroblasts and microglia/macrophages(Shibahara, Ago, Tachibana, et al., 2020).

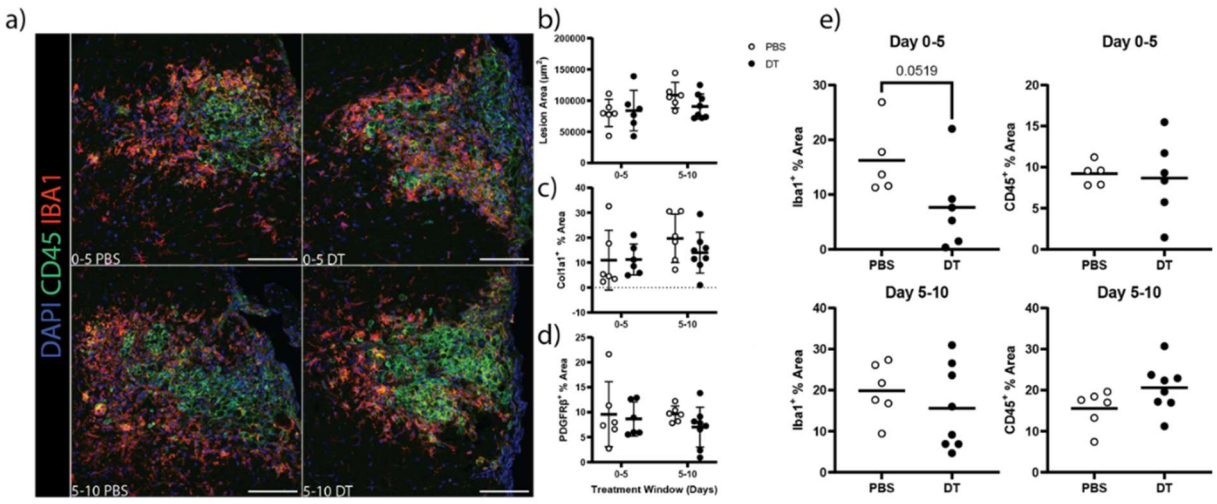

Figure 2.4) CX3CR1-iDTR mediated microglia/macrophage depletion experiment. a) Representative confocal images of CD45 and Iba1 immunoreactivity in PBS and DT treatment groups 7 days after LPC injection. Graphs of b) Lesion ROI area, percentage of ROI positive for c) Col1a1 and d) PDGFRβ. e) graphs quantifying the percentage of ROI positive for Iba1 and CD45 in 0-5 and 5-10 treatment groups. Sample sizes n = as shown number of mice across two experiments. b-d) Two-way ANOVA followed by a Tukey's multiple comparisons; e) Two-tailed, unpaired t-test comparing groups. Mean shown as horizontal lines.

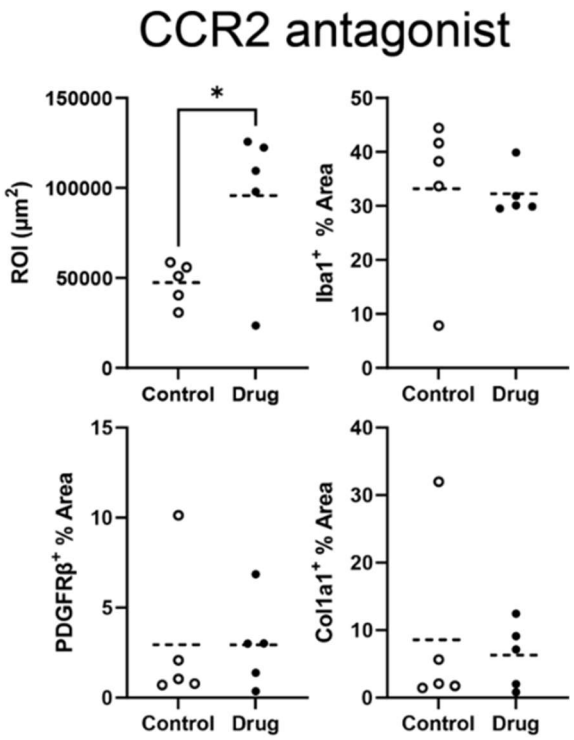

Figure 2.5) CCR2-antagonist monocyte depletion experiment. Graphs showing lesion ROI (top left), percent of ROI positive for Iba1 (top right), PDGFRβ (bottom left), Col1a1 (bottom right). Two-tailed, unpaired t-test comparing groups. Significance is indicated as *P < 0.05, Sample sizes n = as shown number of mice from one experiment. Mean shown as horizontal line.

2.4.5) CNS Fibroblasts impair OPCs by inhibiting their differentiation

Fibroblasts express many factors inhibitory for OPC function including inhibitory ECM components, NOTCH1, and Wnts(DeSisto et al., 2020; Dorrier, Aran, et al., 2021; Yahn et al., 2020). We sought to determine whether fibroblasts were associated with impaired OPC function and impaired myelination. As such, LPC lesioned tissue sections were labeled with OLIG2 for oligodendrocyte lineage cells and PDGFRβ for fibroblasts. We first characterized the axon pathology and OPC timeline in LPC (Fig 2.6). Lesions had intense MBP staining indicative of myelin debris and GFAP immunoreactivity primarily around the rim of the lesion, though some remained within the lesion (Fig 2.6a). The density of axons was reduced in LPC lesions but there were no clear axonal swellings that would indicate ongoing injury (Fig 2.6a-c). Consistent with previous studies(Jensen et al., 2018) the OPC response is significant 7 dpi and declines to normal levels by 21 days (Fig 2.6 d-f).

Following 7, 14 and 21 days after LPC injection OLIG2+ cells were entirely lacking within PDGFRβ occupied areas (Fig 2.7a, b). To determine if this translated to reduced levels of newly myelinating oligodendrocytes, LPC demyelination was induced in CSPG4-Cre;Mapt-eGFP mice, allowing for identification of oligodendrocyte lineage cells based on GFP expression(Ghorbani et al., 2022). GFP+ immunoreactivity was minimal 7 dpi though it increased at 14 dpi (Fig 2.7c). As well, the fibroblast occupied niche within the lesion contained significantly less GFP+ staining compared to the rest of the lesion (Fig 2.7c, d).

While there is a decrease in axon density after LPC (Fig 2.7a-c), there was no difference in NFH+ axon density between the fibroblast occupied niche and the rest of the lesion (Fig 2.8a,b). This suggests fibroblasts in LPC lesions are an obstacle to the OPC regenerative response.

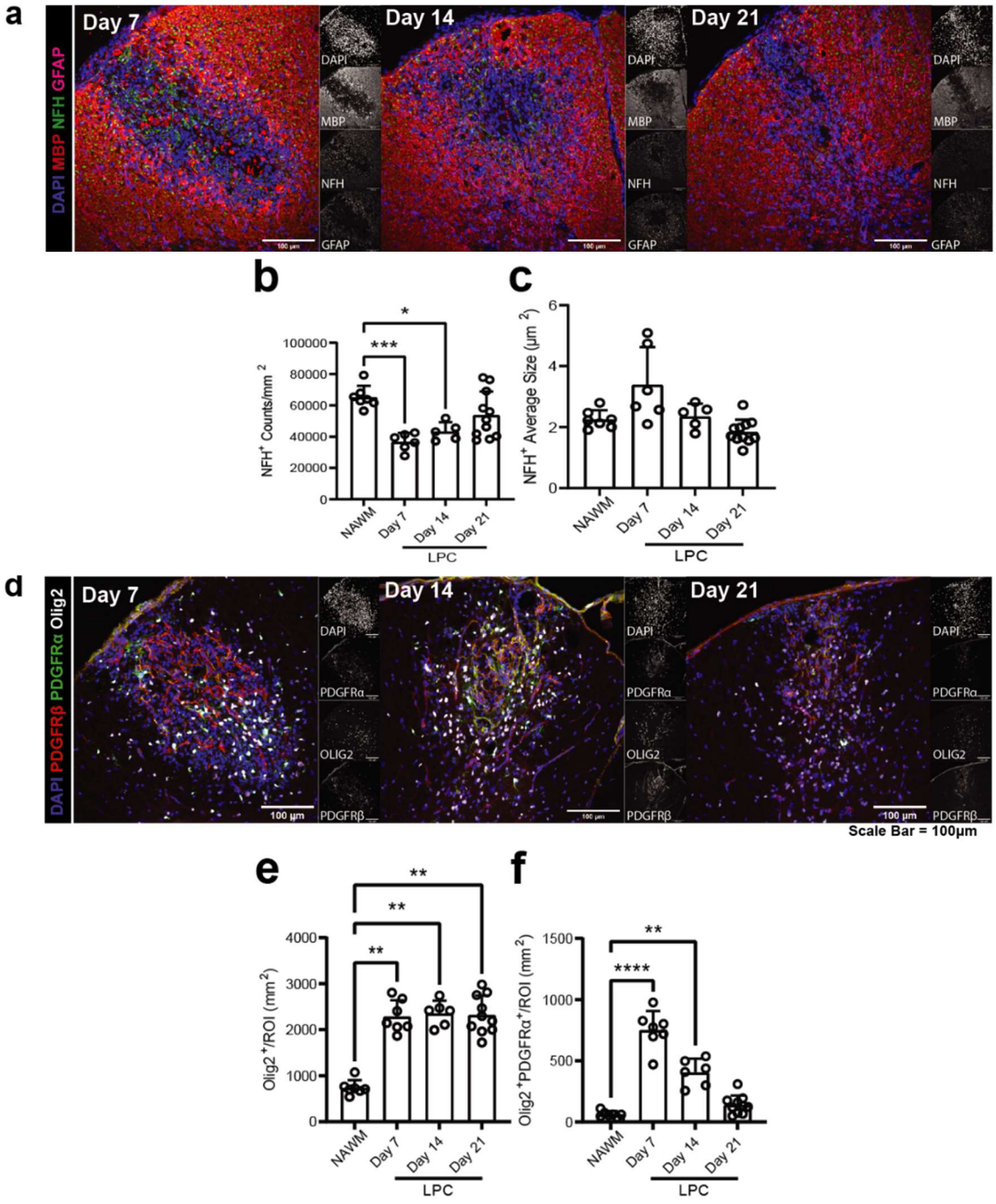

Figure 2.6) Characterization of lesion pathology and oligodendrocyte responses a, d) Representative confocal images of day 7, 14, and 21 LPC lesions labelled with a) DAPI (blue), MBP (red), NFH (white), GFAP (magenta), c) DAPI (blue), PDGFRα (green), PDGFRβ (red), Olig2

(white). b-f) Graphs comparing NAWM to LPC lesions 7, 14, and 21 dpi b) axon (NFH^+) counts/mm^2, c) axon (NFH^+) average size, e) oligodendrocyte lineage cell ($Olig2^+$) counts/ROI, f) oligodendrocyte progenitor cell ($Olig2^+PDGFR\alpha^+$) counts/ROI. Significance is indicated as *P < 0.05, **P < 0.01, ***P < 0.001, ****P < 0.0001. Sample sizes n = as shown number of mice from at least two experiments. Kruskal-Wallis followed by a Dunn's multiple comparisons. Data are the mean ± s.d.

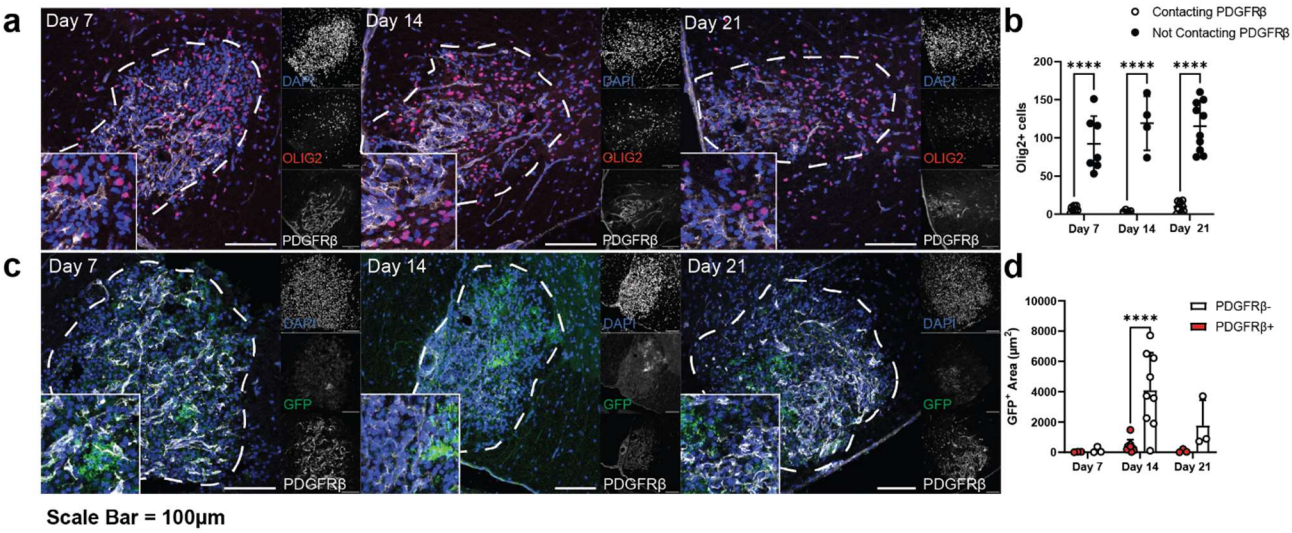

Figure 2.7) Oligodendrocytes do not occupy fibroblast niche in LPC lesions. a, c) Representative confocal images of day 7, 14, and 21 LPC lesions labelled with a) DAPI (blue), Olig2 (red), PDGFRβ (white), c) DAPI (blue), GFP (green), PDGFRβ (white). b) Graphs comparing Olig2-positive cells contacting or note contracting PDGFRβ-positive immunoreactivity 7, 14, and 21 dpi. d) Graph comparing GFP-positive area in PDGFRβ-positive and PDGFRβ-negative regions of LPC lesions 7, 14, and 21 dpi. Significance is indicated as *P < 0.05, **P < 0.01, ***P < 0.001, ****P < 0.0001. Sample sizes n = as shown number of mice from b) at least two experiments d) one experiment (day 7 and 21) and two experiments (day 14). Kruskal-Wallis followed by a Dunn's multiple comparisons. Mean is shown by horizontal lines.

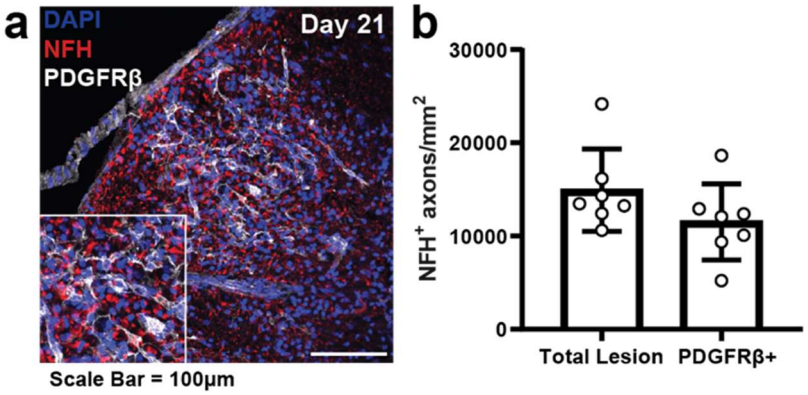

Figure 2.8) Axon densities are unchanged in fibroblast niche. a) Representative confocal images of day 21 LPC lesions labelled with a) DAPI (blue), NFH (red), PDGFRβ (white), b) Graph comparing PDGFRβ-positive niche compared with whole lesion. Sample sizes n = as shown number of mice from two experiments. Two-tailed, unpaired t-test comparing groups. Data are the mean ± s.d.

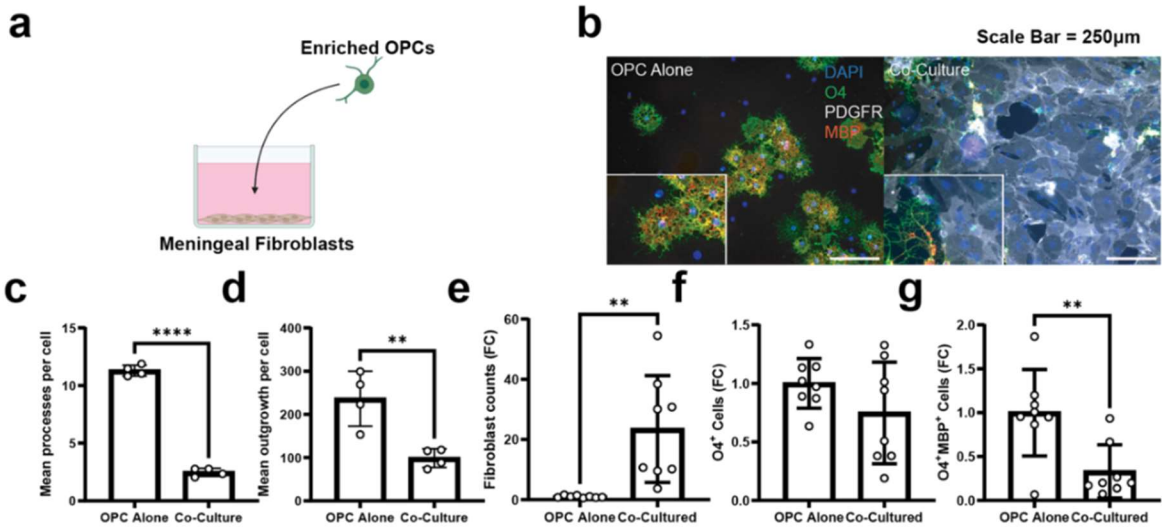

Figure 2.9) Fibroblasts impeded OPC differentiation in vitro. a) Schematic of experimental design. OPC enriched cultures were added to meningeal fibroblast cultures. b) representative widefield microscopy images of OPC cultured alone or with meningeal fibroblasts labelled with DAPI (blue), PDGFRβ (white), O4 (green), MBP (red). c-g) Graphs comparing OPCs cultured alone with co-cultures. c) mean $O4^+$ processes per cell, d) mean $O4^+$ outgrowth per cell, e) fold change in $PDGFR\beta^+$ fibroblast counts, f) fold change in $O4^+$ cells OPCs, g) fold change in $O4^+MBP^+$ mature oligodendrocytes. Olig2-positive cells contacting or note contracting PDGFRβ-positive immunoreactivity 7, 14, and 21 dpi. d) Graph comparing GFP-positive area in PDGFRβ-positive and PDGFRβ-negative regions of LPC lesions 7, 14, and 21 dpi. Significance is indicated as *P < 0.05, **P < 0.01, ***P < 0.001, ****P < 0.0001. Sample sizes n = as shown c,d) number of technical replicates, e-g) number of technical replicates from two experiments. Two-tailed, unpaired t-test comparing groups. Data are the mean ± s.d.

To test the hypothesis that CNS fibroblasts impair OPC responses, we cultured meningeal fibroblasts and OPCs together (Fig 2.9a, b). OPCs cultured in the presence of meningeal fibroblasts had significantly fewer mean processes and outgrowth per cell (Fig 2.9c-e) despite no change in the density of O4+ OPCs (Fig 2.9f). As well, there were significantly fewer MBP+O4+ cells in the co-cultures (Fig 2.9g).

Next, we increased the number of fibroblasts in culture, and this resulted in further reduction in OPC differentiation (Fig 2.10a-c). Surprisingly, staggering the order in which cells were added to co-cultures did not have an effect on the inhibition (Fig 2.10d-f). To test whether the fibroblasts inhibitory effects were due to cell-cell interactions or soluble factors we cultured OPCs with fibroblasts or fibroblast culture medium (Fig 2.10g-j). Though culturing OPCs in fibroblast conditioned medium did appear to reduce indications of differentiation, only co-cultures showed significant reductions Fig 2.10g-j). These data provides evidence that CNS fibroblasts can impair OPC differentiation in a cell-cell dependent manner and may contribute to reduced myelination.

To seek to test the hypothesis that fibroblasts impair OPC differentiation in vivo, we used two methods to attempt to deplete CNS fibroblasts. First, an adeno-Cre system to express thymidine kinase in PDGFRβ+ cells was used. Treatment of thymidine kinase expressing cells with ganciclovir causes these cells to undergo apoptosis in proliferating cells (Fig 2.11a). Following LPC mice were treated for 14 days with ganciclovir but this resulted in no change in lesion or PDGFRβ volumes (Fig 2.11b-f). We then used an inducible diphtheria toxin receptor (DTR) mediated cell ablation model. DTR expression was induced by Cre expression in PDGFRβ+ cells following tamoxifen treatment. Mice were injected I.P. with diphtheria toxin (DT) daily for 7 days after LPC. There were no significant differences in lesion or PDGFRβ volume between DT and control groups (Fig 2.12).

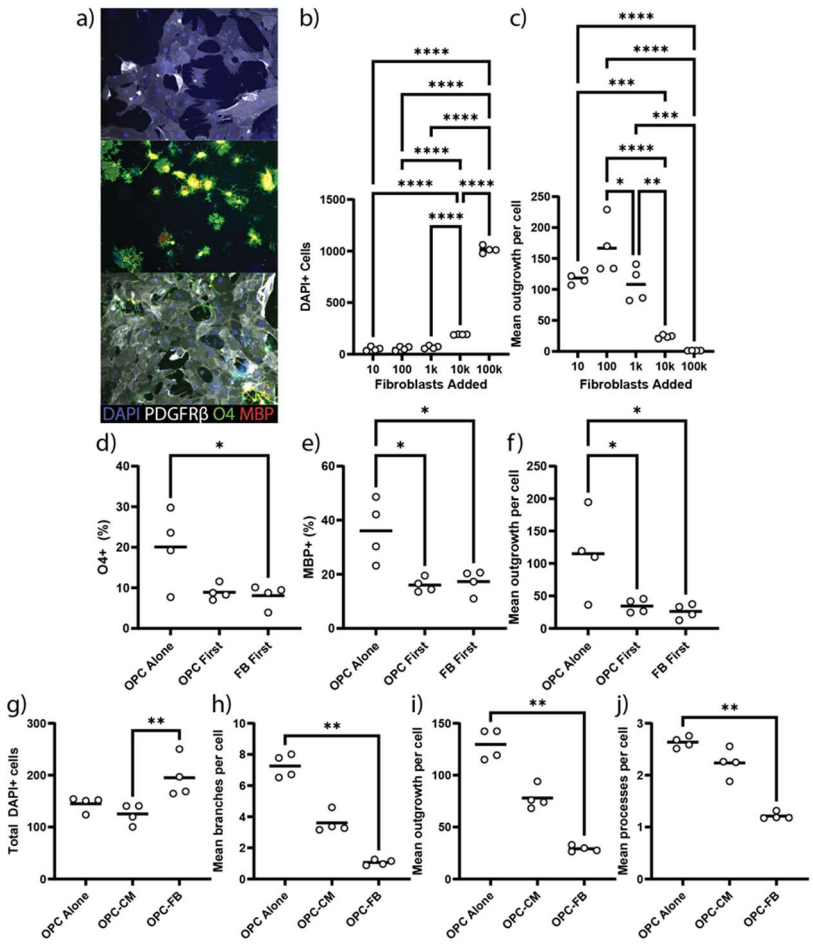

Figure 2.10) Fibroblasts reduce OPC differentiation in a dose dependent manner. a) Representative widefield microscopy images of fibroblasts alone (top), OPCs alone (middle), and co-cultures (bottom) labelled with DAPI (blue), PDGFRβ (white), O4 (green), MBP (red). b) Graphs comparing total DAPI$^+$ cells with 10, 100, 1k, 10k, 100k fibroblasts added. c) Mean outgrowth per cell with 10, 100, 1k, 10k, 100k fibroblasts added. d-f) Graphs comparing OPCs cultured alone, added before fibroblasts or after fibroblasts showing d) percentage of culture O4-positive, e) percentage of culture MBP-positive, f) mean outgrowth per cell. g-j) Graphs comparing OPCs cultured alone, with fibroblast conditioned medium (CM), or with fibroblasts showing g) total DAPI$^+$ cells, O4$^+$ h) mean branches per cell, i) mean outgrowth per cell, j) mean processes per cell. Significance is indicated as *P < 0.05, **P < 0.01, ***P < 0.001, ****P < 0.0001. Sample sizes n = as shown number of technical replicates. Kruskal-Wallis followed by a Dunn's multiple comparisons. Mean shown as horizontal line.

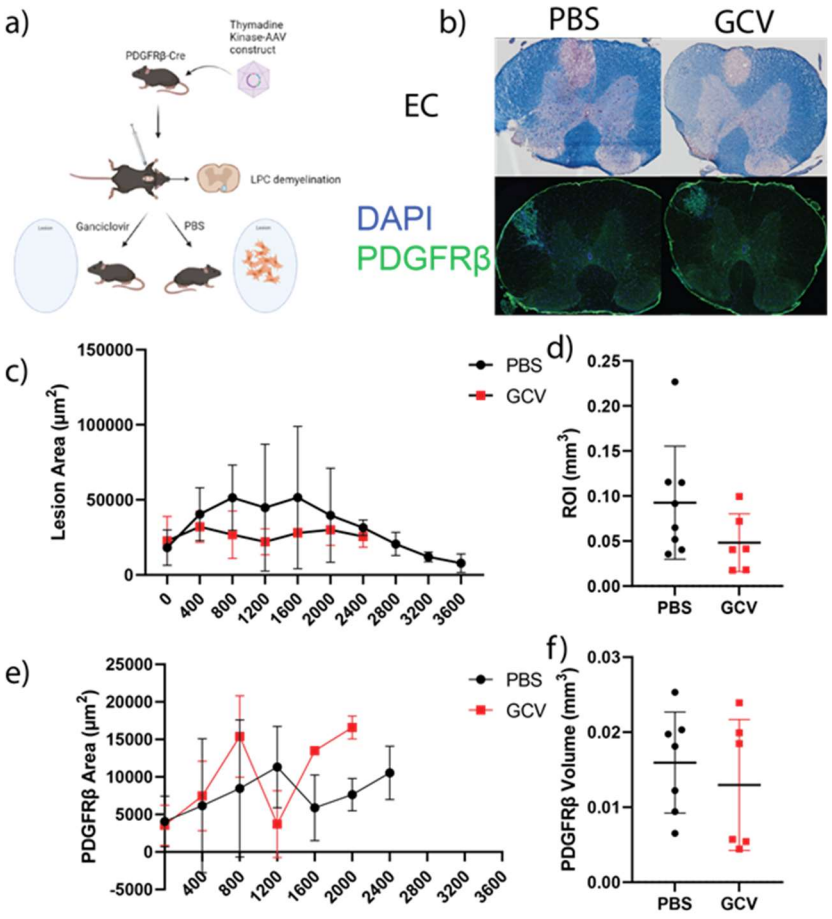

Figure 2.11) PDGFRβ-TK adeno-cre system did not deplete fibroblasts. a) Schematic of AAV-Cre recombinase system and experimental design. b) Representative widefield microscopy images of eriochrome cyanine (EC) and immunofluorescent labeling of DAPI (blue) and PDGFRβ (green). c, e) histograms showing lesion and PDGFRβ spread. d, f) graphs quantifying d) lesion volume in c, f) PDGFRβ volume in e. Sample sizes c, d) n = 8 PBS, n = 6 GCV, e, f) n = 7 PBS, n = 6 GCV from two experiments. Two-tailed, unpaired t-test comparing groups.

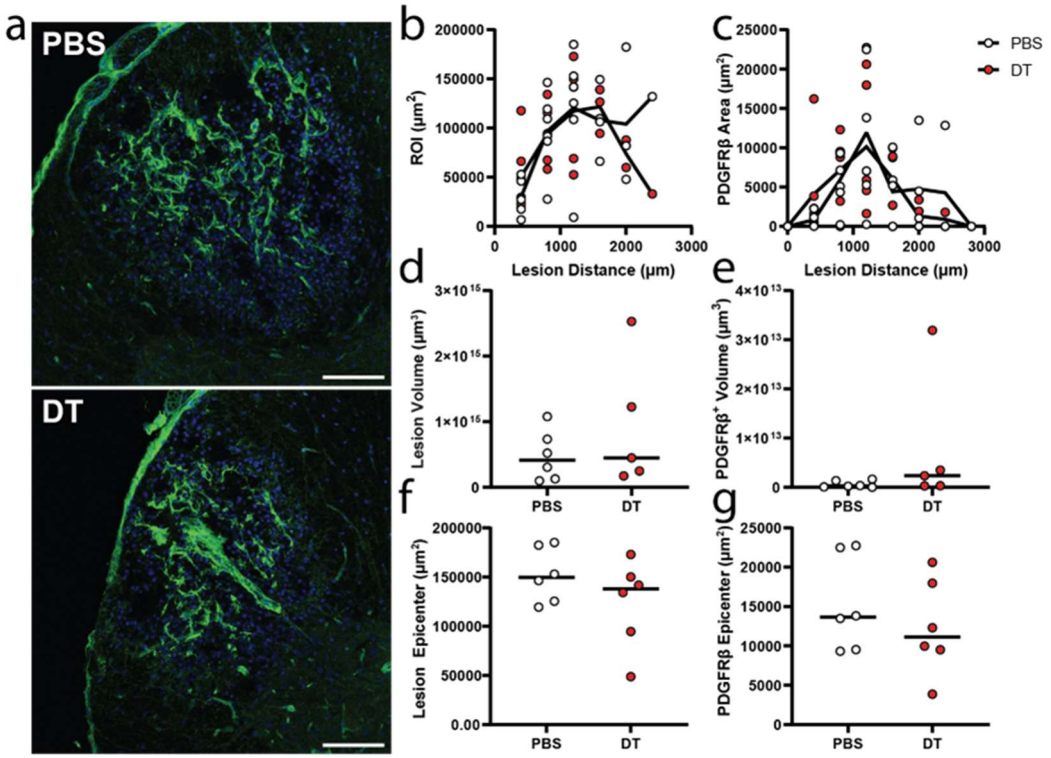

Figure 2.12) PDGFRβ-DTR mice treated with diphtheria did not deplete fibroblasts. a) representative confocal images of PBS and DT treated mice labeled with DAPI (blue), PDGFRβ (green). b, c) histograms showing lesion and PDGFRβ spread. d, e) Graphs showing total d) lesion volume, e) PDGFRβ volume. f, g) Graphs showing peak area of f) lesion epicentre, g) PDGFRβ epicentre. Sample size, n = 6 mice for all groups from two experiments. Two-tailed, unpaired t-test comparing groups

2.5) Discussion

Previous work has demonstrated that CNS fibroblasts are elevated in CNS lesions following acute, chronic, and neuroinflammatory insults(D. O. Dias et al., 2021; Dorrier, Jones, et al., 2021). We have demonstrated that the elevation of fibroblasts spatially and temporally parallels the microglia/macrophage response and has detrimental effects on OPC function.

Prior investigation into the involvement of CNS fibroblasts in OPC function used the EAE neuroinflammation model of MS(Dorrier, Aran, et al., 2021; Yahn et al., 2020). The stochastic nature of lesion formation in EAE makes it difficult to accurately study CNS regeneration. In contrast, the defined course of injury and recovery as well as the reproducible spatial position of lesions makes the toxin induced LPC model ideal for studying regenerative processes(Keough et al., 2015; Kotter et al., 2005; Ousman & David, 2000; Plemel, Michaels, et al., 2017).

Immune-fibroblast interactions have been shown to be critical for cancer and immune tolerance(Buechler, Fu, et al., 2021; Nitta et al., 2020). In both LPC and MS lesions we observe fibroblasts in close proximity to immune cells. In LPC the onset of inflammation closely aligns with the incidence of fibroblast elevation. Indeed, we describe here that meningeal fibroblasts showed greater migration when added to BMDM cultures compared to medium alone. There are undoubtedly many factors expressed by macrophages that influence fibroblast responses. Expression of TGF-β, amphiregulin (Areg), PDGF, and IL-6 by macrophages act on fibroblasts to influence their activation, proliferation, and migration(Buechler, Fu, et al., 2021). Interestingly, many of these factors are found in significant levels in lesions of LPC and MS(Hinks & Franklin, 1999; Wheeler et al., 2023). Additional research is needed to elucidate the in vivo role of inflammation on the fibroblast populations in CNS injury.

It is likely that the models used in our study to deplete microglia/macrophages were unsuccessful due to more rapid than anticipated hematopoietic cell turnover(Patel et al., 2021). The CX3CR1-DTR model used to deplete microglia and CNS associated macrophages involves a 3-4 week waiting period following tamoxifen treatment to allow for monocyte renewal(Plemel et al.,

2020). However, the half-life of blood monocytes is 20-50 hours which may have resulted in DTR- cells obscuring any depletion that occurred(Patel et al., 2021).

We find that the elevation of fibroblasts in CNS lesions does not occur immediately but reaches its peak at 7 days. The existence of fibrosis in LPC lesions has been previously described at the ultrastructural level but comprehensive descriptions have been lacking(Blakemore et al., 1977; Dorrier, Aran, et al., 2021). Despite the partial reduction in lesion size at later points of LPC, fibroblasts remained at comparable levels throughout the injury. This consistent presence of fibroblasts in the core of the LPC lesions allows them access to OPCs, microglia/macrophages, and injured and degenerating axons at critical stages of regeneration(Blakemore et al., 1977; G. J. Duncan et al., 2017; Plemel, Michaels, et al., 2017).

The fibroblast occupied niche within LPC lesions has a scarcity of oligodendrocyte lineage cells and newly myelinating oligodendrocytes. While it remains uncertain whether fibroblasts occupy these regions due to a lack of oligodendrocytes or vice versa we have shown that CNS fibroblasts have the potential to impede OPC function. This is despite the similar axonal density between fibroblast occupied regions and the rest of the lesion area. CNS fibroblasts express an array of ECM inhibitory to OPC function including FN1 and Col1a1(Dorrier, Aran, et al., 2021). As well, secretion of ECM by CNS fibroblasts creates and maintains defined tissue niches during development and inflammation(DeSisto et al., 2020; Pikor et al., 2015). Further studies are needed to determine whether CNS fibroblasts cells contribute to the formation of specific regional environments in CNS lesions.

The lack of fibroblast depletion in the PDGFRβ-DTR and GCV models that we utilized makes it difficult to conclude with certainty that fibroblasts are responsible for impeding oligodendrocyte lineage cells and newly myelinating oligodendrocytes in certain areas of the lesion. The PHP.eB AAV vector used in this study has broad tropism for CNS cells(Chan et al., 2017; Mathiesen et al., 2020). The uptake of this AAV occurs through LY6A and PKD2(Jang et al., 2022). Transcriptomic studies of CNS vascular cells suggests that these receptors are expressed at low levels by fibroblasts potentially explaining the lack of depletion(Vanlandewijck et al., 2018).

Alternatively, CNS fibroblasts have significant self-renewal capacity and may be able to overcome depletion(Dorrier, Aran, et al., 2021; Xu et al., 2022). Finally, it is possible that other cells normally negative for PDGFRβ such as endothelial cells or meningeal epithelial barrier cells undergo endothelial and epithelial to mesenchymal transition upregulation genes normally expressed by fibroblasts(Derk et al., 2021; Sun et al., 2022).

In summary, our findings of this chapter provide a characterization of the fibroblast response following CNS injury, identifies potential mechanisms of their elevation in the LPC lesion environment, and proposes fibroblasts as mediators of OPC function. In the next chapter we expand our focus to investigate the potential consequences of aging on the fibroblast response to injury in the CNS.

Chapter 3: Aging exacerbates the fibroblast response to CNS injury

3.1) Abstract

In light of findings from chapter 2 that show that fibroblasts are elevated in LPC lesions and that macrophages can promote their migration, this chapter investigates the influence of age in regulating the fibroblast response to CNS injury. These findings represent the first characterization of how age affects the fibroblast response to CNS injury.

The findings presented in this chapter are in preparation for publication.

Author contributions to this chapter include S. Ghorbani for EAE tissue used in figure 3.2, C. Li and D. Moezzi for meningeal tissue used to generate fibroblast cultures used in figures 3.7, M. MØrch for help generating BMDMs used in figure 3.7. All other experiments, and the writing of this chapter, were completed by B.M. Lozinski. V.W. Yong supervised B.M. Lozinski, M. MØrch, C. Li, D. Moezzi, and S. Ghorbani, and contributed input.

3.2) Introduction

In most organs, fibroblasts are the cells responsible for deposition and maintenance of tissue extracellular matrix (ECM)(Rodrigues et al., 2019). During tissue injury fibroblasts display a range of functions including ECM remodeling, growth factor and cytokine secretion, and providing mechanical stability, that are critical for tissue regeneration(Ashcroft et al., 1997; Y. Chen et al., 2021; Yuan et al., 2022). Recently, fibroblasts have been increasingly recognized for their involvement following injury to the central nervous system (CNS)(Dorrier, Aran, et al., 2021; Goritz et al., 2011; Soderblom et al., 2013; Yahn et al., 2020). These fibroblasts originating in the meninges and perivascular spaces around blood vessels become elevated in the CNS parenchyma(D. O. Dias et al., 2021). CNS fibroblasts are essential for sealing the site of injury and ablating them results in open tissue defects(Goritz et al., 2011). However, they are potent producers of ECM components such as collagen and fibronectin that inhibit CNS regeneration(D.

O. Dias et al., 2018; Dorrier, Aran, et al., 2021; Stoffels et al., 2014). Regeneration in the form of axonal regrowth does not normally occur in the CNS after injury(Sofroniew, 2018). However, regeneration of myelin sheaths by oligodendrocytes that mature from oligodendrocyte progenitor cells (OPCs) is commonly seen in demyelinating diseases such as multiple sclerosis (MS)(Franklin & Simons, 2022).

During the course of aging, tissues display declines in function and regenerative capacity(López-Otín et al., 2023). Intrinsic deficits in fibroblasts and other stem cell populations contribute to this impaired regeneration and contribute to chronic injuries and diseases(Ashcroft et al., 1997; Eming et al., 2014). Common traits of aging tissues include elevated levels of inflammatory molecules and increased fibrosis(Chambers et al., 2021; Doles et al., 2012; Stearns-Reider et al., 2017). Similar age-associated deficits are seen in the CNS and during remyelination(S. Shen et al., 2008). As previously shown(Bolte et al., 2023; Dorrier, Aran, et al., 2021), CNS fibroblasts express several ECM components inhibitory to OPC function and are associated with reduced OPC response to injury. However, it is unknown whether CNS fibroblasts display similar age-associated deficits as described in other organs(Y. Chen et al., 2021).

We hypothesize that the fibroblast response after a CNS injury suffers from age-associated dysfunction that is the result of known age-associated traits, such as a dysregulated immune response, and that these contribute to age-associated OPC dysregulation. Here, we test this hypothesis.

3.3) Methods

3.3.1) Mice

All experiments were conducted with ethics approval from the Animal Care Committee at the University of Calgary under regulations of the Canadian Council of Animal Care. Six-10 week and 52-week-old female C57BL/6J mice were acquired from Jackson laboratories. Female mice were used to replicate the prevalence of MS in females. Male and female CD1 pups of postnatal day 0-2 were used for OPC and meningeal fibroblast cultures. C57BL6 female mice 6-10 weeks of age were used for BMDM cultures. All mice were maintained on a 12-h light/dark cycle with food (Pico-Vac Mouse Diet 20) and water given ad libitum.

3.3.2) Spinal Cord Surgery

Lysolecithin/lysophosphatidylcholine (LPC) demyelination was accomplished as previously described(Keough et al., 2015). Mice were anaesthetized with intraperitoneal injections of ketamine (100 $mgkg^{-1}$) and xylazine (10 $mgkg^{-1}$). Buprenorphine (0.05 $mgkg^{-1}$) was injected subcutaneously immediately prior to surgery and 12 h post-surgery as an analgesic. The surgery site was shaved and disinfected with 70% ethanol and betadine. Ophthalmic gel was applied to both eyes to prevent drying throughout the surgery and recovery period. Animals were positioned on a stereotaxic frame and a midline incision 2-3 cm long was made between the shoulder blades using a #11 scalpel blade. The T2 vertebra was exposed by separating the muscle and adipose tissue with a retractor. The intervertebral space between T3 and T4 was identified using T2 as a landmark. The T3-T4 tissue was blunt dissected apart and the dura was removed using a 30-gauge metal needle. Using a 32-gauge needle attached to a 10 µL Hamilton syringe, 0.5 µL of 1% w/v LPC (Sigma-Aldrich, L1381) was injected into the ventral column of the spinal cord at a rate of 0.25 $\mu Lmin^{-1}$ for 2 min. The needle was left in place for 2 min following the injection to avoid back flow. The muscle and skin were then sutured, and mice were placed in a thermally controlled environment for recovery.

3.3.3) Experimental autoimmune encephalomyelitis (EAE) induction

Young (8-week) and middle-aged (52-week) female C56BL6 mice (Jackson Laboratories) were subcutaneously injected with 50µg per 100 µL MOG 35-55 peptide (Protein and Nucleic Acid Facility, Stanford University School of Medicine) in complete Freund's adjuvant supplemented with 4mgmL^{-1} heat-inactivated Mycobacterium tuberculosis H36a (Sigma-Aldrich). A total of 50 µL emulsion was deposited on either side of the tail base. Pertussis toxin (300 ng per 200 µL; 180, List Biological Laboratories) was intraperitoneally injected on days 0 and 2 after MOG immunization. Daily monitoring of EAE mice was performed, and the mice were scored on a 0-15 scale(Weaver et al., 2005). For the tail, 0 signifies no signs, a score of 1 represents a half-paralyzed tail and a score of 2 reflects a fully paralyzed tail. For each of the hind- or forelimbs, 0 is for no signs, a score of 1 is given to a mouse with a weak or altered gait, 2 represents paresis, while a score of 3 reflects a fully paralyzed limb. Mortality corresponds to a score of 15.

3.3.4) Spinal Cord Tissue Isolation

LPC and EAE mice were anaesthetized with intraperitoneal injections of ketamine (100 mgkg^{-1}) and xylazine (10 mgkg^{-1}). LPC spinal cords were collected at 3-, 7-, 14-, or 21-days post-surgery. EAE mice were euthanized, and spinal cords collected 12 days post onset of clinical signs with average EAE scores of 7.8 (young) and 7.6 (middle-aged) on a 15-point scale. Mice were then transcardially perfused with a total of 15mL of PBS. Spinal cords were dissected from the back of the mouse, and the tissue between the lower cervical and lower thoracic (LPC) or thoracic (EAE) regions was collected into 4% paraformaldehyde (PFA) in PBS for 24-hour fixation. Spinal cords were then transferred to 30% w/v sucrose solution for dehydration for at least 72-hours. Spinal cords were then frozen in FSC 22 frozen section media (Leica). Using a cryostat (ThermoFisher Scientific), spinal cord tissue was coronally cut in 20µm sections onto Superfrost Plus microscope slides (VWR) and stored at -20^{o}C until analysis.

3.3.5) Immunofluorescence staining

Slides were thawed at room temperature then rehydrated with PBS for 10 minutes and permeabilized with 0.2% TritonX-100 in PBS for 10 minutes. Tissue was blocked by adding hose serum blocking solution (0.01 M PBS, 10% horse serum, 1% bovine serum albumin (BSA), 0.1% cold fish skin gelatin, 0.1% Triton-X100, and 0.05% Tween-20) for 1 hour at room temperature. Primary antibodies were resuspended in antibody dilution buffer (PBS, 1% BSA, 0.1% cold fish stain gelation, 0.1% Triton X-100) and added to tissue overnight at RT. Slides were then washed three times, 5 minutes each, using PBS, and stained with TrueBlack Lipofuscin Autofluorescence Quencher according to the manufacturer's instructions (Biotium) for 2 min at room temperature. Tissues were washed three more times, 5 minutes each, then incubated with secondary antibodies and 1 μgmL^{-1} of DAPI resuspended in antibody dilution buffer for 1 hour at RT. Slides were then washed three more times, 5 minutes each, and coverslips were mounted onto slides using Fluoromount-G solution (SouthernBiotech). EAE slides were thawed at RT, fixed with 4% PFA for 10 minutes, washed twice with PBS. All remaining steps are the same as above.

For multiplexed images, sections were stained as detailed above. After slides were imaged, they were submerged in PBS for 5 minutes and coverslips were carefully lifted from the slide using forceps. Sections were then treated for 5-minutes at RT with NewBlot Nitro 5X stripping buffer (Li-Cor Biosciences)(Maric et al., 2021). Slides were then blocked for 1 hour at room temperature and the remaining steps were listed above. Sections were stripped no more than 24 hours after imaging the previous set of stains.

Antibodies used for immunofluorescence identification of specific targets: anti-mouse myelin basic protein (MBP, BioLegend, PA1-10008), anti-mouse Periostin (POSTN, R&D Systems, AF2955), anti-mouse α-smooth muscle actin-Cy3 (αSMA, Millipore, C6198), anti-mouse Fibronectin (FN1, Millipore, AB2033), anti-mouse leukocyte common antigen conjugated to alexafluor 488 (CD45-AF488, Biolegend, 103122), anti-mouse/human platelet derived growth factor receptor β (PDGFRβ, R&D Systems, AF1042), anti-mouse ionized calcium-binding adaptor molecule1 (Iba1, Wako, 019-19741), Collagen Type I Alpha 1 Chain (Col1a1, Invitrogen, PA1-

26204), anti-mouse sulfatide O4 (R&D Systems, MAB1326), anti-mouse Arginase 1 (Arg1, BioLegend, 678802), major histocompatibility complex class II (MHCII, Thermofisher, 13-5321-82). The following secondary antibodies from Jackson ImmunoResearch were used at 1:400 dilution: Alexa Fluor 488 donkey anti-mouse IgM, Alexa Fluor 488 donkey anti-rabbit IgG, Alexa Fluor 488 donkey anti-rat IgG, Alexa Fluor 488 donkey anti-goat IgG, cyanine Cy3 donkey anti-goat IgG, cyanine Cy3 donkey anti-chicken IgY, Alexa Fluor 647 donkey anti-rat IgG, Alexa Fluor 647 donkey anti-rabbit IgG

3.3.6) Confocal Immunofluorescence Microscopy

Laser confocal immunofluorescence images were acquired at RT using the Leica TCS Sp8 laser confocal microscope or Leica Sp8 Falcon. Images acquired on the Leica TCS were done using a ×25/0.5 NA water objective. The 405-nm, 488-nm, 552-nm and 640-nm lasers were used to excite the fluorophores from antibodies bound to samples and detected by two low-dark-current Hamamatsu PMT detectors and two high-sensitivity hybrid detectors on the Sp8. Images acquired on the Leica SP8 Falcon were done using a x20/0.8 NA air objective with 405nm and white light laser (470-670nm) used to excite the fluorophores from antibodies bound to samples. Fluorescence was detected by one low-dark-current Hamamatsu PMT detector, one cooled high sensitivity, single molecule detection hybrid detector, and two high sensitivity hybrid detectors. All images were acquired using the following parameters: in 8 bits, in a z-stack using unidirectional scanning, 1 times frame averaging, 1 airy unit pinhole, ×1 zoom, 0.57 µm or 1 µm per optical section, and 2,048 x 2,048 or 1024 x 1024 pixels x–y resolution. Equal laser, gain and offset settings to maximize contrast and minimize saturation were consistently used for all samples within each set of experiments. For volume measurements every section with a lesion was imaged. For all other analysis, lesion epicentres were acquired. For mice with EAE, at least 6 images were taken of inflamed areas as determined by CD45 stain for each biological replicate for analysis.

3.3.7) Cell Culture

3.3.7.1) Mouse meningeal fibroblasts

Brains from postnatal day P0-2 CD1 mouse pups were isolated, the meninges were removed using a dissection microscope and transferred to serum free RPMI buffer (Sigma) on ice until all meninges were collected. Meninges were then digested for 18 minutes at 37^{o}C in 1 μgmL^{-1} DNase I (Sigma) and 3.7 μgmL^{-1} collagenase D (Sigma) triturating every 6 minutes. Meninges were centrifuged at 300xg for 3 minutes and supernatant was discarded. Cells were resuspended in growth medium (DMEM (Gibco) supplemented with 10% FBS, 1% non-essential amino-acids (NEAA), 1% GlutaMAX, 1% sodium pyruvate, and 1% Penicillin- Streptomycin (all from Gibco). Cells were then transferred to T-75 flasks and incubated at 37^{o}C with 5% CO_2. Medium was changed every 3 days and cells were passaged when 90% confluent. Cells were passaged by adding 2.5% trypsin for 5 minutes at 37^{o}C. Trypsin was inactivated by adding growth medium, then cells were centrifuged at 300xg for 10 minutes. Cells were resuspended in 10mL of growth medium and run through 100 μm filter. Filtered cells were transferred to either T-75 flasks, or 96-well plates. Cells were used after at least one passage.

3.3.7.2) Mouse Bone marrow derived macrophages (BMDMs)

Mice were sterilized and hair and skin cleared from the lower half of the mouse to expose the lower limbs. Femurs from C57BL6 mice 12 months old were collected in calcium and magnesium free Hank's buffered salt solution (HBSS), and then cells from bone marrow were collected by flushing with DMEM supplemented with 10FBS, 1% Penicillin- Streptomycin and 1% Glutamax (all Gibco) using a 12mL syringe and 25g needle. Samples were then centrifuged at 300xg for 10 minutes, supernatant was discarded cells were then resuspended in BMDM culture medium (10% supernatant from L929 cell line enriched in macrophage-colony stimulating factor], 10% FBS, 1% penicillin-streptomycin, 2% minimum essential medium (MEM) nonessential amino acid solution (all except L929 from Gibco). Cells were cultured in 100mm culture plates at 37^{o}C with 8.5% CO_2 for 9 days with half-medium change at day 5 and full change at day 7. On day 9

BMDMs were collected by adding 3mL of cold PBS and scraping cells off of the plates. Cell suspensions were collected into 50mL tubes and centrifuged at 300xg for 10 minutes, then supernatant was discarded, and cells were resuspended in 1mL of BMDM culture medium for counting.

3.3.8) Transwell migration assay

BMDMs were plated in 24 well plates at a density of 260,000 cells/cm^2 overnight at 37°C with 8.5% CO_2. Cells were serum starved in BMDM culture medium with 1% FBS for 24 hours prior to experiments. Meningeal fibroblasts were added to transwell inserts (Corning, 29442-120) at a density of 150,000 cells/cm^2. Fibroblasts were allowed to migrate for 16-18 hours after which they were fixed and stained. Cells remaining in the upper chamber were removed using a cotton swab after which inserts were fixed with acid alcohol (1% HCl in 95% ethanol) for 15 minutes, washed in PBS for 5 minutes, transferred to hematoxylin for 15 minutes, and washed in PBS again for 1 minutes. Inserts were cut out using a #11 scalpel and mounted on Superfrost Plus microscope slides (VWR) using a small amount of water to adhere and Fluoromount-G solution (SouthernBiotech) to apply coverslips. Mounted transwell inserts were imaged on an Olympus VS110 slide scanner on a 10x/0.4 NA objective and VS-ASW-S5 (V2.9) with Batch Converter software.

3.3.9) Fluorescent image analysis

Leica Application Suite X was used for image acquisition, ImageJ was used for image threshold and particle analysis, and QuPath 0.3.1 was used for transwell and slide scanner image analysis. The z-stacks of confocal images were analyzed using ImageJ. For each image z-stack, maximum-intensity projections were created for each channel/marker. All images were blinded prior to analysis. ROI for lesions were drawn using DAPI or MBP for LPC lesions and DAPI or CD45 for EAE lesions. Threshold intensity was determined using at least 3 images. The Analyze Particles function was then used to create a mask and to quantify the positive signals in each ROI using size

exclusion of 2-infinity. Threshold intensity, size exclusion, and circularity settings for particle analysis were kept constant across all samples for each experimental set. For the representative images shown, the maximum-intensity projection of each channel/marker in a z-stack was merged and displayed using pseudocolors in ImageJ. Only the brightness and contrast settings were adjusted, and consistently between samples, to better display the images.

3.3.10) Quantitative fluorescence microscopy analysis

Labeled cells in 96-well flat-bottom black/clear plates were imaged using a ×10/0.5 NA air objective on an ImageXpress Micro XLS High-Content Analysis system (Molecular Devices). The following filters were used for detection: DAPI, excitation of 387/11 and emission of 447/60; FITC, excitation of 482/35 and emission of 536/40; Cy3, excitation of 531/40 and emission of 593/40; and Cy5, excitation of 628/40 and emission of 692/40. For each well of cells, 9–12 FOVs were imaged for quantitative analysis. Multiwavelength cell scoring analysis in the MetaXpress High-Content Image Acquisition and Analysis software (Molecular Devices) was used to quantify cell survival from the fluorescence microscopy images gathered. For fold change values, all numbers were divided by the mean of the control samples. The fold-change values from all samples and experiments were then plotted for statistical analysis. For the representative images shown, each channel/marker for the sample was merged and displayed using pseudocolors. Only the brightness and contrast settings were adjusted, and consistently between samples, to better display the images.

3.3.11) Luminex

BMDMs from young (10-12 week-old) and middle-aged (52 week-old) mice were isolated as previously described. 30,000 cells were plated in DMEM supplemented with 10% FBS, 1% Pen/Strep, and 1% Glutamax in a 96 well round bottom plate overnight at 37^{o}C with 8.5% CO_2. Cells were changed to 1% FBS medium for 2 hours and stimulated with LPS (100ng/ml)/IFN-γ (10ng/ml), IL-4 (20ng/ml)/IL-13 (10ng/ml), or 1% medium alone for 48 hours. Then, cells were spun at 3000xg for 5 minutes and 100 µL were collected in 0.65mL tubes and stored at -80C. For cytokine

measurements, supernatants were sent to Eve Technologies for Mouse Cytokine 32-Plex Discovery Assay®. Stimulating factors used to stimulate BMDMS include: Lipopolysaccharide (LPS, Sigma, L2630-10MG), Interferon-γ (IFN-γ, Peprotech, 315-05), Interleukin-4 (IL-4, Peprotech, 214-14), IL-13 (Peprotech, 201-13).

3.3.12) Statistical analysis

Data was collated using Microsoft Excel. Graphs were generated using GraphPad Prism 8. Data shown are the individual data points, whereby each point on a bar graph represents a biological replicate (for in vivo experiments) or replicate (for in vitro experiments), and the mean ± s.d. No statistical methods were used to predetermine sample sizes, but our sample sizes were similar to those reported in previous publications(Dong et al., 2021; Plemel et al., 2020; Rawji et al., 2020). No inclusion or exclusion criteria were used unless otherwise stated. Animals and tissue culture samples were randomized when assigned to various experimental groups and conditions. Data collection and analysis were not performed blind to the conditions of the experiment (unless otherwise stated), as all image and data analysis were completed with the same acquisition conditions and analysis thresholds. Statistical tests are as listed in figure legends. Asterisks indicate significance where *P < 0.05, **P < 0.01, ***P < 0.001.

3.4) Results

3.4.1) Aging exacerbates fibroblast accumulation in LPC lesions

We began by looking at LPC lesions in young and middle-aged mice 7- 14-, and 21-days post injury (dpi). These timepoints were chosen as they correspond with a period of substantial OPC repopulation (7 dpi), onset of remyelination (14 dpi), and when there is robust remyelination (21 dpi)(Ruckh et al., 2012). LPC lesioned tissue from young (6-10 week) and middle-aged (48-52 week) old mice were stained for fibroblasts (PDGFRβ), demyelination (intense MBP fragmented profiles), and ECM deposition (Col1a1) (Fig 3.1a). There was no difference in the lesion volume, fibroblast response, or ECM deposition after 7 days (Fig 3.1b-d, k-m). While there was no change in the fibroblast response the proportion of the lesion positive for PDGFRβ was greater in the middle-aged mice (Fig 3.1n). By 14 days LPC lesions in middle-aged mice were significantly larger though there were no statistical differences in PDGFRβ or Col1a1 (Fig 3.1e-g, p-t). After 21 days the aging lesions were larger and had greater PDGFRβ and Col1a1 immunoreactivity than young lesions (Fig 3.1h-j, u-w). Though there was an increase in the proportion of the lesion positive for PDGFRβ in middle-aged mice there was no difference in Col1a1 between age groups (Fig 3.1x, y).

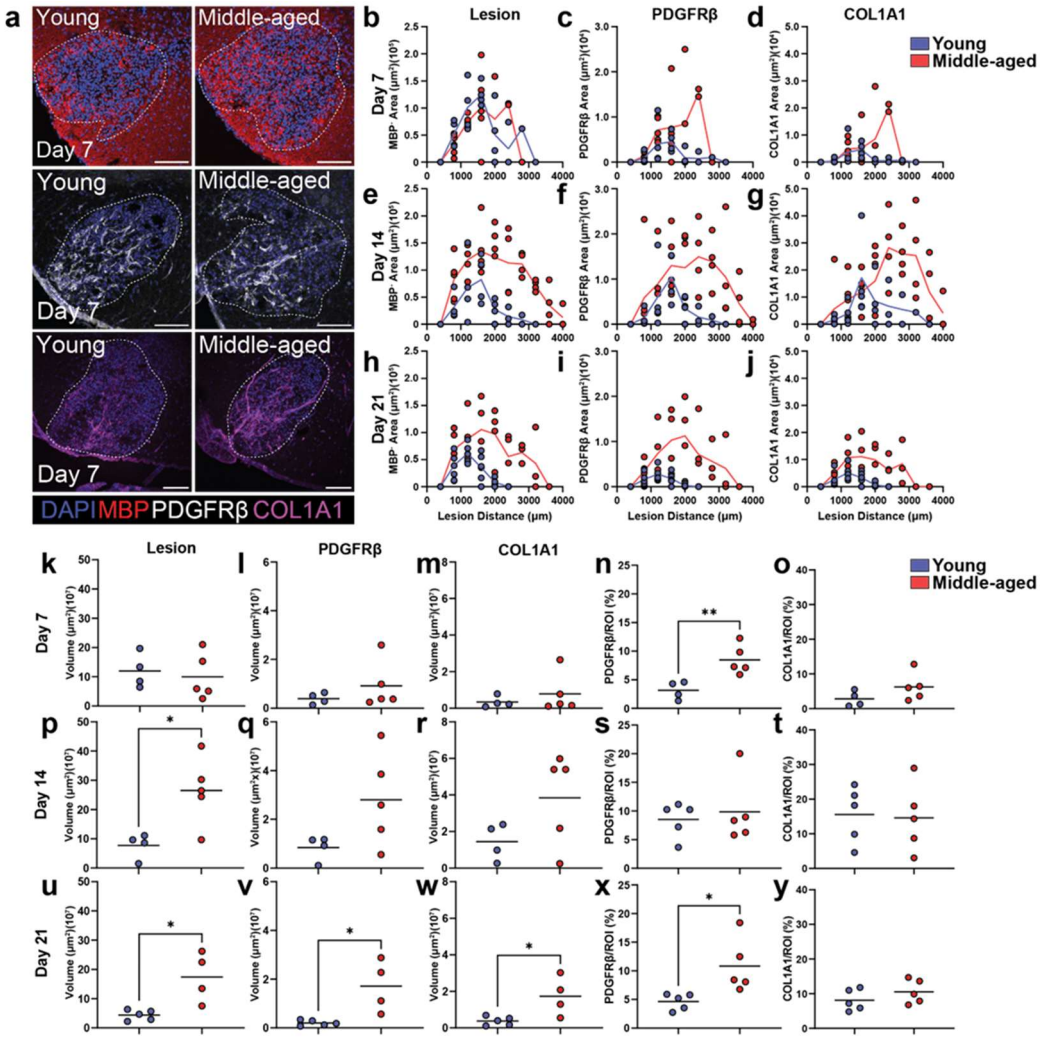

Figure 3.1) Elevation of fibroblasts is exacerbated by age. a) Representative images of young (2-3 month) and middle-aged (12 month) old mice 7 days post injury (dpi) labelled for DAPI (blue), MBP (red), PDGFRβ (white), Col1a1 (magenta). b-j) Histograms of b-d) day 7, e-g) day 14, h-j) day 21 LPC lesions showing b, e, h) spinal cord lesion spread, c, f, i) PDGFRβ spread, d, g, j) Col1a1 spread. k-o) Graphs showing day 7 LPC lesion quantifications. p-t) Graphs showing day 14 LPC lesion quantifications. u-y) Graphs showing day 21 lesion quantifications. k, p, u) Lesion volumes; l, p, v) PDGFRβ volumes; m, r, w) Col1a1 volumes; n, s, x) percent of lesion regions of interest (ROI) positive for PDGFRβ; o, t, y) percent of lesion ROI positive for Col1a1. Sample size n = number of mice from two experiments. Significance is indicated as *P < 0.05, **P < 0.01. Two-tailed, unpaired t-test comparing young and middle-aged mice. Mean shown as horizontal lines.

3.4.2) Fibroblast response is increased in aging EAE mice

As the effect of age on fibroblast responses in the CNS is poorly explored, we looked to validate these findings in the inflammatory demyelinating experimental autoimmune encephalomyelitis (EAE) model(Ghorbani et al., 2022). The disease course followed the histopathology as there was no difference in clinical scores at the time of tissue collection (Fig 3.2a, c). Inflammatory spinal cord lesions were identified by CD45 immunoreactivity (Fig 3.2b). Similar to LPC lesions in middle-aged mice the areas of ongoing inflammation in middle-aged EAE mice displayed greater amounts of PDGFRβ positivity (Fig 3.2b, d).

3.4.3) More fibroblast activation in middle-aged LPC lesions

We next looked at whether the prominent fibroblast presence in middle-aged LPC lesions coincided with altered levels of fibroblast activation. Fibroblasts can become activated by several means including TGF-β and PDGF signaling(Makino et al., 2017; Verrecchia et al., 2001) leading to upregulation of cytoskeletal and ECM genes including smooth muscle actin (SMA) and fibronectin (FN1)(Buechler, Pradhan, et al., 2021; Dorrier, Aran, et al., 2021). As the fibroblast response does not appear prior to 7 dpi in the LPC model we looked in LPC 7 dpi lesions for SMA and FN1 overlapping with PDGFRβ to determine activation. A significant increase in the overlap of PDGFRβ with SMA in middle-aged LPC lesions occurred 7 dpi (Fig 3.3c-d).

One limitation of using SMA as a marker of activation in the CNS is the expression of SMA by smooth muscle cells found on arteries and arterioles(Vanlandewijck et al., 2018). Since PDGFRβ+ cells can be found in proximity to CD31+ endothelial cells within LPC lesions (Fig 3.4) it cannot be ruled out that some amount of SMA positivity in PDGFRβ+ areas represent staining of smooth muscle cells. We therefore looked at FN1, another marker of activation in fibroblasts(Walker et al., 2019). The increase in FN1 in PDGFRβ+ fibroblasts 7 dpi was comparable to the increase in SMA (Fig 3.3).

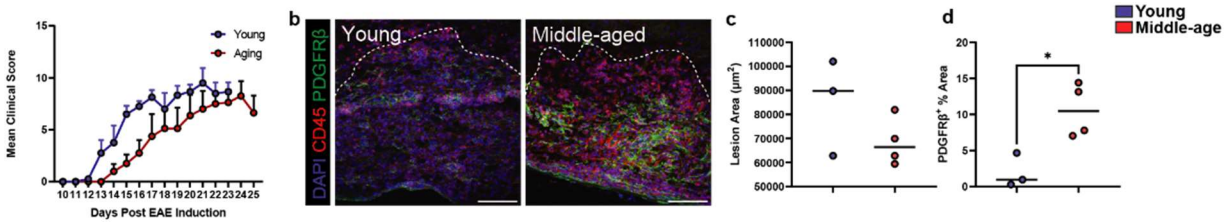

Figure 3.2) Fibroblast response is exacerbated in middle-aged EAE mice. a) Daily average EAE clinical score to day 25. b) Representative confocal images of young and middle-aged EAE lesions labeled with DAPI (blue), CD45 (red), PDGFRβ (green). c) Graph showing quantification of lesion ROI. d) Percentage of lesion ROI positive for PDGFRβ. Sample size n = average of 6 FOV per mouse, n = 4 middle- aged mice, n = 3 young mice. Significance is indicated as *P < 0.05, **P < 0.01, ***P < 0.001. Two-tailed, unpaired t-test comparing young and middle-aged mice. Mean shown as horizontal lines.

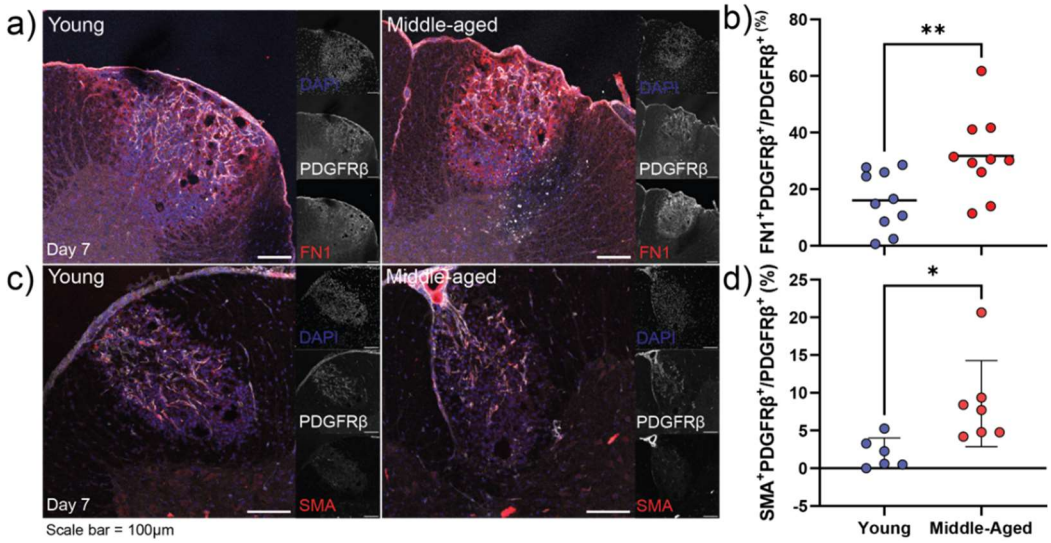

Figure 3.3) Fibroblasts in middle-aged LPC lesions display greater activation. a, c) Representative confocal images of day 7 LPC lesions in young and middle-aged mice labelled for a) DAPI (blue), PDGFRβ (white), FN1 (red), c) DAPI (blue), PDGFRβ (white), SMA (red). b, d) Graphs showing proportion of PDGFRβ-positive area overlapped with b) FN1, d) SMA. Sample size n = as shown number of mice from two experiments. Significance is indicated as *P < 0.05, **P < 0.01, ***P < 0.001. Two-tailed, unpaired t-test comparing young and middle-aged mice. Data is mean ± s.d.

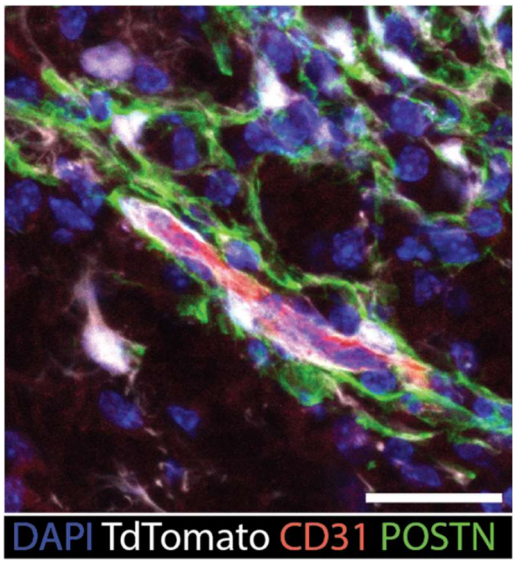

Figure 3.4) PDGFRβ-positive cells do not specifically reside around vasculature. Representative confocal image of LPC lesion in PDGFRβ-Ai9 mice showing PDGFRβ (TdTomato) both in proximity to CD31 endothelial cells and away from them.

3.4.4) Attenuation of immune phenotypes in middle-aged lesions

Macrophages and microglia are the most abundant immune cells in LPC lesions(Ousman & David, 2000; Plemel et al., 2020). Macrophages engage in reciprocal interactions with fibroblasts during homeostasis and injury and become dysfunctional with age(Chambers et al., 2021; X. Zhou et al., 2018). We asked whether an altered immune response occurred in middle-aged mice synchronous with the exacerbated fibroblast response. As macrophages are known to undergo phenotypic changes over the course of injury(Duffield, Forbes, et al., 2005; Miron et al., 2013) we looked at early and later periods of LPC injury. LPC lesions 7- and 21-dpi were investigated using a pan-leukocyte marker (CD45), pan-myeloid cell marker (Iba1), markers of M1-like macrophages (MHCII) and M2-like polarization (Arg1). Iba1 reactivity was reduced in day 7 middle-aged lesions though there was no change in CD45 expression (Fig 3.5a-c). As well, middle-aged lesions 7 dpi had decreased MHCII expression and increased Arg1 expression. From 7-to-21 dpi, young LPC lesions have reduced Iba1 and MHCII expression with CD45 and Arg1 levels remaining stable (Fig 3.5b-e). Conversely, the middle-aged lesions display increased CD45 levels and reduced Arg1 (Fig 3.5b, e). These results are suggestive of a disrupted and attenuated immune response with aging.

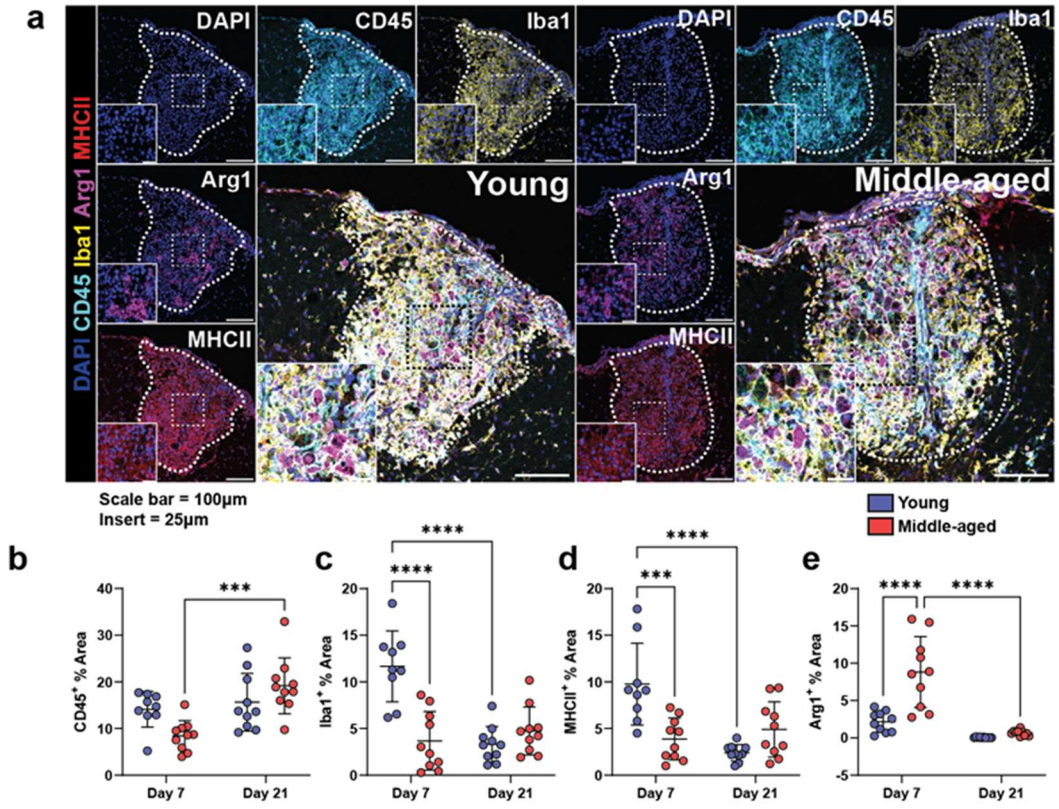

Figure 3.5) Immune phenotypes are attenuated in middle-aged LPC lesions. a) representative multiplexed confocal image of young and middle-aged LPC lesions 7 days after injection showing DAPI (blue), CD45 (cyan), Iba1 (yellow), Arg1 (magenta), MHCII (red). b) graphs quantifying percent of lesion ROI positive for CD45, Iba1, MHCII, Arg1 in 7 and 21 dpi LPC lesions. Sample size n = as shown number of mice from two experiments. Significance is indicated as *P < 0.05, **P < 0.01, ***P < 0.001, ****P < 0.0001. Two-way ANOVA with a Tukey's multiple comparisons of day 7 and 21 LPC lesions in young and middle-aged mice. Data is mean ± s.d.

3.4.5) Aging BMDMs have altered responses to inflammatory cytokines

Previous studies have shown that the lesion environment becomes disordered during aging(Michaels et al., 2020). To investigate how age affects macrophage responses to inflammatory signals bone marrow monocyte derived macrophages (BMDMs) from young and middle-aged mice were polarized in vitro. Conditioned media from young and middle-aged BMDMs stimulated with IFN-γ/LPS, IL-4/IL-13, or medium alone were collected for a Luminex Mouse Cytokine 32-Plex Discovery Assay® (Fig 3.6a). Most age-associated cytokine changes identified by Luminex Elisa were from IFN-γ/LPS stimulation (Fig 3.6a). The chemokines MIP1a/CCL3, MIP1b/CCL4, RANTES/CCL5, and KC/CXCL1 were all elevated in the middle-aged IFN-γ/LPS group (Fig 3.6b). As well, IL12p40 and IL-17 were elevated while G-CSF was reduced in the middle-aged IFN-γ/LPS group were also significantly altered with age.

3.4.6) Aged BMDMs have diminished capacity to promote fibroblast migration

We then asked whether there were functional consequences of macrophage aging for the fibroblast response. BMDMs from young and middle-aged mice were cultured in the lower compartment of a Boyden chamber and meningeal fibroblasts were added to the upper chamber (Fig 3.7a). Interestingly, young BMDMs promoted greater migration of fibroblasts across the transwell membrane while middle-aged BMDMs displayed similar densities of DAPI as the negative control (Fig 3.7b, c).

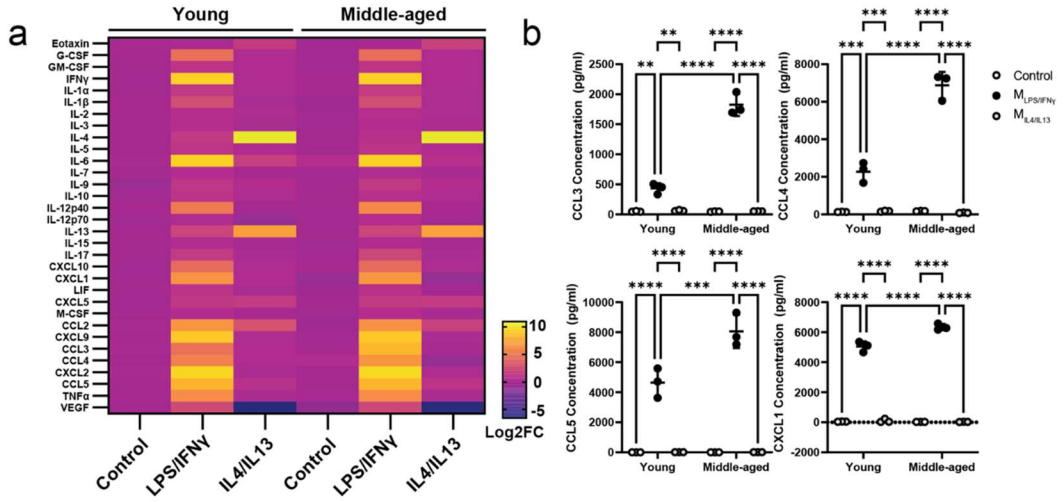

Figure 3.6) Middle-aged BMDMs have altered response to inflammatory stimulus. a) Heatmap Luminex Mouse Cytokine 32-Plex Discovery Assay® panel showing Log2 fold changes in concentration of cytokines following stimulation in young and middle-aged BMDMs. b) Quantification of chemokines significantly elevated in middle-aged BMDMs. Sample size n = 3 technical replicates per group, samples run in triplicate. Significance is indicated as *P < 0.05, **P < 0.01, ***P < 0.001, ****P < 0.0001. Two-way ANOVA with a Tukey's multiple comparisons of control, $M_{LPS/IFN\gamma}$, and $M_{IL\text{-}4/IL\text{-}13}$ stimulation of young and middle-aged BMDMs. Data is mean ± s.d.

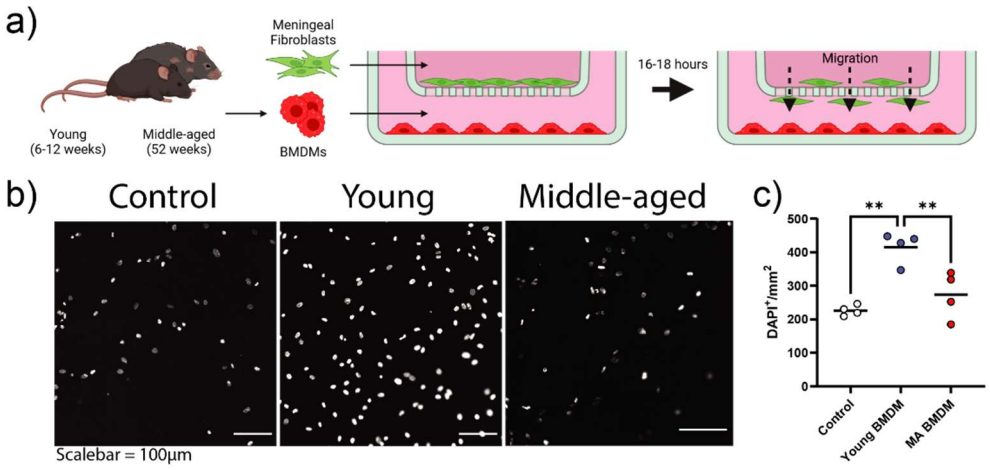

Figure 3. 7) Aging BMDMs fail to promote fibroblast migration in vitro. a) Schematic of transwell migration assay. b) Representative widefield microscopy images of transwell inserts without BMDMs or with BMDMs from young or middle-aged mice. c) quantification of $DAPI^+$ cell density. Kruskal-Wallis followed by a Dunn's multiple comparisons. Sample size n = 4 inserts per group, averaged over 4 fields of view per insert. Significance is indicated as *P < 0.05, **P < 0.01, ***P < 0.001, ****P < 0.0001. Mean shown as horizontal line.

3.5) Discussion

Fibroblasts become elevated in the CNS parenchyma following LPC injury. Their elevation occurs concurrent with microglia/macrophage recruitment to the lesion site(Plemel et al., 2020). In CNS lesions fibroblasts have detrimental effects on regenerative processes including axon regrowth and remyelination. Organs such as the lung, liver, and kidney have reduced regenerative ability in response to injury due partly to age-associated intrinsic changes to tissue resident fibroblasts and greater inflammation(Ashcroft et al., 1997; Y. Chen et al., 2021; Salzer et al., 2018). Following traumatic brain injury meningeal fibroblasts are known to undergo significant alteration in transcriptomic profiles(Bolte et al., 2023). However, it is unknown whether age affects the ability of CNS fibroblasts to respond to parenchymal injury.

We show here that CNS fibroblasts respond more to injury in the middle-aged CNS compared with the young CNS. The aging CNS is prone to injury and neurodegeneration(Dong et al., 2022; Wyss-coray, 2015). That was confirmed here with significantly larger LPC lesions in the middle-aged LPC lesions. It is possible that this contributed to the elevation in fibroblasts in the middle-aged LPC lesions though the proportion of the lesion positive for PDGFRβ was also larger. Likely, inducing a more significant injury is able to influence fibroblast levels in the CNS. This may explain why the representation of fibroblasts in the CNS is more apparent in traumatic injuries such as contusion spinal cord injuries compared to neuroinflammation such as that seen in MS. Injury to the CNS releases alarmins such as IL-1α and ATP that cause neuroinflammation as well as regulate calcium dynamics, proliferation, and survival of fibroblasts(Dong et al., 2021; Gasse et al., 2007).

As well, we show that fibroblasts in middle-aged lesions had elevated levels of activation markers FN1 and SMA. This would suggest a higher level of ECM production and potentially greater tissue fibrosis although later time points are needed for verification. Furthermore, it is unclear whether the expression of ECM like FN1 and COL1A1 directly translate into their integration into the tissue stroma. Aging fibroblasts have been shown to display reduced matrix adhesion and

impaired integration of ECM into the tissue matrix(Chandrasekhar et al., 1983; Takaya et al., 2022). This could be potentially important as ECM components can act as receptor ligands potentially exacerbating injury in the aged CNS. Fibronectin can bind and activate toll-like receptors (TLRs) leading to expression of inflammatory cytokines like IL-1β and TNF and enhancing T cell proliferation(Fei et al., 2018; Lasarte et al., 2007).

In the previous chapter we showed that the fibroblast response occurs alongside the microglia/macrophage response. As well, previous reports have demonstrated that immune cells are affected during aging(Dong et al., 2022; Mrdjen et al., 2018; Rawji et al., 2020). Middle-aged lesions displayed greater levels of Arginase 1, a commonly used marker of anti-inflammatory macrophages(Jensen et al., 2018). Arg1 is potentially important for elevations in ECM seen in middle-aged lesions as it is associated with collagen metabolism(Witte & Barbul, 2003). Urea is converted into L-ornithine at which point it is converted into polyamines necessary for proliferation and L-proline which makes up 10% of the amino acids in collagen(Karna et al., 2020; Z. Li et al., 2022). However, despite its association with collagen levels and tissue fibrosis, depleting Arg1 in macrophages significantly worsens fibrosis(Pesce et al., 2009). As well, it has been made apparent that single markers may obscure from a broader spectrum of gene expression(Locatelli et al., 2018; Ransohoff, 2016). In EAE many Arg1 positive cells express varying levels of inducible nitric oxide synthase (iNOS) highlighting the complexity within immune responses(Locatelli et al., 2018). However, it is clear the aging immune response is diminished from that of the young. This previously was shown to include improper debris removal(Rawji et al., 2020), greater inflammatory phenotypes(Dong et al., 2022), and contributes to age-associated remyelination impairment(Ruckh et al., 2012). Our findings describing reduced immune cell numbers is consistent with previous descriptions of immune cell subsets in age-related disorders such as Alzheimer's disease(Mrdjen et al., 2018).

As well, we describe that middle-aged BMDMs increase expression of several genes in response to LPS/IFN-γ including CCL3, CCL4, CCL5, and CXCL1. LPS and IFN-γ pathways converge through NFkB, AP1, and IRF(Pulido-Salgado et al., 2018) though all age-affected

proteins were downstream of NFkB(Naamane et al., 2007). Interestingly, NFkB is known to underly age-associated tissue inflammation and several target genes such as *Il1b and Lgals3* are elevated in aging LPC lesions(Michaels et al., 2020; O'Brown et al., 2015). Whether NFkB signaling specifically drives age-related immune dysfunction in aging LPC lesions, and what effect this has on the fibroblast response are unknown.

Taking the expression of several chemokines with our findings from the previous chapter suggest a role for macrophages in promoting fibroblast migration; thus, we hypothesized that aged macrophages would promote increased migration of fibroblasts. Unexpectedly the aged macrophages had reduced migration similar to the controls. It is possible that middle-aged BMDMs promote differentiation of the fibroblasts reducing their migratory potential. This is consistent with the elevated activation of fibroblasts in middle-aged LPC lesions.

We propose that age exacerbates the fibroblast response to CNS injury potentially as a result of a disordered immune response. This chapter contributes to our knowledge of how CNS injuries are affected by age by providing the first description of age-associated exacerbation of the CNS fibroblast response after neural injury.

Chapter 4: Exercise rapidly alters proteomes in mice following spinal cord demyelination

4.1) Abstract

Following the results of the previous chapters that describe fibroblast responses to injury including in age, and the inhibitory effect of fibroblasts for OPC differentiation, the purpose of this chapter was to investigate the ability of physical activity/exercise to modulate the environmental milieu of the CNS following LPC injection. Exercise affords broad benefits for PwMS including less fatigue, depression, and improved cognition. In animal models of MS, exercise has been shown to improve remyelination, decrease blood–brain barrier permeability and reduce leukocyte infiltration. Despite these benefits many PwMS refrain from engaging in physical activity. This barrier to participation in exercise may be overcome by uncovering and describing the mechanisms by which exercise promotes beneficial changes in the CNS. Here, we show that acute bouts of exercise in mice profoundly alters the proteome in demyelinating lesions. Following lysolecithin induced demyelination of the ventral spinal cord, mice were given immediate access to a running wheel for 4 days. Lesioned spinal cords and peripheral blood serum were then subjected to tandem mass tag labeling shotgun proteomics workflow to identify alteration in protein levels. We identified 86 significantly upregulated and 85 downregulated proteins in the lesioned spinal cord as well as 14 significantly upregulated and 11 downregulated proteins in the serum following acute exercise. Altered pathways following exercise in demyelinated mice include oxidative stress response, metabolism, and transmission across chemical synapses. Similar acute bout of exercise in naïve mice also changed several proteins in the serum and spinal cord, including those for metabolism and anti-oxidant responses. Improving our understanding of the mechanisms and duration of activity required to influence the injured CNS should motivate PwMS and other conditions to embrace exercise as part of their therapy to manage CNS disability.

Chapter 4 is a published original manuscript and was the joint effort of Brian Mark Lozinski, Luiz Gustavo Nogueira de Almeida, Claudia Silva, Dr. Yifei Dong, Dennis Brown, Sameeksha Chopra, Dr. Wee Yong, and Dr Antoine Dufour. The citation for the article is listed below:

Lozinski BM, de Almeida LGN, Silva C, Dong Y, Brown D, Chopra S, Yong VW, Dufour A. Exercise rapidly alters proteomes in mice following spinal cord demyelination. Sci Rep. 2021 Mar 31;11(1):7239. This is a pre-copyedited, author-produced version of an article accepted for publication in Scientific Reports following peer review. The version of record is available online at https://www.nature.com/articles/s41598-021-86593-5 and https://doi.org/10.1038/s41598-021-86593-5.

Author contributions to this chapter are as follows. Brian M. Lozinski did LPC surgeries, spinal cord harvest, tissue sectioning, immunohistochemical stains and immunofluorescence stains, images sections, analyzed images and data and wrote the manuscript. Luiz .G.N. de Almeida collected and analyzed the data and wrote the manuscript. Claudia Silva and Dennis Brown helped in the collection of tissue and serum. Dr. Yifei Dong helped in collection of samples, data analysis and wrote the manuscript. Sameeksha Chopra helped in running the proteomics. Dr. Wee Yong. and Dr. Antoine Dufour designed the study, analyzed the data, and wrote the manuscript. All authors reviewed the manuscript. Cristian Santa-Maria provided middle-aged exercise tissues used in addendum, Brian M. Lozinski generated young exercise and sedentary tissue, did LPC surgeries, harvested spinal cords, stained, imaged, and analyzed images and data.

4.2) Introduction

Multiple sclerosis (MS) is an inflammatory neurodegenerative disorder in which immune cells enter the central nervous system (CNS) and destroy myelin and myelin-producing oligodendrocytes, as well as neurons and axons(Lassmann, 2018). Studies in people with MS (PwMS) have found that exercise improves outcomes of physical fitness such as fatigue and mobility, as well as CNS related outcomes such as cognition and white matter integrity(Felippe et al., 2019; Motl et al., 2017; Sandroff et al., 2019). Physical activity performed in a regimented fashion with the purpose of improving physical fitness delineates exercise from physical activity itself(Motl et al., 2017). The prior consensus surrounding exercise for PwMS was that their well-being would suffer a detrimental effect due to heat sensitivity and potential aggravation of symptoms(van Praag, 2009). However, as recent studies demonstrate immunomodulatory and clinical benefits of exercise, there is a paradigm shift that now considers exercise as a potential adjunctive therapy for MS and other neurological diseases(Motl et al., 2017; Petzinger et al., 2013), or even as a preventative therapy for those at risk for developing MS(Dalgas et al., 2019). In the inflammatory experimental autoimmune encephalomyelitis (EAE) rodent model of MS, exercise has the potential to delay disease onset and decrease severity of disability(Bernardes et al., 2016; Fainstein et al., 2019; Le Page et al., 1994; Rossi et al., 2009).

Exercise can benefit PwMS in many ways. For example, it has peripheral immunomodulatory effects and promotes the release of anti-inflammatory myokines from the contracting muscle, and it also induces regulatory anti-inflammatory microglia activity within the CNS(Benatti & Pedersen, 2015; Gentile et al., 2019; Jensen & Wee Yong, 2014). Exercise also promotes neurogenesis and gliogenesis through mechanisms that include the elevation of neurotrophic factors(Frodermann et al., 2019; Guo et al., 2019; Jensen & Yong, 2016; Lassmann, 2018; Scheiman et al., 2019). Moreover, exercise in mice facilitates remyelination following lysolecithin-induced spinal cord demyelination(Jensen et al., 2018). Interestingly, exercise was found to work synergistically with clemastine, a known pro-remyelinating drug, to further increase remyelination(Jensen et al., 2018). The concept of exercise as a co-therapeutic administered with

other medications has been termed “MedXercise”, by combining the terms Medication and eXercise (reviewed elsewhere(Lozinski & Yong, 2020)) and may promote further recovery.

Acute bouts of exercise can modulate thousands of molecules in serum samples from human subjects(Sacks et al., 2018). For instance, it can rapidly increase the blood levels of myeloperoxidase (MPO), which is known to recruit macrophages to damaged sites, revealing a potential benefit for PwMS(Reihmane et al., 2012; Sacks et al., 2018). Additionally, it can increase the levels of neuroactive metabolites, such as acetylcholine and kynurenic acid, linking acute exercise to mental health and antidepressant activity(Agudelo et al., 2014; Sacks et al., 2018). However, little is known about the molecular players capable of bridging the effects of acute and chronic responses to exercise.

Despite the apparent benefits of exercise in MS and rodent MS models, PwMS engage in significantly less physical activity than the healthy population(Klaren et al., 2013). Recent consensus for activity levels for PwMS by a group of experts in the field recommend encouraging at least 150 min per week(Kalb et al., 2020). However, besides ambulatory symptoms, the lack of mechanistic understandings on how the CNS is affected by exercise has hampered efforts to motivate PwMS to exercise(Motl et al., 2017). The available evidence from human and animal studies is inconclusive regarding questions such as when exercise should be initiated in relation to relapses, how much is required, and what intensity or paradigm will produce the greatest benefit.

Here, we profiled the spinal cord and serum of mice using quantitative shotgun proteomics to address whether short bouts of exercise may influence the peripheral blood and CNS of naïve animals and following LPC-induced spinal cord demyelination. Our approach has the potential to identify changes at the micro-environment or systemic level, by analyzing the spinal cord and serum, respectively. We demonstrate that access to voluntary running wheel activity over four days is sufficient to induce significant protein level changes within the lesioned spinal cords associated with oxidative stress, metabolism, neurotransmission and proteolytic remodeling of the extracellular matrix. These results provide insight into the impact of exercise on demyelinating injuries.

4.3) Methods

4.3.1) Animals

All experiments were conducted with ethics approval from the Animal Care Committee at the University of Calgary under regulations of the Canadian Council of Animal Care. All mice used were female C57BL/6 mice at 6–12 weeks of age acquired from Charles River (Montreal, Canada). Female mice were used to depict the prevalence of MS in women more accurately. Mice were between 18–21 g in body weight and were maintained on a 12-h light/dark cycle with food (Pico-Vac Mouse Diet 20) and water given ad libitum.

4.3.2) Lysolecithin (lysophosphatidylcholine)-induced demyelination

Demyelination was accomplished as previously described(Keough et al., 2015). Mice were anaesthetized using ketamine (100 mg/kg) and xylazine (10 mg/kg) injected intraperitoneally. Skin overlying surgical site was shaved and disinfected with 70% ethanol and iodine. Ophthalmic gel was applied to both eyes to prevent drying, and buprenorphine (0.05 mg/kg) was injected subcutaneously immediately prior to surgery and 12 h post-surgery as an analgesic. Animals were positioned on a stereotaxic frame and a midline incision approximately 5 cm long was made between the shoulder blades using a #15 scalpel blade. A retractor was used to separate the muscle and adipose tissue to expose the spinal column. The prominent T2 vertebra was used as a landmark to find the T3–T4 intervertebral space. Tissue in the T3–T4 gap was then blunt dissected apart using forceps and spring scissors, and the dura was removed using a 30-gauge metal needle. Using a 32-gauge needle attached to a 10 µL Hamilton syringe, 0.5 µL of 1% lysolecithin/lysophosphatidylcholine (LPC) (Sigma-Aldrich, L1381) was injected into the ventral column of the spinal cord at a rate of 0.25 µL/min for 2 min. The needle was left in place for 2 min following the injection to avoid back flow, followed by suturing of the muscle and skin. Mice were then placed in a thermally controlled environment for recovery.

4.3.3) Exercise paradigm

Immediately following recovery from surgery (~ 1–2 h post-surgery), exercising animals were singly housed in modified rat cages19 with 5 inch running wheels mounted to the wire lid for 4 days. Wheels were connected to a computer system running a software to monitor wheel revolutions (developed in LabVIEW). Rotations per minute (rpm) were recorded in 10-min bins generating an average rpm over that 10-min period. Sedentary control animals were singly housed in modified rat cages with the running wheel placed on the ground as environmental enrichment control. Naïve animals were given access to running wheel cages at the same time as LPC animals.

4.3.4) Serum and tissue collection for proteomics

For the proteomics experiment, serum and lesioned spinal cords were collected from eight different female C57BL6 mice per group and two mice were pooled per sample: naïve without exercise (n = 4), naïve with exercise (n = 4), LPC lesioned without exercise (n = 4) and LPC lesioned with exercise (n = 4). Tissue was harvested 4 h into the dark cycle when animals had reached peak running for 2 h. Mice were anaesthetized using ketamine (100 mg/kg) and xylazine (10 mg/kg) injected intraperitoneally, and 500 µL of whole blood was drawn from the heart using a 1 mL syringe with a 25-gauge needle and collected in a 1.5 mL microcentrifuge tube. Mice were then transcardially perfused with 15 mL of room temperature phosphate-buffered saline (PBS) solution. Spinal tissue from the lower cervical to lower thoracic region was dissected. Tissue was placed on a dissecting microscope set up with dry ice and 2-methylbutane (Sigma-Aldrich) placed underneath the stage allowing for the tissue to be frozen to avoid protein degradation. Spinal cords were trimmed to 5 mm around the lesion site then cut into quarter-sections to include the lesion area. Lesioned quarter-sections from 2 mice were pooled into one sample in a 1.5 mL microcentrifuge tube to allow for sufficient protein levels and left on dry ice until harvesting was finished. Tissue was stored at – 80 °C until the proteomics experiments were performed. Tissue collection for immunohistochemistry followed a different methodology described below.

Whole blood was spun at 1300 rpm (160 g) for 10 min at 4 °C. Supernatant was removed using a pipette being careful to avoid disrupting the red blood cell pellet. As in spinal cords, serum from 2 animals from the same group were pooled, for a final n = 4 sample (from 8 mice) per group.

4.3.5) Quantitative shotgun proteomics using tandem mass tags (TMT) labeling

The four groups of mice were subjected to a quantitative shotgun proteomics analysis. Serum or tissue were lysed in a buffer composed of 1% SDS, 200 mM HEPES (pH 8.0), 100 mM ammonium bicarbonate, 10 mM EDTA and protease inhibitor complete tablets (Roche, 4693159001). Disulfide bonds of 100 µg of total protein were reduced with 10 mM Tris(2-carboxyethyl) phosphine hydrochloride (Thermo Fisher Scientific) at 55 °C for 1 h. The proteins were then alkylated by incubation with 15 mM iodoacetamide (VWR) for 25 min in the dark at room temperature. Proteins were precipitated out of solution by adding 600 µL of ice-cold acetone and incubated at – 20 °C overnight. Samples were centrifuged at 8000g for 10 min before resuspension in 100 µL of 50 mM triethyl ammonium bicarbonate. Proteins were then trypsinized (Thermo Fisher Scientific) overnight at a 1:10 enzyme-to-substrate ratio. For TMT 6-plex labeling, 0.8 mg of TMT reagent (Thermo Fisher Scientific) was resuspended in 41 µL of acetonitrile (ACN), samples were spun down quickly at 2000 rpm (380g) for 10 s, and samples were incubated at room temperature for 1 h. The labelling reaction was quenched by adding 8 µL of 5% hydroxylamine and incubated for 15 min at 25 °C. Peptides with different labels were combined before 100% formic acid was added to each sample to reach a volumetric concentration of 1% formic acid. Samples were spun at 5000 rpm (2350g) for 10 min and then desalted using Sep-Pak C18 columns (Waters, 130 mg WAT023501). Sep-Pak columns were conditioned with 1 × 3 mL 90% methanol/0.1% TFA, 1 × 2 mL 0.1% formic acid. Each sample was loaded onto a column and washed with 1 × 3 mL 0.1% TFA/5% methanol. Peptides were eluted off the column with 1 × 1 mL 50% ACN/0.1% formic acid and lyophilized. Peptides were resuspended in 1% formic acid and a BCA assay (Thermo Fisher Scientific) was used to determine the concentration of peptide in each sample. Samples were dried down and stored at – 80 °C.

4.3.6) High performance liquid chromatography (HPLC) and mass spectrometry

All liquid chromatography and mass spectrometry experiments were carried out by the Southern Alberta Mass Spectrometry (SAMS) core facility at the University of Calgary, Canada. To assure consistency in data collection, HPLC and mass spectrometry data acquisition was replicated from our previous publication(M. H. Gordon et al., 2019). In detail, analysis was performed on an Orbitrap Fusion Lumos Tribrid mass spectrometer (Thermo Fisher Scientific) operated with Xcalibur (version 4.0.21.10) and coupled to a Thermo Scientific Easy-nLC (nanoflow Liquid Chromatography) 1200 system. Tryptic peptides (2 µg) were loaded onto a C18 trap (75 µm × 2 cm; Acclaim PepMap 100, P/N 164946; Thermo Fisher Scientific) at a flow rate of 2 µL/min of solvent A (0.1% formic acid and 3% acetonitrile in LC- mass spectrometry grade water). Peptides were eluted using a 120 min gradient from 5 to 40% (5% to 28% in 105 min followed by an increase to 40% B in 15 min) of solvent B (0.1% formic acid in 80% LC- mass spectrometry grade acetonitrile) at a flow rate of 0.3 µL/min and separated on a C18 analytical column (75 um × 50 cm; PepMap RSLC C18; P/N ES803; Thermo Fisher Scientific). Peptides were then electrosprayed using 2.3 kV voltage into the ion transfer tube (300 °C) of the Orbitrap Lumos operating in positive mode. The Orbitrap first performed a full mass spectrometry scan at a resolution of 120,000 FWHM to detect the precursor ion having a mass-to-charge ratio (m/z) between 375 and 1575 and a + 2 to + 4 charge. The Orbitrap AGC (Auto Gain Con109roll) and the maximum injection time were set at 4e5 and 50 ms, respectively. The Orbitrap was operated using the top speed mode with a 3 s cycle time for precursor selection. The most intense precursor ions presenting a peptidic isotopic profile and having an intensity threshold of at least 2e4 were isolated using the quadrupole (isolation window of m/z 0.7) and fragmented with HCD (38% collision energy) in the ion routing Multipole. The fragment ions (MS2) were analyzed in the Orbitrap at a resolution of 15,000. The AGC, the maximum injection time and the first mass were set at 1e5, 105 ms and 100, respectively. Dynamic exclusion was enabled for 45 s to avoid acquisition of the same precursor ion having a similar m/z (plus or minus 10 ppm).

4.3.7) Proteomic data and bioinformatics analysis.

Spectral data were matched to peptide sequences in the murine UniProt protein database using the Andromeda algorithm(Cox et al., 2011) as implemented in the MaxQuant(Cox & Mann, 2008) software package v.1.6.0.1, at a peptide-spectrum match false discovery rate (FDR) of < 0.01. Search parameters included a mass tolerance of 20 p.p.m. for the parent ion, 0.5 Da for the fragment ion, carbamidomethylation of cysteine residues (+ 57.021464 Da), variable N-terminal modification by acetylation (+ 42.010565 Da), and variable methionine oxidation (+ 15.994915 Da). TMT 6-plex labels 126–131 were defined as labels for relative quantification. The cleavage site specificity was set to Trypsin/P (search for free N-terminus and for only lysines), with up to two missed cleavages allowed. Next, quantified proteins were filtered using the Perseus software(Tyanova et al., 2016). Proteins that have more than two replicates with zero values in more than one group were removed. Filtered proteins were normalized using the CycLoess approach via NormalizerDE package31 using the R language (v3.6.0)(R Core Team, 2019). An average of the normalized results for each group was calculated and followed by the ratio of each group comparison. The ratios were log(2) transformed and the significant outlier cut-off values were determined after log(2) transformation by boxplot-and-whiskers analysis using the BoxPlotR tool(M. Spitzer et al., 2014).

4.3.8) Heatmaps

The results from the BoxplotR analysis were used in the heatmaps. Data analysis was accomplished using the R software(R Core Team, 2019). The plot was generated using the heatmap.2 function from the gplots package(Warnes et al., 2015).

4.3.9) Reactome pathway analysis

To identify protein–protein interaction, the STRING (Search Tool for the Retrieval of Interacting Genes) database(Szklarczyk et al., 2019) was used to illustrate interconnectivity among proteins. Protein interaction relationship is encoded into networks in the STRING v11 database (https:// string- db. Org). Our data was analyzed using the Mus musculus as our model organism at a false discovery rate of 5%. Proteins belonging to specific pathways were selected and their ratios were plotted as heatmaps.

4.3.10) Immunohistochemistry

For histology, lesioned spinal cords were collected from five different female C57BL6 mice per group: LPC lesioned without exercise (n = 5) and LPC lesioned with exercise (n = 5). The experiment was performed in duplicates, for a total of twenty mice. Tissue was harvested 4 h into the dark cycle when animals had reached peak running for 2 h. Mice were transcardially perfused with 15 mL of room temperature PBS followed by 15 mL of ice cold 4% paraformaldehyde (PFA). The spinal cord was dissected from the lower cervical to lower thoracic regions and post fixed in 4% PFA overnight at 4 °C, then cryoprotected in 30% sucrose for 3 days. Cords were cut into 5 mm sections with the lesion site in the centre and frozen in FSC 22 Frozen Section Media (Leica). Spinal cords were cut coronally into 20 µm sections on a cryostat (Thermo Fischer Scientific) onto Superfrost Plus microscope slides (VWR). Sections were stored at – 20 °C until staining and analysis. Slides with coronal sections were warmed to room temperature for 5 min. For myelin basic protein (MBP) staining, slides were delipidated with concurrent washes of 50%, 70%, 90%, 95%, 100%, 95%, 90%, 70%, and 50% ethanol. Slides were rehydrated for 10 min in PBS, then permeabilized with 0.2% Triton-X100 in PBS for 10 min. Slides were then blocked for 1 h at room temperature using horse blocking buffer (PBS, 10% horse serum, 1% BSA, 0.1% cold fish stain gelation, 0.1% Triton X-100, 0.05% Tween-20) and IgG Fab fragments (20 µg/mL). Staining for NFH, Olig2, PDGFRα, CC, and CX32 did not require delipidating steps. After blocking, primary antibodies were added in antibody dilution buffer (PBS, 1% BSA, 0.1% cold fish stain gelation, 0.1%

Triton X-100) overnight at 4 °C. Sections were washed three times with 0.05% Tween-20 in PBS for 5 min each, followed by 1 h of incubation with secondary antibodies in antibody dilution buffer (1/400 from manufacturer stock) and Nuclear Yellow (1/800) at room temperature. Sections were then washed three more times with 0.05% Tween-20 in PBS for 5 min each then mounted using Fluoromount-G solution (SouthernBiotech). The following antibodies were used: Olig2 (Millipore AB9610, R&D AF 2418), PDGFRα (R&D AF1062), CC1 (Millipore OP80-100UG), MBP (Abcam AB7349), NFH (Encor RPCA-NFH), GFAP (Biolegend 829401), GJB1 (Invitrogen 71-0600). The following Jackson laboratory secondary antibodies were used: Cyanine Cy3 donkey anti-chicken IgY, Cyanine Cy3 donkey anti-rat IgG, Alexa Fluor 594 donkey anti-mouse IgG, Alexa Fluor 488 donkey anti-rat IgG, Alexa Fluor 647 donkey anti-rat IgG, Alexa Fluor 657 donkey anti-rabbit IgG.

4.3.11) Confocal microscopy

Confocal images were taken on the Leica TCS Sp8 laser confocal microscope using the 10 × air objective and 25 × 0.5 NA water objective. The 405 nm, 488 nm, 552 nm, and 640 nm lasers were used to excite fluorophores with detection by 2 low dark current Hamamatsu PMT detectors and two high sensitivity hybrid detectors. Images were acquired in 8-bits, in a z-stack bidirectionally, with 2-times line average, and at 0.57 μm optical sections. Laser levels were maintained across all sections of common stains, and secondary alone controls were used to account for non-specific secondary fluorescence. Images were blinded and analyzed using ImageJ (RRID: SCR_003070).

4.3.12) Statistical analysis

For sample size calculation, it was used previously published studies as a reference(Jensen et al., 2018), using as a baseline the least sensitive method. The Shapiro–Wilk test was used to assess data normality and the F-test was used to evaluate if the variances of two groups are equal. Normal data were evaluated using the Student t-test, while non-normal data was assessed using the Mann–Whitney test. For the proteomics analysis, it was applied an interquartile

boxplot analysis to determine the proteins differentially expressed(M. Spitzer et al., 2014). The FDR was generated by the bioinformatic tools used for pathway analysis. The R software(Warnes et al., 2015), GraphPad Prism version 9, and Microsoft Excel were used for the statistical analysis.

4.3.13) Ethical standards

Our study was carried out in compliance with the ARRIVE guidelines.

4.4) Results

4.4.1) Exercise in naïve mice alters the spinal cord proteome

To evaluate the impact of exercise on the CNS and serum, we subjected mice to short-term bouts of exercise and compared to sedentary control. Running animals had free access to a running wheel over 4 days, while sedentary animals were given a locked wheel as environmental enrichment control. Mice ran during their night cycle and rested during the day as determined from the number of runs per 10 min bin (Fig. 4.1a,b). Four hours into day 4 and during the animal's active night cycle, serum and spinal cords at T3–T4 were collected and subjected to a quantitative shotgun proteomics work- flow labelled with tandem mass tags (TMT) 6-plex kits (Fig. 4.1a). Mice subjected to LPC-surgery had reduced exercise activity in the first and second day after surgery but attained similar levels by the end of the third day (Fig. 4.1b); over the 4 days, LPC-surgery mice ran significantly shorter distances than the naïve animals (Fig. 4.1c).

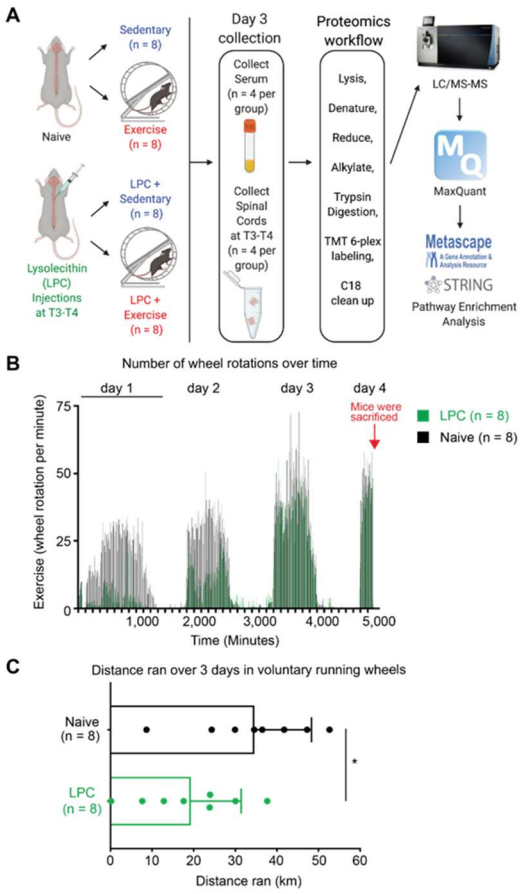

Figure 4.1) Workflow and running wheel activity. The LPC mice recovered for ~ 1–2 h post-surgery and the same rest period was given to naïve mice. Naïve and LPC animals were given access to a running wheel, or a wheel on its side immediately following recovery. (A) Schematic demonstrating experimental workflow. Animals were subjected to LPC surgery or not, then housed with an unlocked or locked running wheel. Serum and tissue were collected on the 4th day (4 h into the running cycle) and subjected to a quantitative shotgun proteomics workflow. Spinal cords and serum were pooled in groups of 2 for adequate protein concentrations (n = 4 of 2 pooled samples, n = 8 total). Figure was drawn using BioRender. The data was analyzed using the freely available MaxQuant software v.1.6.0.1 (https:// www. maxqu ant. org). (B) Running wheel data of naïve and LPC mice. Revolutions were monitored and binned in 10-min increments. Figure was drawn using Prism. (C) Quantification of total distance run over a 4-day period for naïve (n = 8) and LPC (n = 8) mice. Student's t-test was used for statistics. *P < 0.05.

We first examined protein changes in non-lesioned naïve mice that exercised on the running wheel to determine if short term exercise could alter the CNS proteome. Compared to their sedentary naïve controls, there were 115 significantly upregulated proteins and 67 significantly downregulated proteins in the spinal cord following exercise as determined by an interquartile boxplot analysis (Fig. 4.2a, b). Pathway enrichment analyses were performed using STRING(Szklarczyk et al., 2019) and Metascape(Y. Zhou et al., 2019) and revealed various altered pathways (Fig. 4.2c and 4.3). Upregulated proteins in the CNS included those associated with membrane trafficking (e.g. Snx2: sorting nexin-2), the extracellular matrix (e.g. Bgn: biglycan, Col's: collagens) (Fig. 4.2c), glutathione anti-oxidant responses (e.g. Mgst1: microsomal glutathione S-transferase 1, Gstk1: glutathione S-transferase kappa 1), metabolism (e.g. Acsl1: long chain fatty acid CoA ligase 1, Mgll: monoglyceride lipase) and myelination (Mbp: myelin basic protein, Myrf: myelin regulatory factor) (Fig. 4.3A,C). Downregulated proteins in exercising mice (i.e. higher in sedentary mice) included those related to metabolism of nucleotides (e.g. Gart: Trifunctional purine biosynthetic protein adenosine-3) (Fig. 4.2C) and Golgi-ER transport (e.g. Copa: Coatomer submit alpha, Dctn4: dynactin subunit 4) (Fig 4.3B,C).

In the serum of naïve exercising animals there were 9 upregulated proteins including those related to detoxification of oxygen species (Gpx3: glutathione peroxidase 3, Prdx2: peroxiredoxin-1), and platelet degranulation (Fgb: fibrinogen beta chain, Ecm1: extracellular matrix protein 1) (Fig 4.4A,B,D). Exercising naïve mice had 11 downregulated proteins (i.e. higher in sedentary mice) including those associated with plasma lipoprotein assembly (ApoA4: Apolipoprotein A-4, ApoB: Apolipoprotein B-100) (Fig 4.4A,C,D). Our findings suggest that acute exercise in naïve mice can alter both the CNS and serum proteomes. Proteins associated with anti-oxidant responses are concurrently elevated in spinal cord and serum of naïve exercising mice.

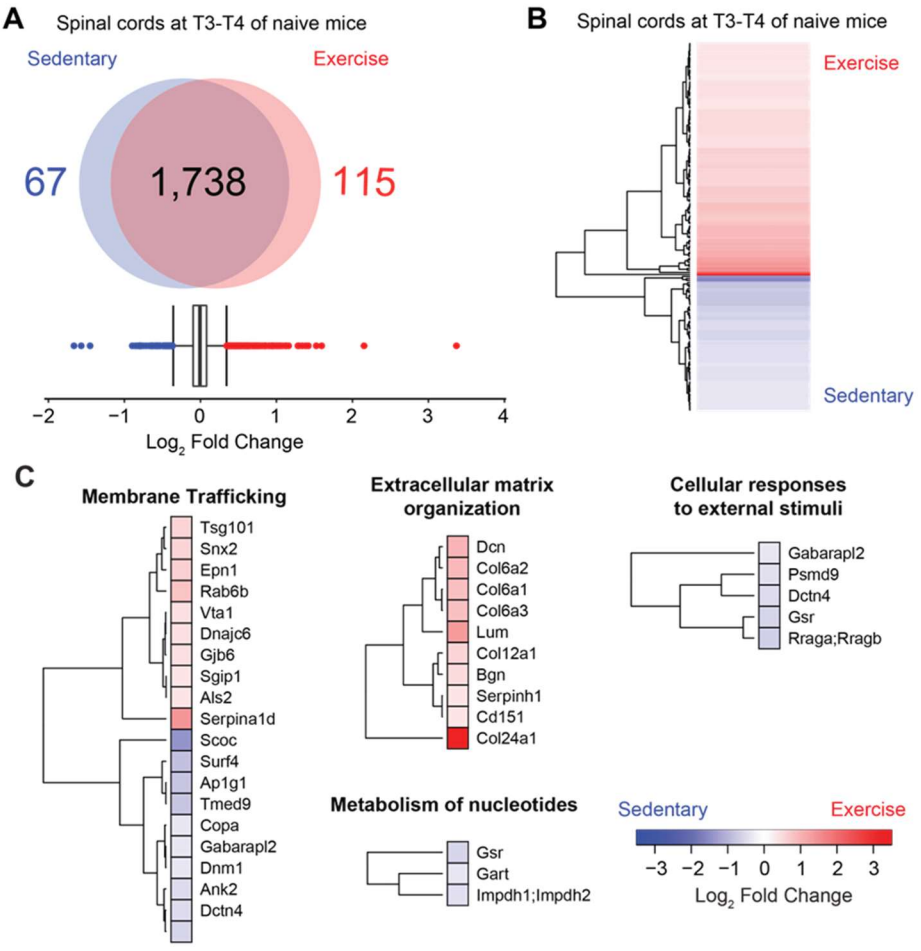

Figure 4.2) Effect of exercise on naïve spinal cord proteome after 4 days of running. Red, significantly elevated in the exercise group; Blue, significantly elevated in the sedentary group. (A) Quantification of differentially expressed proteins as determined by interquartile box plot analysis. A false discovery rate (FDR) of 1% was applied to the database search on MaxQuant. (B) Heatmap of differentially expressed proteins in naïve spinal cord tissue. (C) Heatmap of proteins and associated reactome pathways as determined by STRING (https:// string- db. org). A false discovery rate (FDR) for each pathway was added on the left of each heatmap. Interquartile box plot analysis was used for statistics. Data analysis was accomplished using the R software(R Core Team, 2019). The plot was generated using the heatmap.2 function from the gplots package(Warnes et al., 2015).

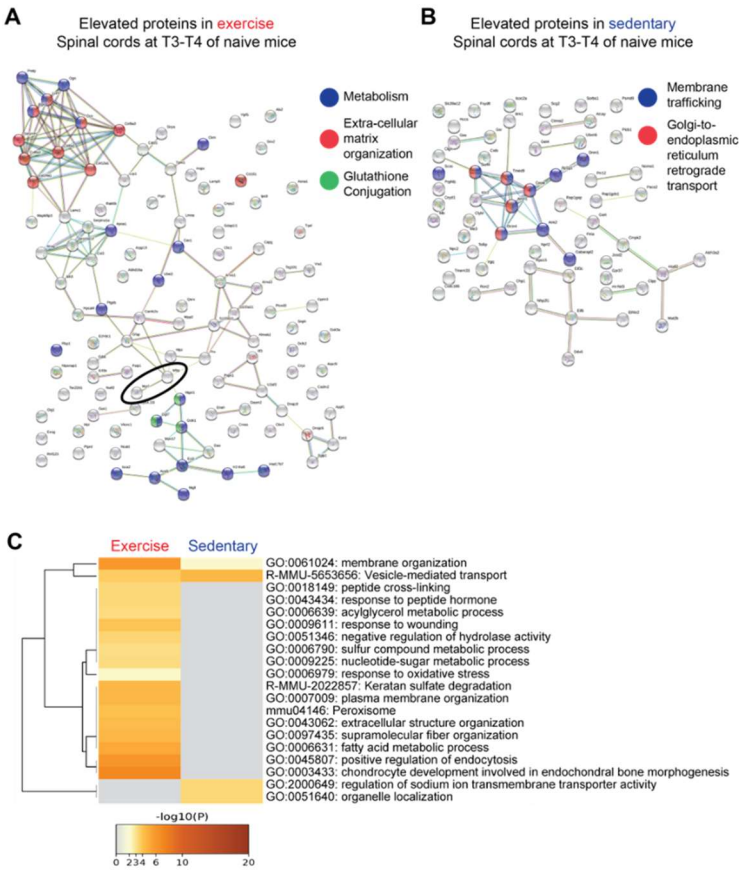

Figure 4.3) Protein-protein interactions and meta-analysis of significantly altered naïve spinal cord proteins after 4 days of running. STRING-db analysis of proteins significantly changing in the A) exercise group and B) sedentary group. Significantly changed reactome pathways are colored in each group. $P < 0.05$ as determined by False Discovery rate (FDR). C) Metascape analysis of the significantly changed proteins for each group. Terms with a $p < 0.01$ are shown.

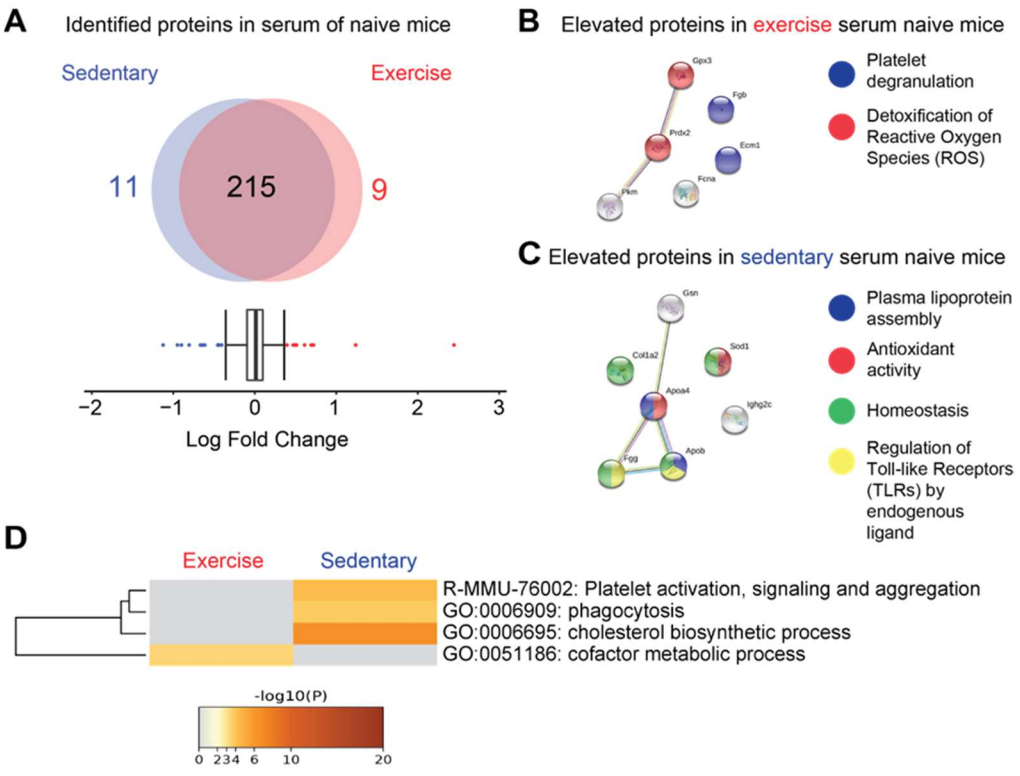

Figure 4.4) Protein-protein interactions and meta-analysis of significantly altered naïve serum proteins after 4 days of running. A) Quantification of significantly changed proteins as determined by interquartile box plot analysis. STRING-db analysis of proteins significantly changing in the B) exercise group and C) sedentary group. Significantly changed reactome pathways are colored in each group. $P < 0.05$ as determined by False Discovery rate (FDR). D) Metascape analysis of the significantly changed proteins for each group. Terms with a $p < 0.01$ are shown.

4.4.2) Demyelination following LPC injection

Next, we determined whether demyelinated CNS also have altered proteomes in response to exercise. To model the environment of a demyelinated MS lesion, we injected LPC into the spinal cords of mice(Keough et al., 2015) and compared it to naïve uninjured mice. LPC-injected mice were placed in individual cages with a running wheel immediately after recovery from surgery in the LPC group. Following LPC injection, there was demyelination as verified by eriochrome cyanine staining, and a loss of mature OLIG2 + CC1 + oligodendrocytes within the lesion; the number of OLIG2 + PDGFRα + oligodendrocyte progenitor cells (OPC) in the lesion appeared increased at 3 days post lesion (dpi) compared to the contralateral uninjured side (Fig. 4.5a, b). There was increased detection of MBP positive myelin debris, visible loss of axons, and a lack of GFAP positive astrocytes within the lesion (Fig. 4.5c). These results affirm the creation of a demyelinated lesion against which exercise in previous experiments 19 promoted oligodendrogenesis at later time points, and they provide the substrate to evaluate the proteomics of exercise following demyelination.

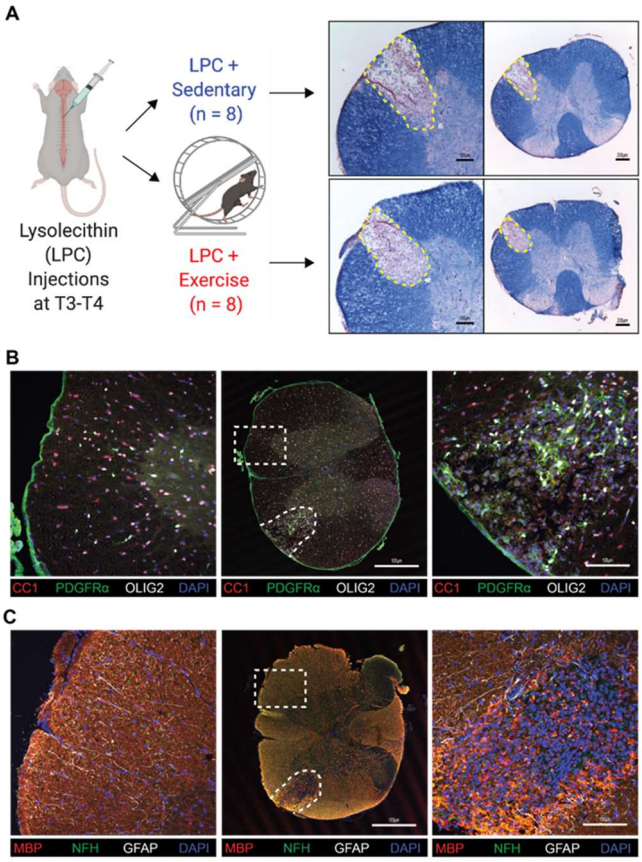

Figure 4.5) Impact of LPC surgery on mice subjected to running wheel. (A) Workflow and representative eriochrome cyanine-stained sections with lesion in the ventrolateral white matter delineated by dashed lines. Figure was drawn using BioRender. (B) Representative images of LPC lesion (left) and contralateral normal appearing white matter (right) 4 days post injury stained for mature oligodendrocytes (CC1) in red, OPCs (PDGFRα) in green, oligodendrocyte lineage cells (OLIG2) in white, and DNA (DAPI) in blue. (C) Representative images of LPC lesion 4 days post injury stained for myelin and myelin debris (MBP) in red, axons (NFH) in green, and astrocytes (GFAP) in white, and DNA (DAPI) in blue. In both (B) and (C), the lesion is outlined by the irregular dashed line while the non-involved contralateral site is denoted by the rectangle dashed line. Scale bar represents 100 μm.

4.4.3) Wheel running induces significant protein changes within the lesioned spinal cord

We identified 1920 proteins within the spinal cord of LPC demyelinated mice, and 248 proteins in the serum (Figs. 4.6a,b, 4.7a). Of the identified proteins, 86 were significantly upregulated and 85 were significantly downregulated in the lesioned spinal cords of exercising mice compared to sedentary demyelinated controls (Fig. 4.6a, b); 14 were upregulated and 11 downregulated in the serum (Fig. 4.7a, b). Compared to sedentary demyelinated mice, wheel running following demyelination increased proteins associated with metabolism (e.g. Ndufb9: NADH dehydrogenase [ubiquinone] 1 beta subcomplex subunit 9, Pgam2: phosphoglycerate mutase 2), glutathione anti-oxidant responses (Mgst1: microsomal glutathione S-transferase 1), transmission across chemical synapse (e.g. Ncald: neurocalcin delta) and proteolytic activity (e.g. ADAM10: a disintegrin and metalloprotease 10, Serpin1b: leukocyte elastase inhibitor B) (Fig. 4.6c, Fig 4.8). Conversely, exercise decreased proteins (i.e. elevated in sedentary over exercise spinal cords) associated with glucose metabolism (Gnpda1: Glucosamine-6-phosphate isomerase 1, Slc25a10: mitochondrial phosphate carrier protein); the gap junction protein, connexin 32 (Gjb1, gap junction beta1 protein), and MBP and Myrf were also reduced in exercising demyelinated samples (Fig. 4.6c, Fig 4.8). In the serum of exercising animals, proteins associated with the innate immune system were downregulated (Orm1: Alpha-1-acid glycoprotein-1, Orm2), and anti-oxidant proteins (Sod1: superoxide dismutase 1, Prdx2: peroxiredoxin-2) were upregulated (Fig. 4.7c, Fig 4.9). This shows that acute amounts of exercise are sufficient to profoundly alter the proteome of the spinal cord and serum in both naïve and LPC demyelinated animals.

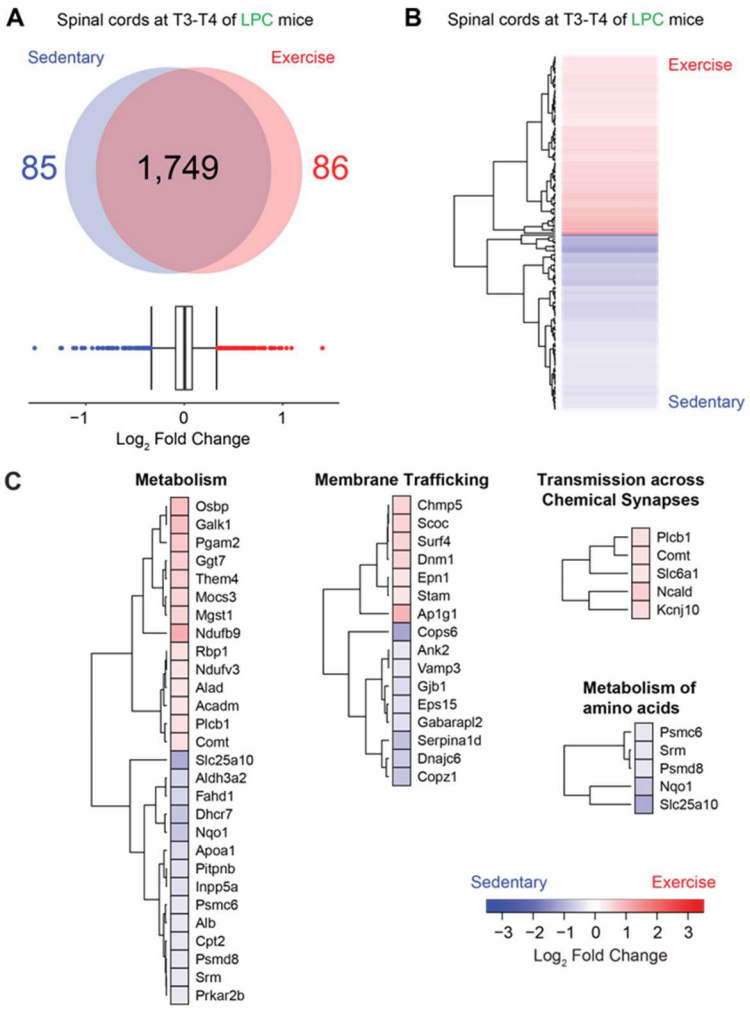

Figure 4.6) Effect of exercise on LPC demyelinated spinal cord proteome after 4 days of running wheel. (A) Quantification of differentially expressed proteins in LPC demyelinated spinal cord 4 dpi as determined by interquartile box plot analysis. A false discovery rate (FDR) of 1% was applied to the database search on MaxQuant. (B) Heatmap of differentially expressed proteins in LPC demyelinated spinal cord. C) Heatmap of proteins and associated reactome pathways as determined by STRING (https:// string- db. Org). A false discovery rate (FDR) for each pathway was added on the left of each heatmap. Interquartile box plot analysis was used for statistics. Data analysis was accomplished using the R software(R Core Team, 2019). The plot was generated using the heatmap.2 function from the gplots package(Warnes et al., 2015)

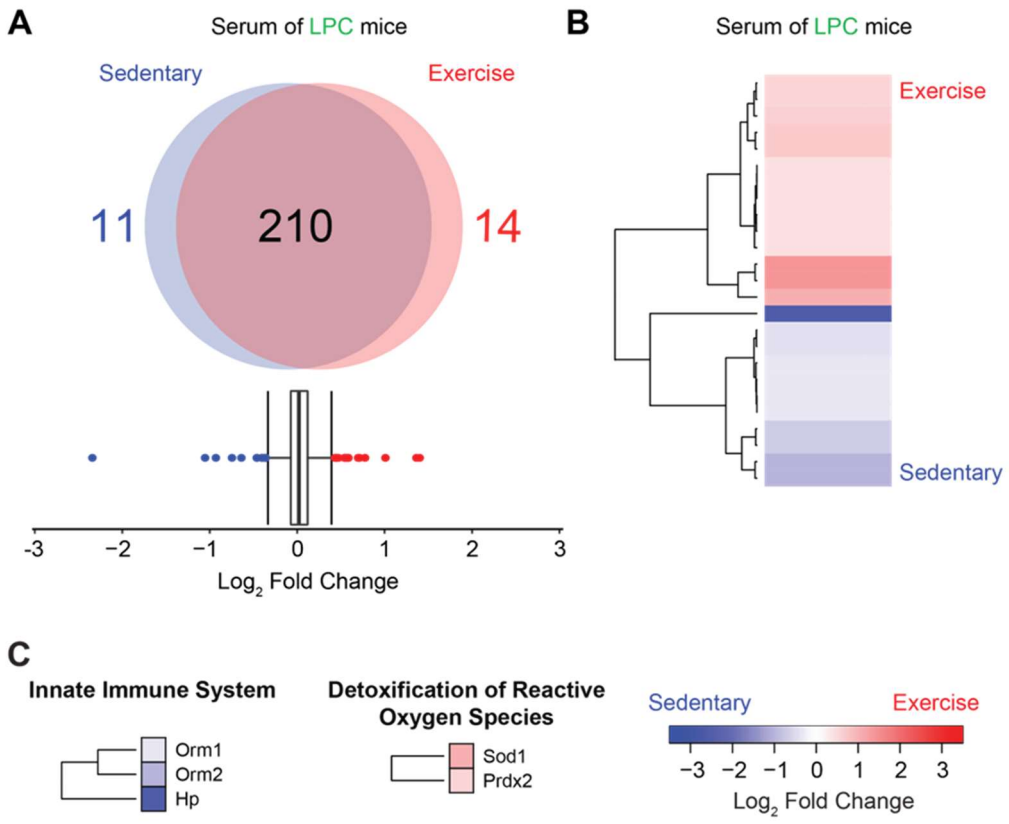

Figure 4.7) Effect of exercise on LPC demyelinated serum proteome after 4 days of running wheel. (A) Quantification of differentially expressed proteins in LPC demyelinated serum 4 dpi as determined by interquartile box plot analysis. A false discovery rate (FDR) of 1% was applied to the database search on MaxQuant. (B) Heatmap of differentially expressed proteins in LPC demyelinated serum. (C) Heatmap of proteins and associated reactome pathways as determined by STRING (https:// string- db. Org). A false discovery rate (FDR) for each pathway was added on the left of each heatmap. Interquartile box plot analysis was used for statistics. Data analysis was accomplished using the R software(R Core Team, 2019). The plot was generated using the heatmap.2 function from the gplots package(Warnes et al., 2015)

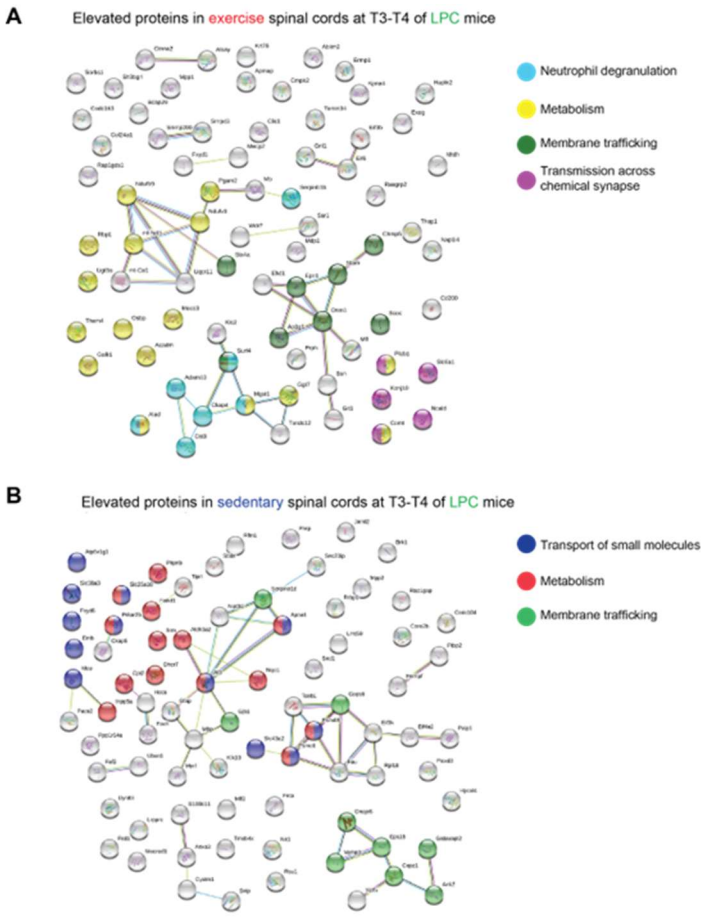

Figure 4.8) Protein-protein interactions of significantly altered LPC demyelinated spinal cord proteins after 4 days of running wheel access. STRING-db analysis of proteins significantly changing in the A) exercise group and B) sedentary group. Significantly changed reactome pathways are colored in each group. $P < 0.05$ as determined by False Discovery rate (FDR).

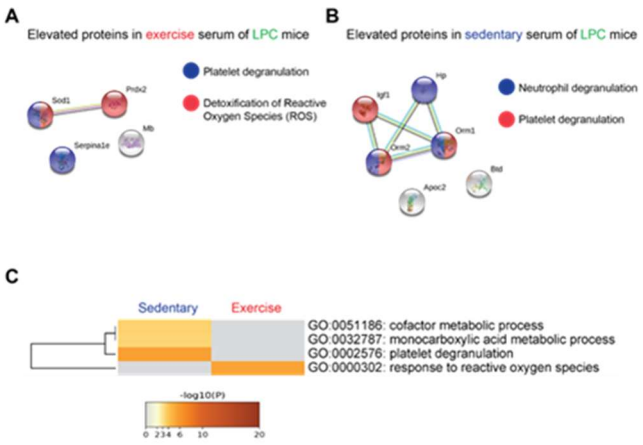

Figure 4.9) Protein-protein interactions of significantly altered LPC demyelinated mouse serum proteins after 4 days of running wheel access. STRING-db analysis of proteins significantly changing in the A) exercise group and B) sedentary group. Significantly changed reactome pathways are colored in each group. $P < 0.05$ as determined by False Discovery rate (FDR). C) Metascape analysis of the significantly changed proteins for each group. Terms with a $p < 0.01$ are shown.

4.4.4) Proteomes commonly elevated by exercise in naïve and demyelinated spinal cords

We addressed whether there were proteins commonly elevated by exercise in naïve and LPC-demyelinated spinal cords. The Venn diagram in Fig. 4.10a shows 14 proteins elevated by exercise in both the LPC and naïve animals including those associated with oxidative stress response (Mgst1: microsomal glutathione S-transferase 1, Ggt7: gamma-glutamyl transferase 7 involved in the metabolism of glutathione), extracellular matrix (Col24a1: collagen alpha-1 chain), protease activity (Cst3: cystatin-C), transcription/translation (Eif3b: Eukaryotic translation initiation factor 3 subunit B, Hist1h2al: a histone) and metabolism (Rbp1: retinol-binding protein) (Fig. 4.10b). Others elevated by exercise are Clic1 (Chloride intracellular channel protein 1), Epin1 (epsin-1 associated with endocytosis), Exog (a mitochondria nuclease), Ncald (Neuron-specific calcium-binding protein hippocalcin), and Prph (peripherin/vimentin). Finally, twelve proteins were commonly downregulated by exercise in the spinal cord of naïve and LPC mice (Fig. 4.10b). They include Fxyd6 (FXYD domain-containing ion transport regulator 6), Hccs (cytochrome c-type heme lyase), Brk1 (protein BRICK 1), Cdk17/18 (cyclin-dependent kinase-17 or 18), Pacs2 (phosphofurin acidic cluster sorting protein 2), Gnpda1/2 (glucosamine-6-phosphate isomerase 1 or 2), Aldh3a2 (aldehyde dehydrogenase), Fnta (protein farnesyltransferase), Eif4g1/3 (eukaryotic translation initiation factor 4 gamma 1 or 3), Gabarapl2 (gamma-aminobutyric acid receptor-associated protein-like 2), Rap1gap (Rap1 GTPase-activating protein 1) and Ank2 (ankyrin-2).

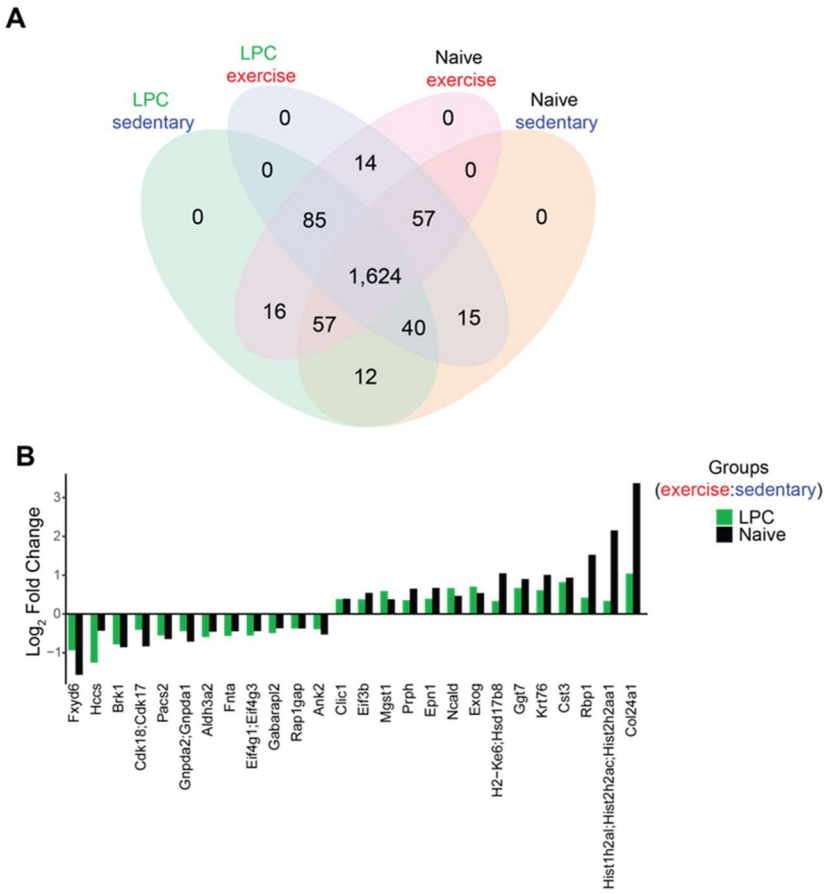

Figure 4.10) Comparison of shared proteins from the naïve and LPC of sedentary and exercising spinal cord proteome. (A) Venn diagram of enriched proteins in each of the 4 experimental groups after boxplot analysis. A total of 1624 proteins were not statistically enriched in any of the groups. 14 common upregulated and 12 common downregulated proteins between naïve and LPC exercising animals are shown in bold. (B) Bar plot showing the 14 proteins upregulated and the 12 proteins downregulated in both the naïve and LPC mice. Data analysis was accomplished using the R software(R Core Team, 2019). The plot was generated using the heatmap.2 function from the gplots package(Warnes et al., 2015).

4.4.5) Validation by immunofluorescence microscopy of decrease of connexin-32 and myelin basic protein in 4-day lesion of exercising animals.

We sought to validate the findings of proteomics by immunofluorescent staining of coronal spinal cord sections. An antibody each to a marker of metabolism (Pgam2) and anti-oxidant enzyme (Mgst1) was first attempted but signals of immunofluorescence were unconvincing in any sections. We next chose antibodies to structural proteins such as the gap junction protein, connexin-32, and MBP, which have been pointed out above to be reduced in exercising demyelinated mice. Using immunofluorescence, we found that while lesion size at 4 days post-LPC did not differ between exercising and sedentary groups (Fig. 4.11a, b), there was a significant decrease in the amount of both connexin-32 and MBP immunoreactivity within the lesion environment of exercising animals (Fig. 4.7c, d). As MBP immunoreactivity within the LPC lesion at early time points post-injury (and which is devoid of eriochrome cyanine as in Fig. 4.5) is indicative of myelin debris37, the decrease in MBP in lesion of exercising mice may represent the more rapid clearance of myelin debris that is inhibitory to repair processes.

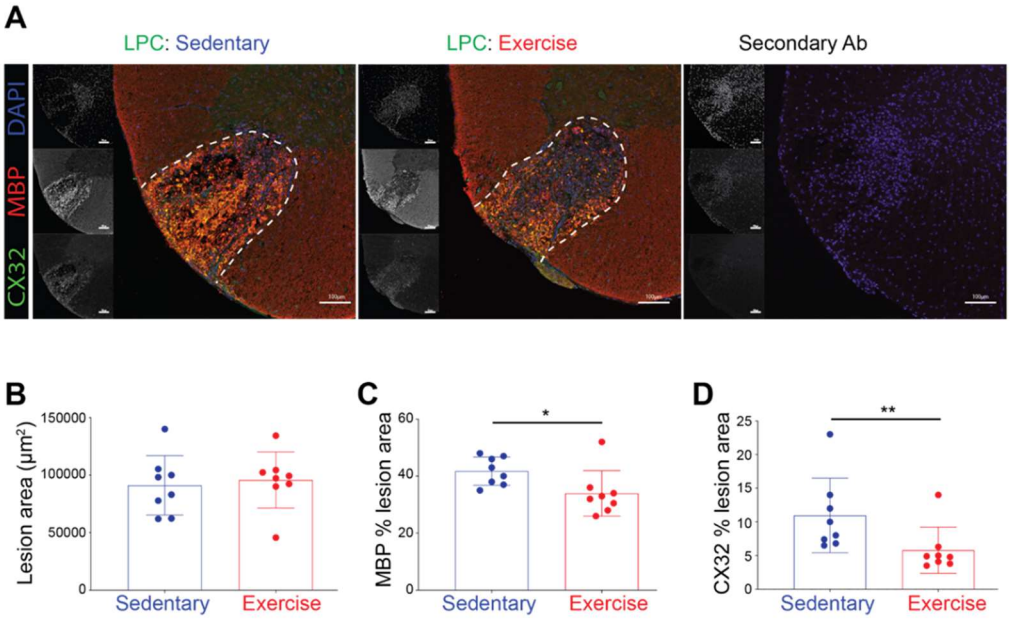

Figure 4.11) Immunofluorescence microscopy of LPC mice validation of shotgun proteomics analysis. (A) Representative images of LPC mice from the sedentary control, exercising animals, and secondary control for connexin-32 (CX32), and myelin (MBP). Scale bar denotes 100 µm. (B) Quantification of lesion area. (C) Quantification of percent of lesion that is MBP-positive. *$p < 0.05$. (D) Quantification of percent of lesion that is CX32-positive. **$p < 0.01$. A Mann–Whitney test was used for statistics. Each point is of a single animal, and the bar represents mean ± SD (n of 8 per group).

4.5) Discussion

There is unanimity that exercise benefits general health. For brain health, several reports demonstrate that exercise modulates the brain's connectome and even its structure(Kjolhede et al., 2018; Prakash et al., 2010; Prosperini et al., 2014). There is now an extensive literature that exercise improves cognition, fatigue, depression and mood in PwMS(Dalgas et al., 2019; Motl et al., 2017). In animal studies, outcomes of exercise in healthy mice or those modeling neurological conditions include reduced neuroinflammation or blood–brain barrier breakdown, neurogenesis, oligodendrogenesis, neuroprotection and remyelination(Frodermann et al., 2019; Guo et al., 2019; Jensen & Yong, 2016; Lassmann, 2018; Scheiman et al., 2019). The mechanisms by which exercise promotes CNS wellbeing appear to be multiple, such as the generation of brain-derived neurotrophic factor, reducing pro-inflammatory responses, modulating microglia activity, and ameliorating oxidative stress (reviewed elsewhere(Di Liegro et al., 2019; Gentile et al., 2019; Jensen & Wee Yong, 2014; Negaresh et al., 2018). Endurance (treadmill running) training in rodents decreased oxidative stress in the spinal cord, while increasing levels of the Nrf2 transcription factor and downstream anti-oxidant enzymes(Souza et al., 2016). Exercise also promotes neurotransmission and multiple signaling pathways in brain cells(Di Liegro et al., 2019; Jensen & Yong, 2016). Molecular mediators of the benefits of exercise include muscle-derived myokine FNDC5/irisin that prevents neurodegeneration and rescues memory impairment in a model of Alzheimer's disease, and liver-derived glycosylphosphatidylinositol- specific phospholipase D1 that improves cognition in aged mice(Horowitz et al., 2020; Lourenco et al., 2019). Despite the increasing knowledge of the mechanisms of exercise, it is not known how quickly they are affected.

Here, using quantitative shotgun proteomics, we report that a short bout of exercise changes numerous proteins in blood and spinal cord of naïve and demyelinated mice. Running activity of demyelinated mice was low to modest in the first 2 days and was similar to naïve controls only by the fourth day. Thus, the proteomic changes from tissues harvested 4 h into running at day 4 (Fig. 4.1) are reasonably the result of less than 2 days of running. Unanswered questions are

whether the proteomic changes would be affected after a single running episode, or whether some would be long-lasting after exercise is stopped. Regardless, with a short bout of running, the results are remarkable, as over 150 proteins are up- or down-regulated in the spinal cord of both naïve and demyelinated mice. Fewer altered proteins are detected in the serum, likely the result of our technical detection of a smaller number of proteins (248) in the serum compared to the spinal cord (1920 proteins) of LPC demyelinated mice (Figs. 4.6A, 7A). The quick alteration of numerous proteins in the CNS may help explain the brain changes in humans soon after exercise. For example, a single 50-min vigorous intensity cycling on a stationary bicycle in healthy subjects improved their prefrontal cortex-dependent cognition that lasted up to 2 h after exercise(Basso et al., 2020). A single 40-min bout of harness-supported treadmill walking in highly progressed PwMS increases brain excitability, which indicates higher potential for neuroplasticity, and it is more pronounced in individuals with higher aerobic fitness. Although this feature was observed only on the hemisphere less affected by the disease, it shows the importance of exercise in PwMS and the potential for changes in the CNS even following acute exercise(Chaves et al., 2020). In evaluating the changes to the proteomes in the spinal cord of demyelinated mice after exercise, we found that markers of anti-oxidant responses, metabolism, neurotransmission and proteolytic remodeling of the extracellular matrix are commonly elevated by exercise. The last is notable since subsequent repair after injury would require extracellular matrix remodeling(Jong et al., 2019). Elevation of anti-oxidant responses are also notable. Markers of oxidative stress are increased within MS lesions where they have been implicated in axonal damage and demyelination(Gilgun-sherki et al., 2004; Haider et al., 2011; Lassmann, 2018). In the EAE model of MS, the primary anti-oxidant glutathione is upregulated following voluntary wheel running(Benson et al., 2015). Consistent with this report, we found elevation of Mgst1 and Ggt7 in the exercising LPC-demyelinated spinal cord. Mgst1 has both glutathione transferase and peroxidase functions which makes it particularly potent at attenuating oxidative stress injuries(Bräutigam et al., 2018; Schaffert, 2011). Thus, exercise-induced upregulation of these antioxidants may help mitigate injury-related oxidative damage. We attempted to corroborate these findings by looking at markers of oxidative injury such as malondialdehyde (MDA), 8-Oxo-2′-deoxyguanosine (8-OhDG), and 4-hydroxynonenal (4-HNE).

Due to limitations with high antibody background staining and thus specificity we were unable to corroborate differences in overall oxidative stress. However, we hypothesize that any difference would likely be seen later in lifespan of the lesion after these oxidative stress response proteins have had time to function. We also found increased expression of Sod1 and Prdx2 in the serum of exercising mice. Decreased total antioxidant capacity has been noted in the serum of PwMS(Hadžović-džuvo et al., 2010; Mezzaroba et al., 2020). Taken together, the combined spinal cord and serum upregulation of antioxidants suggests that exercise produces the necessary components to handle the pro-oxidants commonly seen in MS. Changes in metabolism influence cell function(Afridi et al., 2020; Pearce & Pearce, 2013). Metabolic reprogramming such as the reliance of aerobic glycolysis for rapid energy supply occurs in cells when responding to injury and infection(Afridi et al., 2020; Jellusova, 2018; Kaushik et al., 2019; Seki & Gaultier, 2017). For example, macrophages rely on aerobic glycolysis to transmigrate into the parenchyma from perivascular cuffs in the EAE model(Shechter et al., 2013). Additionally, microglia are thought to use oxidative phosphorylation for homeostatic or tissue repair functions(Miron et al., 2013; Shechter et al., 2013) but switch to aerobic glycolysis when pro-inflammatory(Lauro & Limatola, 2020). Our proteomic analysis identified significant changes in metabolism-related proteins. For example, upregulation of Pgam2 suggests a general rise in glycolysis while increased expression of proteins associated with mitochondria (Ndufb9, Ndufv3, mt-Nd3) suggests elevated oxidative phosphorylation. These metabolic changes could be downstream of the transcriptional co-activator PGC1α (peroxisome proliferator-activated receptor gamma coactivator 1-alpha), which mediates exercise-enhanced remyelination in mice(Jensen et al., 2018). Impressively, exercise in naïve mice also elevated numerous proteins (115) in the naïve spinal cord of mice, with smaller changes (9 elevated) noted in the serum. This finding may help account for the benefit of exercise not only for general health, but also for CNS wellbeing in the absence of any pathology. Common pathways elevated by exercise in the naïve or demyelinated CNS include those related to anti-oxidants and metabolism. Namely, the upregulation of metabolism upon exercise was identified by 16 and 18 proteins in the LPC (FDR = 3.16 × 10–2) and naïve (FDR = 1.29 × 10–2) samples, respectively. Among the 34 proteins, they shared only Ggt7, Mgst1 and Rbp1, indicating that exercise has a

wide effect on protein expression in the spinal cord tissue, modulating the levels of multiple proteins within a specific biological function. For the proteins commonly enriched in sedentary mice, Fxyd6 had the highest log fold change, -1.56 naïve and -0.93 LPC. Experimental evidence indicates that the FXYD family of transmembrane proteins can associate and modulate the transport properties of Na,K-ATPase(Crambert & Geering, 2003; Geering, 2006), an enzyme responsible for regulating the Na+ and K+ gradients across the cell membrane(Young et al., 2008). Dysfunction of Na,K-ATPase may play a central role in MS, as loss of axonal Na,K-ATPase is linked to neurological decline in chronic stages of the disease(Young et al., 2008). Although the exact impact of Fxyd6 on Na,K-ATPase is not completely known, its regulation by exercise, independently of LPC, suggests a beneficial and protective role for PwMS. These findings may also help explain why MS is less common in those that exercise versus those that do not, supporting the suggestion that exercise may prevent MS(Dalgas et al., 2019; Wesnes et al., 2017). We note that while several pathways have been identified by Metascape and STRING analyses for exercise-induced changes, and several proteins have been highlighted, these proteins may serve several functions in different pathways. For instance, Mgst1 is highlighted in both anti-oxidant and metabolism pathways in our analyses. Also, not all existing proteins have been identified in the serum and spinal cord in this study, a limitation of mass spectrometry, so other exercise-induced changes remain to be discovered. When comparing the proteomics findings to the transcriptomics results from a previous study published by our group(Jensen et al., 2018), it is not possible to see a clear correlation between both techniques, even though it was analyzed in the same type of LPC-induced demyelinating lesions. However, this lack of correlation may be explained by the number of days post lesion (dpl) analyzed in each experiment, as the proteomics approach was performed on 3 dpl and the transcriptomics analyzed samples at 5 and 10 dpl. Nonetheless, proteomics identified 4 members of the mitogen-activated protein kinases (Mapk) family (Mapk1, Mapk3, Mapk15, and Mapk10) with minimal alterations in their fold change, while the ERK/MAPK signaling pathway was enriched at 5 dpl on the transcriptomics data and presented the lowest p-value (2 × 10–5). This suggests that the MAPK pathway is part of a delayed response induced by exercise and most likely to be detected at the protein level on day 5 and onwards. LPC demyelination provides a useful

model for subsequent remyelination(Keough et al., 2016). However, it models the repopulation of oligodendrocyte lineage cells after demyelination in MS and does not replicate every facet of the disease. We acknowledge that this is not a classical immune mediated lesion as is seen in MS or EAE, but rather a toxin induced injury. LPC has been useful because of the well characterized injury and a reliable course of resolution. Following cell death and lesion formation there is a rapid increase in the innate immune response by day 3. Some limitations of this model include the dearth of an adaptive immune response. While lymphocytes have been shown to be present early in lesion formation, the short lifespan and focal nature of the lesion restricts the immune response to an innate one. By day 7 following lesion formation, the repair process has begun and OPCs accumulate in the lesion. By two weeks, remyelination begins to occur and is robust by three weeks. For the purposes of this study, to investigate what changes exercise induces in naïve and demyelinated tissue, LPC is a useful model. LPC produces rapid and complete demyelination within the first day of application(Plemel, Michaels, et al., 2017), and the eriochrome cyanine staining shows a complete loss of intact myelin at day 4 (Fig. 4.5A). Nonetheless, myelin debris is still manifest within the lesion at this point, as noted by MBP immunoreactivity (Fig. 4.11) within the lesion that is intense due presumably to exposure of antibody epitopes in the degraded myelin. In previous work, we found that exercise promotes myelin debris removal by 3–4 days of injury(Jensen et al., 2018), likely resulting in the lower MBP immunoreactivity in the lesion of exercising mice herein (Fig. 4.11). This is important in demyelinating injuries in which myelin debris is inhibitory to OPCs(Keough et al., 2015; Rawji et al., 2020) and would need to be cleared. However, we did not find phagocytosis-associated proteins to be elevated in the exercise LPC group, but endocytosis-associated proteins were increased (Chmp5: Charged multivesicular body protein 5, Dnm1: Dynamin-1, Ehd1: EH domain- containing protein 1, Epn1: Epsin-1, Git1: ARF GTPase-activating protein GIT1, and Stam: Signal transducing adapter molecule 1). In the lysolecithin-injury, OPCs begin repopulating within 3 days but differentiation to oligodendrocytes occurs later (approximately day 7). This may reconcile the result that Myrf, a transcriptional factor expressed in mature myelinating oligodendrocytes that promotes the expression of myelin genes (Emery 2009), is downregulated in the LPC spinal cord by exercise, as the day four post-LPC time

point is not yet timely for myelin formation. Conversely, Myrf is elevated by exercise in the naïve spinal cord (Fig 4.3), suggestive of activity-dependent myelin formation in the homeostatic CNS(Jensen & Yong, 2016). In summary, we provide a protein level landscape of how exercise alters the CNS. The rapid elevation of numerous proteins involved in several pathways, particularly anti-oxidative and metabolic responses, not only following demyelination but also in the healthy state, is remarkable. These rapid changes help reconcile the observations that short bouts of exercise can influence the brain. A finer dissection of the crucial proteins may provide direction for future studies of exercise to promote repair responses in MS and other neurological conditions. Finally, the profound changes to the proteome induced by exercise may provide a lesion milieu particularly conducive for a pro-remyelinating medication to act upon. This integration of Medication and eXercise or “MedXercise” may lay the foundation for future strategies to maximize regeneration of the injured CNS.

4.6) Post-publication Addendum

My graduate project initially focused on the mechanisms by which exercise provides benefits for remyelination. This direction did not end up being worthwhile and therefore the focus of my project changed to fibroblasts. At the point in time when our proteomics experiment was published in Scientific Reports(Lozinski et al., 2021), fibroblasts had not entered into my project. As such, fibroblasts did not feature in this chapter. Instead, the focus of this chapter was primarily how physical activity alters the LPC and systemic environments and whether this could suggest beneficial outcomes. Given the findings of the previous chapters describing the fibroblast response to CNS injury and our proteomic findings showing a significantly altered LPC lesion environment after only 4 days of running, we looked into the fibroblast response in LPC lesions of young and middle-aged mice following 21 days of wheel running. We were interested in investigating whether wheel running was able to attenuate the fibroblast response including in LPC lesions of aging mice. Exercise has been shown to induce transcriptional and functional changes in fibroblasts and other mural cell populations including in the CNS(Lighthouse et al., n.d.; Morland et al., 2017). As well, exercise was found to reverse age-related deficits in cortical PDGFRβ+ cell numbers and

function(Soto et al., 2015). Therefore, we hypothesized that exercise would affect the fibroblast response including in aging mice. We looked at 21 days after LPC injection to study the endpoint effects of exercise on fibroblast responses. We find that 21 days of voluntary wheel running in young and middle-aged mice did not result in changes to the lesion size (Fig 4.12a, b) or fibroblast response (Fig 4.12c). As well, there were no changes in the proportion of Olig2+ oligodendrocyte lineage cells within the fibroblast niche (Fig 4.12d). Thus, while acute bouts of exercise are capable of significantly altering the proteome of naïve and LPC demyelinated spinal cords this does not translate into significant differences in young and middle-aged fibroblast responses, at least when studied at 21 days after LPC.

Previous reports have shown that exercise promotes oligodendrogenesis and remyelination(Jensen et al., 2018). It is very likely that while fibroblasts are sufficient to inhibit OPC response following LPC, they are likely not necessary for it. This is true of many inhibitors of OPC response. For instance, CSPGs are capable of inhibiting OPC differentiation but aren't required for this as shown by the inhibitory effects of high molecular weight hyaluronan(Back et al., 2005; Keough et al., 2015; Lau et al., 2012).

Though exercise has known effects on the phenotypes of fibroblasts in the muscle, heart, and tendons(Docherty et al., 2022; J. Li et al., 2022; Lighthouse et al., n.d.; W. Wei et al., 2023), these are all organs immediately affected by the biomechanics of exercise. Stretch, compression, and shear forces directly affect these organs resulting in a more direct mechanism of action affecting fibroblasts. Indeed, fibroblasts sense these mechanical forces integrating them and altering their gene expression as a result(MacKenna, 2000; Y. Zhou et al., 2013).

There is currently no known direct effect of physical activity on fibroblast functions in the CNS. Though we did not observe any effect in LPC lesions it may be too significant of a traumatic injury for exercise to display therapeutic benefits. Exercise is known to act on the barrier regions where CNS fibroblasts reside. For instance, exercise restores age-related deficits in neurovascular function in an APOE dependent manner(Soto et al., 2015) and increases cerebral angiogenesis through lactate signaling(Morland et al., 2017). As well, exercise has been shown to affect the

meninges, increasing the glymphatic clearance through the subarachnoid space to the deep cervical lymph nodes(He et al., 2017).

In conclusion, the findings in this addendum to chapter 4 indicate that the fibroblast response in young and middle-aged mice remains unchanged when animals were given voluntary access to a running wheel for 21 days.

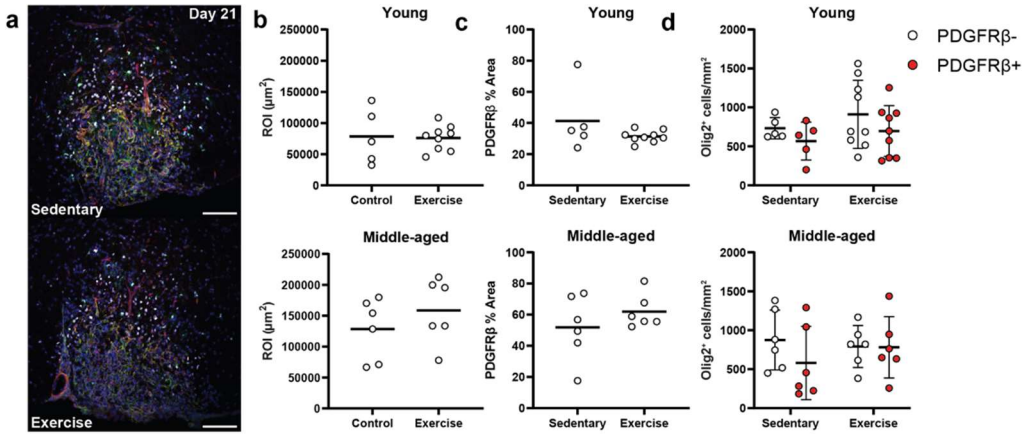

Figure 4.12) Exercise does not significantly alter the young or middle-aged fibroblast response following LPC. a) representative confocal images of sedentary and exercise LPC lesions 21 days after injection labeled with DAPI (blue), PDGFRβ (red), PDGFRα (green), and Olig2 (white). b) Graphs showing lesion ROI defined by DAPI hypercellularity. c) Graphs showing the percentage of lesion ROI positive for PDGFRβ. d) Graph showing the Olig2+ counts/mm^2 in the PDGFRβ+ fibroblast occupied niche compared to the rest of the lesion ROI. Data are from two independent experiments. b,c) Two-tailed, unpaired *t*-test comparing exercise and sedentary groups 21-days post injection. Mean shown as horizontal lines. d) Kruskal-Wallis followed by a Dunn's multiple comparisons. Sample size n = as shown number of mice from one experiment. Mean shown as horizontal line.

Chapter 5: General summary and discussion

5.1) General summary

The overall goal of this thesis was to characterize and study the causes and outcomes of the fibroblast response to central nervous system (CNS) injury. As well, we sought to investigate the effect of aging and aerobic exercise on this response. Fibroblasts are the main contributor of extracellular matrix (ECM) components during wound healing and are known to be affected with age. In the CNS, fibroblasts are normally restricted to the meninges, perivascular space, and choroid plexus(Dorrier, Jones, et al., 2021). Following traumatic or neuroinflammatory injury they become elevated in the parenchyma where they negatively influence regenerative processes such as axon regrowth(Sofroniew, 2018). We investigated how CNS fibroblasts respond to focal lysolecithin (LPC) induced demyelination of the spinal cord white matter, the mechanisms promoting their response, and whether physical activity could affect the promotion and outcomes of their response.

Chapter 2 (aim 1) characterizes the spatial and temporal fibroblast response in LPC lesions. As well, it details the presence of PDGFRβ+ cells in normal appearing white matter (NAWM) and multiple sclerosis (MS) lesions. Expression of the fibroblast activation markers smooth muscle actin (SMA), fibronectin (FN1), and periostin (POSTN) were seen at 7-and-21- days post injury (dpi). Interestingly, while SMA and POSTN increased from 7-to-21-days, the level of FN1 overlap with PDGFRβ+ fibroblasts were reduced. Proteases that digest fibronectin, including MMP7, are expressed most highly 14 dpi in LPC(P. Wang et al., 2018). As well, microglia/macrophage levels are reduced by 21 dpi and can also express fibronectin which may contribute to the reduction at that time(Masuda et al., 2019). We also demonstrate that fibroblasts are elevated in regions densely populated by immune cells in LPC and MS. Likely, macrophages and fibroblasts contribute to the others presence in CNS injury(Yokota et al., 2017; X. Zhou et al., 2018). We show that the microglia/macrophage response precedes the fibroblast response and that bone marrow monocyte derived macrophages (BMDMs) promote fibroblast migration. Once elevated in LPC lesions,

fibroblasts occupy areas that are vacant of oligodendrocytes, including newly myelinating oligodendrocytes. OPCs cultured in the presence of fibroblasts display reduced levels of differentiation including MBP expression and process outgrowth. The results from this chapter suggest that fibroblasts are elevated in CNS lesions, potentially due to macrophage soluble factors, after which fibroblasts can impair OPC differentiation.

Chapter 3 (aim 2) investigates the effects of age on the fibroblast response to LPC injury. We found that LPC lesions in middle-aged mice eventually are significantly larger and have a greater fibroblast presence. Fibroblasts were also elevated in EAE lesions in middle-aged mice. This is of interest based on our findings in chapter 2 showing the potential of fibroblasts to limit OPC differentiation. Previous studies have implicated age as a factor contributing to remyelination failure(Rawji et al., 2020; Ruckh et al., 2012; Sim et al., 2002). The potential of age-associated elevation of fibroblasts in the CNS contributing to remyelination impairment is intriguing but requires further investigation. LPC lesions in middle-aged mice show a greater amount of SMA+ and FN1+ fibroblasts 7 dpi. Though SMA labels arteries and arterioles we find that most PDGFRβ+ cells are not found around CD31+ vasculature. This chapter then builds from chapter 2, investigating how age-associated immune changes contribute to the fibroblast response. We demonstrate that the immune response in LPC lesions of middle-aged mice is dampened and abnormal. Further, we find that BMDMs derived from middle-aged mice have abnormal responses to inflammatory stimulation including increased expression of chemokines CCL3, CCL4, CCL5, and CXCL1. Microglia/macrophage expressing CCL3 and CCL4 are expanded during LPC injury and in aging (Hammond 2019). Interestingly, middle-aged BMDMs displayed reduced ability to stimulate fibroblast migration. This is counter to previous literature that has shown macrophages contribute to age-related fibrosis by upregulating fibroblast chemokines such as (C-X-C motif) ligand 13 (Cxcl13) and plexin B3 (Plxnb3)(Landry et al., 2022). However, it is possible that middle-aged macrophages upregulate factors that inhibit fibroblast activation such as prostaglandin E2 (PGE2)(J. Chen et al., 2022; Fortier et al., n.d.; W.-S. Lee et al., 2014; E. S. White et al., 2005; K. E. White et al., 2008). This chapter highlighted age as a factor in enhancing the elevation of fibroblasts in the parenchyma following LPC induced injury.

Chapter 4 (aim 3) describes the how voluntary wheel running affects the spinal cord and serum proteomes following LPC. As well, we briefly describe whether voluntary wheel running affects the fibroblast response to injury. We detail how naïve mice and mice subjected to LPC demyelination display significantly altered proteomes when given voluntary access to a running wheel for 4 days. In particular, this chapter highlights how acute bouts of physical activity induces protein level changes in the LPC demyelinated spinal cord related to metabolism, membrane trafficking, synaptic transmission, and amino acid metabolism and serum of LPC mice related to the innate immune system and detoxification of reactive oxygen species. This is of interest as oxidized macromolecules such as lipids are capable of inducing tissue injury(Dong et al., 2021). Expression of anti-oxidant proteins such as Ggt7 and Mgst1 highlight the potentially protective role of exercise to limit injurious oxidized macromolecules in the CNS(Dong et al., 2021; Haider et al., 2011). We also describe that voluntary wheel running was insufficient to alter the fibroblast response to LPC in young and middle-aged mice. No difference in lesion size or PDGFRβ immunoreactivity was seen after 21 days of running and may support that the fibroblast response is a function of injury size although this requires additional investigation. Overall, findings of chapter 4 show that short bouts of physical activity are sufficient to significantly alter the spinal cord and serum proteomes in potentially beneficial ways but that these do not have immediate impacts on the elevation of fibroblasts in the LPC lesion of young and middle-aged mice.

5.2) Limitations and future directions

5.2.1) Aim 1/Chapter 2 Limitations and future directions

Chapter 2 characterizes the response of CNS fibroblasts to focal LPC induced injury. We used PDGFRβ antibodies and inducible Cre recombinase mice to label fibroblasts. The limitation of this approach is the potential to label mural cell populations like smooth muscle cells and pericytes. Other reporters such as the Col1a1-eGFP and Tbx18-Cre have been used to label fibroblasts previously. As well, several markers including peptidase inhibitor 16 (Pi16), collagen 15a1 (Col15a1), and dermatopontin (Dpt) have been described as universal fibroblast markers and

are present in homeostatic CNS fibroblasts(Buechler, Pradhan, et al., 2021; Vanlandewijck et al., 2018). These could be used in future to validate our findings and for isolation of cells using fluorescence activated cell sorting (FACS). This would make future transcriptomic characterization of LPC lesion fibroblasts possible without potential polluting mural cells.

We describe that macrophages have the ability to promote fibroblast migration in vitro. Future studies can build from this work to further to understand the specific mechanisms that regulate fibroblast recruitment. Microglia and macrophages express chemokines during injury including CCL3 and CCL4 that can be recognized by fibroblasts(Hammond et al., 2019). As well, we did not investigate fibroblast recruitment of microglia/macrophage which is a more commonly described phenomenon(Pakshir et al., 2019; Shook et al., 2018; Sinha et al., 2022). It is likely that fibroblasts contribute to the turnover of immune cells that occur in the CNS(Lloyd et al., n.d.). Fibroblasts regulate macrophage recruitment through secreted and mechanical signals, and express chemoattractant proteins including CCL2, CXCL9, and CXCL10 in the injured CNS(Dorrier, Aran, et al., 2021; Pakshir et al., 2019). Indeed, we see LPC lesion fibroblasts upregulate contractile proteins like smooth muscle actin suggesting a contractile phenotype though more investigation is warranted into how fibroblasts influence the immune response in CNS injury.

An additional aspect that we did not investigate are potential subtypes of LPC lesion. Fibroblast populations can be highly heterogeneous between organs but also within an organ(Plikus et al., 2021). These subpopulations can be variably stimulated by soluble factors such as Wnt(Rock et al., 2011). Transcriptomic studies of embryonic meningeal fibroblasts identify unique transcriptional states of fibroblasts in the dura, arachnoid, and pia fibroblasts(DeSisto et al., 2020). As well, dermal fibroblasts are subdivided into mesenchymal, pro-inflammatory, and secretory populations during skin injury(Deng et al., 2021). While we have shown that fibroblasts are elevated in LPC lesions it is of interest to investigate the potential for further subtypes of fibroblasts in LPC injury.

In this thesis, we focused on the involvement of fibroblasts in LPC lesions. LPC is a phospholipid that exerts non-specific and widespread cell damage(Plemel, Michaels, et al., 2017).

It remains unclear whether fibroblasts will respond similarly to a specific demyelinating lesion. Indeed, in the bleomycin model of lung fibrosis injection of bleomycin intradermally over several weeks compared to a single intratracheal dose results in different signaling cascades(Singh et al., 2017; Wilson et al., 2010). It is possible that acute traumatic injuries in the CNS promote robust fibroblast activation while mild injuries that accumulate over time may not. Transection and balloon catheter induced spinal cord injury models both result in significant fibrosis(D. O. Dias et al., 2021; Fukuda et al., 2005). As well, delaying regeneration following cerebrovascular injury exacerbated collagen deposition(Mastorakos et al., 2021). Investigations into how CNS fibroblasts respond to varying amounts of trauma will help to yield information regarding the mechanisms that regulate fibroblast elevation in the CNS.

We also described an inhibitory effect of fibroblasts on oligodendrocyte progenitor cell (OPC) differentiation. We did not investigate the specific molecules that modulate the OPC response. Fibroblasts express many inhibitory ECM components during CNS injury. Genetic deletion of specific ECM components using Cre recombinase excision at LoxP sites would allow future studies to determine the role of fibroblast derived ECM on oligodendrocyte dynamics. Besides production of ECM, meningeal fibroblasts express factors including Wnt and BMP that are inhibitory to OPC responses(Fancy et al., 2009; Petersen et al., 2017). It is of value for future studies to investigate the role of fibroblast derived ECM and non-ECM components in regulating the OPC response to injury.

Additionally, future studies can directly observe fibroblast responses to CNS injury by utilizing ex vivo imaging systems together with acute injuries such as transection of LPC injection(Rawji et al., 2018). When done in tissue isolated from reporter animals would allow for the direct live imaging of fibroblasts in response to CNS injury. As well, reporter lines can be crossed such as PDGFRβ-Ai9 with CX3CR1-GFP or PDGFRα-GFP to study the interaction of fibroblasts with immune cells and OPCs.

5.2.2) Aim 2/Chapter 3 Limitations and future directions

A limitation of using immunofluorescence to identify cell populations is the inability to reliably quantify individual cell expression. While IMARIS provides a platform to visualize individual cells this is inadequate for studying fibroblasts in LPC lesions as cell boundaries are not well defined. Other methods, such as histoflow cytometry, utilize machine learning algorithms to define cellular boundaries and quantify the cellular localization of proteins within individual cells. Though this is a technically challenging method that requires substantial amounts of tissue it can be used in future to try to define individual fibroblast populations at the single cell level(R. W. Jain et al., 2023). More traditional methods of phenotyping cells using flow cytometry provide the ability to characterize many more markers, up to 100, than is possible using immunofluorescence staining. However, flow cytometry lacks the spatial resolution that histoflow cytometry provides, and the process of isolating cells from the central nervous system can result in phenotypic changes in cells(Gosselin et al., 2014; R. W. Jain et al., 2023). Since fibroblasts are adhesive cells that are influenced by their environment the dissociation method used to isolate the cells can result in phenotypic and abundance differences(Uniken Venema et al., 2022). Therefore, while many studies have tried to use transgenic reporters like PDGFRβ and Col1a1 there is no unified protocol(Dorrier, Aran, et al., 2021; Tsata et al., 2021). In situ hybridization methods like RNA-scope or spatial transcriptomics offer some methods of validating the findings of the other techniques though these have limitations in sensitivity and resolution(F. Wang et al., 2012).

An additional limitation for our findings of chapter 3 was the lack of available middle-aged PDGFRβ-Ai9 reporter mice at the time of our study. While in our hands the specificity of the PDGFRβ antibodies is high it is possible for cells to differentially express genes during inflammation. For example, TMEM119 labeling of microglia is sufficient only during homeostasis while it becomes downregulated during inflammation making it inadequate to identify microglial populations(Vankriekelsvenne et al., 2022). Inducible reporters such as our PDGFRβ-Cre^{ERT2} mice provide one method of avoiding this issue. As previously mentioned, reporter mice are commonly used for isolating cells from tissue(DeSisto et al., 2020; Dorrier, Aran, et al., 2021). Future directions

would be able to further elucidate the differences between young and aging mice using reporters to isolate cells for transcriptomic and proteomic analysis. This has been used in other studies to identify changing immune populations following oxidized phosphatidylcholine induced neurodegeneration(Dong et al., 2021).

Using bone marrow derived macrophages have limited translatability to cells in vivo. As well, it is difficult to recapitulate the inflammatory environment found with in CNS lesions. Attempts have been made to overcome some of these limitations by supplementing cells with M-CSF, TGF-β, and IL-34 though these may not be present during inflammation(Dong & Yong, 2019). The same can be said for using stimulation paradigms such as IFN-γ/LPS and IL-4/IL-13 to stimulate traditional M1-like and M2-like macrophage phenotypes. Future studies should rely on in vivo or high throughput models such as those described above including flow cytometry or transcriptomics to characterize the aging immune phenotypes. These have been used in other models to show that microglia/macrophages become more inflammatory with age expressing markers including osteopontin (Spp1) and galectin-3 (Lgals3) and contribute to neurodegeneration(Dong et al., 2022; Xue et al., 2023).

Another assay that can be improved upon is the transwell migration assay using a Boyden chamber. Fibroblasts in the CNS are surrounded in three dimensions by extracellular matrix which provide anchoring and stability. Indeed, fibroblast functions can be affected by the matrix they are growth on(Parker et al., 2014). More modern systems of in vitro migration assays utilize micropillar arrays and allow for three-dimensional high throughput measurement of cell migration(S.-Y. Lee et al., 2022).

5.2.3) Aim 3/Chapter 4 Limitations and future directions

A major limitation of chapter 4 is the lack of further description of cellular responses in exercising mice. There is substantial interest in the effects of physical activity on the CNS and health. Indeed, physical activity has a number of benefits for people with MS. As a multimodal intervention it is thought that physical activity exerts benefits for the CNS through peripheral and

CNS specific effects. These include immunomodulation, metabolic reprogramming, neuro and gliogenesis, and vascular effects(Guo et al., 2019). Previous studies found that voluntary wheel running promoted oligodendrogenesis and remyelination(Jensen et al., 2018). This is thought to occur by modulation of peroxisome proliferator-activated receptor γ (PPARG) coactivator 1 α (PGC1α). PGC1α is a transcriptional coactivator of metabolism related genes.

We also found that physical activity significantly affected genes related to metabolism in the LPC lesions CNS(Lozinski et al., 2021). It is unknown whether exercise induced metabolic changes have impacts on specific cells. Lactate production is a well described outcome of exercise and has cerebrovascular effects(Morland et al., 2017). As well, cells often rely on glycolysis for specific functions. Microglia/macrophages are highly glycolytic in EAE and MS perivascular cuffs allowing for their transmigration into the parenchyma(Kaushik et al., 2019). As well, oligodendrocytes rely on glycolysis to maintain myelin an axonal integrity(Fünfschilling et al., 2012). It is unknown whether these sorts of processes are affected by exercise. Additional studies into the specific cellular metabolic outcomes of exercise could provide clarity.

As well, our proteomics study looked only in young exercising animals. The effect of physical activity in aging animals subject to injury is not known. Exercise in aging animals does have substantial effects on cognitive outcomes due to regulating neurogenesis and plasticity(Bouchard & Villeda, 2015). We described that exercise did not alter the LPC lesion area or fibroblast accumulation in young or middle-aged lesions. We were not able to make direct comparisons between young and middle-aged exercising cohorts due to these experiments occurring at different times with changes to experimental variables such as the surgeon and age of lysolecithin used. The lack of an effect of exercise on LPC lesion fibroblast accumulation may be due to the significance and acute nature of the LPC model that may obscure potential exercise induced effects on fibroblasts. Brain derived neurotrophic factor (BDNF) is one factor produced during exercise that promotes neuronal survival and plasticity(Wrann et al., 2013). Expression of BDNF in the injured spinal cord reduced fibrotic scarring and promoted axon regeneration by reducing astrocytic STAT3 phosphorylation and reactivity(Holt et al., 2019; A. Jain et al., 2006;

Khan et al., 2018). Whether exercise induces levels of BDNF, or other factors, sufficient to elicit such effects is unknown. This provides several directions for future studies. Determination of the outcomes of exercise for the aging CNS remains unknown but would provide insight for the application of physical activity for the injured CNS of aged individuals. As well, it is unclear whether therapeutic or prophylactic application of exercise will be more efficacious for influencing the injured CNS. Though we describe here and in previous studies (Jensen 2018) that acute exercise can have robust effects, most individuals suffering from chronic disorders do not exercise often(Klaren et al., 2013). Finally, exercise induced factors such as BDNF and irisin have benefits for the CNS but there is no information on their role on CNS fibroblasts, particularly in injury. Of note, irisin, a muscle derived myokine, has been shown to limit cardiac fibrosis by limiting oxidative stress(R.-R. Chen et al., 2019). Whether BDNF, Irisin, or other exercise associated soluble factors can influence CNS fibroblasts would be a novel direction of interest.

5.3) General future directions

A general future area of study should be to consider the effects of CNS fibroblasts on immune privilege and infiltration of the CNS. The CNS is generally immune privileged and maintain highly regulated borders in the blood-brain barrier, meninges, and choroid plexus(Engelhardt et al., 2017). As fibroblasts have well described tissue remodeling and immune regulatory functions, they are well positioned to influence perivascular cuff formation and immune infiltration into the parenchyma. Fibroblasts occupy all of the CNS border regions and have been shown to have immune regulatory functions in the meninges of EAE mice(Pikor et al., 2015).

Infiltration of immune cells into the CNS parenchyma drives pathology and disability in MS. As well, we have shown that fibroblasts are primarily restricted to the perivascular space in MS tissue. Studies have illustrated how fibroblasts contribute to tissue remodeling including vascular remodeling by secretion of ECM(Bonney et al., 2022; Henderson et al., 2020; Rajan et al., 2020). As well, fibroblasts produce a range of immune modulatory cytokines including IL-6, TNF-α, and CCL2 that recruit and polarize immune cells(Bautista-Hernández et al., 2017; Correa-Gallegos et al., 2021). Many ECM components can act as ligands for immune cell receptors during injury that

upregulates proteases and inflammatory cytokines contributing to further pathology(Ghorbani & Yong, 2021; Pu et al., 2018; Stephenson et al., 2018). What is lacking is a coherent understanding of the spatial and temporal interactions between fibroblasts and immune cells in the perivascular space, the consequences of their dysfunction and ablation, and how these contribute to MS pathology.

5.4) Conclusions

This thesis covers the involvement of central nervous system fibroblasts in lysolecithin mediated CNS injury including during aging and the effect of physical activity in altering the environment of lysolecithin lesions. An original finding is the description that fibroblasts become elevated in lysolecithin lesions, that this may result from macrophage signals, and can negatively influence oligodendrocyte progenitor cell differentiation. The second original finding is the exacerbation of the fibroblast response in aging lysolecithin lesions, potentially as the result of a dysfunctional and impaired immune response. Another novel finding is the spatial restriction of newly myelinating oligodendrocytes from fibroblast occupied niches in the lysolecithin lesion. As well, we find that fibroblasts act directly on oligodendrocyte progenitor cells to inhibit their differentiation. Finally, an additional novel finding is that short bouts of physical activity is capable of robustly alter lysolecithin demyelinated spinal cord proteins related to metabolism, synaptic trafficking, and amino acid metabolism. Surprisingly, despite the significant effect of exercise on the lysolecithin lesion environment this did not affect the fibroblast response in young and middle-aged exercising mice. Altogether, I hope that this thesis contributes to the developing and intriguing field of central nervous system fibroblasts and their involvement in central nervous system injuries.

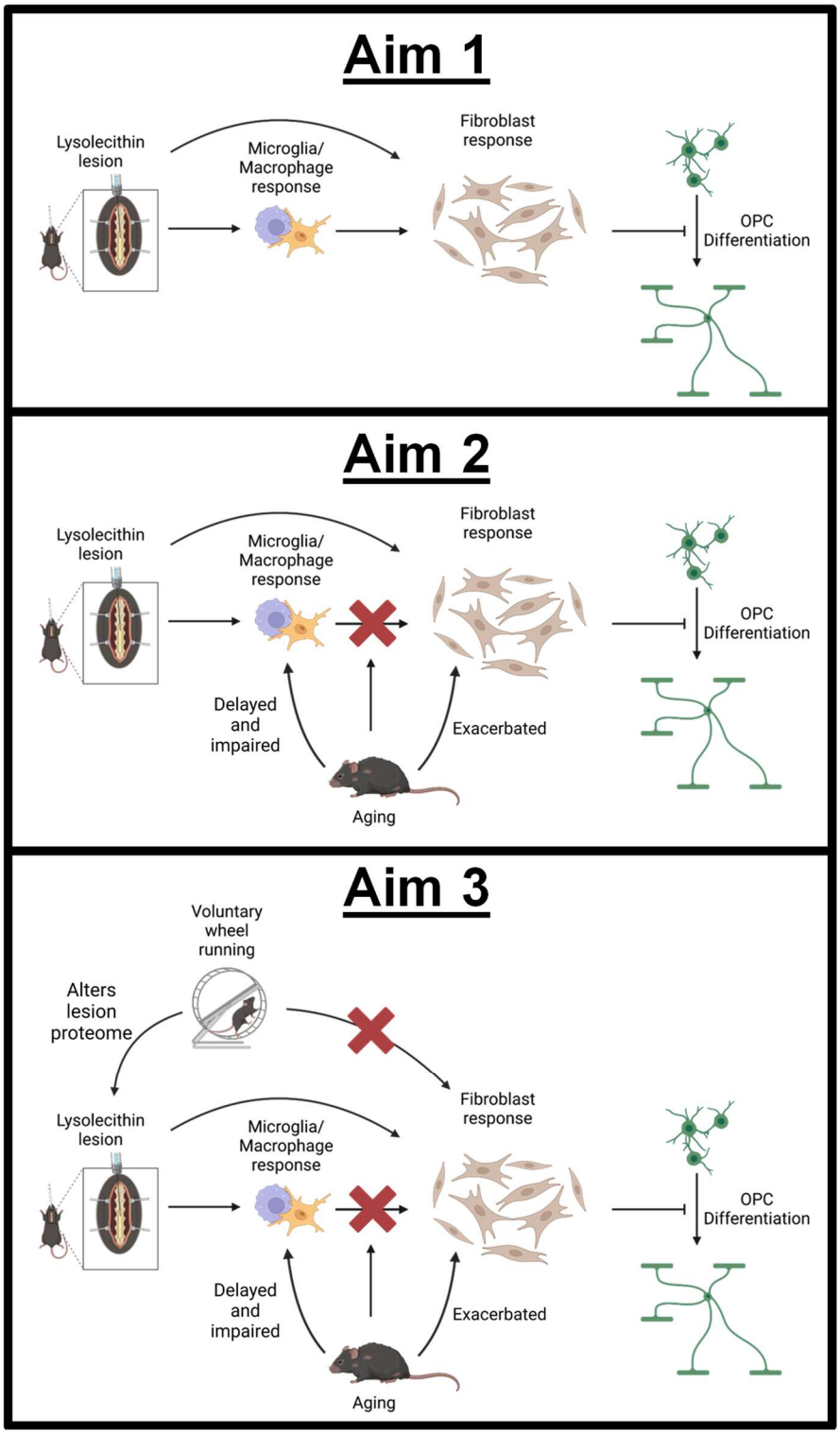

Figure 5.1) Overview schematics demonstrating findings of each aim.

6.0: References

Abbasi, S., Sinha, S., Labit, E., Rosin, N. L., Yoon, G., Rahmani, W., Jaffer, A., Sharma, N., Hagner, A., Shah, P., Arora, R., Yoon, J., Islam, A., Uchida, A., Chang, C. K., Stratton, J. A., Scott, R. W., Rossi, F. M. V., Underhill, T. M., & Biernaskie, J. (2020). Distinct Regulatory Programs Control the Latent Regenerative Potential of Dermal Fibroblasts during Wound Healing. *Cell Stem Cell*, *27*(3), 396-412.e6. https://doi.org/10.1016/j.stem.2020.07.008

Absinta, M., Maric, D., Gharagozloo, M., Garton, T., Smith, M. D., Jin, J., Fitzgerald, K. C., Song, A., Liu, P., Lin, J., Wu, T., Johnson, K. R., Mcgavern, D. B., Schafer, D. P., Calabresi, P. A., & Reich, D. S. (2021). A lymphocyte – microglia – astrocyte axis in chronic active multiple sclerosis. *Nature*, *November 2020*. https://doi.org/10.1038/s41586-021-03892-7

Afridi, R., Kim, J. H., Rahman, M. H., & Suk, K. (2020). Metabolic Regulation of Glial Phenotypes: Implications in Neuron–Glia Interactions and Neurological Disorders. *Frontiers in Cellular Neuroscience*, *14*(February), 1–17. https://doi.org/10.3389/fncel.2020.00020

Agrawal, S., Anderson, P., Durbeej, M., Van Rooijen, N., Ivars, F., Opdenakker, G., & Sorokin, L. M. (2006). Dystroglycan is selectively cleaved at the parenchymal basement membrane at sites of leukocyte extravasation in experimental autoimmune encephalomyelitis. *Journal of Experimental Medicine*, *203*(4), 1007–1019. https://doi.org/10.1084/jem.20051342

Agudelo, L. Z., Femenía, T., Orhan, F., Porsmyr-Palmertz, M., Goiny, M., Martinez-Redondo, V., Correia, J. C., Izadi, M., Bhat, M., Schuppe-Koistinen, I., Pettersson, A. T., Ferreira, D. M. S., Krook, A., Barres, R., Zierath, J. R., Erhardt, S., Lindskog, M., & Ruas, J. L. (2014). Skeletal muscle PGC-1α1 modulates

kynurenine metabolism and mediates resilience to stress-induced depression. *Cell*, *159*(1), 33–45. https://doi.org/10.1016/j.cell.2014.07.051

Ajami, B., Bennett, J. L., Krieger, C., McNagny, K. M., & Rossi, F. M. V. (2011). Infiltrating monocytes trigger EAE progression, but do not contribute to the resident microglia pool. *Nature Neuroscience*, *14*(9), 1142–1149. https://doi.org/10.1038/nn.2887

Akbar, N., Sandroff, B. M., Wylie, G. R., Strober, L. B., Smith, A., Goverover, Y., Motl, R. W., DeLuca, J., & Genova, H. (2020). Progressive resistance exercise training and changes in resting-state functional connectivity of the caudate in persons with multiple sclerosis and severe fatigue: A proof-of-concept study. *Neuropsychological Rehabilitation*, *30*(1), 54–66. https://doi.org/10.1080/09602011.2018.1449758

Albert, M., Antel, J., Brück, W., & Stadelmann, C. (2007). Extensive cortical remyelination in patients with chronic multiple sclerosis. *Brain Pathology*, *17*(2), 129–138. https://doi.org/10.1111/j.1750-3639.2006.00043.x

Allen, I. V., McQuaid, S., Mirakhur, M., & Nevin, G. (2001). Pathological abnormalities in the normal-appearing white matter in multiple sclerosis. *Neurological Sciences*, *22*(2), 141–144. https://doi.org/10.1007/s100720170012

Almeida, R. G. (2018). The rules of attraction in central nervous system myelination. *Frontiers in Cellular Neuroscience*, *12*(October), 1–9. https://doi.org/10.3389/fncel.2018.00367

Anderson, M. A., Burda, J. E., Ren, Y., Ao, Y., O'Shea, T. M., Kawaguchi, R., Coppola, G., Khakh, B. S., Deming, T. J., & Sofroniew, M. V. (2016). Astrocyte scar formation aids central nervous system axon regeneration. *Nature*, *532*(7598), 195–200. https://doi.org/10.1038/nature17623

Anderson, M. A., O'Shea, T. M., Burda, J. E., Ao, Y., Barlatey, S. L., Bernstein, A. M., Kim, J. H., James, N. D., Rogers, A., Kato, B., Wollenberg, A. L., Kawaguchi, R., Coppola, G., Wang, C., Deming, T. J., He, Z., Courtine, G., & Sofroniew, M. V. (2018). Required growth facilitators propel axon regeneration across complete spinal cord injury. *Nature*, *561*(7723), 396–400. https://doi.org/10.1038/s41586-018-0467-6

Andreuzzi, E., Fejza, A., Polano, M., Poletto, E., Camicia, L., Carobolante, G., Tarticchio, G., Todaro, F., Di Carlo, E., Scarpa, M., Scarpa, M., Paulitti, A., Capuano, A., Canzonieri, V., Maiero, S., Fornasarig, M., Cannizzaro, R., Doliana, R., Colombatti, A., … Mongiat, M. (2022). Colorectal cancer development is affected by the ECM molecule EMILIN-2 hinging on macrophage polarization via the TLR-4/MyD88 pathway. *Journal of Experimental & Clinical Cancer Research : CR*, *41*, 60. https://doi.org/10.1186/s13046-022-02271-y

Armstrong, R. C., Le, T. Q., Frost, E. E., Borke, R. C., & Vana, A. C. (2002). Absence of Fibroblast Growth Factor 2 Promotes Oligodendroglial Repopulation of Demyelinated White Matter. *The Journal of Neuroscience*, *22*(19), 8574–8585. https://doi.org/10.1523/JNEUROSCI.22-19-08574.2002

Ashcroft, G. S., Horan, M. A., & Ferguson, M. W. J. (1997). Aging is associated with reduced deposition of specific extracellular matrix components, an upregulation of angiogenesis, and an altered inflammatory response in a murine incisional wound healing model. *Journal of Investigative Dermatology*, *108*(4), 430–437. https://doi.org/10.1111/1523-1747.ep12289705

Back, S. A., Tuohy, T. M. F., Chen, H., Wallingford, N., Craig, A., Struve, J., Ning, L. L., Banine, F., Liu, Y., Chang, A., Trapp, B. D., Bebo, B. F., Rao, M. S., & Sherman, L. S. (2005). Hyaluronan accumulates in demyelinated lesions and inhibits

oligodendrocyte progenitor maturation. *Nature Medicine*, *11*(9), 966–972. https://doi.org/10.1038/nm1279

Bacmeister, C. M., Barr, H. J., Mcclain, C. R., Thornton, M. A., Nettles, D., Welle, C. G., & Hughes, E. G. (2020). Motor learning promotes remyelination via new and surviving oligodendrocytes. *Nature Neuroscience*. https://doi.org/10.1038/s41593-020-0637-3

Baek, S.-S. (2016). Role of exercise on the brain. *Journal of Exercise Rehabilitation*, *12*(5), 380–385. https://doi.org/10.12965/jer.1632808.404

Bageghni, S. A., Hemmings, K. E., Yuldasheva, N. Y., Maqbool, A., Gamboa-Esteves, F. O., Humphreys, N. E., Jackson, M. S., Denton, C. P., Francis, S., Porter, K. E., Ainscough, J. F. X., Pinteaux, E., Drinkhill, M. J., & Turner, N. A. (2019). Fibroblast-specific deletion of IL-1 receptor-1 reduces adverse cardiac remodeling following myocardial infarction. *JCI Insight*, *4*(17). https://doi.org/10.1172/jci.insight.125074

Bansal, R., Magge, S., & Winkler, S. (2003). Specific inhibitor of FGF receptor signaling: FGF-2-mediated effects on proliferation, differentiation, and MAPK activation are inhibited by PD173074 in oligodendrocyte-lineage cells. *Journal of Neuroscience Research*, *74*(4), 486–493. https://doi.org/10.1002/jnr.10773

Baranzini, S. E., Mudge, J., van Velkinburgh, J. C., Khankhanian, P., Khrebtukova, I., Miller, N. a, Zhang, L., Farmer, A. D., Bell, C. J., Kim, R. W., May, G. D., Woodward, J. E., Caillier, S. J., McElroy, J. P., Gomez, R., Pando, M. J., Clendenen, L. E., Ganusova, E. E., Schilkey, F. D., … Kingsmore, S. F. (2010). Genome, epigenome and RNA sequences of monozygotic twins discordant for multiple sclerosis. *Nature*, *464*(7293), 1351–1356. https://doi.org/10.1038/nature08990

Baranzini, S. E., & Oksenberg, J. R. (2017). The Genetics of Multiple Sclerosis: From 0 to 200 in 50 Years. *Trends in Genetics*, *33*(12), 960–970. https://doi.org/10.1016/j.tig.2017.09.004

Barres, B. A., & Raff, M. C. (1993). Proliferation of oligodendrocyte precursor cells depends on electrical activity in axons. *Nature*, *361*(6409), 258–260. https://doi.org/10.1038/361258a0

Basso, J. C., Shang, A., Elman, M., Karmouta, R., & Suzuki, W. A. (2020). Acute Exercise Improves Prefrontal Cortex but not Hippocampal Function in Healthy Adults. *Journal Ofthe International Neuropsychological Society*, *21*(2015), 791–801. https://doi.org/10.1017/S135561771500106X

Bautista-Hernández, L. A., Gómez-Olivares, J. L., Buentello-Volante, B., & Bautista-de Lucio, V. M. (2017). Fibroblasts: The Unknown Sentinels Eliciting Immune Responses Against Microorganisms. *European Journal of Microbiology & Immunology*, *7*(3), 151–157. https://doi.org/10.1556/1886.2017.00009

Beecham, A. H., Patsopoulos, N. A., Xifara, D. K., Davis, M. F., Kemppinen, A., Cotsapas, C., Shah, T. S., Spencer, C., Booth, D., Goris, A., Oturai, A., Saarela, J., Fontaine, B., Hemmer, B., Martin, C., Zipp, F., D'Alfonso, S., Martinelli-Boneschi, F., Taylor, B., … McCauley, J. L. (2013). Analysis of immune-related loci identifies 48 new susceptibility variants for multiple sclerosis. *Nature Genetics*, *45*(11), 1353–1362. https://doi.org/10.1038/ng.2770

Benatti, F. B., & Pedersen, B. K. (2015). Exercise as an anti-inflammatory therapy for rheumatic diseases—Myokine regulation. *Nature Reviews Rheumatology*, *11*(2), 86–97. https://doi.org/10.1038/nrrheum.2014.193

Bengtsson, S. L., Nagy, Z., Skare, S., Forsman, L., Forssberg, H., & Ullén, F. (2005). Extensive piano practicing has regionally specific effects on white matter

development. *Nature Neuroscience*, *8*(9), 1148–1150. https://doi.org/10.1038/nn1516

Benson, C., Paylor, J. W., Tenorio, G., Winship, I., Baker, G., & Kerr, B. J. (2015). Voluntary wheel running delays disease onset and reduces pain hypersensitivity in early experimental autoimmune encephalomyelitis (EAE). *Experimental Neurology*, *271*, 279–290. https://doi.org/10.1016/j.expneurol.2015.05.017

Bergles, D. E., & Richardson, W. D. (2016). Oligodendrocyte development and plasticity. *Cold Spring Harbor Perspectives in Biology*, *8*(2), 1–28. https://doi.org/10.1101/cshperspect.a020453

Bernardes, D., Brambilla, R., Bracchi-Ricard, V., Karmally, S., Dellarole, A., Carvalho-Tavares, J., & Bethea, J. R. (2016). Prior regular exercise improves clinical outcome and reduces demyelination and axonal injury in experimental autoimmune encephalomyelitis. *Journal of Neurochemistry*, *136*, 63–73. https://doi.org/10.1111/jnc.13354

Bethlehem, R. A. I., Seidlitz, J., White, S. R., Vogel, J. W., Anderson, K. M., Adamson, C., Adler, S., Alexopoulos, G. S., Anagnostou, E., Areces-Gonzalez, A., Astle, D. E., Auyeung, B., Ayub, M., Bae, J., Ball, G., Baron-Cohen, S., Beare, R., Bedford, S. A., Benegal, V., … Alexander-Bloch, A. F. (2022). Brain charts for the human lifespan. *Nature*, *604*(7906), 525–533. https://doi.org/10.1038/s41586-022-04554-y

Bitterman, P. B., & Henke, C. A. (1991). Fibroproliferative Disorders. *Chest*, *99*(3), 81S-84S. https://doi.org/10.1378/chest.99.3_Supplement.81S

Bjornevik, K., Cortese, M., Healy, B. C., Kuhle, J., Mina, M. J., Leng, Y., Elledge, S. J., Niebuhr, D. W., Scher, A. I., Munger, K. L., & Ascherio, A. (2022). Longitudinal analysis reveals high prevalence of Epstein-Barr virus associated with multiple

sclerosis. *Science (New York, N.Y.)*, *301*(January), 296–301. https://doi.org/10.1126/science.abj8222

Blakemore, W. F., Eames, R. A., Smith, K. J., & Mcdonald, W. I. (1977). Remyelination in the spinal cord of the cat following intraspinal injections of lysolecithin. *Journal of the Neurological Sciences*, *33*(1–2), 31–43. https://doi.org/10.1016/0022-510X(77)90179-4

Bö, L., Peterson, J. W., Mørk, S., Hoffman, P. A., Gallatin, M., Ransohoff, R. M., & Trapp, B. D. (1996). Distribution of Immunoglobulin Superfamily Members ICAM-1, -2, -3, and the β2 Integrin LFA-1 in Multiple Sclerosis Lesions. *Journal of Neuropathology and Experimental Neurology*, *55*(10), 1060–1072. https://doi.org/10.1097/00005072-199655100-00006

Bodini, B., Veronese, M., García-Lorenzo, D., Battaglini, M., Poirion, E., Chardain, A., Freeman, L., Louapre, C., Tchikviladze, M., Papeix, C., Dollé, F., Zalc, B., Lubetzki, C., Bottlaender, M., Turkheimer, F., & Stankoff, B. (2016). Dynamic Imaging of Individual Remyelination Profiles in Multiple Sclerosis. *Annals of Neurology*, *79*(5), 726–738. https://doi.org/10.1002/ana.24620

Bolte, A. C., Shapiro, D. A., Dutta, A. B., Ma, W. F., Bruch, K. R., Kovacs, M. A., Marco, A. R., Ennerfelt, H. E., & Lukens, J. R. (2023). The meningeal transcriptional response to traumatic brain injury and aging. *ELife*, *12*, 1–38. https://doi.org/10.7554/eLife.81154

Bonnans, C., Chou, J., & Werb, Z. (2014). Remodelling the extracellular matrix in development and disease. *Nature Reviews Molecular Cell Biology*, *15*(12), 786–801. https://doi.org/10.1038/nrm3904

Bonney, S. K., Sullivan, L. T., Cherry, T. J., Daneman, R., & Shih, A. Y. (2022). Distinct features of brain perivascular fibroblasts and mural cells revealed by in vivo two-

photon imaging. *Journal of Cerebral Blood Flow & Metabolism*, *42*(6), 966–978. https://doi.org/10.1177/0271678X211068528

Bonzano, L., Pedullà, L., Tacchino, A., Brichetto, G., Battaglia, M. A., Mancardi, G. L., & Bove, M. (2019). Upper limb motor training based on task-oriented exercises induces functional brain reorganization in patients with multiple sclerosis. *Neuroscience*, *410*, 150–159. https://doi.org/10.1016/j.neuroscience.2019.05.004

Boothby, I. C., Kinet, M. J., Boda, D. P., Kwan, E. Y., Clancy, S., Cohen, J. N., Habrylo, I., Lowe, M. M., Pauli, M., Yates, A. E., Chan, J. D., Harris, H. W., Neuhaus, I. M., Mccalmont, T. H., Molofsky, A. B., & Rosenblum, M. D. (2021). Early-life inflammation primes a T helper 2 cell – fibroblast niche in skin. *Nature*, *January*. https://doi.org/10.1038/s41586-021-04044-7

Bosch-Queralt, M., Firzner, D., Cantuti-Castelvetri, L., Weil, M., Su, M., Sen, P., & Ruhwedel, T. (2018). Defective cholesterol clearance limits remyelination in the aged central nervous system. *Science*, *688*, 684–688.

Böttcher, C., Van Der Poel, M., Fernández-Zapata, C., Schlickeiser, S., Leman, J. K. H., Hsiao, C. C., Mizee, M. R., Adelia, Vincenten, M. C. J., Kunkel, D., Huitinga, I., Hamann, J., & Priller, J. (2020). Single-cell mass cytometry reveals complex myeloid cell composition in active lesions of progressive multiple sclerosis. *Acta Neuropathologica Communications*, *8*(1), 1–18. https://doi.org/10.1186/s40478-020-01010-8

Bouchard, J., & Villeda, S. A. (2015). Aging and brain rejuvenation as systemic events. *Journal of Neurochemistry*, *132*(1), 5–19. https://doi.org/10.1111/jnc.12969

Boyd, A., Zhang, H., & Williams, A. (2013). Insufficient OPC migration into demyelinated lesions is a cause of poor remyelination in MS and mouse models. *Acta Neuropathologica*, *125*(6), 841–859. https://doi.org/10.1007/s00401-013-1112-y

Bramow, S., Frischer, J. M., Lassmann, H., Koch-Henriksen, N., Lucchinetti, C. F., Sørensen, P. S., & Laursen, H. (2010). Demyelination versus remyelination in progressive multiple sclerosis. *Brain*, *133*(10), 2983–2998. https://doi.org/10.1093/brain/awq250

Brändle, S. M., Obermeier, B., Senel, M., Bruder, J., Mentele, R., Khademi, M., Olsson, T., Tumani, H., Kristoferitsch, W., Lottspeich, F., Wekerle, H., Hohlfeld, R., & Dornmair, K. (2016). Distinct oligoclonal band antibodies in multiple sclerosis recognize ubiquitous self-proteins. *Proceedings of the National Academy of Sciences of the United States of America*, *113*(28), 7864–7869. https://doi.org/10.1073/pnas.1522730113

Bräutigam, L., Zhang, J., Dreij, K., Spahiu, L., Holmgren, A., Abe, H., Tew, K. D., Townsend, D. M., Kelner, M. J., & Morgenstern, R. (2018). Redox Biology MGST1 , a GSH transferase / peroxidase essential for development and hematopoietic stem cell di ff erentiation. *Redox Biology*, *17*(April), 171–179. https://doi.org/10.1016/j.redox.2018.04.013

Brown, J. W. L., Cunniffe, N. G., Prados, F., Kanber, B., Jones, J. L., Needham, E., Georgieva, Z., Rog, D., Pearson, O. R., Overell, J., MacManus, D., Samson, R. S., Stutters, J., ffrench-Constant, C., Gandini Wheeler-Kingshott, C. A. M., Moran, C., Flynn, P. D., Michell, A. W., Franklin, R. J. M., … Coles, A. J. (2021). Safety and efficacy of bexarotene in patients with relapsing-remitting multiple sclerosis (CCMR One): A randomised, double-blind, placebo-controlled, parallel-group, phase 2a study. *The Lancet Neurology*, *20*(9), 709–720. https://doi.org/10.1016/S1474-4422(21)00179-4

Brownlee, W. J., Hardy, T. A., Fazekas, F., & Miller, D. H. (2017). Diagnosis of multiple sclerosis: Progress and challenges. *The Lancet*, *389*(10076), 1336–1346. https://doi.org/10.1016/S0140-6736(16)30959-X

Brügger, M. D., & Basler, K. (2023). The diverse nature of intestinal fibroblasts in development, homeostasis, and disease. *Trends in Cell Biology*, *0*(0). https://doi.org/10.1016/j.tcb.2023.03.007

Buechler, M. B., Fu, W., & Turley, S. J. (2021). Fibroblast-macrophage reciprocal interactions in health, fibrosis, and cancer. *Immunity*, *54*(5), 903–915. https://doi.org/10.1016/j.immuni.2021.04.021

Buechler, M. B., Pradhan, R. N., Krishnamurty, A. T., Cox, C., Calviello, A. K., Wang, A. W., Yang, Y. A., Tam, L., Caothien, R., Roose-Girma, M., Modrusan, Z., Arron, J. R., Bourgon, R., Müller, S., & Turley, S. J. (2021). Cross-tissue organization of the fibroblast lineage. *Nature*, *593*(7860), 575–579. https://doi.org/10.1038/s41586-021-03549-5

Buttery, P. C. (1999). *Laminin-2/Integrin Interactions Enhance Myelin Membrane Formation by Oligodendrocytes*. *212*, 199–212.

Cai, D., Chen, S., Prasad, M., He, L., Wang, X., Choesmel-cadamuro, V., Sawyer, J. K., Danuser, G., & Montell, D. J. (2014). *Mechanical Feedback through E-Cadherin Promotes Direction Sensing during Collective Cell Migration*. https://doi.org/10.1016/j.cell.2014.03.045

Cai, J., Qi, Y., Hu, X., Tan, M., Liu, Z., Zhang, J., Li, Q., Sander, M., & Qiu, M. (2005). Generation of Oligodendrocyte Precursor Cells from Mouse Dorsal Spinal Cord Independent of Nkx6 Regulation and Shh Signaling. *Neuron*, *45*(1), 41–53. https://doi.org/10.1016/j.neuron.2004.12.028

Calvo, F., Ege, N., Grande-Garcia, A., Hooper, S., Jenkins, R. P., Chaudhry, S. I., Harrington, K., Williamson, P., Moeendarbary, E., Charras, G., & Sahai, E. (2013). Mechanotransduction and YAP-dependent matrix remodelling is required for the generation and maintenance of cancer-associated fibroblasts. *Nature Cell Biology*, *15*(6), Article 6. https://doi.org/10.1038/ncb2756

Ceccato, T. L., Starbuck, R. B., Hall, J. K., Walker, C. J., Brown, T. E., Killgore, J. P., Anseth, K. S., & Leinwand, L. A. (2020). Defining the Cardiac Fibroblast Secretome in a Fibrotic Microenvironment. *Journal of the American Heart Association: Cardiovascular and Cerebrovascular Disease*, *9*(19), e017025. https://doi.org/10.1161/JAHA.120.017025

Chambers, E. S., Vukmanovic-stejic, M., Shih, B. B., Trahair, H., Subramanian, P., Devine, O. P., Glanville, J., Gilroy, D., Rustin, M. H. A., Freeman, T. C., Mabbott, N. A., & Akbar, A. N. (2021). Recruitment of inflammatory monocytes by senescent fibroblasts inhibits antigen-specific tissue immunity during human aging. *Nature Aging*, *1*(January). https://doi.org/10.1038/s43587-020-00010-6

Chan, K. Y., Jang, M. J., Yoo, B. B., Greenbaum, A., Ravi, N., Wu, W. L., Sánchez-Guardado, L., Lois, C., Mazmanian, S. K., Deverman, B. E., & Gradinaru, V. (2017). Engineered AAVs for efficient noninvasive gene delivery to the central and peripheral nervous systems. *Nature Neuroscience*, *20*(8), 1172–1179. https://doi.org/10.1038/nn.4593

Chandrasekhar, S., Sorrentino, J. A., & Millis, A. J. (1983). Interaction of fibronectin with collagen: Age-specific defect in the biological activity of human fibroblast fibronectin. *Proceedings of the National Academy of Sciences of the United States of America*, *80*(15), 4747–4751.

Chang, A., Nishiyama, A., Peterson, J., Prineas, J., & Trapp, B. D. (2000). NG2-positive oligodendrocyte progenitor cells in adult human brain and multiple sclerosis lesions. *Journal of Neuroscience*, *20*(17), 6404–6412. https://doi.org/10.1523/JNEUROSCI.20-17-06404.2000

Chang, A., Tourtellotte, W., Rudick, R., & Trapp, B. D. (2002). Premyelinating Oligodendrocytes in Chronic Lesions of Multiple Sclerosis. *N Engl J Med*, *346*(3), 165–173.

Chari, D. M., Crang, A. J., & Blakemore, W. F. (2003). Decline in rate of colonization of oligodendrocyte progenitor cell (OPC)-depleted tissue by adult OPCs with age. *Journal of Neuropathology and Experimental Neurology*, *62*(9), 908–916. https://doi.org/10.1093/jnen/62.9.908

Chari, D., Zhao, C., Kotter, M., Blakemore, W., & Franklin, R. (2006). Corticosteroids Delay Remyelination of Experimental Demyelination in the Rodent Central Nervous System. *Journal of Neuroscience Researchesearch*, *83*, 594–605. https://doi.org/10.1002/jnr

Charles, P., Hernandez, M. P., Stankoff, B., Aigrot, M. S., Colin, C., Rougon, G., Zalc, B., & Lubetzki, C. (2000). Negative regulation of central nervous system myelination by polysialylated-neural cell adhesion molecule. *Proceedings of the National Academy of Sciences of the United States of America*, *97*(13), 7585–7590. https://doi.org/10.1073/pnas.100076197

Chaves, A. R., Devasahayam, A. J., Liam, P., Pretty, R. W., & Plougman, M. (2020). Exercise-Induced Brain Excitability Changes in Progressive Multiple Sclerosis: A Pilot Study. *JNPT*, *44*, 132–144. https://doi.org/10.1097/NPT.0000000000000308

Chen, J., Deng, J. C., Zemans, R. L., Bahmed, K., Kosmider, B., Zhang, M., Peters-Golden, M., & Goldstein, D. R. (2022). Age-induced prostaglandin E2 impairs mitochondrial fitness and increases mortality to influenza infection. *Nature Communications*, *13*(1), Article 1. https://doi.org/10.1038/s41467-022-34593-y

Chen, R.-R., Fan, X.-H., Chen, G., Zeng, G.-W., Xue, Y.-G., Liu, X.-T., & Wang, C.-Y. (2019). Irisin attenuates angiotensin II-induced cardiac fibrosis via Nrf2 mediated inhibition of ROS/ TGFβ1/Smad2/3 signaling axis. *Chemico-Biological Interactions*, *302*, 11–21. https://doi.org/10.1016/j.cbi.2019.01.031

Chen, Y., Pu, Q., Ma, Y., Zhang, H., Ye, T., Zhao, C., Huang, X., Ren, Y., Qiao, L., Liu, H. M., Esmon, C. T., Ding, B. S., & Cao, Z. (2021). Aging Reprograms the

Hematopoietic-Vascular Niche to Impede Regeneration and Promote Fibrosis. *Cell Metabolism*, *33*(2), 395-410.e4. https://doi.org/10.1016/j.cmet.2020.11.019

Chong, S. Y. C., Rosenberg, S. S., Fancy, S. P. J., Zhao, C., Shen, Y.-A. A., Hahn, A. T., McGee, A. W., Xu, X., Zheng, B., Zhang, L. I., Rowitch, D. H., Franklin, R. J. M., Lu, Q. R., & Chan, J. R. (2012). Neurite outgrowth inhibitor Nogo-A establishes spatial segregation and extent of oligodendrocyte myelination. *Proceedings of the National Academy of Sciences*, *109*(4), 1299–1304. https://doi.org/10.1073/pnas.1113540109

Christy, A. L., Walker, M. E., Hessner, M. J., & Brown, M. A. (2013). Mast cell activation and neutrophil recruitment promotes early and robust inflammation in the meninges in EAE. *Journal of Autoimmunity*, *42*, 50–61. https://doi.org/10.1016/j.jaut.2012.11.003

Coman, I., Aigrot, M. S., Seilhean, D., Reynolds, R., Girault, J. A., Zalc, B., & Lubetzki, C. (2006). Nodal, paranodal and juxtaparanodal axonal proteins during demyelination and remyelination in multiple sclerosis. *Brain*, *129*(12), 3186–3195. https://doi.org/10.1093/brain/awl144

Cooper, J. G., Sicard, D., Sharma, S., Van Gulden, S., McGuire, T. L., Cajiao, M. P., Tschumperlin, D. J., & Kessler, J. A. (2020). Spinal Cord Injury Results in Chronic Mechanical Stiffening. *Journal of Neurotrauma*, *37*(3), 494–506. https://doi.org/10.1089/neu.2019.6540

Correa-Gallegos, D., Jiang, D., & Rinkevich, Y. (2021). Fibroblasts as confederates of the immune system. *Immunological Reviews*, *302*(1), 147–162. https://doi.org/10.1111/imr.12972

Couly, G. F., Coltey, P. M., & Douarin, N. M. L. (1992). The developmental fate of the cephalic mesoderm in quail-chick chimeras. *Development*, *114*, 1–15.

Couly, G. F., & Douarin, N. M. L. (1987). Mapping of the Early Neural Primordium in Quail-Chick Chimeras. *Developmental Biology*, *120*, 198–214.

Covarrubias, A. J., Perrone, R., Grozio, A., & Verdin, E. (2021). NAD+ metabolism and its roles in cellular processes during ageing. *Nature Reviews Molecular Cell Biology*, *22*(2), Article 2. https://doi.org/10.1038/s41580-020-00313-x

Cox, J., & Mann, M. (2008). MaxQuant enables high peptide identification rates, individualized p.p.b.-range mass accuracies and proteome-wide protein quantification. *Nature Biotechnology*, *26*(12), 1367–1372. https://doi.org/10.1038/nbt.1511

Cox, J., Neuhauser, N., Michalski, A., Scheltema, R. A., Olsen, J. V., & Mann, M. (2011). Andromeda: A Peptide Search Engine Integrated into the MaxQuant Environment. *Journal of Proteome Research*, *10*(4), 1794–1805. https://doi.org/10.1021/pr101065j

Crambert, G., & Geering, K. (2003). FXYD Proteins: New Tissue-Specific Regulators of the Ubiquitous Na , K-ATPase Peptide hormones. *Pharmacology*, *January*, 1–9.

Czopka, T., ffrench-Constant, C., & Lyons, D. A. (2013). Individual oligodendrocytes have only a few hours in which to generate new myelin sheaths invivo. *Developmental Cell*, *25*(6), 599–609. https://doi.org/10.1016/j.devcel.2013.05.013

D'Alessandro, R., Vignatelli, L., Lugaresi, A., Baldin, E., Granella, F., Tola, M. R., Malagù, S., Motti, L., Neri, W., Galeotti, M., Santangelo, M., Fiorani, L., Montanari, E., Scandellari, C., Benedetti, M. D., & Leone, M. (2013). Risk of multiple sclerosis following clinically isolated syndrome: A 4-year prospective study. *Journal of Neurology*, *260*(6), 1583–1593. https://doi.org/10.1007/s00415-013-6838-x

Dalgas, U., Langeskov-Christensen, M., Stenager, E., Riemenschneider, M., & Hvid, L. G. (2019). Exercise as Medicine in Multiple Sclerosis—Time for a Paradigm Shift: Preventive, Symptomatic, and Disease-Modifying Aspects and Perspectives. *Current Neurology and Neuroscience Reports*, *19*(11), 88. https://doi.org/10.1007/s11910-019-1002-3

Dani, N., Herbst, R. H., McCabe, C., Green, G. S., Kaiser, K., Head, J. P., Cui, J., Shipley, F. B., Jang, A., Dionne, D., Nguyen, L., Rodman, C., Riesenfeld, S. J., Prochazka, J., Prochazkova, M., Sedlacek, R., Zhang, F., Bryja, V., Rozenblatt-Rosen, O., … Lehtinen, M. K. (2021). A cellular and spatial map of the choroid plexus across brain ventricles and ages. *Cell*, *184*(11), 3056-3074.e21. https://doi.org/10.1016/j.cell.2021.04.003

De La Fuente, A. G., Lange, S., Silva, M. E., Gonzalez, G. A., Tempfer, H., van Wijngaarden, P., Zhao, C., Di Canio, L., Trost, A., Bieler, L., Zaunmair, P., Rotheneichner, P., O'Sullivan, A., Couillard-Despres, S., Errea, O., Mäe, M. A., Andrae, J., He, L., Keller, A., … Rivera, F. J. (2017). Pericytes Stimulate Oligodendrocyte Progenitor Cell Differentiation during CNS Remyelination. *Cell Reports*, *20*(8), 1755–1764. https://doi.org/10.1016/j.celrep.2017.08.007

Demerens, C., Stankoff, B., Logak, M., Anglade, P., Allinquant, B., Couraud, F., Zalc, B., & Lubetzki, C. (1996). Induction of myelination in the central nervous system by electrical activity. *Proceedings of the National Academy of Sciences*, *93*(18), 9887–9892. https://doi.org/10.1073/pnas.93.18.9887

Dendrou, C. A., Fugger, L., & Friese, M. A. (2015). Immunopathology of multiple sclerosis. *Nature Reviews Immunology*, *15*(9), 545–558. https://doi.org/10.1038/nri3871

Deng, C. C., Hu, Y. F., Zhu, D. H., Cheng, Q., Gu, J. J., Feng, Q. L., Zhang, L. X., Xu, Y. P., Wang, D., Rong, Z., & Yang, B. (2021). Single-cell RNA-seq reveals fibroblast

heterogeneity and increased mesenchymal fibroblasts in human fibrotic skin diseases. *Nature Communications*, *12*(1), 1–16. https://doi.org/10.1038/s41467-021-24110-y

Derk, J., Jones, H. E., Como, C., Pawlikowski, B., & Siegenthaler, J. A. (2021). Living on the Edge of the CNS: Meninges Cell Diversity in Health and Disease. *Frontiers in Cellular Neuroscience*, *15*. https://www.frontiersin.org/articles/10.3389/fncel.2021.703944

DeSisto, J., O'Rourke, R., Jones, H. E., Pawlikowski, B., Malek, A. D., Bonney, S., Guimiot, F., Jones, K. L., & Siegenthaler, J. A. (2020). Single-Cell Transcriptomic Analyses of the Developing Meninges Reveal Meningeal Fibroblast Diversity and Function. *Developmental Cell*, *54*(1), 43-59.e4. https://doi.org/10.1016/j.devcel.2020.06.009

Di Liegro, C. M., Schiera, G., Proia, P., & Di Liegro, I. (2019). Physical Activity and Brain Health. *Genes*, *10*, 720. https://doi.org/10.3389/fphys.2019.01550

Dias, D. (2020). Pericyte-derived fibrotic scarring is conserved across diverse central nervous system lesions. *The Poets, II: Mary Fage*, 189–192. https://doi.org/10.4324/9781315237787-31

Dias, D. O., Kalkitsas, J., Kelahmetoglu, Y., Estrada, C. P., Tatarishvili, J., Holl, D., Jansson, L., Banitalebi, S., Amiry-Moghaddam, M., Ernst, A., Huttner, H. B., Kokaia, Z., Lindvall, O., Brundin, L., Frisén, J., & Göritz, C. (2021). Pericyte-derived fibrotic scarring is conserved across diverse central nervous system lesions. *Nature Communications*, *12*(1). https://doi.org/10.1038/s41467-021-25585-5

Dias, D. O., Kim, H., Holl, D., & Carle, M. (2018). Reducing Pericyte-Derived Scarring Promotes Recovery after Spinal Cord Injury Article Reducing Pericyte-Derived

Scarring Promotes Recovery after Spinal Cord Injury. *Cell*, 153–165. https://doi.org/10.1016/j.cell.2018.02.004

Díaz-Castro, B., Robel, S., & Mishra, A. (2023). Astrocyte Endfeet in Brain Function and Pathology: Open Questions. *Annual Review of Neuroscience*, *46*(1), 101–121. https://doi.org/10.1146/annurev-neuro-091922-031205

Dickendesher, T. L., Baldwin, K. T., Mironova, Y. A., Koriyama, Y., Raiker, S. J., Askew, K. L., Wood, A., Geoffroy, C. G., Zheng, B., Liepmann, C. D., Katagiri, Y., Benowitz, L. I., Geller, H. M., & Giger, R. J. (2012). NgR1 and NgR3 are receptors for chondroitin sulfate proteoglycans. *Nature Neuroscience*, *15*(5), Article 5. https://doi.org/10.1038/nn.3070

Distler, J. H. W., Györfi, A. H., Ramanujam, M., Whitfield, M. L., Königshoff, M., & Lafyatis, R. (2019). Shared and distinct mechanisms of fibrosis. *Nature Reviews Rheumatology*, *15*(12), 705–730. https://doi.org/10.1038/s41584-019-0322-7

Docherty, S., Harley, R., McAuley, J. J., Crowe, L. A. N., Pedret, C., Kirwan, P. D., Siebert, S., & Millar, N. L. (2022). The effect of exercise on cytokines: Implications for musculoskeletal health: a narrative review. *BMC Sports Science, Medicine and Rehabilitation*, *14*(1), 5. https://doi.org/10.1186/s13102-022-00397-2

Doles, J., Storer, M., Cozzuto, L., Roma, G., & Keyes, W. M. (2012). Age-associated inflammation inhibits epidermal stem cell function. *Genes and Development*, *26*(19), 2144–2153. https://doi.org/10.1101/gad.192294.112

Dong, Y., D'Mello, C., Pinsky, W., Lozinski, B. M., Kaushik, D. K., Ghorbani, S., Moezzi, D., Brown, D., Melo, F. C., Zandee, S., Vo, T., Prat, A., Whitehead, S. N., & Yong, V. W. (2021). Oxidized phosphatidylcholines found in multiple sclerosis lesions mediate neurodegeneration and are neutralized by microglia. *Nature Neuroscience*, *24*(4), 489–503. https://doi.org/10.1038/s41593-021-00801-z

Dong, Y., Jain, R. W., Lozinski, B. M., Mello, C. D., Visser, F., Ghorbani, S., Zandee, S., Brown, D. I., Prat, A., Xue, M., & Yong, V. W. (2022). Single-cell and spatial RNA sequencing identify perturbators of microglial functions with aging. *Nature Aging*. https://doi.org/10.1038/s43587-022-00205-z

Dong, Y., & Yong, V. W. (2019). When encephalitogenic T cells collaborate with microglia in multiple sclerosis. *Nature Reviews Neurology*. https://doi.org/10.1038/s41582-019-0253-6

Donovan, J., Shiwen, X., Norman, J., & Abraham, D. (2013). Platelet-derived growth factor alpha and beta receptors have overlapping functional activities towards fibroblasts. *Fibrogenesis & Tissue Repair*, *6*, 10. https://doi.org/10.1186/1755-1536-6-10

Dorrier, C. E., Aran, D., Haenelt, E. A., Sheehy, R. N., Hoi, K. K., Pintarić, L., Chen, Y., Lizama, C. O., Cautivo, K. M., Weiner, G. A., Popko, B., Fancy, S. P. J., Arnold, T. D., & Daneman, R. (2021). CNS fibroblasts form a fibrotic scar in response to immune cell infiltration. *Nature Neuroscience*, *24*(FebruarY). https://doi.org/10.1038/s41593-020-00770-9

Dorrier, C. E., Jones, H. E., Pintarić, L., Siegenthaler, J. A., & Daneman, R. (2021). Emerging roles for CNS fibroblasts in health, injury and disease. *Nature Reviews Neuroscience*, *0123456789*. https://doi.org/10.1038/s41583-021-00525-w

Duffield, J. S., Forbes, S. J., Constandinou, C. M., Clay, S., Partolina, M., Vuthoori, S., Wu, S., Lang, R., & Iredale, J. P. (2005). Selective depletion of macrophages reveals distinct, opposing roles during liver injury and repair. *Journal of Clinical Investigation*, *115*(1), 56–65. https://doi.org/10.1172/JCI200522675

Duffield, J. S., Tipping, P. G., Kipari, T., Cailhier, J. F., Clay, S., Lang, R., Bonventre, J. V., & Hughes, J. (2005). Conditional ablation of macrophages halts progression

of crescentic glomerulonephritis. *American Journal of Pathology*, *167*(5), 1207–1219. https://doi.org/10.1016/S0002-9440(10)61209-6

Duncan, G. J., Plemel, J. R., Assinck, P., Manesh, S. B., Muir, F. G. W., Hirata, R., Berson, M., Liu, J., Wegner, M., Emery, B., Moore, G. R. W., & Tetzlaff, W. (2017). Myelin regulatory factor drives remyelination in multiple sclerosis. *Acta Neuropathologica*, *134*(3), 403–422. https://doi.org/10.1007/s00401-017-1741-7

Duncan, G. J., Simkins, T. J., Emery, B., & Duncan, G. J. (2021). *Neuron-Oligodendrocyte Interactions in the Structure and Integrity of Axons*. *9*(March). https://doi.org/10.3389/fcell.2021.653101

Duncan, I. D., Brower, A., Kondo, Y., Curlee, J. F., & Schultz, R. D. (2009). Extensive remyelination of the CNS leads to functional recovery. *Proceedings of the National Academy of Sciences of the United States of America*, *106*(16), 6832–6836. https://doi.org/10.1073/pnas.0812500106

Duncan, I. D., Marik, R. L., Broman, A. T., & Heidari, M. (2017). Thin myelin sheaths as the hallmark of remyelination persist over time and preserve axon function. *Proceedings of the National Academy of Sciences of the United States of America*, *114*(45), E9685–E9691. https://doi.org/10.1073/pnas.1714183114

Emery, B. (2010). Regulation of oligodendrocyte differentiation. *Science*, *330*(November), 359–362.

Emery, B., Agalliu, D., Cahoy, J. D., Watkins, T. A., Dugas, J. C., Mulinyawe, S. B., Ibrahim, A., Ligon, K. L., Rowitch, D. H., & Barres, B. A. (2009). Myelin Gene Regulatory Factor Is a Critical Transcriptional Regulator Required for CNS Myelination. *Cell*, *138*(1), 172–185. https://doi.org/10.1016/j.cell.2009.04.031

Eming, S. A., Martin, P., & Tomic-Canic, M. (2014). Wound repair and regeneration: Mechanisms, signaling, and translation. *Science Translational Medicine*, *6*(265). https://doi.org/10.1126/scitranslmed.3009337

Engelhardt, B., Vajkoczy, P., & Weller, R. O. (2017). The movers and shapers in immune privilege of the CNS. *Nature Publishing Group*, *18*(2), 123–131. https://doi.org/10.1038/ni.3666

Fainstein, N., Tyk, R., Touloumi, O., Lagoudaki, R., Goldberg, Y., Agranyoni, O., Navon-Venezia, S., Katz, A., Grigoriadis, N., Ben-Hur, T., & Einstein, O. (2019). Exercise intensity-dependent immunomodulatory effects on encephalomyelitis. *Annals of Clinical and Translational Neurology*, *6*(9), 1647–1658. https://doi.org/10.1002/acn3.50859

Fancy, S. P. J., Baranzini, S. E., Zhao, C., Yuk, D. I., Irvine, K. A., Kaing, S., Sanai, N., Franklin, R. J. M., & Rowitch, D. H. (2009). Dysregulation of the Wnt pathway inhibits timely myelination and remyelination in the mammalian CNS. *Genes and Development*, *23*(13), 1571–1585. https://doi.org/10.1101/gad.1806309

Fei, D., Meng, X., Yu, W., Yang, S., Song, N., Cao, Y., Jin, S., Dong, L., Pan, S., & Zhao, M. (2018). Fibronectin (FN) cooperated with TLR2/TLR4 receptor to promote innate immune responses of macrophages via binding to integrin β1. *Virulence*, *9*(1), 1588–1600. https://doi.org/10.1080/21505594.2018.1528841

Felippe, L. A., Salgado, P. R., De Souza Silvestre, D., Smaili, S. M., & Christofoletti, G. (2019). A controlled clinical trial on the effects of exercise on cognition and mobility in adults with multiple sclerosis. *American Journal of Physical Medicine and Rehabilitation*, *98*(2), 97–102. https://doi.org/10.1097/PHM.0000000000000987

Ferguson, B., Matyszak, M. K., Esiri, M. M., & Perry, V. H. (1997). Axonal damage in acute multiple sclerosis lesions. *Brain*, *120*(3), 393–399. https://doi.org/10.1093/brain/120.3.393

Feys, P., Moumdjian, L., Halewyck, F. V., Wens, I., Eijnde, B. O., Wijmeersch, B. V., Popescu, V., & Asch, P. V. (2017). Effects of an individual 12-week community-

located “start-to-run” program on physical capacity, walking, fatigue, cognitive function, brain volumes, and structures in persons with multiple sclerosis. *Multiple*, *25*(1), 92–103. https://doi.org/10.1177/https

Filippi, M., Bar-Or, A., Piehl, F., Preziosa, P., Solari, A., Vukusic, S., & Rocca, M. A. (2018). Multiple sclerosis. *Nature Reviews Disease Primers*, *4*(1), 1–27. https://doi.org/10.1038/s41572-018-0041-4

Fisher, D., Xing, B., Dill, J., Li, H., Hoang, H. H., Zhao, Z., Yang, X.-L., Bachoo, R., Cannon, S., Longo, F. M., Sheng, M., Silver, J., & Li, S. (2011). Leukocyte Common Antigen-Related Phosphatase Is a Functional Receptor for Chondroitin Sulfate Proteoglycan Axon Growth Inhibitors. *The Journal of Neuroscience*, *31*(40), 14051–14066. https://doi.org/10.1523/JNEUROSCI.1737-11.2011

Flachenecker, P., Bures, A. K., Gawlik, A., Weiland, A.-C., Kuld, S., Gusowski, K., Streber, R., Pfeifer, K., & Tallner, A. (2020). Efficacy of an Internet-Based Program to Promote Physical Activity and Exercise after Inpatient Rehabilitation in Persons with Multiple Sclerosis: A Randomized, Single-Blind, Controlled Study. *International Journal of Environmental Research and Public Health*, *17*(12), 4544. https://doi.org/10.3390/ijerph17124544

Fortier, S. M., Penke, L. R., King, D., Pham, T. X., Ligresti, G., & Peters-Golden, M. (n.d.). Myofibroblast dedifferentiation proceeds via distinct transcriptomic and phenotypic transitions. *JCI Insight*, *6*(6), e144799. https://doi.org/10.1172/jci.insight.144799

Franklin, R. J. M., & Simons, M. (2022). CNS remyelination and inflammation: From basic mechanisms to therapeutic opportunities. *Neuron*, *110*(21), 3549–3565. https://doi.org/10.1016/j.neuron.2022.09.023

Freeman, S. A., Desmazières, A., Simonnet, J., Gatta, M., Pfeiffer, F., Aigrot, M. S., Rappeneau, Q., Guerreiro, S., Michel, P. P., Yanagawa, Y., Barbin, G., Brophy,

P. J., Fricker, D., Lubetzki, C., & Sol-Foulon, N. (2015). Acceleration of conduction velocity linked to clustering of nodal components precedes myelination. *Proceedings of the National Academy of Sciences*, *112*(3). https://doi.org/10.1073/pnas.1419099112

Frodermann, V., Rohde, D., Courties, G., Severe, N., Schloss, M. J., Amatullah, H., McAlpine, C. S., Cremer, S., Hoyer, F. F., Ji, F., van Koeverden, I. D., Herisson, F., Honold, L., Masson, G. S., Zhang, S., Grune, J., Iwamoto, Y., Schmidt, S. P., Wojtkiewicz, G. R., … Nahrendorf, M. (2019). Exercise reduces inflammatory cell production and cardiovascular inflammation via instruction of hematopoietic progenitor cells. *Nature Medicine*, *25*(11), 1761–1771. https://doi.org/10.1038/s41591-019-0633-x

Frost, E. E., Nielsen, J. A., Le, T. Q., & Armstrong, R. C. (2003). PDGF and FGF2 regulate oligodendrocyte progenitor responses to demyelination. *Journal of Neurobiology*, *54*(3), 457–472. https://doi.org/10.1002/neu.10158

Fukuda, S., Nakamura, T., Kishigami, Y., Endo, K., Azuma, T., Fujikawa, T., Tsutsumi, S., & Shimizu, Y. (2005). New canine spinal cord injury model free from laminectomy. *Brain Research Protocols*, *14*(3), 171–180. https://doi.org/10.1016/j.brainresprot.2005.01.001

Fünfschilling, U., Supplie, L. M., Mahad, D., Boretius, S., Saab, A. S., Edgar, J., Brinkmann, B. G., Kassmann, C. M., Tzvetanova, I. D., Möbius, W., Diaz, F., Meijer, D., Suter, U., Hamprecht, B., Sereda, M. W., Moraes, C. T., Frahm, J., Goebbels, S., & Nave, K. A. (2012). Glycolytic oligodendrocytes maintain myelin and long-term axonal integrity. *Nature*, *485*(7399), 517–521. https://doi.org/10.1038/nature11007

Gasse, P., Mary, C., Guenon, I., Noulin, N., Charron, S., Schnyder-Candrian, S., Schnyder, B., Akira, S., Quesniaux, V. F. J., Lagente, V., Ryffel, B., & Couillin, I.

(2007). IL-1R1/MyD88 signaling and the inflammasome are essential in pulmonary inflammation and fibrosis in mice. *Journal of Clinical Investigation*, *117*(12), 3786–3799. https://doi.org/10.1172/JCI32285

Gay, D., & Esiri, M. (1991). Blood-Brain Barrier Damage in Acute Multiple Sclerosis Plaques. *Brain*, *114*(1), 557–572. https://doi.org/10.1093/brain/114.1.557

Geering, K. (2006). FXYD proteins: New regulators of Na-K-ATPase. *American Journal of Physiology - Renal Physiology*, *290*(2). https://doi.org/10.1152/ajprenal.00126.2005

Gentile, A., Musella, A., De Vito, F., Rizzo, F. R., Fresegna, D., Bullitta, S., Vanni, V., Guadalupi, L., Stampanoni Bassi, M., Buttari, F., Centonze, D., & Mandolesi, G. (2019). Immunomodulatory Effects of Exercise in Experimental Multiple Sclerosis. *Frontiers in Immunology*, *10*(September), 1–8. https://doi.org/10.3389/fimmu.2019.02197

Ghorbani, S., Jelinek, E., Jain, R., Buehner, B., Li, C., Lozinski, B. M., Sarkar, S., Kaushik, D. K., Dong, Y., Wight, T. N., Karimi-Abdolrezaee, S., Schenk, G. J., Strijbis, E. M., Geurts, J., Zhang, P., Ling, C. C., & Yong, V. W. (2022). Versican promotes T helper 17 cytotoxic inflammation and impedes oligodendrocyte precursor cell remyelination. *Nature Communications*, *13*(1), 1–18. https://doi.org/10.1038/s41467-022-30032-0

Ghorbani, S., & Yong, V. W. (2021). The extracellular matrix as modifier of neuroinflammation and remyelination in multiple sclerosis. *Brain*. https://doi.org/10.1093/brain/awab059

Gibson, E. M., Purger, D., Mount, C. W., Goldstein, A. K., Lin, G. L., Wood, L. S., Inema, I., Miller, S. E., Bieri, G., Zuchero, J. B., Barres, B. A., Woo, P. J., Vogel, H., & Monje, M. (2014). Neuronal Activity Promotes Oligodendrogenesis and Adaptive

Myelination in the Mammalian Brain. *Science*, *344*(6183), 480–481. https://doi.org/10.1126/science.1254446

Giles, D. A., Duncker, P. C., Wilkinson, N. M., Washnock-Schmid, J. M., & Segal, B. M. (2018). CNS-resident classical DCs play a critical role in CNS autoimmune disease. *Journal of Clinical Investigation*, *128*(12), 5322–5334. https://doi.org/10.1172/JCI123708

Gilgun-sherki, Y., Melamed, E., & Offen, D. (2004). The role of oxidative stress in the pathogenesis of multiple sclerosis: The need for effective antioxidant therapy. *Journal of Neurology*, *251*, 261–268. https://doi.org/10.1007/s00415-004-0348-9

Goldman, S. A., & Kuypers, N. J. (2015). How to make an oligodendrocyte. *Development*, 3983–3995. https://doi.org/10.1242/dev.126409

Goldschmidt, T., Antel, J., Konig, F. B., Bruck, W., & Kuhlmann, T. (2009). Remyelination capacity of the MS brain decreases with disease chronicity. *Neurology*, *72*(22), 1914–1921.

Gordon, G. R. J., Choi, H. B., Rungta, R. L., Ellis-Davies, G. C. R., & MacVicar, B. A. (2008). Brain metabolism dictates the polarity of astrocyte control over arterioles. *Nature*, *456*(7223), Article 7223. https://doi.org/10.1038/nature07525

Gordon, M. H., Anowai, A., Young, D., Das, N., Campden, R. I., Sekhon, H., Myers, Z., Mainoli, B., Chopra, S., Thuy-Boun, P. S., Kizhakkedathu, J., Bindra, G., Jijon, H. B., Heitman, S., Yates, R., Wolan, D. W., Edgington-Mitchell, L. E., MacNaughton, W. K., & Dufour, A. (2019). N-Terminomics/TAILS Profiling of Proteases and Their Substrates in Ulcerative Colitis. *ACS Chemical Biology*, *14*(11), 2471–2483. https://doi.org/10.1021/acschembio.9b00608

Goritz, C., Dias, D., Tomilin, N., Barbacid, M., Shupliakov, O., & Frisen, J. (2011). A Pericyte Origin of Spinal Cord Scar Tissue. *Science*, *333*(July), 238–243. https://doi.org/10.1126/science.1203165

Gosselin, D., Link, V. M., Romanoski, C. E., Fonseca, G. J., Eichenfield, D. Z., Spann, N. J., Stender, J. D., Chun, H. B., Garner, H., Geissmann, F., & Glass, C. K. (2014). Environment drives selection and function of enhancers controlling tissue-specific macrophage identities. *Cell*, *159*(6), 1327–1340. https://doi.org/10.1016/j.cell.2014.11.023

Goverman, J. M. (2011). Immune Tolerance in Multiple Sclerosis. *Immunological Reviews*, *241*(1), 228–240. https://doi.org/10.1111/j.1600-065X.2011.01016.x

Green, A. J., Gelfand, J. M., Cree, B. A., Bevan, C., Boscardin, W. J., Mei, F., Inman, J., Arnow, S., Devereux, M., Abounasr, A., Nobuta, H., Zhu, A., Friessen, M., Gerona, R., von Büdingen, H. C., Henry, R. G., Hauser, S. L., & Chan, J. R. (2017). Clemastine fumarate as a remyelinating therapy for multiple sclerosis (ReBUILD): A randomised, controlled, double-blind, crossover trial. *The Lancet*, *390*(10111), 2481–2489. https://doi.org/10.1016/S0140-6736(17)32346-2

Gritsch, S., Lu, J., Thilemann, S., Wo, S., Bruttger, J., Karram, K., Ruhwedel, T., Blanfeld, M., Vardeh, D., Waisman, A., Nave, K., & Kuner, R. (2014). Oligodendrocyte ablation triggers central pain independently of innate or adaptive immune responses in mice. *Nature Communications*. https://doi.org/10.1038/ncomms6472

Guo, L. Y., Lozinski, B., & Yong, V. W. (2019). Exercise in multiple sclerosis and its models: Focus on the central nervous system outcomes. *Journal of Neuroscience Research*, *3*(98), 509–523. https://doi.org/10.1002/jnr.24524

Hadžović-džuvo, A., Lepara, O., Valjevac, A., & Avdagić, N. (2010). Serum total antioxidant capacity in patients with multiple sclerosis. *BOSNIAN JOURNAL OF BASIC MEDICAL SCIENCES*, *11*(1), 33–36.

Haider, L., Fischer, M. T., Frischer, J. M., Bauer, J., Ho, R., Esterbauer, H., Binder, C. J., & Witztum, J. L. (2011). Oxidative damage in multiple sclerosis lesions ¨. *Brain*, *134*, 1914–1924. https://doi.org/10.1093/brain/awr128

Haimon, Z., Frumer, G. R., Kim, J.-S., Trzebanski, S., Haffner-Krausz, R., Ben-Dor, S., Porat, Z., Muschaweckh, A., Chappell-Maor, L., Boura-Halfon, S., Korn, T., & Jung, S. (2022). Cognate microglia–T cell interactions shape the functional regulatory T cell pool in experimental autoimmune encephalomyelitis pathology. *Nature Immunology*, *23*(12), Article 12. https://doi.org/10.1038/s41590-022-01360-6

Hammond, T. R., Dufort, C., Dissing-Olesen, L., Giera, S., Young, A., Wysoker, A., Walker, A. J., Gergits, F., Segel, M., Nemesh, J., Marsh, S. E., Saunders, A., Macosko, E., Ginhoux, F., Chen, J., Franklin, R. J. M., Piao, X., McCarroll, S. A., & Stevens, B. (2019). Single-Cell RNA Sequencing of Microglia throughout the Mouse Lifespan and in the Injured Brain Reveals Complex Cell-State Changes. *Immunity*, *0*(0), 1–19. https://doi.org/10.1016/J.IMMUNI.2018.11.004

Harlow, D. E., Saul, K. E., Komuro, H., & Macklin, W. B. (2015). Myelin Proteolipid Protein Complexes with v Integrin and AMPA Receptors In Vivo and Regulates AMPA-Dependent Oligodendrocyte Progenitor Cell Migration through the Modulation of Cell-Surface GluR2 Expression. *Journal of Neuroscience*, *35*(34), 12018–12032. https://doi.org/10.1523/JNEUROSCI.5151-14.2015

Hayflick, L. (1965). The limited in vitro lifetime of human diploid cell strains. *Experimental Cell Research*, *37*(3), 614–636. https://doi.org/10.1016/0014-4827(65)90211-9

He, X., Liu, D., Zhang, Q., Liang, F., Dai, G., Zeng, J., Pei, Z., Xu, G., & Lan, Y. (2017). Voluntary Exercise Promotes Glymphatic Clearance of Amyloid Beta and Reduces the Activation of Astrocytes and Microglia in Aged Mice. *Frontiers in Molecular Neuroscience*, *10*, 144. https://doi.org/10.3389/fnmol.2017.00144

Henderson, N. C., Arnold, T. D., Katamura, Y., Giacomini, M. M., Rodriguez, J. D., McCarty, J. H., Pellicoro, A., Raschperger, E., Betsholtz, C., Ruminski, P. G., Griggs, D. W., Prinsen, M. J., Maher, J. J., Iredale, J. P., Lacy-Hulbert, A., Adams, R. H., & Sheppard, D. (2013). Targeting of αv integrin identifies a core molecular pathway that regulates fibrosis in several organs. *Nature Medicine*, *19*(12), 1617–1624. https://doi.org/10.1038/nm.3282

Henderson, N. C., Rieder, F., & Wynn, T. A. (2020). Fibrosis: From mechanisms to medicines. *Nature*, *587*(7835), 555–566. https://doi.org/10.1038/s41586-020-2938-9

Herbert, A. L., Fu, M., Drerup, C. M., Gray, R. S., Harty, B. L., Ackerman, S. D., O'Reilly-Pol, T., Johnson, S. L., Nechiporuk, A. V., Barres, B. A., & Monk, K. R. (2017). Dynein/dynactin is necessary for anterograde transport of *Mbp* mRNA in oligodendrocytes and for myelination in vivo. *Proceedings of the National Academy of Sciences*, *114*(43), E9153–E9162. https://doi.org/10.1073/pnas.1711088114

Herriges, M., & Morrisey, E. E. (2014). Lung development: Orchestrating the generation and regeneration of a complex organ. *Development (Cambridge, England)*, *141*(3), 502–513. https://doi.org/10.1242/dev.098186

Hinks, G. L., & Franklin, R. J. M. (1999). Distinctive patterns of PDGF-A, FGF-2, IGF-I, and TGF-β1 gene expression during remyelination of experimentally-induced spinal cord demyelination. *Molecular and Cellular Neurosciences*, *14*(2), 153–168. https://doi.org/10.1006/mcne.1999.0771

Holt, L. M., Hernandez, R. D., Pacheco, N. L., Torres Ceja, B., Hossain, M., & Olsen, M. L. (2019). Astrocyte morphogenesis is dependent on BDNF signaling via astrocytic TrkB.T1. *ELife*, *8*, e44667. https://doi.org/10.7554/eLife.44667

Horowitz, A. M., Fan, X., Bieri, G., Smith, L. K., Sanchez-diaz, C. I., Schroer, A. B., Gontier, G., Casaletto, K. B., Kramer, J. H., Williams, K. E., & Villeda, S. A. (2020). Blood factors transfer beneficial effects of exercise on neurogenesis and cognition to the aged brain. *Science*, *173*(July), 167–173.

Horssen, J. V., Bo, L., Vos, C. M. P., Virtanen, I., & Vries, H. E. D. (2005). *Basement Membrane Proteins in Multiple Sclerosis-Associated Inflammatory Cuffs: Potential Role in Influx and Transport of Leukocytes*. *64*(8), 722–729.

Howell, O. W., Schulz-Trieglaff, E. K., Carassiti, D., Gentleman, S. M., Nicholas, R., Roncaroli, F., & Reynolds, R. (2015). Extensive grey matter pathology in the cerebellum in multiple sclerosis is linked to inflammation in the subarachnoid space. *Neuropathology and Applied Neurobiology*, *41*(6), 798–813. https://doi.org/10.1111/nan.12199

Huang, J. K., Jarjour, A. A., Nait Oumesmar, B., Kerninon, C., Williams, A., Krezel, W., Kagechika, H., Bauer, J., Zhao, C., Evercooren, A. B.-V., Chambon, P., ffrench-Constant, C., & Franklin, R. J. M. (2011). Retinoid X receptor gamma signaling accelerates CNS remyelination. *Nature Neuroscience*, *14*(1), Article 1. https://doi.org/10.1038/nn.2702

Huang, J.-Y., Wang, Y.-X., Gu, W.-L., Fu, S.-L., Li, Y., Huang, L.-D., Zhao, Z., Hang, Q., Zhu, H.-Q., & Lu, P.-H. (2012). Expression and function of myelin-associated proteins and their common receptor NgR on oligodendrocyte progenitor cells. *Brain Research*, *1437*, 1–15. https://doi.org/10.1016/j.brainres.2011.12.008

Hughes, E. G., Kang, S. H., Fukaya, M., & Bergles, D. E. (2013). Oligodendrocyte progenitors balance growth with self-repulsion to achieve homeostasis in the adult brain. *Nature Neuroscience*, *16*(6), 668–676. https://doi.org/10.1038/nn.3390

Hughes, E. G., Orthmann-Murphy, J. L., Langseth, A. J., & Bergles, D. E. (2018). Myelin remodeling through experience-dependent oligodendrogenesis in the adult somatosensory cortex. *Nature Neuroscience*, *21*(5), 696–706. https://doi.org/10.1038/s41593-018-0121-5

Iacobaeus, E., Sugars, R. V., Törnqvist Andrén, A., Alm, J. J., Qian, H., Frantzen, J., Newcombe, J., Alkass, K., Druid, H., Bottai, M., Röyttä, M., & Le Blanc, K. (2017). Dynamic Changes in Brain Mesenchymal Perivascular Cells Associate with Multiple Sclerosis Disease Duration, Active Inflammation, and Demyelination. *Stem Cells Translational Medicine*, *6*(10), 1840–1851. https://doi.org/10.1002/sctm.17-0028

Ibrahim, I., Tintera, J., Skoch, A., Jirů, F., Hlustik, P., Martinkova, P., Zvara, K., & Rasova, K. (2011). Fractional anisotropy and mean diffusivity in the corpus callosum of patients with multiple sclerosis: The effect of physiotherapy. *Neuroradiology*, *53*(11), 917–926. https://doi.org/10.1007/s00234-011-0879-6

International Multiple Sclerosis Genetics Consortium, Harroud, A., Stridh, P., McCauley, J. L., Saarela, J., Van Den Bosch, A. M. R., Engelenburg, H. J., Beecham, A. H., Alfredsson, L., Alikhani, K., Amezcua, L., Andlauer, T. F. M., Ban, M., Barcellos, L. F., Barizzone, N., Berge, T., Berthele, A., Bittner, S., Bos, S. D., … Stefánsson, K. (2023). Locus for severity implicates CNS resilience in progression of multiple sclerosis. *Nature*, *619*(7969), 323–331. https://doi.org/10.1038/s41586-023-06250-x

Irvine, K. A., & Blakemore, W. F. (2008). Remyelination protects axons from demyelination-associated axon degeneration. *Brain*, *131*, 1464–1477. https://doi.org/10.1093/brain/awn080

Ito, M., Yang, Z., Andl, T., Cui, C., Kim, N., Millar, S. E., & Cotsarelis, G. (2007). Wnt-dependent de novo hair follicle regeneration in adult mouse skin after wounding. *Nature*, *447*(7142), 316–320. https://doi.org/10.1038/nature05766

Jagannath, V. A., Filippini, G., Borges do Nascimento, I. J., Di Pietrantonj, C., Robak, E. W., & Whamond, L. (2018). Vitamin D for the management of multiple sclerosis. *The Cochrane Database of Systematic Reviews*, *2018*(9), CD008422. https://doi.org/10.1002/14651858.CD008422.pub3

Jain, A., Kim, Y.-T., McKeon, R. J., & Bellamkonda, R. V. (2006). In situ gelling hydrogels for conformal repair of spinal cord defects, and local delivery of BDNF after spinal cord injury. *Biomaterials*, *27*(3), 497–504. https://doi.org/10.1016/j.biomaterials.2005.07.008

Jain, R. W., Elliott, D. A., & Yong, V. W. (2023). Single Cell Analysis of High-Parameter Histology Images Using Histoflow Cytometry. *The Journal of Immunology*, *210*(12), 2038–2049. https://doi.org/10.4049/jimmunol.2200700

Jain, R. W., & Yong, V. W. (2021). B cells in central nervous system disease: Diversity, locations and pathophysiology. *Nature Reviews Immunology*, *0123456789*. https://doi.org/10.1038/s41577-021-00652-6

Jang, S., Shen, H. K., Ding, X., Miles, T. F., & Gradinaru, V. (2022). Structural basis of receptor usage by the engineered capsid AAV-PHP.eB. *Molecular Therapy - Methods and Clinical Development*, *26*(September), 343–354. https://doi.org/10.1016/j.omtm.2022.07.011

Jeffery, N. D., & Blakemore, W. F. (1997). Locomotor deficits induced by experimental spinal cord demyelination are abolished by spontaneous remyelination. *Brain*, *120*(1), 27–37. https://doi.org/10.1093/brain/120.1.27

Jellusova, J. (2018). Cross-talk between signal transduction and metabolism in B cells. *Immunology Letters*, *201*(November), 1–13. https://doi.org/10.1016/j.imlet.2018.11.003

Jensen, S. K., Michaels, N. J., Ilyntskyy, S., Keough, M. B., Kovalchuk, O., & Yong, V. W. (2018). Multimodal Enhancement of Remyelination by Exercise with a Pivotal Role for Oligodendroglial PGC1α. *Cell Reports*, *24*(12), 3167–3179. https://doi.org/10.1016/j.celrep.2018.08.060

Jensen, S. K., & Wee Yong, V. (2014). Microglial modulation as a mechanism behind the promotion of central nervous system well-being by physical exercise. *Clinical and Experimental Neuroimmunology*, *5*(2), 188–201. https://doi.org/10.1111/cen3.12093

Jensen, S. K., & Yong, V. W. (2016). Activity-Dependent and Experience-Driven Myelination Provide New Directions for the Management of Multiple Sclerosis. *Trends in Neurosciences*, *39*(6), 356–365. https://doi.org/10.1016/j.tins.2016.04.003

Jepson, S., Vought, B., Gross, C. H., Gan, L., Austen, D., Frantz, J. D., Zwahlen, J., Lowe, D., Markland, W., & Krauss, R. (2012). LINGO-1, a Transmembrane Signaling Protein, Inhibits Oligodendrocyte Differentiation and Myelination through Intercellular Self-interactions. *The Journal of Biological Chemistry*, *287*(26), 22184–22195. https://doi.org/10.1074/jbc.M112.366179

Jiang, X., Iseki, S., Maxson, R. E., Sucov, H. M., & Morriss-Kay, G. M. (2002). Tissue Origins and Interactions in the Mammalian Skull Vault. *Developmental Biology*, *241*(1), 106–116. https://doi.org/10.1006/dbio.2001.0487

Jones, L. K., O'Sullivan, K. M., Semple, T., Kuligowski, M. P., Fukami, K., Ma, F. Y., Nikolic-Paterson, D. J., Holdsworth, S. R., & Kitching, A. R. (2009). IL-1RI

deficiency ameliorates early experimental renal interstitial fibrosis. *Nephrology Dialysis Transplantation*, *24*(10), 3024–3032. https://doi.org/10.1093/ndt/gfp214

Jong, J. M. D., Wang, P., Oomkens, M., & Baron, W. (2019). Remodeling of the interstitial extracellular matrix in white matter multiple sclerosis lesions: Implications for remyelination (failure). *Journal of Neuroscience Research*, *98*, 1370–1397. https://doi.org/10.1002/jnr.24582

Kalb, R., Brown, T. R., Coote, S., Costello, K., Dalgas, U., Garmon, E., Giesser, B., Halper, J., Karpatkin, H., Keller, J., Ng, A. V., Pilutti, L. A., Rohrig, A., Van Asch, P., Zackowski, K., & Motl, R. W. (2020). Exercise and lifestyle physical activity recommendations for people with multiple sclerosis throughout the disease course. *Multiple Sclerosis Journal*, 1–11. https://doi.org/10.1177/1352458520915629

Kalron, A., Dolev, M., Greenberg-Abrahami, M., Menascu, S., Frid, L., Avrech-Shezifi, S., Harari, G., Magalashvili, D., & Achiron, A. (2021). Physical activity behavior in people with multiple sclerosis during the COVID-19 pandemic in Israel: Results of an online survey. *Multiple Sclerosis and Related Disorders*, *47*, 102603. https://doi.org/10.1016/j.msard.2020.102603

Kang, I., Harten, I. A., Chang, M. Y., Braun, K. R., Sheih, A., Nivison, M. P., Johnson, P. Y., Workman, G., Kaber, G., Evanko, S. P., Chan, C. K., Merrilees, M. J., Ziegler, S. F., Kinsella, M. G., Frevert, C. W., & Wight, T. N. (2017). Versican Deficiency Significantly Reduces Lung Inflammatory Response Induced by Polyinosine-Polycytidylic Acid Stimulation. *The Journal of Biological Chemistry*, *292*(1), 51–63. https://doi.org/10.1074/jbc.M116.753186

Kantarci, O. H., Lebrun, C., Siva, A., Keegan, M. B., Azevedo, C. J., Inglese, M., Tintoré, M., Newton, B. D., Durand-Dubief, F., Amato, M. P., De Stefano, N., Sormani, M. P., Pelletier, D., & Okuda, D. T. (2016). Primary Progressive Multiple Sclerosis

Evolving From Radiologically Isolated Syndrome. *Annals of Neurology*, *79*(2), 288–294. https://doi.org/10.1002/ana.24564

Kaplan, M. R., Cho, M.-H., Ullian, E. M., Isom, L. L., Levinson, S. R., & Barres, B. A. (2001). Differential Control of Clustering of the Sodium Channels Na v 1.2 and Na v 1.6 at Developing CNS Nodes of Ranvier purification and culture of retinal ganglion cells (RGCs), optic nerve astrocytes, and optic nerve oligodendro-cytes (Barres et al we have b. *Neuron*, *30*, 105–119.

Kaplan, M. R., Meyer-Franke, A., Lambert, S., Bennett, V., Duncan, I. D., Levinson, S. R., & Barres, B. A. (1997). Induction of sodium channel clustering by oligodendrocytes. *Nature*, *386*(6626), Article 6626. https://doi.org/10.1038/386724a0

Karna, E., Szoka, L., Huynh, T. Y. L., & Palka, J. A. (2020). Proline-dependent regulation of collagen metabolism. *Cellular and Molecular Life Sciences*, *77*(10), 1911–1918. https://doi.org/10.1007/s00018-019-03363-3

Kaushik, D. K., Rho, J. M., Yong, V. W., Kaushik, D. K., Bhattacharya, A., Mirzaei, R., Rawji, K. S., Ahn, Y., & Rho, J. M. (2019). Enhanced glycolytic metabolism supports transmigration of brain-infiltrating macrophages in multiple sclerosis Graphical abstract Find the latest version: Enhanced glycolytic metabolism supports transmigration of brain-infiltrating macrophages in multipl. *The Journal of Clinical Investigation*, *129*(8), 3277–3292.

Keough, M. B., Jensen, S. K., & Wee Yong, V. (2015). Experimental demyelination and remyelination of murine spinal cord by focal injection of lysolecithin. *Journal of Visualized Experiments*, *2015*(97), 1–8. https://doi.org/10.3791/52679

Keough, M. B., Rogers, J. A., Zhang, P., Jensen, S. K., Stephenson, E. L., Chen, T., Hurlbert, M. G., Lau, L. W., Rawji, K. S., Plemel, J. R., Koch, M., Ling, C. C., & Yong, V. W. (2016). An inhibitor of chondroitin sulfate proteoglycan synthesis

promotes central nervous system remyelination. *Nature Communications*, *7*, 1–12. https://doi.org/10.1038/ncomms11312

Kermode, A. G., Thompson, A. J., Tofts, P., Macmanus, D. G., Kendall, B. E., Kingsley, D. P. E., Moseley, I. F., Rudge, P., & Mcdonald, W. I. (1990). Breakdown of the blood-brain barrier precedes symptoms and other mri signs of new lesions in multiple sclerosis: Pathogenetic and clinical implications. *Brain*, *113*(5), 1477–1489. https://doi.org/10.1093/brain/113.5.1477

Kettenmann, H., & Ranson, B. R. (1988). Electrical coupling between astrocytes and between oligodendrocytes studied in mammalian cell cultures. *Glia*, *1*(1), 64–73. https://doi.org/10.1002/glia.440010108

Khan, I. U., Yoon, Y., Kim, A., Jo, K. R., Choi, K. U., Jung, T., Kim, N., Son, Y., Kim, W. H., & Kweon, O.-K. (2018). Improved Healing after the Co-Transplantation of HO-1 and BDNF Overexpressed Mesenchymal Stem Cells in the Subacute Spinal Cord Injury of Dogs. *Cell Transplantation*, *27*(7), 1140–1153. https://doi.org/10.1177/0963689718779766

Kim, S., Takahashi, H., Lin, W.-W., Descargues, P., Grivennikov, S., Kim, Y., Luo, J.-L., & Karin, M. (2009). Carcinoma-produced factors activate myeloid cells through TLR2 to stimulate metastasis. *Nature*, *457*(7225), Article 7225. https://doi.org/10.1038/nature07623

Kim, T. W., & Sung, Y. H. (2017). Regular exercise promotes memory function and enhances hippocampal neuroplasticity in experimental autoimmune encephalomyelitis mice. *Neuroscience*, *346*, 173–181. https://doi.org/10.1016/j.neuroscience.2017.01.016

Kivisäkk, P., Mahad, D. J., Callahan, M. K., Trebst, C., Tucky, B., Wei, T., Wu, L., Baekkevold, E. S., Lassmann, H., Staugaitis, S. M., Campbell, J. J., & Ransohoff, R. M. (2003). Human cerebrospinal fluid central memory CD4 $^{+}$ T cells: Evidence

for trafficking through choroid plexus and meninges via P-selectin. *Proceedings of the National Academy of Sciences*, *100*(14), 8389–8394. https://doi.org/10.1073/pnas.1433000100

Kjellén, L., & Lindahl, U. (1991). Proteoglycans: Structures and Interactions. *Annual Review of Biochemistry*, *60*(1), 443–475. https://doi.org/10.1146/annurev.bi.60.070191.002303

Kjellén, L., & Lindahl, U. (2018). Specificity of glycosaminoglycan–protein interactions. *Current Opinion in Structural Biology*, *50*, 101–108. https://doi.org/10.1016/j.sbi.2017.12.011

Kjolhede, T., Siemonsen, S., Wenzel, D., Stellman, J.-P., Ringgaard, S., Pedersen, B. G., Stenager, E., Petersen, T., Vissing, K., Heesen, C., & Dalgas, U. (2018). Can resistance training impact MRI outcomes in relapsing-remitting multiple sclerosis? *Multiple Sclerosis Journal*, *9*(6), 259–261. https://doi.org/10.1177/https

Klaren, R. E., Motl, R. W., Dlugonski, D., Sandroff, B. M., & Pilutti, L. A. (2013). Objectively Quantified Physical Activity in Persons With Multiple Sclerosis. *Archives of Physical Medicine and Rehabilitation*, *94*(12), 2342–2348. https://doi.org/10.1016/j.apmr.2013.07.011

Klineova, S., & Lublin, F. D. (2018). Clinical course of multiple sclerosis. *Cold Spring Harbor Perspectives in Medicine*, *8*(9), 1–12. https://doi.org/10.1101/cshperspect.a028928

Koch, M., Mostert, J., Heersema, D., & De Keyser, J. (2007). Progression in multiple sclerosis: Further evidence of an age dependent process. *Journal of the Neurological Sciences*, *255*(1–2), 35–41. https://doi.org/10.1016/j.jns.2007.01.067

Kohman, R. A., DeYoung, E. K., Bhattacharya, T. K., Peterson, L. N., & Rhodes, J. S. (2012). Wheel running attenuates microglia proliferation and increases

expression of a proneurogenic phenotype in the hippocampus of aged mice. *Brain, Behavior, and Immunity*, *26*(5), 803–810. https://doi.org/10.1016/j.bbi.2011.10.006

Kornek, B., Storch, M. K., Weissert, R., Wallstroem, E., Stefferl, A., Olsson, T., Linington, C., Schmidbauer, M., & Lassmann, H. (2000). Multiple sclerosis and chronic autoimmune encephalomyelitis: A comparative quantitative study of axonal injury in active, inactive, and remyelinated lesions. *American Journal of Pathology*, *157*(1), 267–276. https://doi.org/10.1016/S0002-9440(10)64537-3

Kotter, M. R., Zhao, C., Van Rooijen, N., & Franklin, R. J. M. (2005). Macrophage-depletion induced impairment of experimental CNS remyelination is associated with a reduced oligodendrocyte progenitor cell response and altered growth factor expression. *Neurobiology of Disease*, *18*(1), 166–175. https://doi.org/10.1016/j.nbd.2004.09.019

Krasemann, S., Madore, C., Cialic, R., Baufeld, C., Calcagno, N., El Fatimy, R., Beckers, L., O'Loughlin, E., Xu, Y., Fanek, Z., Greco, D. J., Smith, S. T., Tweet, G., Humulock, Z., Zrzavy, T., Conde-Sanroman, P., Gacias, M., Weng, Z., Chen, H., … Butovsky, O. (2017). The TREM2-APOE Pathway Drives the Transcriptional Phenotype of Dysfunctional Microglia in Neurodegenerative Diseases. *Immunity*, *47*(3), 566-581.e9. https://doi.org/10.1016/j.immuni.2017.08.008

Krogsgaard, M., Wucherpfennig, K. W., Canella, B., Hansen, B. E., Svejgaard, A., Pyrdol, J., Ditzel, H., Raine, C., Engberg, J., & Fugger, L. (2000). Visualization of Myelin Basic Protein (Mbp) T Cell Epitopes in Multiple Sclerosis Lesions Using a Monoclonal Antibody Specific for the Human Histocompatibility Leukocyte Antigen (Hla)-Dr2–Mbp 85–99 Complex. *Journal of Experimental Medicine*, *191*(8), 1395–1412. https://doi.org/10.1084/jem.191.8.1395

Kuhlmann, T., Ludwin, S., Prat, A., Antel, J., Brück, W., & Lassmann, H. (2017). An updated histological classification system for multiple sclerosis lesions. *Acta Neuropathologica*, *133*(1), 13–24. https://doi.org/10.1007/s00401-016-1653-y

Kuhlmann, T., Miron, V., Cuo, Q., Wegner, C., Antel, J., & Brück, W. (2008). Differentiation block of oligodendroglial progenitor cells as a cause for remyelination failure in chronic multiple sclerosis. *Brain*, *131*(7), 1749–1758. https://doi.org/10.1093/brain/awn096

Kuppe, C., Ibrahim, M. M., Kranz, J., Zhang, X., Ziegler, S., Perales-Patón, J., Jansen, J., Reimer, K. C., Smith, J. R., Dobie, R., Wilson-Kanamori, J. R., Halder, M., Xu, Y., Kabgani, N., Kaesler, N., Klaus, M., Gernhold, L., Puelles, V. G., Huber, T. B., … Kramann, R. (2021). Decoding myofibroblast origins in human kidney fibrosis. *Nature*, *589*(7841), 281–286. https://doi.org/10.1038/s41586-020-2941-1

Kutzelnigg, A., & Lassmann, H. (2014). Pathology of multiple sclerosis and related inflammatory demyelinating diseases. *Handbook of Clinical Neurology*, *122*, 15–58. https://doi.org/10.1016/B978-0-444-52001-2.00002-9

Kutzelnigg, A., Lucchinetti, C. F., Stadelmann, C., Brück, W., Rauschka, H., Bergmann, M., Schmidbauer, M., Parisi, J. E., & Lassmann, H. (2005). Cortical demyelination and diffuse white matter injury in multiple sclerosis. *Brain*, *128*(11), 2705–2712. https://doi.org/10.1093/brain/awh641

Lam, M. A., Hemley, S. J., Najafi, E., Vella, N. G. F., Bilston, L. E., & Stoodley, M. A. (2017). The ultrastructure of spinal cord perivascular spaces: Implications for the circulation of cerebrospinal fluid. *Scientific Reports*, *7*(1), Article 1. https://doi.org/10.1038/s41598-017-13455-4

Landry, D. A., Yakubovich, E., Cook, D. P., Fasih, S., Upham, J., & Vanderhyden, B. C. (2022). Metformin prevents age-associated ovarian fibrosis by modulating the

immune landscape in female mice. *Science Advances*, *8*(35), eabq1475. https://doi.org/10.1126/sciadv.abq1475

Lanz, T. V., Brewer, R. C., Ho, P. P., Moon, J.-S., Jude, K. M., Fernandez, D., Fernandes, R. A., Gomez, A. M., Nadj, G.-S., Bartley, C. M., Schubert, R. D., Hawes, I. A., Vazquez, S. E., Iyer, M., Zuchero, J. B., Teegen, B., Dunn, J. E., Lock, C. B., Kipp, L. B., … Robinson, W. H. (2022). Clonally Expanded B Cells in Multiple Sclerosis Bind EBV EBNA1 and GlialCAM. *Nature*. https://doi.org/10.1038/s41586-022-04432-7

Lappano, R., Talia, M., Cirillo, F., Rigiracciolo, D. C., Scordamaglia, D., Guzzi, R., Miglietta, A. M., De Francesco, E. M., Belfiore, A., Sims, A. H., & Maggiolini, M. (2020). The IL1β-IL1R signaling is involved in the stimulatory effects triggered by hypoxia in breast cancer cells and cancer-associated fibroblasts (CAFs). *Journal of Experimental & Clinical Cancer Research*, *39*(1), 153. https://doi.org/10.1186/s13046-020-01667-y

Lappe-Siefke, C., Goebbels, S., Gravel, M., Nicksch, E., Lee, J., Braun, P. E., & Nave, K.-A. (2003). Disruption of Cnp1 uncouples oligodendroglial functions in axonal support and myelination. *Nature Genetics*, *36*(1–2), 161–171. https://doi.org/10.1038/ng1095

Lasarte, J. J., Casares, N., Gorraiz, M., Hervás-Stubbs, S., Arribillaga, L., Mansilla, C., Durantez, M., Llopiz, D., Sarobe, P., Borrás-Cuesta, F., Prieto, J., & Leclerc, C. (2007). The Extra Domain A from Fibronectin Targets Antigens to TLR4-Expressing Cells and Induces Cytotoxic T Cell Responses In Vivo. *The Journal of Immunology*, *178*(2), 748–756. https://doi.org/10.4049/jimmunol.178.2.748

Lassmann, H. (2018). Multiple sclerosis pathology. *Cold Spring Harbor Perspectives in Medicine*, *8*(3), 1–16. https://doi.org/10.1101/cshperspect.a028936

Lassmann, H., & Bradl, M. (2017). Multiple sclerosis: Experimental models and reality. *Acta Neuropathologica*, *133*(2), 223–244. https://doi.org/10.1007/s00401-016-1631-4

Lau, L. W., Keough, M. B., Haylock-jacobs, S., Sloka, S., Stirling, D. P., Cua, R., Axinia, D., Rivest, S., & Yong, V. W. (2012). Chondroitin Sulfate Proteoglycans in Demyelinated Lesions Impair Remyelination. *Annals of Neurology*. https://doi.org/10.1002/ana.23599

Lauro, C., & Limatola, C. (2020). Metabolic Reprograming of Microglia in the Regulation of the Innate Inflammatory Response. *Frontiers in Immunology*, *11*(March), 1–8. https://doi.org/10.3389/fimmu.2020.00493

Le Page, C., Ferry, A., & Rieu, M. (1994). Effect of muscular exercise on chronic relapsing experimental autoimmune encephalomyelitis. *J Appl Physiol (1985)*, *77*(5), 2341–2347. https://doi.org/10.1152/jappl.1994.77.5.2341

Learmonth, Y. C., Pilutti, L. A., Herring, M. P., Motl, R. W., Chan, B., & Metse, A. P. (2021). Safety of exercise training in multiple sclerosis: A protocol for an updated systematic review and meta-analysis. *Systematic Reviews*, *10*, 208. https://doi.org/10.1186/s13643-021-01751-0

Lee, S.-Y., Park, L. M., Oh, Y. J., Choi, D. H., & Lee, D. W. (2022). High Throughput 3D Cell Migration Assay Using Micropillar/Microwell Chips. *Molecules*, *27*(16), 5306. https://doi.org/10.3390/molecules27165306

Lee, W.-S., Lim, J.-H., Sung, M.-S., Lee, E.-G., Oh, Y.-J., & Yoo, W.-H. (2014). Ethyl acetate fraction from Angelica sinensis inhibits IL-1β-induced rheumatoid synovial fibroblast proliferation and COX-2, PGE2, and MMPs production. *Biological Research*, *47*(1), 41. https://doi.org/10.1186/0717-6287-47-41

Leiton, C. V., Aranmolate, A., Eyermann, C., Menezes, M. J., Escobar-Hoyos, L. F., Husain, S., Winder, S. J., & Colognato, H. (2015). Laminin promotes

metalloproteinase-mediated dystroglycan processing to regulate oligodendrocyte progenitor cell proliferation. *Journal of Neurochemistry*, *135*(3), 522–538. https://doi.org/10.1111/jnc.13241

Levine, J. M., & Reynolds, R. (1999). Activation and proliferation of endogenous oligodendrocyte precursor cells during ethidium bromide-induced demyelination. *Experimental Neurology*, *160*(2), 333–347. https://doi.org/10.1006/exnr.1999.7224

Li, J., Wang, Z., Li, C., Song, Y., Wang, Y., Bo, H., & Zhang, Y. (2022). Impact of Exercise and Aging on Mitochondrial Homeostasis in Skeletal Muscle: Roles of ROS and Epigenetics. *Cells*, *11*(13), 2086. https://doi.org/10.3390/cells11132086

Li, Y., He, X., Kawaguchi, R., Zhang, Y., Wang, Q., Monavarfeshani, A., Yang, Z., Chen, B., Shi, Z., Meng, H., Zhou, S., Zhu, J., Jacobi, A., Swarup, V., Popovich, P. G., Geschwind, D. H., & He, Z. (2020). Microglia-organized scar-free spinal cord repair in neonatal mice. *Nature*, *587*(7835), 613–618. https://doi.org/10.1038/s41586-020-2795-6

Li, Z., Wang, L., Ren, Y., Huang, Y., Liu, W., Lv, Z., Qian, L., Yu, Y., & Xiong, Y. (2022). Arginase: Shedding light on the mechanisms and opportunities in cardiovascular diseases. *Cell Death Discovery*, *8*(1), Article 1. https://doi.org/10.1038/s41420-022-01200-4

Lighthouse, J. K., Burke, R. M., Velasquez, L. S., Dirkx, R. A., Aiezza, A., Moravec, C. S., Alexis, J. D., Rosenberg, A., & Small, E. M. (n.d.). Exercise promotes a cardioprotective gene program in resident cardiac fibroblasts. *JCI Insight*, *4*(1), e92098. https://doi.org/10.1172/jci.insight.92098

Lloyd, A. F., Davies, C. L., Holloway, R. K., Labrak, Y., Ireland, G., Carradori, D., Dillenburg, A., Borger, E., Soong, D., Richardson, J. C., Kuhlmann, T., Williams, A., Pollard, J. W., Rieux, A., Priller, J., & Miron, V. E. (n.d.). Central nervous

system regeneration is driven by microglia necroptosis and repopulation. *Nature Neuroscience*. https://doi.org/10.1038/s41593-019-0418-z

Locatelli, G., Theodorou, D., Kendirli, A., Jordão, M. J. C., Staszewski, O., Phulphagar, K., Cantuti-Castelvetri, L., Dagkalis, A., Bessis, A., Simons, M., Meissner, F., Prinz, M., & Kerschensteiner, M. (2018). Mononuclear phagocytes locally specify and adapt their phenotype in a multiple sclerosis model. *Nature Neuroscience*, *21*(9), 1196–1208. https://doi.org/10.1038/s41593-018-0212-3

Locatelli, G., Wörtge, S., Buch, T., Ingold, B., Frommer, F., Sobottka, B., Krüger, M., Karram, K., Bühlmann, C., Bechmann, I., Heppner, F. L., Waisman, A., & Becher, B. (2012). Primary oligodendrocyte death does not elicit anti-CNS immunity. *Nature Neuroscience*, *15*(4), 543–550. https://doi.org/10.1038/nn.3062

Longoni, G., Brown, R. A., Aubert-Broche, B., Grover, S. A., Branson, H. M., Fetco, D., Bar-Or, A., Marrie, R. A., Motl, R. W., Louis Collins, D., Narayanan, S., Arnold, D. L., Banwell, B., & Ann Yeh, E. (2018). Physical activity and dentate gyrus volume in pediatric acquired demyelinating syndromes. *Neurology: Neuroimmunology and NeuroInflammation*, *5*(6), 1–7. https://doi.org/10.1212/NXI.0000000000000499

López-Otín, C., Blasco, M. A., Partridge, L., Serrano, M., & Kroemer, G. (2023). Hallmarks of aging: An expanding universe. *Cell*, *186*(2), 243–278. https://doi.org/10.1016/j.cell.2022.11.001

Lorenz, H. P., Whitby, D. J., Longaker, M. T., & Adzick, N. S. (1993). Fetal wound healing: The ontogeny of scar formation in the non-human primate. *Annals of Surgery*, *217*(4), 391–396. https://doi.org/10.1097/00000658-199304000-00011

Lourenco, M. V., Frozza, R. L., Freitas, G. B. D., Zhang, H., Kincheski, G. C., Ribeiro, F. C., Gonçalves, R. A., Clarke, J. R., Beckman, D., Staniszewski, A., Berman, H., Guerra, L. A., Forny-germano, L., Meier, S., Wilcock, D. M., Souza, J. M. D.,

Alves-leon, S., & Prado, V. F. (2019). Exercise-linked FNDC5/irisin rescues synaptic plasticity and memory defects in Alzheimer's models. *Nature Medicine*, *25*(January), 165–175. https://doi.org/10.1038/s41591-018-0275-4

Lozinski, B. M., de Almeida, L. G. N., Silva, C., Dong, Y., Brown, D., Chopra, S., Yong, V. W., & Dufour, A. (2021). Exercise rapidly alters proteomes in mice following spinal cord demyelination. *Scientific Reports*, *11*(1). https://doi.org/10.1038/s41598-021-86593-5

Lozinski, B. M., & Yong, V. W. (2020). Exercise and the brain in multiple sclerosis. *Multiple Sclerosis Journal*, *00*(0), 1–6. https://doi.org/10.1177/1352458520969099

Lucchinetti, C., Brück, W., Parisi, J., Scheithauer, B., Rodriguez, M., & Lassmann, H. (1999). A quantitative analysis of oligodendrocytes in multiple sclerosis lesions. A study of 113 cases. *Brain*, *122*(12), 2279–2295. https://doi.org/10.1093/brain/122.12.2279

Machado-Santos, J., Saji, E., Tröscher, A. R., Paunovic, M., Liblau, R., Gabriely, G., Bien, C. G., Bauer, J., & Lassmann, H. (2018). The compartmentalized inflammatory response in the multiple sclerosis brain is composed of tissue-resident CD8+ T lymphocytes and B cells. *Brain*, *141*(7), 2066–2082. https://doi.org/10.1093/brain/awy151

MacKenna, D. (2000). Role of mechanical factors in modulating cardiac fibroblast function and extracellular matrix synthesis. *Cardiovascular Research*, *46*(2), 257–263. https://doi.org/10.1016/S0008-6363(00)00030-4

Maeda, Y., Solanky, M., Menonna, J., Chapin, J., Li, W., & Dowling, P. (2001). Platelet-derived growth factor-α receptor-positive oligodendroglia are frequent in multiple sclerosis lesions. *Annals of Neurology*, *49*(6), 776–785. https://doi.org/10.1002/ana.1015

Magliozzi, R., Howell, O. W., Reeves, C., Roncaroli, F., Nicholas, R., Serafini, B., Aloisi, F., & Reynolds, R. (2010). A Gradient of neuronal loss and meningeal inflammation in multiple sclerosis. *Annals of Neurology*, *68*(4), 477–493. https://doi.org/10.1002/ana.22230

Mahmoudi, S., Mancini, E., Xu, L., Moore, A., Jahanbani, F., Hebestreit, K., Srinivasan, R., Li, X., Devarajan, K., Prélot, L., Ang, C. E., Shibuya, Y., Benayoun, B. A., Chang, A. L. S., Wernig, M., Wysocka, J., Longaker, M. T., Snyder, M. P., & Brunet, A. (2019). Heterogeneity in old fibroblasts is linked to variability in reprogramming and wound healing. In *Nature* (Vol. 574, Issue 7779). Springer US. https://doi.org/10.1038/s41586-019-1658-5

Makino, K., Makino, T., Stawski, L., Mantero, J. C., Lafyatis, R., Simms, R., & Trojanowska, M. (2017). Blockade of PDGF Receptors by Crenolanib Has Therapeutic Effect in Patient Fibroblasts and in Preclinical Models of Systemic Sclerosis. *Journal of Investigative Dermatology*, *137*(8), 1671–1681. https://doi.org/10.1016/j.jid.2017.03.032

Mandolesi, G., Bullitta, S., Fresegna, D., Vito, F. D., Romana, F., Musella, A., Guadalupi, L., Vanni, V., Stampanoni, M., Buttari, F., Teresa, M., & Centonze, D. (2019). Voluntary running wheel attenuates motor deterioration and brain damage in cuprizone-induced demyelination. *Neurobiology of Disease*, *129*(May), 102–117. https://doi.org/10.1016/j.nbd.2019.05.010

Maric, D., Jahanipour, J., Li, X. R., Singh, A., Mobiny, A., Van Nguyen, H., Sedlock, A., Grama, K., & Roysam, B. (2021). Whole-brain tissue mapping toolkit using large-scale highly multiplexed immunofluorescence imaging and deep neural networks. *Nature Communications*, *12*, 1550. https://doi.org/10.1038/s41467-021-21735-x

Marlatt, M. W., Potter, M. C., Lucassen, P. J., & van Praag, H. (2012). Running throughout middle-age improves memory function, hippocampal neurogenesis,

and BDNF levels in female C57BL/6J mice. *Developmental Neurobiology*, *72*(6), 943–952. https://doi.org/10.1002/dneu.22009

Marschallinger, J., Iram, T., Zardeneta, M., Lee, S. E., Lehallier, B., Haney, M. S., Pluvinage, J. V., Mathur, V., Hahn, O., Morgens, D. W., Kim, J., Tevini, J., Felder, T. K., Wolinski, H., Bertozzi, C. R., Bassik, M. C., Aigner, L., & Wyss-Coray, T. (2020). Lipid-droplet-accumulating microglia represent a dysfunctional and proinflammatory state in the aging brain. *Nature Neuroscience*, *23*(2), 194–208. https://doi.org/10.1038/s41593-019-0566-1

Mascharak, S., des Jardins-Park, H. E., Davitt, M. F., Griffin, M., Borrelli, M. R., Moore, A. L., Chen, K., Duoto, B., Chinta, M., Foster, D. S., Shen, A. H., Januszyk, M., Kwon, S. H., Wernig, G., Wan, D. C., Lorenz, H. P., Gurtner, G. C., & Longaker, M. T. (2021). Preventing Engrailed-1 activation in fibroblasts yields wound regeneration without scarring. *Science*, *372*(6540). https://doi.org/10.1126/science.aba2374

Massagué, J. (2012). TGFβ signalling in context. *Nature Reviews Molecular Cell Biology*, *13*(10), 616–630. https://doi.org/10.1038/nrm3434

Mastorakos, P., Mihelson, N., Luby, M., Burks, S. R., Johnson, K., Hsia, A. W., Witko, J., Frank, J. A., Latour, L., & McGavern, D. B. (2021). Temporally distinct myeloid cell responses mediate damage and repair after cerebrovascular injury. *Nature Neuroscience*, *24*(2), 245–258. https://doi.org/10.1038/s41593-020-00773-6

Masuda, T., Sankowski, R., Staszewski, O., Böttcher, C., Amann, L., Sagar, Scheiwe, C., Nessler, S., Kunz, P., van Loo, G., Coenen, V. A., Reinacher, P. C., Michel, A., Sure, U., Gold, R., Grün, D., Priller, J., Stadelmann, C., & Prinz, M. (2019). Spatial and temporal heterogeneity of mouse and human microglia at single-cell resolution. *Nature*, *566*(7744), 388–392. https://doi.org/10.1038/s41586-019-0924-x

Mathiesen, S. N., Lock, J. L., Schoderboeck, L., Abraham, W. C., & Hughes, S. M. (2020). CNS Transduction Benefits of AAV-PHP.eB over AAV9 Are Dependent on Administration Route and Mouse Strain. *Molecular Therapy - Methods & Clinical Development*, *19*, 447–458. https://doi.org/10.1016/j.omtm.2020.10.011

McGee, H. M., Schmidt, B., Booth, C. J., Yancopoulos, G. D., Valenzuela, D. M., Murphy, A. J., Stevens, S., Flavell, R. A., & Horsley, V. (2013). Interleukin-22 promotes fibroblast- mediated wound repair in the skin. *The Journal of Investigative Dermatology*, *133*(5), 1321–1329. https://doi.org/10.1038/jid.2012.463

McGinley, M. P., Goldschmidt, C. H., & Rae-Grant, A. D. (2021). Diagnosis and Treatment of Multiple Sclerosis: A Review. *JAMA*, *325*(8), 765. https://doi.org/10.1001/jama.2020.26858

McKinnon, R. D., Matsui, T., Dubois-Dalcq, M., & Aaronsont, S. A. (1990). FGF modulates the PDGF-driven pathway of oligodendrocyte development. *Neuron*, *5*(5), 603–614. https://doi.org/10.1016/0896-6273(90)90215-2

McKinnon, R. D., Smith, C., Behar, T., Smith, T., & Dubois-Dalcq, M. (1993). Distinct effects of bFGF and PDGF on oligodendrocyte progenitor cells. *Glia*, *7*(3), 245–254. https://doi.org/10.1002/glia.440070308

McWhorter, F. Y., Wang, T., Nguyen, P., Chung, T., & Liu, W. F. (2013). Modulation of macrophage phenotype by cell shape. *Proceedings of the National Academy of Sciences of the United States of America*, *110*(43), 17253–17258. https://doi.org/10.1073/pnas.1308887110

Mei, F., Fancy, S. P. J., Shen, Y. A., Niu, J., Zhao, C., Presley, B., Miao, E., Lee, S., Mayoral, S. R., Redmond, S. A., Etxeberria, A., Xiao, L., Franklin, R. J. M., Green, A., Hauser, S. L., & Chan, J. R. (2014). Micropillar arrays as a high-

throughput screening platform for therapeutics in multiple sclerosis. *Nature Medicine*, *20*(8), 954–960. https://doi.org/10.1038/nm.3618

Mei, F., Lehmann-Horn, K., Shen, Y. A. A., Rankin, K. A., Stebbins, K. J., Lorrain, D. S., Pekarek, K., Sagan, S. A., Xiao, L., Teuscher, C., von Büdingen, H. C., Wess, J., Josh Lawrence, J., Green, A. J., Fancy, S. P. J., Zamvil, S. S., & Chan, J. R. (2016). Accelerated remyelination during inflammatory demyelination prevents axonal loss and improves functional recovery. *ELife*, *5*(September), 1–21. https://doi.org/10.7554/eLife.18246

Merkler, D., Boretius, S., Stadelmann, C., Ernsting, T., Michaelis, T., Frahm, J., & Brück, W. (2005). Multicontrast MRI of remyelination in the central nervous system. *NMR in Biomedicine*, *18*(6), 395–403. https://doi.org/10.1002/nbm.972

Mezzaroba, L., Name, A., Simão, C., Oliveira, S. R., Flauzino, T., Alfieri, D. F., Lice, W., Jennings, D. C., Kallaur, A. P., Alysson, M., Lozovoy, B., Kaimen-maciel, D. R., Maes, M., Maria, E., & Reiche, V. (2020). Antioxidant and Anti-inflammatory Diagnostic Biomarkers in Multiple Sclerosis: A Machine Learning Study. *Molecular Neurobiology*, *57*, 2167–2178.

Mi, S., Miller, R. H., Lee, X., Scott, M. L., Shulag-Morskaya, S., Shao, Z., Chang, J., Thill, G., Levesque, M., Zhang, M., Hession, C., Sah, D., Trapp, B., He, Z., Jung, V., McCoy, J. M., & Pepinsky, R. B. (2005). LINGO-1 negatively regulates myelination by oligodendrocytes. *Nature Neuroscience*, *8*(6), 745–751. https://doi.org/10.1038/nn1460

Michaels, N. J., Lemmon, K., Plemel, J. R., Jensen, S. K., Mishra, M. K., Brown, D., Rawji, K. S., Koch, M., & Yong, V. W. (2020). Aging-Exacerbated Acute Axon and Myelin Injury Is Associated with Microglia-Derived Reactive Oxygen Species and Is Alleviated by the Generic Medication Indapamide. *The Journal of*

Neuroscience, *40*(44), 8587–8600. https://doi.org/10.1523/JNEUROSCI.1098-20.2020

Micu, I., Plemel, J. R., Caprariello, A. V., Nave, K. A., & Stys, P. K. (2017). Axo-myelinic neurotransmission: A novel mode of cell signalling in the central nervous system. *Nature Reviews Neuroscience*, *19*(1), 49–57. https://doi.org/10.1038/nrn.2017.128

Mifflin, K. A., Frieser, E., Benson, C., Baker, G., & Kerr, B. J. (2017). Voluntary wheel running differentially affects disease outcomes in male and female mice with experimental autoimmune encephalomyelitis. *Journal of Neuroimmunology*, *305*, 135–144. https://doi.org/10.1016/j.jneuroim.2017.02.005

Milner, R., Edwards, G., & Streuli, C. (1996). *A Role in Migration for the ⎵ v ⅟ 1 Integrin Expressed on Oligodendrocyte Precursors*. *16*(22), 7240–7252.

Miron, V. E., Boyd, A., Zhao, J. W., Yuen, T. J., Ruckh, J. M., Shadrach, J. L., Van Wijngaarden, P., Wagers, A. J., Williams, A., Franklin, R. J. M., & Ffrench-Constant, C. (2013). M2 microglia and macrophages drive oligodendrocyte differentiation during CNS remyelination. *Nature Neuroscience*, *16*(9), 1211–1218. https://doi.org/10.1038/nn.3469

Mohan, H., Krumbholz, M., Sharma, R., Eisele, S., Junker, A., Sixt, M., Newcombe, J., Wekerle, H., Hohlfeld, R., Lassmann, H., & Meinl, E. (2010). *Extracellular Matrix in Multiple Sclerosis Lesions: Fibrillar Collagens , Biglycan and Decorin are Upregulated and Associated with Infiltrating Immune Cells*. *20*, 966–975. https://doi.org/10.1111/j.1750-3639.2010.00399.x

Moore, C. S., Cui, Q., Warsi, N. M., Durafourt, B. A., Zorko, N., Owen, D. R., Antel, J. P., & Bar-or, A. (2015). *Direct and Indirect E ects of Immune and Central Nervous*

System– Resident Cells on Human Oligodendrocyte Progenitor Cell Di erentiation . *194*, 761–772. https://doi.org/10.4049/jimmunol.1401156

Morland, C., Andersson, K. A., Haugen, Ø. P., Hadzic, A., Kleppa, L., Gille, A., Rinholm, J. E., Palibrk, V., Diget, E. H., Kennedy, L. H., Stølen, T., Hennestad, E., Moldestad, O., Cai, Y., Puchades, M., Offermanns, S., Vervaeke, K., Bjørås, M., Wisløff, U., … Bergersen, L. H. (2017). Exercise induces cerebral VEGF and angiogenesis via the lactate receptor HCAR1. *Nature Communications*, *8*(7491), 1–9. https://doi.org/10.1038/ncomms15557

Motl, R. W., & Sandroff, B. M. (2015). Benefits of Exercise Training in Multiple Sclerosis. *Current Neurology and Neuroscience Reports*, *15*(9), 1–9. https://doi.org/10.1007/s11910-015-0585-6

Motl, R. W., Sandroff, B. M., Kwakkel, G., Dalgas, U., Feinstein, A., Heesen, C., Feys, P., & Thompson, A. J. (2017). Exercise in patients with multiple sclerosis. *The Lancet Neurology*, *16*(10), 848–856. https://doi.org/10.1016/S1474-4422(17)30281-8

Mouw, J. K., Ou, G., & Weaver, V. M. (2014). Extracellular matrix assembly: A multiscale deconstruction. *Nature Reviews Molecular Cell Biology*, *15*(12), Article 12. https://doi.org/10.1038/nrm3902

Mrdjen, D., Pavlovic, A., Hartmann, F. J., Schreiner, B., Utz, S. G., Leung, B. P., Lelios, I., Heppner, F. L., Kipnis, J., Merkler, D., Greter, M., & Becher, B. (2018). High-Dimensional Single-Cell Mapping of Central Nervous System Immune Cells Reveals Distinct Myeloid Subsets in Health, Aging, and Disease. *Immunity*, *48*(2), 380-395.e6. https://doi.org/10.1016/j.immuni.2018.01.011

Mundt, S., Mrdjen, D., Utz, S. G., Greter, M., Schreiner, B., & Becher, B. (2019). Conventional DCs sample and present myelin antigens in the healthy CNS and

allow parenchymal T cell entry to initiate neuroinflammation. *Science Immunology*.

Murray, P. D., Mcgavern, D. B., Sathornsumetee, S., & Rodriguez, M. (2001). Spontaneous remyelination following extensive demyelination is associated with improved neurological function in a viral model of multiple sclerosis. *Brain*, *124*(7), 1403–1416. https://doi.org/10.1016/j.physbeh.2017.03.040

Naamane, N., van Helden, J., & Eizirik, D. L. (2007). In silico identification of NF-kappaB-regulated genes in pancreatic beta-cells. *BMC Bioinformatics*, *8*, 55. https://doi.org/10.1186/1471-2105-8-55

Natrajan, M. S., De La Fuente, A. G., Crawford, A. H., Linehan, E., Nuñez, V., Johnson, K. R., Wu, T., Fitzgerald, D. C., Ricote, M., Bielekova, B., & Franklin, R. J. M. (2015). Retinoid X receptor activation reverses age-related deficiencies in myelin debris phagocytosis and remyelination. *Brain*, *138*(12), 3581–3597. https://doi.org/10.1093/brain/awv289

Nawaz, S., Sánchez, P., Schmitt, S., Snaidero, N., Mitkovski, M., Velte, C., Brückner, B. R., Alexopoulos, I., Czopka, T., Jung, S. Y., Rhee, J. S., Janshoff, A., Witke, W., Schaap, I. A. T., Lyons, D. A., & Simons, M. (2015). Actin Filament Turnover Drives Leading Edge Growth during Myelin Sheath Formation in the Central Nervous System. *Developmental Cell*, *34*(2), 139–151. https://doi.org/10.1016/j.devcel.2015.05.013

Negaresh, R., Motl, R. W., Mokhtarzade, M., Dalgas, U., Patel, D., Shamsi, M. M., Majdinasab, N., Ranjbar, R., Zimmer, P., & Baker, J. S. (2018). Effects of exercise training on cytokines and adipokines in multiple Sclerosis: A systematic review. *Multiple Sclerosis and Related Disorders*, *24*(March), 91–100. https://doi.org/10.1016/j.msard.2018.06.008

Neumann, B., Baror, R., Zhao, C., Segel, M., Dietmann, S., Rawji, K. S., Foerster, S., McClain, C. R., Chalut, K., van Wijngaarden, P., & Franklin, R. J. M. (2019). Metformin Restores CNS Remyelination Capacity by Rejuvenating Aged Stem Cells. *Cell Stem Cell*, *25*(4), 473-485.e8. https://doi.org/10.1016/j.stem.2019.08.015

Nitta, T., Tsutsumi, M., Nitta, S., Muro, R., Suzuki, E. C., Nakano, K., Tomofuji, Y., Sawa, S., Okamura, T., Penninger, J. M., & Takayanagi, H. (2020). Fibroblasts as a source of self-antigens for central immune tolerance. *Nature Immunology*, *21*(10), 1172–1180. https://doi.org/10.1038/s41590-020-0756-8

Nouchi, T., Tanaka, Y., Tsukada, T., Sato, C., & Marumo, F. (1991). Appearance of α-smooth-muscle-actin-positive cells in hepatic fibrosis. *Liver*, *11*(2), 100–105. https://doi.org/10.1111/j.1600-0676.1991.tb00499.x

O'Brown, Z. K., Van Nostrand, E. L., Higgins, J. P., & Kim, S. K. (2015). The Inflammatory Transcription Factors NFκB, STAT1 and STAT3 Drive Age-Associated Transcriptional Changes in the Human Kidney. *PLoS Genetics*, *11*(12), e1005734. https://doi.org/10.1371/journal.pgen.1005734

Olsson, T., Barcellos, L. F., & Alfredsson, L. (2016). Interactions between genetic, lifestyle and environmental risk factors for multiple sclerosis. *Nature Reviews Neurology*, *13*(1), 26–36. https://doi.org/10.1038/nrneurol.2016.187

Oluich, L., Stratton, J. A. S., Xing, Y. L., Ng, S. W., Cate, H. S., Sah, P., Windels, F., Kilpatrick, T. J., & Merson, T. D. (2012). *Targeted Ablation of Oligodendrocytes Induces Axonal Pathology Independent of Overt Demyelination*. *32*(24), 8317–8330. https://doi.org/10.1523/JNEUROSCI.1053-12.2012

Orentas, D. M., Hayes, J. E., Dyer, K. L., & Miller, R. H. (1999). Sonic hedgehog signaling is required during the appearance of spinal cord oligodendrocyte

precursors. *Development*, *126*(11), 2419–2429. https://doi.org/10.1242/dev.126.11.2419

Ousman, S. S., & David, S. (2000). Lysophosphatidylcholine induces rapid recruitment and activation of macrophages in the adult mouse spinal cord. *Glia*, *30*(1), 92–104. https://doi.org/10.1002/(SICI)1098-1136(200003)30:1<92::AID-GLIA10>3.0.CO;2-W

Pakshir, P., Alizadehgiashi, M., Wong, B., Coelho, N. M., Chen, X., Gong, Z., Shenoy, V. B., McCulloch, C., & Hinz, B. (2019). Dynamic fibroblast contractions attract remote macrophages in fibrillar collagen matrix. *Nature Communications*, *10*(1), 1–17. https://doi.org/10.1038/s41467-019-09709-6

Parker, M. W., Rossi, D., Peterson, M., Smith, K., Sikstroṁ, K., White, E. S., Connett, J. E., Henke, C. A., Larsson, O., & Bitterman, P. B. (2014). Fibrotic extracellular matrix activates a profibrotic positive feedback loop. *Journal of Clinical Investigation*, *124*(4), 1622–1635. https://doi.org/10.1172/JCI71386

Patani, R., Balaratnam, M., Vora, A., & Reynolds, R. (2007). Remyelination can be extensive in multiple sclerosis despite a long disease course. *Neuropathology and Applied Neurobiology*, *33*(3), 277–287. https://doi.org/10.1111/j.1365-2990.2007.00805.x

Patel, A. A., Ginhoux, F., & Yona, S. (2021). Monocytes, macrophages, dendritic cells and neutrophils: An update on lifespan kinetics in health and disease. *Immunology*, *163*(3), 250–261. https://doi.org/10.1111/imm.13320

Patrikios, P., Stadelmann, C., Kutzelnigg, A., Rauschka, H., Schmidbauer, M., Laursen, H., Sorensen, P. S., Brück, W., Lucchinetti, C., & Lassmann, H. (2006). Remyelination is extensive in a subset of multiple sclerosis patients. *Brain*, *129*(12), 3165–3172. https://doi.org/10.1093/brain/awl217

Pearce, E. L., & Pearce, E. J. (2013). Metabolic pathways in immune cell activation and quiescence. *Immunity*, *38*(4), 633–643. https://doi.org/10.1016/j.immuni.2013.04.005

Pendleton, J. C., Shamblott, M. J., Gary, D. S., Belegu, V., Hurtado, A., Malone, M. L., & Mcdonald, J. W. (2013). Chondroitin sulfate proteoglycans inhibit oligodendrocyte myelination through PTP σ. *Experimental Neurology*, *247*, 113–121. https://doi.org/10.1016/j.expneurol.2013.04.003

Peng, D., Fu, M., Wang, M., Wei, Y., & Wei, X. (2022). Targeting TGF-β signal transduction for fibrosis and cancer therapy. *Molecular Cancer*, *21*(1), 1–20. https://doi.org/10.1186/s12943-022-01569-x

Pesce, J. T., Ramalingam, T. R., Mentink-Kane, M. M., Wilson, M. S., Kasmi, K. C. E., Smith, A. M., Thompson, R. W., Cheever, A. W., Murray, P. J., & Wynn, T. A. (2009). Arginase-1-expressing macrophages suppress Th2 cytokine-driven inflammation and fibrosis. *PLoS Pathogens*, *5*(4). https://doi.org/10.1371/journal.ppat.1000371

Petersen, M. A., Ryu, J. K., Chang, K. J., Etxeberria, A., Bardehle, S., Mendiola, A. S., Kamau-Devers, W., Fancy, S. P. J., Thor, A., Bushong, E. A., Baeza-Raja, B., Syme, C. A., Wu, M. D., Rios Coronado, P. E., Meyer-Franke, A., Yahn, S., Pous, L., Lee, J. K., Schachtrup, C., … Akassoglou, K. (2017). Fibrinogen Activates BMP Signaling in Oligodendrocyte Progenitor Cells and Inhibits Remyelination after Vascular Damage. *Neuron*, *96*(5), 1003-1012.e7. https://doi.org/10.1016/j.neuron.2017.10.008

Petzinger, G. M., Fisher, B. E., McEwen, S., Beeler, J. A., Walsh, J. P., & Jakowec, M. W. (2013). Exercise-enhanced neuroplasticity targeting motor and cognitive circuitry in Parkinson's disease. *The Lancet Neurology*, *12*(7), 716–726. https://doi.org/10.1016/S1474-4422(13)70123-6

Philippot, C., Griemsmann, S., Jabs, R., Seifert, G., Kettenmann, H., & Steinhäuser, C. (2021). Astrocytes and oligodendrocytes in the thalamus jointly maintain synaptic activity by supplying metabolites. *Cell Reports*, *34*(3), 108642. https://doi.org/10.1016/j.celrep.2020.108642

Pikor, N. B., Astarita, J. L., Summers-Deluca, L., Galicia, G., Qu, J., Ward, L. A., Armstrong, S., Dominguez, C. X., Malhotra, D., Heiden, B., Kay, R., Castanov, V., Touil, H., Boon, L., O'Connor, P., Bar-Or, A., Prat, A., Ramaglia, V., Ludwin, S., … Gommerman, J. L. (2015). Integration of Th17- and Lymphotoxin-Derived Signals Initiates Meningeal-Resident Stromal Cell Remodeling to Propagate Neuroinflammation. *Immunity*, *43*(6), 1160–1173. https://doi.org/10.1016/j.immuni.2015.11.010

Pilutti, L. A., Platta, M. E., Motl, R. W., & Latimer-Cheung, A. E. (2014). The safety of exercise training in multiple sclerosis: A systematic review. *Journal of the Neurological Sciences*, *343*(1–2), 3–7. https://doi.org/10.1016/j.jns.2014.05.016

Plemel, J. R., Liu, W., & Yong, V. W. (2017). Remyelination therapies: A new direction and challenge in multiple sclerosis. *Nat Rev Drug Discov*, *16*. https://doi.org/10.1038/nrdnrd.2017.115

Plemel, J. R., Manesh, S. B., Sparling, J. S., & Tetzlaff, W. (2013). Myelin inhibits oligodendroglial maturation and regulates oligodendrocytic transcription factor expression: Myelin Inhibits Oligodendroglial Maturation. *Glia*, *61*(9), 1471–1487. https://doi.org/10.1002/glia.22535

Plemel, J. R., Michaels, N. J., Weishaupt, N., Caprariello, A. V., Keough, M. B., Rogers, J. A., Yukseloglu, A., Lim, J., Patel, V. V., Rawji, K. S., Jensen, S. K., Teo, W., Heyne, B., Whitehead, S. N., Stys, P. K., & Yong, V. W. (2017). Mechanisms of lysophosphatidylcholine-induced demyelination: A primary lipid disrupting myelinopathy. *Glia*, *66*(2), 327–347. https://doi.org/10.1002/glia.23245

Plemel, J. R., Stratton, J. A., Michaels, N. J., Rawji, K. S., Zhang, E., Sinha, S., Baaklini, C. S., Dong, Y., Ho, M., Thorburn, K., Friedman, T. N., Jawad, S., Silva, C., Caprariello, A. V., Hoghooghi, V., Yue, J., Jaffer, A., Lee, K., Kerr, B. J., … Yong, V. W. (2020). Microglia response following acute demyelination is heterogeneous and limits infiltrating macrophage dispersion. *Science Advances*, *6*(3), eaay6324. https://doi.org/10.1126/sciadv.aay6324

Plikus, M. V., Wang, X., Sinha, S., Forte, E., Thompson, S. M., Herzog, E. L., Driskell, R. R., Rosenthal, N., Biernaskie, J., & Horsley, V. (2021). Fibroblasts: Origins, definitions, and functions in health and disease. *Cell*, *184*(15), 3852–3872. https://doi.org/10.1016/j.cell.2021.06.024

Pohl, H. B. F., Porcheri, C., Mueggler, T., Bachmann, L. C., Martino, G., Riethmacher, D., Franklin, R. J. M., Rudin, M., & Suter, U. (2011). Genetically Induced Adult Oligodendrocyte Cell Death Is Associated with Poor Myelin Clearance, Reduced Remyelination, and Axonal Damage. *Journal of Neuroscience*, *31*(3), 1069–1080. https://doi.org/10.1523/JNEUROSCI.5035-10.2011

Popescu, B., Pirko, I., & Lucchinetti, C. F. (2013). The New Pathology of Multiple Sclerosis. *American Academy of Neurology*, *6*(6), 409–410. https://doi.org/10.1177/135245850000600609

Prakash, R. S., Snook, E. M., Motl, R. W., & Kramer, A. F. (2010). Aerobic fitness is associated with gray matter volume and white matter integrity in multiple sclerosis. *Brain Research*, *1341*, 41–51. https://doi.org/10.1016/j.brainres.2009.06.063

Prineas, J. W., & Connell, F. (1979). Remyelination in Multiple Sclerosis. *Annals of Neurology*, 193–223. https://doi.org/10.1016/B978-0-12-384913-7.00009-5

Prosperini, L., Fanelli, F., Petsas, N., Sbardella, E., Tona, F., Raz, E., Fortuna, D., De Angelis, F., Pozzilli, C., & Pantano, P. (2014). Multiple Sclerosis: Changes in

Microarchitecture of White Matter Tracts after Training with a Video Game Balance Board. *Radiology*, *273*(2), 529–538. https://doi.org/10.1148/radiol.14140168

Psenicka, M. W., Smith, B. C., Tinkey, R. A., & Williams, J. L. (2021). Connecting Neuroinflammation and Neurodegeneration in Multiple Sclerosis: Are Oligodendrocyte Precursor Cells a Nexus of Disease? *Frontiers in Cellular Neuroscience*, *15*, 654284. https://doi.org/10.3389/fncel.2021.654284

Pu, A., Stephenson, E. L., & Yong, V. W. (2018). The extracellular matrix: Focus on oligodendrocyte biology and targeting CSPGs for remyelination therapies. *Glia*, *October 2017*, 1–17. https://doi.org/10.1002/glia.23333

Pulido-Salgado, M., Vidal-Taboada, J. M., Barriga, G. G.-D., Solà, C., & Saura, J. (2018). RNA-Seq transcriptomic profiling of primary murine microglia treated with LPS or LPS + IFNγ. *Scientific Reports*, *8*(1), Article 1. https://doi.org/10.1038/s41598-018-34412-9

Qin, J., Sikkema, A. H., Bij, X. K. V. D., Jonge, J. C. D., Klappe, K., Nies, V., Jonker, J. W., Kok, J. W., Hoekstra, D., & Baron, W. (2017). *GD1a Overcomes Inhibition of Myelination by Fibronectin via Activation of Protein Kinase A : Implications for Multiple Sclerosis*. *37*(41), 9925–9938. https://doi.org/10.1523/JNEUROSCI.0103-17.2017

R Core Team. (2019). *R: A Language and Environment for Statistical Computing*. R Foundation for Statistical Computing. https://www.r-project.org/

Rajan, A. M., Ma, R. C., Kocha, K. M., Zhang, D. J., & Huang, P. (2020). Dual function of perivascular fibroblasts in vascular stabilization in zebrafish. *PLoS Genetics*, *16*(10), e1008800. https://doi.org/10.1371/journal.pgen.1008800

Ransohoff, R. M. (2012). Animal models of multiple sclerosis: The good, the bad and the bottom line. *Nature Neuroscience*, *15*(8), 1074–1077. https://doi.org/10.1038/nn.3168

Ransohoff, R. M. (2016). A polarizing question: Do M1 and M2 microglia exist. *Nature Neuroscience*, *19*(8), 987–991. https://doi.org/10.1038/nn.4338

Rasmussen, M. K., Mestre, H., & Nedergaard, M. (2022). Fluid transport in the brain. *Physiological Reviews*, *102*(2), 1025–1151. https://doi.org/10.1152/physrev.00031.2020

Rawji, K. S., Kappen, J., Tang, W., Teo, W., Plemel, J. R., Stys, P. K., & Yong, V. W. (2018). Deficient Surveillance and Phagocytic Activity of Myeloid Cells Within Demyelinated Lesions in Ageing Mice Visualized by *Ex Vivo* Live Multiphoton Imaging. *The Journal of Neuroscience*, *38*(8), 2341–17. https://doi.org/10.1523/JNEUROSCI.2341-17.2018

Rawji, K. S., Young, A. M. H., Ghosh, T., Michaels, N. J., Mirzaei, R., Kappen, J., Kolehmainen, K. L., Alaeiilkhchi, N., Lozinski, B., Mishra, M. K., Pu, A., Tang, W., Zein, S., Kaushik, D. K., Keough, M. B., Plemel, J. R., Calvert, F., Knights, A. J., Gaffney, D. J., … Yong, V. W. (2020). Niacin-mediated rejuvenation of macrophage/microglia enhances remyelination of the aging central nervous system. *Acta Neuropathologica*, *139*(5), 893–909. https://doi.org/10.1007/s00401-020-02129-7

Reich, D. S., Lucchinetti, C. F., & Calabresi, P. A. (2018). Multiple Sclerosis. *New England Journal of Medicine*, *378*(2), 169–180.

Reihmane, D., Jurka, A., & Tretjakovs, P. (2012). The relationship between maximal exercise-induced increases in serum IL-6, MPO and MMP-9 concentrations. *Scandinavian Journal of Immunology*, *76*(2), 188–192. https://doi.org/10.1111/j.1365-3083.2012.02720.x

Relucio, J., Menezes, M. J., Miyagoe-Suzuki, Y., Takeda, S., & Colognato, H. (2012). Laminin regulates postnatal oligodendrocyte production by promoting oligodendrocyte progenitor survival in the subventricular zone. *Glia*, *60*(10), 1451–1467. https://doi.org/10.1002/glia.22365

Rentsch, N. H., & Rust, R. (2022). “Scary” pericytes: The fibrotic scar in brain and spinal cord lesions. *Trends in Neurosciences*, *45*(1), 6–7. https://doi.org/10.1016/j.tins.2021.10.013

Rock, J. R., Barkauskas, C. E., Cronce, M. J., Xue, Y., Harris, J. R., Liang, J., Noble, P. W., & Hogan, B. L. M. (2011). Multiple stromal populations contribute to pulmonary fibrosis without evidence for epithelial to mesenchymal transition. *Proceedings of the National Academy of Sciences of the United States of America*, *108*(52). https://doi.org/10.1073/pnas.1117988108

Rodrigues, M., Kosaric, N., Bonham, C. A., & Gurtner, G. C. (2019). Wound healing: A cellular perspective. *Physiological Reviews*, *99*(1), 665–706. https://doi.org/10.1152/physrev.00067.2017

Rojas, O. L., Pröbstel, A. K., Porfilio, E. A., Wang, A. A., Charabati, M., Sun, T., Lee, D. S. W., Galicia, G., Ramaglia, V., Ward, L. A., Leung, L. Y. T., Najafi, G., Khaleghi, K., Garcillán, B., Li, A., Besla, R., Naouar, I., Cao, E. Y., Chiaranunt, P., … Gommerman, J. L. (2019). Recirculating Intestinal IgA-Producing Cells Regulate Neuroinflammation via IL-10. *Cell*, *176*(3), 610-624.e18. https://doi.org/10.1016/j.cell.2018.11.035

Rossi, S., Furlan, R., De Chiara, V., Musella, A., Lo Giudice, T., Mataluni, G., Cavasinni, F., Cantarella, C., Bernardi, G., Muzio, L., Martorana, A., Martino, G., & Centonze, D. (2009). Exercise attenuates the clinical, synaptic and dendritic abnormalities of experimental autoimmune encephalomyelitis. *Neurobiology of Disease*, *36*(1), 51–59. https://doi.org/10.1016/j.nbd.2009.06.013

Ruckh, J. M., Zhao, J. W., Shadrach, J. L., Van Wijngaarden, P., Rao, T. N., Wagers, A. J., & Franklin, R. J. M. (2012). Rejuvenation of regeneration in the aging central nervous system. *Cell Stem Cell*, *10*(1), 96–103. https://doi.org/10.1016/j.stem.2011.11.019

Sacks, D., Baxter, B., Campbell, B. C. V., Carpenter, J. S., Cognard, C., Dippel, D., Eesa, M., Fischer, U., Hausegger, K., Hirsch, J. A., Shazam Hussain, M., Jansen, O., Jayaraman, M. V., Khalessi, A. A., Kluck, B. W., Lavine, S., Meyers, P. M., Ramee, S., Rüfenacht, D. A., … Vorwerk, D. (2018). Multisociety Consensus Quality Improvement Revised Consensus Statement for Endovascular Therapy of Acute Ischemic Stroke. *International Journal of Stroke*, *13*(6), 612–632. https://doi.org/10.1177/1747493018778713

Saito, Y., Chikenji, T. S., Matsumura, T., Nakano, M., & Fujimiya, M. (2020). Exercise enhances skeletal muscle regeneration by promoting senescence in fibro-adipogenic progenitors. *Nature Communications*, *11*, 889. https://doi.org/10.1038/s41467-020-14734-x

Salzer, M. C., Lafzi, A., Berenguer-Llergo, A., Youssif, C., Castellanos, A., Solanas, G., Peixoto, F. O., Stephan-Otto Attolini, C., Prats, N., Aguilera, M., Martín-Caballero, J., Heyn, H., & Benitah, S. A. (2018). Identity Noise and Adipogenic Traits Characterize Dermal Fibroblast Aging. *Cell*, *175*(6), 1575-1590.e22. https://doi.org/10.1016/j.cell.2018.10.012

Sandroff, B. M., Baird, J. F., Silveira, S. L., & Motl, R. W. (2019). Response heterogeneity in fitness, mobility and cognition with exercise-training in MS. *Acta Neurologica Scandinavica*, *139*(2), 183–191. https://doi.org/10.1111/ane.13041

Sasaki, M., Black, J. A., Lankford, K. L., Tokuno, H. A., Waxman, S. G., & Kocsis, J. D. (2006). Molecular Reconstruction of Nodes of Ranvier after Remyelination by Transplanted Olfactory Ensheathing Cells in the Demyelinated Spinal Cord. *The*

Journal of Neuroscience, *26*(6), 1803–1812. https://doi.org/10.1523/JNEUROSCI.3611-05.2006

Scalabrini, D., Galimberti, D., Fenoglio, C., Comi, C., De Riz, M., Venturelli, E., Castelli, L., Piccio, L., Ronzoni, M., Lovati, C., Mariani, C., Monaco, F., Bresolin, N., & Scarpini, E. (2005). P-selectin glycoprotein ligand-1 variable number of tandem repeats (VNTR) polymorphism in patients with multiple sclerosis. *Neuroscience Letters*, *388*(3), 149–152. https://doi.org/10.1016/j.neulet.2005.06.059

Schaffert, C. S. (2011). Role of MGST1 in reactive intermediate-induced injury. *World J Gastroenterol*, *17*(20), 2552–2557. https://doi.org/10.3748/wjg.v17.i20.2552

Scheiman, J., Luber, J. M., Chavkin, T. A., MacDonald, T., Tung, A., Pham, L.-D., Wibowo, M. C., Wurth, R. C., Punthambaker, S., Tierney, B. T., Yang, Z., Hattab, M. W., Avila-Pacheco, J., Clish, C. B., Lessard, S., Church, G. M., & Kostic, A. D. (2019). Meta-omics analysis of elite athletes identifies a performance-enhancing microbe that functions via lactate metabolism. *Nature Medicine*, *25*(7), 1104–1109. https://doi.org/10.1038/s41591-019-0485-4

Schultz, V., van der Meer, F., Wrzos, C., Scheidt, U., Bahn, E., Stadelmann, C., Brück, W., & Junker, A. (2017). Acutely damaged axons are remyelinated in multiple sclerosis and experimental models of demyelination. *Glia*, *65*(8), 1350–1360. https://doi.org/10.1002/glia.23167

Schulze, C., Wetzel, F., Kueper, T., Malsen, A., Muhr, G., Jaspers, S., Blatt, T., Wittern, K.-P., Wenck, H., & Käs, J. A. (2010). Stiffening of Human Skin Fibroblasts with Age. *Biophysical Journal*, *99*(8), 2434–2442. https://doi.org/10.1016/j.bpj.2010.08.026

Scolding, N., Franklin, R., Stevens, S., Heldin, C. H., Compston, A., & Newcombe, J. (1998). Oligodendrocyte progenitors are present in the normal adult human CNS

and in the lesions of multiple sclerosis. *Brain*, *121*(12), 2221–2228. https://doi.org/10.1093/brain/121.12.2221

Segel, M., Neumann, B., Hill, M. F. E., Isabell, P., Viscomi, C., Zhao, C., Young, A., Agley, C. C., Thompson, A. J., Gonzalez, G. A., Sharma, A., Holmqvist, S., Rowitch, D. H., Franze, K., Franklin, R. J. M., & Chalut, K. J. (2019). Niche stiffness underlies the ageing of central nervous system progenitor cells. *Nature*. https://doi.org/10.1038/s41586-019-1484-9

Seki, S. M., & Gaultier, A. (2017). Exploring non-metabolic functions of glycolytic enzymes in immunity. *Frontiers in Immunology*, *8*(NOV), 1–8. https://doi.org/10.3389/fimmu.2017.01549

Sellers, D. L., Maris, D. O., & Horner, P. J. (2009). Postinjury Niches Induce Temporal Shifts in Progenitor Fates to Direct Lesion Repair after Spinal Cord Injury. *The Journal of Neuroscience*, *29*(20), 6722–6733. https://doi.org/10.1523/JNEUROSCI.4538-08.2009

Seyfried, N. T., McVey, G. F., Almond, A., Mahoney, D. J., Dudhia, J., & Day, A. J. (2005). Expression and Purification of Functionally Active Hyaluronan-binding Domains from Human Cartilage Link Protein, Aggrecan and Versican. *Journal of Biological Chemistry*, *280*(7), 5435–5448. https://doi.org/10.1074/jbc.M411297200

Shahidi, S. H., Kordi, M. R., Rajabi, H., Malm, C., Shah, F., & Quchan, A. S. K. (2020). Exercise modulates the levels of growth inhibitor genes before and after multiple sclerosis. *Journal of Neuroimmunology*, *341*(January), 577172. https://doi.org/10.1016/j.jneuroim.2020.577172

Shearer, M. C., Niclou, S. P., Brown, D., Asher, R. A., Holtmaat, A. J. G. D., Levine, J. M., Verhaagen, J., & Fawcett, J. W. (2003). The astrocyte/meningeal cell interface is a barrier to neurite outgrowth which can be overcome by

manipulation of inhibitory molecules or axonal signalling pathways. *Molecular and Cellular Neuroscience*, *24*(4), 913–925. https://doi.org/10.1016/j.mcn.2003.09.004

Shechter, R., Miller, O., Yovel, G., Rosenzweig, N., London, A., Kim, K., Klein, E., Kalchenko, V., Bendel, P., Sergio, A., Jung, S., & Schwartz, M. (2013). Recruitment of Beneficial M2 Macrophages to Injured Spinal Cord Is Orchestrated by Remote Brain Choroid Plexus. *Immunity*, *38*(3), 555–569. https://doi.org/10.1016/j.immuni.2013.02.012.Recruitment

Shen, S., Sandoval, J., Swiss, V. A., Li, J., Dupree, J., Franklin, R. J. M., & Casaccia-Bonnefil, P. (2008). Age-dependent epigenetic control of differentiation inhibitors is critical for remyelination efficiency. *Nature Neuroscience*, *11*(9), 1024–1034. https://doi.org/10.1038/nn.2172

Shen, Y., Tenney, A. P., Busch, S. A., Horn, K. P., Cuascut, F. X., Liu, K., He, Z., Silver, J., & Flanagan, J. G. (2009). PTPσ Is a Receptor for Chondroitin Sulfate Proteoglycan, an Inhibitor of Neural Regeneration. *Science*, *326*(5952), 592–596. https://doi.org/10.1126/science.1178310

Shibahara, T., Ago, T., Nakamura, K., Tachibana, M., Yoshikawa, Y., Komori, M., Yamanaka, K., Wakisaka, Y., & Kitazono, T. (2020). Pericyte-mediated tissue repair through PDGFRβ promotes peri-infarct astrogliosis, oligodendrogenesis, and functional recovery after acute ischemic stroke. *ENeuro*, *7*(2), 1–20. https://doi.org/10.1523/ENEURO.0474-19.2020

Shibahara, T., Ago, T., Tachibana, M., Nakamura, K., Yamanaka, K., Kuroda, J., Wakisaka, Y., & Kitazono, T. (2020). Reciprocal Interaction Between Pericytes and Macrophage in Poststroke Tissue Repair and Functional Recovery. *Stroke*, *October*, 3095–3106. https://doi.org/10.1161/strokeaha.120.029827

Shields, S. A., Gilson, J. M., Blakemore, W. F., & Franklin, R. J. M. (1999). Remyelination occurs as extensively but more slowly in old rats compared to young rats following gliotoxin-induced CNS demyelination. *Glia*, *28*(1), 77–83. https://doi.org/10.1002/(SICI)1098-1136(199910)28:1<77::AID-GLIA9>3.0.CO;2-F

Shook, B. A., Wasko, R. R., Rivera-Gonzalez, G. C., Salazar-Gatzimas, E., López-Giráldez, F., Dash, B. C., Muñoz-Rojas, A. R., Aultman, K. D., Zwick, R. K., Lei, V., Arbiser, J. L., Miller-Jensen, K., Clark, D. A., Hsia, H. C., & Horsley, V. (2018). Myofibroblast proliferation and heterogeneity are supported by macrophages during skin repair. *Science*, *362*(6417). https://doi.org/10.1126/science.aar2971

Shoulders, M. D., & Raines, R. T. (2009). COLLAGEN STRUCTURE AND STABILITY. *Annual Review of Biochemistry*, *78*, 929–958. https://doi.org/10.1146/annurev.biochem.77.032207.120833

Sikkema, A. H., Stoffels, J. M. J., Wang, P., Basedow, F. J., Bulsink, R., Bajramovic, J. J., & Baron, W. (2018). Fibronectin aggregates promote features of a classically and alternatively activated phenotype in macrophages. *Journal of Neuroinflammation*, *15*, 218. https://doi.org/10.1186/s12974-018-1238-x

Sim, F. J., Zhao, C., Penderis, J., & Franklin, R. J. M. (2002). The Age-Related Decrease in CNS Remyelination Efficiency Is Attributable to an Impairment of Both Oligodendrocyte Progenitor Recruitment and Differentiation. *Journal of Neuroscience*, *22*(7), 2451–2459.

Singh, B., Kasam, R. K., Sontake, V., Wynn, T. A., & Madala, S. K. (2017). Repetitive intradermal bleomycin injections evoke T-helper cell 2 cytokine-driven pulmonary fibrosis. *American Journal of Physiology - Lung Cellular and Molecular Physiology*, *313*(5), L796–L806. https://doi.org/10.1152/ajplung.00184.2017

Sinha, S., Sparks, H. D., Labit, E., Robbins, H. N., Gowing, K., Jaffer, A., Kutluberk, E., Arora, R., Raredon, M. S. B., Cao, L., Swanson, S., Jiang, P., Hee, O., Pope, H., Workentine, M., Todkar, K., Sharma, N., Bharadia, S., Chockalingam, K., … Biernaskie, J. (2022). Fibroblast inflammatory priming determines regenerative versus fibrotic skin repair in reindeer. *Cell*, *185*(25), 4717-4736.e25. https://doi.org/10.1016/j.cell.2022.11.004

Sloane, J. A., Batt, C., Ma, Y., Harris, Z. M., Trapp, B., & Vartanian, T. (2010). Hyaluronan blocks oligodendrocyte progenitor maturation and remyelination through TLR2. *Proceedings of the National Academy of Sciences of the United States of America*, *107*(25), 11555–11560. https://doi.org/10.1073/pnas.1006496107

Smith, K. J., Blakemore, W. F., & McDonald, W. I. (1979). Central remyelination restores secure conduction. *Nature*, *280*(5721), 395–396. https://doi.org/10.1038/280395a0

Smith, K. J., Blakemore, W. F., & Mcdonald, W. I. (1981). The Restoration of Conduction by Central Remyelination. *Brain*, *104*, 383–404. https://doi.org/10.1093/brain/104.2.383

Smith, M. H., Gao, V. R., Periyakoil, P. K., Kochen, A., DiCarlo, E. F., Goodman, S. M., Norman, T. M., Donlin, L. T., Leslie, C. S., & Rudensky, A. Y. (2023). Drivers of heterogeneity in synovial fibroblasts in rheumatoid arthritis. *Nature Immunology*, *24*(7), Article 7. https://doi.org/10.1038/s41590-023-01527-9

Snaidero, N., Möbius, W., Czopka, T., Hekking, L. H. P., Mathisen, C., Verkleij, D., Goebbels, S., Edgar, J., Merkler, D., Lyons, D. A., Nave, K. A., & Simons, M. (2014). Myelin membrane wrapping of CNS axons by PI(3,4,5)P3-dependent polarized growth at the inner tongue. *Cell*, *156*(1–2), 277–290. https://doi.org/10.1016/j.cell.2013.11.044

Snaidero, N., Velte, C., Myllykoski, M., Raasakka, A., Ignatev, A., Werner, H. B., Erwig, M. S., Möbius, W., Kursula, P., Nave, K. A., & Simons, M. (2017). Antagonistic Functions of MBP and CNP Establish Cytosolic Channels in CNS Myelin. *Cell Reports*, *18*(2), 314–323. https://doi.org/10.1016/j.celrep.2016.12.053

Sobel, R. A. (2001). The extracellular matrix in multiple sclerosis: An update. *Brazilian Journal of Medical and Biological Research*, *34*(5), 603–609. https://doi.org/10.1590/S0100-879X2001000500007

Sobel, R. A., & Mitchell, M. E. (1989). Fibronectin in multiple sclerosis lesions. *American Journal of Pathology*, *135*(1), 161–168.

Soderblom, C., Luo, X., Blumenthal, E., Bray, E., Lyapichev, K., Ramos, J., Krishnan, V., Lai-Hsu, C., Park, K. K., Tsoulfas, P., & Lee, J. K. (2013). Perivascular fibroblasts form the fibrotic scar after contusive spinal cord injury. *Journal of Neuroscience*, *33*(34), 13882–13887. https://doi.org/10.1523/JNEUROSCI.2524-13.2013

Sofroniew, M. V. (2018). Dissecting spinal cord regeneration perspective. *Nature*, *557*(7705), 343–350. https://doi.org/10.1038/s41586-018-0068-4

Sofroniew, M. V. (2020). Astrocyte Reactivity: Subtypes , States , and Functions in CNS Innate Immunity. *Trends in Immunology*, *41*(9), 758–770. https://doi.org/10.1016/j.it.2020.07.004

Soliman, H., Theret, M., Scott, W., Hill, L., Underhill, T. M., Hinz, B., & Rossi, F. M. V. (2021). Multipotent stromal cells: One name, multiple identities. *Cell Stem Cell*, *28*(10), 1690–1707. https://doi.org/10.1016/j.stem.2021.09.001

Soriano, P. (1997). The PDGFα receptor is required for neural crest cell development and for normal patterning of the somites. *Development*, *124*(14), 2691–2700. https://doi.org/10.1242/dev.124.14.2691

Sorokin, L. (2010). The impact of the extracellular matrix on inflammation. *Nature Reviews Immunology*, *10*(10), 712–723. https://doi.org/10.1038/nri2852

Soto, I., Graham, L. C., Richter, H. J., Simeone, S. N., Radell, J. E., Grabowska, W., Funkhouser, W. K., Howell, M. C., & Howell, G. R. (2015). APOE Stabilization by Exercise Prevents Aging Neurovascular Dysfunction and Complement Induction. *PLoS Biology*, *13*(10), 1–33. https://doi.org/10.1371/journal.pbio.1002279

Souza, P. S., Gonçalves, E. D., Pedroso, G. S., Farias, H. R., Junqueira, S. C., Marcon, R., Tuon, T., Cola, M., Silveira, P. C. L., Santos, A. R., Calixto, J. B., Souza, C. T., de Pinho, R. A., & Dutra, R. C. (2016). Physical Exercise Attenuates Experimental Autoimmune Encephalomyelitis by Inhibiting Peripheral Immune Response and Blood-Brain Barrier Disruption. *Molecular Neurobiology*, *54*(6), 4723–4737. https://doi.org/10.1007/s12035-016-0014-0

Spitzer, M., Wildenhain, J., Rappsilber, J., & Tyers, M. (2014). BoxPlotR: A web tool for generation of box plots. *Nature Methods*, *11*(2), 121–122. https://doi.org/10.1038/nmeth.2811

Spitzer, S. O., Sitnikov, S., Kamen, Y., Faria, O. D., Agathou, S., Spitzer, S. O., Sitnikov, S., Kamen, Y., Evans, K. A., & Kronenberg-versteeg, D. (2019). Oligodendrocyte Progenitor Cells Become Regionally Diverse and Heterogeneous with Age Article Oligodendrocyte Progenitor Cells Become Regionally Diverse and Heterogeneous with Age. *Neuron*, 459–471. https://doi.org/10.1016/j.neuron.2018.12.020

Srivastava, T., Diba, P., Dean, J. M., Banine, F., Shaver, D., Hagen, M., Gong, X., Su, W., Emery, B., Marks, D. L., Harris, E. N., Baggenstoss, B., Weigel, P. H., Sherman, L. S., & Back, S. A. (n.d.). A TLR/AKT/FoxO3 immune tolerance–like pathway disrupts the repair capacity of oligodendrocyte progenitors. *The Journal of Clinical Investigation*, *128*(5), 2025–2041. https://doi.org/10.1172/JCI94158

Srivastava, T., Sherman, L. S., & Back, S. A. (2020). Dysregulation of Hyaluronan Homeostasis during White Matter Injury. *Neurochemical Research*, *45*(3), 672–683. https://doi.org/10.1007/s11064-019-02879-1

Stadelmann, C., Timmler, S., Barrantes-Freer, A., & Simons, M. (2019). Myelin in the Central Nervous System: Structure, Function, and Pathology. *Physiological Reviews*, *99*(3), 1381–1431. https://doi.org/10.1152/physrev.00031.2018

Stearns-Reider, K. M., D'Amore, A., Beezhold, K., Rothrauff, B., Cavalli, L., Wagner, W. R., Vorp, D. A., Tsamis, A., Shinde, S., Zhang, C., Barchowsky, A., Rando, T. A., Tuan, R. S., & Ambrosio, F. (2017). Aging of the skeletal muscle extracellular matrix drives a stem cell fibrogenic conversion. *Aging Cell*, *16*(3), 518–528. https://doi.org/10.1111/acel.12578

Steffen, B. J., Breier, G., Butcher, E. C., Schulz, M., & Engelhardt, B. (1996). ICAM-1, VCAM-1, and MAdCAM-1 are expressed on choroid plexus epithelium but not endothelium and mediate binding of lymphocytes in vitro. *The American Journal of Pathology*, *148*(6), 1819–1838.

Stephens, S., Shams, S., Lee, J., Grover, S. A., Longoni, G., Berenbaum, T., Finlayson, M., Motl, R. W., & Yeh, E. A. (2019). Benefits of Physical Activity for Depression and Fatigue in Multiple Sclerosis: A Longitudinal Analysis. *Journal of Pediatrics*, *209*, 226-232.e2. https://doi.org/10.1016/j.jpeds.2019.01.040

Stephenson, E. L., Mishra, M. K., Moussienko, D., Laflamme, N., Rivest, S., Ling, C., & Yong, V. W. (2018). Chondroitin sulfate proteoglycans as novel drivers of leucocyte infiltration in multiple sclerosis. *Brain*, 1094–1110. https://doi.org/10.1093/brain/awy033

Stoffels, J. M. J., Hoekstra, D., Franklin, R. J. M., Baron, W., & Zhao, C. (2014). The EIIIA domain from astrocyte-derived fibronectin mediates proliferation of oligodendrocyte progenitor cells following CNS demyelination. *Glia*.

Strijbis, E. M. M., Kooi, E. J., van der Valk, P., & Geurts, J. J. G. (2017). Cortical remyelination is heterogeneous in multiple sclerosis. *Journal of Neuropathology and Experimental Neurology*, *76*(5), 390–401. https://doi.org/10.1093/jnen/nlx023

Sun, Z., Zhao, H., Fang, D., Davis, C. T., Shi, D. S., Lei, K., Rich, B. E., Winter, J. M., Guo, L., Sorensen, L. K., Pryor, R. J., Zhu, N., Lu, S., Dickey, L. L., Doty, D. J., Tong, Z., Thomas, K. R., Mueller, A. L., Grossmann, A. H., … Zhu, W. (2022). Neuroinflammatory disease disrupts the blood-CNS barrier via crosstalk between proinflammatory and endothelial-to-mesenchymal-transition signaling. *Neuron*, *110*(19), 3106-3120.e7. https://doi.org/10.1016/j.neuron.2022.07.015

Susuki, K., Chang, K.-J., Zollinger, D. R., Liu, Y., Ogawa, Y., Eshed-Eisenbach, Y., Dours-Zimmermann, M. T., Oses-Prieto, J. A., Burlingame, A. L., Seidenbecher, C. I., Zimmermann, D. R., Oohashi, T., Peles, E., & Rasband, M. N. (2013). Three Mechanisms Assemble Central Nervous System Nodes of Ranvier. *Neuron*, *78*(3), 469–482. https://doi.org/10.1016/j.neuron.2013.03.005

Suzuki, N., Hyodo, M., Hayashi, C., Mabuchi, Y., Sekimoto, K., Onchi, C., Sekiguchi, K., & Akazawa, C. (2019). Laminin α2, α4, and α5 Chains Positively Regulate Migration and Survival of Oligodendrocyte Precursor Cells. *Scientific Reports*, *9*(1), Article 1. https://doi.org/10.1038/s41598-019-56488-7

Szklarczyk, D., Gable, A. L., Lyon, D., Junge, A., Wyder, S., Huerta-Cepas, J., Simonovic, M., Doncheva, N. T., Morris, J. H., Bork, P., Jensen, L. J., & Mering, C. von. (2019). STRING v11: Protein–protein association networks with increased coverage, supporting functional discovery in genome-wide experimental datasets. *Nucleic Acids Research*, *47*(D1), D607--D613. https://doi.org/10.1093/nar/gky1131

Takaya, K., Asou, T., & Kishi, K. (2022). Aging Fibroblasts Adversely Affect Extracellular Matrix Formation via the Senescent Humoral Factor Ependymin-Related Protein 1. *Cells*, *11*(23), 3749. https://doi.org/10.3390/cells11233749

Talbott, H. E., Mascharak, S., Griffin, M., Wan, D. C., & Longaker, M. T. (2022). Wound healing, fibroblast heterogeneity, and fibrosis. *Cell Stem Cell*, *29*(8), 1161–1180. https://doi.org/10.1016/j.stem.2022.07.006

Thompson, A. J., Baranzini, S. E., Geurts, J., Hemmer, B., & Ciccarelli, O. (2018). Multiple sclerosis. *The Lancet*, *6736*(18), 1–15. https://doi.org/10.1016/S0140-6736(18)30481-1

Thouvenot, E., Hinsinger, G., Demattei, C., Uygunoglu, U., Castelnovo, G., Pittion-Vouyovitch, S., Okuda, D., Kantarci, O., Pelletier, D., Lehmann, S., Marin, P., Siva, A., & Lebrun, C. (2019). Cerebrospinal fluid chitinase-3-like protein 1 level is not an independent predictive factor for the risk of clinical conversion in radiologically isolated syndrome. *Multiple Sclerosis Journal*, *25*(5), 669–677. https://doi.org/10.1177/1352458518767043

Tinaburri, L., Valente, C., Teson, M., Minafò, Y. A., Cordisco, S., Guerra, L., & Dellambra, E. (2021). The Secretome of Aged Fibroblasts Promotes EMT-Like Phenotype in Primary Keratinocytes from Elderly Donors through BDNF-TrkB Axis. *Journal of Investigative Dermatology*, *141*(4, Supplement), 1052-1062.e12. https://doi.org/10.1016/j.jid.2020.08.019

Tran, J. Q., Rana, J., Barkhof, F., Melamed, I., Gevorkyan, H., Wattjes, M. P., de Jong, R., Brosofsky, K., Ray, S., Xu, L., Zhao, J., Parr, E., & Cadavid, D. (2014). Randomized phase I trials of the safety/tolerability of anti-LINGO-1 monoclonal antibody BIIB033. *Neurology® Neuroimmunology & Neuroinflammation*, *1*(2), e18. https://doi.org/10.1212/NXI.0000000000000018

Trapp, B. D., Peterson, J., Ransohoff, R. M., Rudick, R., Mork, S., & Bo, L. (1998). Axonal transection in the lesions of multiple sclerosis. *N Engl J Med*.

Triarhou, L. C., & Herndon, R. M. (1986). Choline (Lysolecithin) -Induced Demyelination of the Rat Spinal Cord. *Archives of Neurology*, *43*.

Tripathi, A., Parikh, Z. S., Vora, P., Frost, E. E., & Pillai, P. P. (2017). pERK1/2 Peripheral Recruitment and Filopodia Protrusion Augment Oligodendrocyte Progenitor Cell Migration: Combined Effects of PDGF-A and Fibronectin. *Cellular and Molecular Neurobiology*, *37*(2), 183–194. https://doi.org/10.1007/s10571-016-0359-y

Tripathi, R. B., Jackiewicz, M., McKenzie, I. A., Kougioumtzidou, E., Grist, M., & Richardson, W. D. (2017). Remarkable Stability of Myelinating Oligodendrocytes in Mice. *Cell Reports*, *21*(2), 316–323. https://doi.org/10.1016/j.celrep.2017.09.050

Tsai, H. H., Niu, J., Munji, R., Davalos, D., Chang, J., Zhang, H., Tien, A. C., Kuo, C. J., Chan, J. R., Daneman, R., & Fancy, S. P. J. (2016). Oligodendrocyte precursors migrate along vasculature in the developing nervous system. *Science*, *351*(6271), 379–384. https://doi.org/10.1126/science.aad3839

Tsata, V., Möllmert, S., Schweitzer, C., Kolb, J., Möckel, C., Böhm, B., Rosso, G., Lange, C., Lesche, M., Hammer, J., Kesavan, G., Beis, D., Guck, J., Brand, M., & Wehner, D. (2021). A switch in pdgfrb+ cell-derived ECM composition prevents inhibitory scarring and promotes axon regeneration in the zebrafish spinal cord. *Developmental Cell*, *56*(4), 509-524.e9. https://doi.org/10.1016/j.devcel.2020.12.009

Tse, J. M., Cheng, G., Tyrrell, J. A., Wilcox-adelman, S. A., Boucher, Y., & Jain, R. K. (2011). *Mechanical compression drives cancer cells toward invasive phenotype*. https://doi.org/10.1073/pnas.1118910109

Tyanova, S., Temu, T., Sinitcyn, P., Carlson, A., Hein, M. Y., Geiger, T., Mann, M., & Cox, J. (2016). The Perseus computational platform for comprehensive analysis of (prote)omics data. *Nature Methods*, *13*(9), 731–740. https://doi.org/10.1038/nmeth.3901

Uniken Venema, W. T. C., Ramírez-Sánchez, A. D., Bigaeva, E., Withoff, S., Jonkers, I., McIntyre, R. E., Ghouraba, M., Raine, T., Weersma, R. K., Franke, L., Festen, E. A. M., & van der Wijst, M. G. P. (2022). Gut mucosa dissociation protocols influence cell type proportions and single-cell gene expression levels. *Scientific Reports*, *12*(1), Article 1. https://doi.org/10.1038/s41598-022-13812-y

Vallstedt, A., Klos, J. M., & Ericson, J. (2005). Multiple Dorsoventral Origins of Oligodendrocyte Generation in the Spinal Cord and Hindbrain. *Neuron*, *45*, 55–67. https://doi.org/10.1016/j.neuron.2004.12.026

van Horssen, J., Bö, L., Dijkstra, C. D., & de Vries, H. E. (2006). Extensive extracellular matrix depositions in active multiple sclerosis lesions. *Neurobiology of Disease*, *24*(3), 484–491. https://doi.org/10.1016/j.nbd.2006.08.005

Van Horssen, J., Dijkstra, C. D., & De Vries, H. E. (2007). The extracellular matrix in multiple sclerosis pathology. *Journal of Neurochemistry*, *103*(4), 1293–1301. https://doi.org/10.1111/j.1471-4159.2007.04897.x

van Horssen, J., Singh, S., van der Pol, S., Kipp, M., Lim, J. L., Peferoen, L., Gerritsen, W., Kooi, E.-J., Witte, M. E., Geurts, J. J., de Vries, H. E., Peferoen-Baert, R., van den Elsen, P. J., van der Valk, P., & Amor, S. (2012). Clusters of activated microglia in normal-appearing white matter show signs of innate immune activation. *Journal of Neuroinflammation*, *9*, 156. https://doi.org/10.1186/1742-2094-9-156

van Praag, H. (2009). Exercise and the brain: Something to chew on. *Trends in Neurosciences*, *32*(5), 283–290. https://doi.org/10.1016/j.tins.2008.12.007

Vankriekelsvenne, E., Chrzanowski, U., Manzhula, K., Greiner, T., Wree, A., Hawlitschka, A., Llovera, G., Zhan, J., Joost, S., Schmitz, C., Ponsaerts, P., Amor, S., Nutma, E., Kipp, M., & Kaddatz, H. (2022). Transmembrane protein 119 is neither a specific nor a reliable marker for microglia. *Glia*, *70*(6), 1170–1190. https://doi.org/10.1002/glia.24164

Vanlandewijck, M., He, L., Mäe, M. A., Andrae, J., Ando, K., Del Gaudio, F., Nahar, K., Lebouvier, T., Laviña, B., Gouveia, L., Sun, Y., Raschperger, E., Räsänen, M., Zarb, Y., Mochizuki, N., Keller, A., Lendahl, U., & Betsholtz, C. (2018). A molecular atlas of cell types and zonation in the brain vasculature. *Nature*, *554*(7693), 475–480. https://doi.org/10.1038/nature25739

Verrecchia, F., Chu, M. L., & Mauviel, A. (2001). Identification of Novel TGF-β/Smad Gene Targets in Dermal Fibroblasts using a Combined cDNA Microarray/Promoter Transactivation Approach. *Journal of Biological Chemistry*, *276*(20), 17058–17062. https://doi.org/10.1074/jbc.M100754200

Vidal, R., Wagner, J. U. G., Braeuning, C., Fischer, C., Patrick, R., Tombor, L., Muhly-Reinholz, M., John, D., Kliem, M., Conrad, T., Guimarães-Camboa, N., Harvey, R., Dimmeler, S., & Sauer, S. (n.d.). Transcriptional heterogeneity of fibroblasts is a hallmark of the aging heart. *JCI Insight*, *4*(22), e131092. https://doi.org/10.1172/jci.insight.131092

Walker, E. J., Heydet, D., Veldre, T., & Ghildyal, R. (2019). Transcriptomic changes during TGF-β-mediated differentiation of airway fibroblasts to myofibroblasts. *Scientific Reports*, *9*(1), 1–14. https://doi.org/10.1038/s41598-019-56955-1

Wang, F., Flanagan, J., Su, N., Wang, L.-C., Bui, S., Nielson, A., Wu, X., Vo, H.-T., Ma, X.-J., & Luo, Y. (2012). RNAscope. *The Journal of Molecular Diagnostics : JMD*, *14*(1), 22–29. https://doi.org/10.1016/j.jmoldx.2011.08.002

Wang, P., Gorter, R. P., de Jonge, J. C., Nazmuddin, M., Zhao, C., Amor, S., Hoekstra, D., & Baron, W. (2018). MMP7 cleaves remyelination-impairing fibronectin aggregates and its expression is reduced in chronic multiple sclerosis lesions. *Glia*, *66*(8), 1625–1643. https://doi.org/10.1002/glia.23328

Wang, S., Voisin, M.-B., Larbi, K. Y., Dangerfield, J., Scheiermann, C., Tran, M., Maxwell, P. H., Sorokin, L., & Nourshargh, S. (2006). Venular basement membranes contain specific matrix protein low expression regions that act as exit points for emigrating neutrophils. *The Journal of Experimental Medicine*, *203*(6), 1519–1532.

Wanner, I. B., Anderson, M. A., Song, B., Levine, J., Fernandez, A., Gray-Thompson, Z., Ao, Y., & Sofroniew, M. V. (2013). Glial scar borders are formed by newly proliferated, elongated astrocytes that interact to corral inflammatory and fibrotic cells via STAT3-dependent mechanisms after spinal cord injury. *Journal of Neuroscience*, *33*(31), 12870–12886. https://doi.org/10.1523/JNEUROSCI.2121-13.2013

Warnes, G. R., Bolker, B., Bonebakker, L., Gentleman, R., Liaw, W. H. A., Lumley, T., Maechler, M., Magnusson, A., Moeller, S., Schwartz, M., & others. (2015). *gplots: Various R programming tools for plotting data*.

Waxman, S. G., Black, J. A., Duncan, I. D., & Ransom, B. R. (1990). Macromolecular structure of axon membrane and action potential conduction in myelin deficient and myelin deficient heterozygote rat optic nerves. *Journal of Neurocytology*, *19*(1), 11–28. https://doi.org/10.1007/BF01188436

Weaver, A., Da Silva, A. G., Nuttall, R. K., Edwards, D. R., Shapiro, S. D., Rivest, S., & Yong, V. W. (2005). An elevated matrix metalloproteinase (MMP) in an animal model of multiple sclerosis is protective by affecting Th1/Th2 polarization. *The FASEB Journal*, *19*(12), 1668–1670. https://doi.org/10.1096/fj.04-2030fje

Wei, K., Korsunsky, I., Marshall, J. L., Gao, A., Watts, G. F. M., Major, T., Croft, A. P., Watts, J., Blazar, P. E., Lange, J. K., Thornhill, T. S., Filer, A., Raza, K., Donlin, L. T., Siebel, C. W., Buckley, C. D., Raychaudhuri, S., & Brenner, M. B. (2020). Notch signalling drives synovial fibroblast identity and arthritis pathology. *Nature*, *582*(7811), Article 7811. https://doi.org/10.1038/s41586-020-2222-z

Wei, W., Riley, N. M., Lyu, X., Shen, X., Guo, J., Raun, S. H., Zhao, M., Moya-Garzon, M. D., Basu, H., Sheng-Hwa Tung, A., Li, V. L., Huang, W., Wiggenhorn, A. L., Svensson, K. J., Snyder, M. P., Bertozzi, C. R., & Long, J. Z. (2023). Organism-wide, cell-type-specific secretome mapping of exercise training in mice. *Cell Metabolism*, 1–19. https://doi.org/10.1016/j.cmet.2023.04.011

Werkman, I., Sikkema, A. H., Versluijs, J. B., Qin, J., de Boer, P., & Baron, W. (2020). TLR3 agonists induce fibronectin aggregation by activated astrocytes: A role of pro-inflammatory cytokines and fibronectin splice variants. *Scientific Reports*, *10*(1), Article 1. https://doi.org/10.1038/s41598-019-57069-4

Wesnes, K., Myhr, K.-M., Riise, T., Cortese, M., Pugliatti, M., Bostrom, I., Landtblom, A.-M., Wolfson, C., & Bjornevik, K. (2017). Physical activity is associated with a decreased multiple sclerosis risk: The EnvIMS study. *Multiple Sclerosis Journal*, *24*(2), 150–157. https://doi.org/10.1177/https

Wheeler, M. A., Clark, I. C., Lee, H.-G., Li, Z., Linnerbauer, M., Rone, J. M., Blain, M., Akl, C. F., Piester, G., Giovannoni, F., Charabati, M., Lee, J.-H., Kye, Y.-C., Choi, J., Sanmarco, L. M., Srun, L., Chung, E. N., Flausino, L. E., Andersen, B. M., … Quintana, F. J. (2023). Droplet-based forward genetic screening of astrocyte-microglia cross-talk. *Science (New York, N.Y.)*, *379*(6636), 1023–1030. https://doi.org/10.1126/science.abq4822

Wheeler, M. A., Clark, I. C., Tjon, E. C., Li, Z., Zandee, S. E. J., Couturier, C. P., Watson, B. R., Scalisi, G., Alkwai, S., Rothhammer, V., Rotem, A., Heyman, J.

A., Thaploo, S., Sanmarco, L. M., Ragoussis, J., Weitz, D. A., Petrecca, K., Moffitt, J. R., Becher, B., … Quintana, F. J. (2020). MAFG-driven astrocytes promote CNS inflammation. *Nature*, *578*(7796), 593–599. https://doi.org/10.1038/s41586-020-1999-0

White, E. S., Atrasz, R. G., Dickie, E. G., Aronoff, D. M., Stambolic, V., Mak, T. W., Moore, B. B., & Peters-Golden, M. (2005). Prostaglandin E2 Inhibits Fibroblast Migration by E-Prostanoid 2 Receptor–Mediated Increase in PTEN Activity. *American Journal of Respiratory Cell and Molecular Biology*, *32*(2), 135–141. https://doi.org/10.1165/rcmb.2004-0126OC

White, K. E., Ding, Q., Moore, B. B., Peters-Golden, M., Ware, L. B., Matthay, M. A., & Olman, M. A. (2008). Prostaglandin E2 Mediates IL-1β-Related Fibroblast Mitogenic Effects in Acute Lung Injury through Differential Utilization of Prostanoid Receptors. *Journal of Immunology (Baltimore, Md. : 1950)*, *180*(1), 637–646.

Wilson, M. S., Madala, S. K., Ramalingam, T. R., Gochuico, B. R., Rosas, I. O., Cheever, A. W., & Wynn, T. A. (2010). Bleomycin and IL-1β-mediated pulmonary fibrosis is IL-17A dependent. *Journal of Experimental Medicine*, *207*(3), 535–552. https://doi.org/10.1084/jem.20092121

Wilting, J., & Christ, B. (1989). An experimental and ultrastructural study on the development of the avian choroid plexus. *Cell and Tissue Research*, *255*(3), 487–494. https://doi.org/10.1007/BF00218783

Windrem, M. S., Nunes, M. C., Rashbaum, W. K., Schwartz, T. H., Goodman, R. A., McKhann, G., Roy, N. S., & Goldman, S. A. (2004). Fetal and adult human oligodendrocyte progenitor cell isolates myelinate the congenitally dysmyelinated brain. *Nature Medicine*, *10*(1), 93–97. https://doi.org/10.1038/nm974

Winkler, S., Stahl, R. C., Carey, D. J., & Bansal, R. (2002). Syndecan-3 and perlecan are differentially expressed by progenitors and mature oligodendrocytes and accumulate in the extracellular matrix. *Journal of Neuroscience Research*, *69*(4), 477–487. https://doi.org/10.1002/jnr.10311

Witte, M. B., & Barbul, A. (2003). Arginine physiology and its implication for wound healing. *Wound Repair and Regeneration*, *11*(6), 419–423. https://doi.org/10.1046/j.1524-475X.2003.11605.x

Wolswijk, G. (1998). Chronic stage multiple sclerosis lesions contain a relatively quiescent population of oligodendrocyte precursor cells. *Journal of Neuroscience*, *18*(2), 601–609. https://doi.org/10.1523/jneurosci.18-02-00601.1998

Wolswijk, G., & Noble, M. (1992). Cooperation Between PDGF and FGF Converts Slowly Dividing O-2A adult Progenitor Cells to Rapidly Dividing Cells with Characteristics of O _ 2A " nat Progenitor Cells. *The Journal of Cell Biology*, *118*(4), 889–900.

Woodruff, R. H., Fruttiger, M., Richardson, W. D., & Franklin, R. J. M. (2004). Platelet-derived growth factor regulates oligodendrocyte progenitor numbers in adult CNS and their response following CNS demyelination. *Molecular and Cellular Neuroscience*, *25*, 252–262. https://doi.org/10.1016/j.mcn.2003.10.014

Wrann, C. D., White, J. P., Salogiannnis, J., Laznik-Bogoslavski, D., Wu, J., Ma, D., Lin, J. D., Greenberg, M. E., & Spiegelman, B. M. (2013). Exercise induces hippocampal BDNF through a PGC-1α/FNDC5 pathway. *Cell Metabolism*, *18*(5), 649–659. https://doi.org/10.1016/j.cmet.2013.09.008

Wu, Y. J., Pierre, D. P. L., Wu, J., Yee, A. J., & Yang, B. B. (2005). The interaction of versican with its binding partners. *Cell Research*, *15*(7), Article 7. https://doi.org/10.1038/sj.cr.7290318

Wuerfel, J., Paul, F., Beierbach, B., Hamhaber, U., Klatt, D., Papazoglou, S., Zipp, F., Martus, P., Braun, J., & Sack, I. (2010). MR-elastography reveals degradation of tissue integrity in multiple sclerosis. *NeuroImage*, *49*(3), 2520–2525. https://doi.org/10.1016/j.neuroimage.2009.06.018

Wynn, T. A., & Vannella, K. M. (2016). Macrophages in Tissue Repair, Regeneration, and Fibrosis. *Immunity*, *44*(3), 450–462. https://doi.org/10.1016/j.immuni.2016.02.015

Wyss-coray, T. (2015). Ageing, neurodegeneration and brain rejuvenation. *Nature*, *539*. https://doi.org/10.1038/nature20411

Xia, H., Diebold, D., Nho, R., Perlman, D., Kleidon, J., Kahm, J., Avdulov, S., Peterson, M., Nerva, J., Bitterman, P., & Henke, C. (2008). Pathological integrin signaling enhances proliferation of primary lung fibroblasts from patients with idiopathic pulmonary fibrosis. *Journal of Experimental Medicine*, *205*(7), 1659–1672. https://doi.org/10.1084/jem.20080001

Xu, L., Nirwane, A., Xu, T., Kang, M., Devasani, K., & Yao, Y. (2022). Fibroblasts repair blood-brain barrier damage and hemorrhagic brain injury via TIMP2. *Cell Reports*, *41*(8), 111709. https://doi.org/10.1016/j.celrep.2022.111709

Xue, S., Lozinski, B. M., Ghorbani, S., Ta, K., D'Mello, C., Yong, V. W., & Dong, Y. (2023). Elevated Galectin-3 Is Associated with Aging, Multiple Sclerosis, and Oxidized Phosphatidylcholine-Induced Neurodegeneration. *The Journal of Neuroscience*, *43*(25), 4725–4737. https://doi.org/10.1523/JNEUROSCI.2312-22.2023

Yahn, S. L., Li, J., Goo, I., Gao, H., Brambilla, R., & Lee, J. K. (2020). Neurobiology of Disease Fibrotic scar after experimental autoimmune encephalomyelitis inhibits oligodendrocyte di ff erentiation. *Neurobiology of Disease*, *134*(October 2019), 104674. https://doi.org/10.1016/j.nbd.2019.104674

Yeung, M. S. Y., Djelloul, M., Steiner, E., Bernard, S., Salehpour, M., Possnert, G., Brundin, L., & Frisén, J. (2019). Dynamics of oligodendrocyte generation in multiple sclerosis. *Nature*. https://doi.org/10.1038/s41586-018-0842-3

Yeung, M. S. Y., Zdunek, S., Bergmann, O., Bernard, S., Salehpour, M., Alkass, K., Perl, S., Tisdale, J., Possnert, G., Brundin, L., Druid, H., & Frisén, J. (2014). Dynamics of oligodendrocyte generation and myelination in the human brain. *Cell*, *159*(4), 766–774. https://doi.org/10.1016/j.cell.2014.10.011

Yokota, K., Kobayakawa, K., Saito, T., Hara, M., Kijima, K., Ohkawa, Y., & Harada, A. (2017). Periostin Promotes Scar Formation through the Interaction between Pericytes and In fi ltrating Monocytes / Macrophages after Spinal Cord Injury. *The American Journal of Pathology*, *187*(3), 639–653. https://doi.org/10.1016/j.ajpath.2016.11.010

Young, E. A., Fowler, C. D., Kidd, G. J., Chang, A., Rudick, R., Fisher, E., & Trapp, B. D. (2008). Imaging correlates of decreased axonal Na+/K+ ATPase in chronic multiple sclerosis lesions. *Annals of Neurology*, *63*(4), 428–435. https://doi.org/10.1002/ana.21381

Yuan, Q., Ren, Q., Li, L., Tan, H., Lu, M., Tian, Y., Huang, L., Zhao, B., Fu, H., Hou, F. F., Zhou, L., & Liu, Y. (2022). A Klotho-derived peptide protects against kidney fibrosis by targeting TGF-β signaling. *Nature Communications*, *13*(1), 1–14. https://doi.org/10.1038/s41467-022-28096-z

Zhang, K., Grither, W. R., Van Hove, S., Biswas, H., Ponik, S. M., Eliceiri, K. W., Keely, P. J., & Longmore, G. D. (2016). Mechanical signals regulate and activate SNAIL1 protein to control the fibrogenic response of cancer-associated fibroblasts. *Journal of Cell Science*, *129*(10), 1989–2002. https://doi.org/10.1242/jcs.180539

Zhou, X., Franklin, R. A., Adler, M., Carter, T. S., Condiff, E., Adams, T. S., Pope, S. D., Philip, N. H., Meizlish, M. L., Kaminski, N., & Medzhitov, R. (2022). Microenvironmental sensing by fibroblasts controls macrophage population size. *Proceedings of the National Academy of Sciences of the United States of America*, *119*(32), e2205360119. https://doi.org/10.1073/pnas.2205360119

Zhou, X., Franklin, R. A., Adler, M., Jacox, J. B., Bailis, W., Shyer, J. A., Flavell, R. A., Mayo, A., Alon, U., & Medzhitov, R. (2018). Circuit Design Features of a Stable Two-Cell System. *Cell*, *172*(4), 744-757.e17. https://doi.org/10.1016/j.cell.2018.01.015

Zhou, Y., Huang, X., Hecker, L., Kurundkar, D., Kurundkar, A., Liu, H., Jin, T. H., Desai, L., Bernard, K., & Thannickal, V. J. (2013). Inhibition of mechanosensitive signaling in myofibroblasts ameliorates experimental pulmonary fibrosis. *Journal of Clinical Investigation*, *123*(3), 1096–1108. https://doi.org/10.1172/JCI66700

Zhou, Y., Zhou, B., Pache, L., Chang, M., Benner, C., Chanda, S. K., Khodabakhshi, A. H., & Tanaseichuk, O. (2019). Metascape provides a biologist-oriented resource for the analysis of systems-level datasets. *Nature Communications*, *10*. https://doi.org/10.1038/s41467-019-09234-6

Zhu, Y., Soderblom, C., Krishnan, V., Ashbaugh, J., Bethea, J. R., & Lee, J. K. (2015). Hematogenous macrophage depletion reduces the fibrotic scar and increases axonal growth after spinal cord injury. *Neurobiology of Disease*, *74*, 114–125. https://doi.org/10.1016/j.nbd.2014.10.024

Zirngibl, M., Assinck, P., Sizov, A., Caprariello, A. V., & Plemel, J. R. (2022). Oligodendrocyte death and myelin loss in the cuprizone model: An updated overview of the intrinsic and extrinsic causes of cuprizone demyelination. *Molecular Neurodegeneration*, *17*, 34. https://doi.org/10.1186/s13024-022-00538-8

Zrzavy, T., Hametner, S., Wimmer, I., Butovsky, O., Weiner, H. L., & Lassmann, H. (2017). Loss of “homeostatic” microglia and patterns of their activation in active multiple sclerosis. *Brain*, *140*(7), 1900–1913. https://doi.org/10.1093/brain/awx113

Zuchero, J. B., Fu, M. meng, Sloan, S. A., Ibrahim, A., Olson, A., Zaremba, A., Dugas, J. C., Wienbar, S., Caprariello, A. V., Kantor, C., Leonoudakus, D., Lariosa-Willingham, K., Kronenberg, G., Gertz, K., Soderling, S. H., Miller, R. H., & Barres, B. A. (2015). CNS Myelin Wrapping Is Driven by Actin Disassembly. *Developmental Cell*, *34*(2), 152–167. https://doi.org/10.1016/j.devcel.2015.06.011